

# **An Investigation into Noxious Mechanosensation, and the Role of Peripheral Neuron Subpopulations in Pain**

**Alice Morgan Fuller**

A thesis submitted for the degree of Doctor of Philosophy to  
University College London

Wolfson Institute for Biomedical Research  
University College London  
2020

***Declaration***

I, Alice Morgan Fuller confirm that the work presented in this thesis is my own. Where information has been derived from other sources, I can confirm that this has been indicated within this thesis.

## **Abstract**

This thesis uses transgenic mice to explore the role of candidate and known mechanotransducers in acute mechanical pain. It also utilises transgenics to ablate whole populations of sensory neurons in mice to establish what role these also have in pain, both under normal and inflammatory conditions.

The water and ion channel Aquaporin 1 (Aqp1) is preferentially expressed in the small diameter neurons of the peripheral nervous system (PNS). These are responsible for nociception, and Aqp1 has previously been implicated in pain sensation. Its role in acute mechanical pain has not fully been explored. By using global Aqp1 knockout (Aqp1<sup>KO</sup>) mice and mechano-clamp electrophysiology I am the first to demonstrate that Aqp1 contributes to the mechanically activated (MA) currents associated with pain sensing in nociceptors. However, it does not produce MA currents when expressed in naïve cells. Aqp1 is necessary for normal mechanical pain *in vivo* as Aqp1<sup>KO</sup> animals have an increased mechanical pain threshold. Thus, it is unlikely that Aqp1 is a pore-forming component of a noxious mechanotransducer but may form part of a membrane complex essential to mechanical pain sensation.

Piezo2 is a known mammalian mechanotransducer and is responsible for light touch sensation and proprioception. It's contribution to mechanical pain under pathological conditions is established but it's role in acute mechanical pain remains controversial. I generate mice with a nociceptor-specific Piezo2 deletion and again use a combination of electrophysiological and behavioural assays to demonstrate that Piezo2 is not required for acute noxious mechanosensation. Thus, my data confirms that the mechanotransducer responsible for mechanical pain remains ambiguous.

Finally I study the role of the cutaneous population of Parvalbumin-positive (PV+) sensory neurons in pain. This population is required for innocuous mechanical sensation including vibration sensing. By genetically ablating PV+ neurons to generate 'PV<sup>DTA</sup>' mice, I provide evidence that these neurons are necessary for negatively regulating the thermal, mechanical, and inflammatory pain response, as behaving animals are hypersensitive to these insults. I am the first to propose that cutaneous PV+ neurons are responsible for closing the so-called 'pain gate' in the dorsal horn of the spinal cord. Further evidence for this comes from an *in vivo* electrophysiological study of dorsal horn neurons in PV<sup>DTA</sup> mice, which exhibit increased excitability as a consequence of noxious stimulation. *In vivo* DRG neuron imaging in animals

expressing a reporter protein in PV+ sensory neurons show that these neurons are capable of responding to noxious stimuli, thus solidifying this hypothesis.

### ***Impact statement***

My findings exclude a role for Aqp1 and Piezo2 in generating the MA currents responsible for noxious mechanosensation, and encourage the continued search for the channel responsible. My investigation into the contribution of cutaneous PV+ neurons to pain reveals a novel role for PV+ sensory neurons in negatively regulating normal and inflammatory pain. This observation could drastically improve our understanding of current non-pharmacological approaches to pain management.

I am the first to investigate Aqp1's role in mechanotransduction in DRG neurons. Furthermore, where previous reports have been contradictory with respect to Aqp1's role in pain, I demonstrate that Aqp1 does not have a role in noxious thermal sensing but does in mechanical pain, the latter of which has not been previously reported. Despite showing that Aqp1 does not contribute to chronic inflammatory pain, there is a significant upregulation of Aqp1 mRNA in the DRG of wild type (WT) mice under these conditions. Other aquaporins may be capable of compensating for the loss of Aqp1 in Aqp1<sup>KO</sup> animals, thus maintaining inflammatory pain in this instance. As such, further investigation avoiding developmental compensation with the use of Aqp1-specific antagonists in the adult mouse would be exceptionally insightful. Indeed, there are specific antagonists for either the water channel or ion channel components of this protein. The use of these antagonists would also aid our understanding of the component of Aqp1 that is responsible for acute noxious mechanosensation.

In my continued investigation of noxious mechanosensation, I exclude a role for the known mechanotransducer Piezo2 in acute mechanical pain, thus circumventing unnecessary future studies for other groups. As a consequence, the lab has since developed a list of novel mechanotransducer candidates (by comparing the proteomes of undifferentiated versus differentiated neuronal cell lines after mechanical sensitivity characterisation) in the hope of identifying the unknown ion channel responsible for transducing mechanical pain. The group will screen these by performing targeted knockdown of the candidates in DRG neurons, in combination with mechano-clamp electrophysiology. If successful, the identification of a mechanotransducer responsible for mechanical pain could prove an exceptionally important novel therapeutic target. The need for more efficacious pharmacological treatments for chronic pain is clear and urgent as those currently used often cause many unwanted side effects including dependency and in worst cases death.

In addition to these findings, I show that cutaneous PV+ sensory neurons are necessary for the negative regulation of thermal, mechanical, and inflammatory pain. This is a completely novel finding. It indicates that these sensory neurons are responsible for closing the 'pain gate' in the spinal cord, as described over 50 years ago by Melzack and Wall in their gate control theory of pain. My findings pave the way for future research to establish if PV+ neurons are sufficient to induce analgesia under normal and pathological pain conditions. This could be achieved with the use of optogenetics in mice as a means of selectively activating cutaneous PV+ sensory neurons, in conjunction with pain behaviour experiments.

Clinically, these findings may aid our understanding of current non-pharmacological approaches to managing pain. These approaches include electronic devices such as TENS (transcutaneous electrical nerve stimulation) that are capable of stimulating peripheral nerves in such a manner that pain is reduced. The rationale behind this again draws upon the gate control theory which hypothesises that innocuous sensory neuron activation is capable of negatively regulating pain transduced by nociceptors, via dorsal horn circuitry.

## ***Funding***

I would like to thank the following for their funding of this project:



## Contents

<b>1</b>	<b>Introduction .....</b>	<b>19</b>
1.1	Basic neurophysiology in the peripheral somatosensory system .....	20
1.2	Mechanosensation and pain .....	24
1.2.1	Primary afferent neurons and mechanosensory end organs.....	24
1.2.2	Peripheral mechanonociception .....	28
1.2.3	Mechanical pain pathways/circuits in the dorsal horn.....	31
1.2.4	Supraspinal pain pathways.....	38
1.2.5	The transition from acute to chronic pain .....	41
1.2.6	Animal models of pain .....	42
1.2.7	The contribution of peripheral somatosensory neurons to chronic pain 44	
1.2.8	<i>In vivo</i> GCaMP imaging and the PNS .....	46
1.3	The function of Parvalbumin-positive neurons in the nervous system.....	48
1.3.1	PV+ neurons in the brain .....	48
1.3.2	PV+ neurons in the dorsal horn.....	49
1.3.3	PV+ neurons in the PNS.....	51
1.4	The mechanotransducers responsible for touch, proprioception, and pain...52	
1.4.1	The electrophysiological properties of mechanotransducers.....	52
1.4.2	Qualities of a <i>bona fide</i> mechanotransducer.....	54
1.4.3	Invertebrate mechanotransducers and their mammalian homologues	54
1.4.4	Mammalian mechanotransducers .....	56
1.4.5	Gating mechanisms of mechanotransducers.....	59
1.5	Aquaporins and pain .....	62
1.6	The role of voltage gated sodium channels in nociception .....	66
1.7	The proposed contribution of mechanosensitive peripheral sensory neuron subtypes to gating pain in the dorsal horn .....	73
1.8	Cre-lox DNA recombination .....	75
<b>2</b>	<b>Methods .....</b>	<b>76</b>
2.1	Molecular Biology .....	76
2.1.1	Genotyping.....	76
2.1.2	Quantitative RT-PCR .....	78
2.2	Immunohistochemistry .....	80
2.2.1	Tissue Collection.....	80
2.2.2	Sectioning .....	80
2.2.3	Immunostaining and analysis .....	80
2.3	In-situ hybridisation (RNAScope® technology) .....	81
2.4	Behavioural assays .....	82
2.4.1	Motor co-ordination tests in PV <sup>DTA</sup> mice .....	82
2.4.2	Mechanical sensitivity tests .....	83



2.4.3	Thermal sensitivity tests .....	85
2.4.4	Inflammatory pain models.....	86
2.5	GCaMP Imaging.....	88
2.5.1	<i>In vivo</i> GCaMP imaging.....	88
2.5.2	Analysis.....	89
2.6	<i>In vivo</i> electrophysiology of the dorsal horn .....	90
2.6.1	Electrophysiology recordings.....	90
2.6.2	Analysis.....	90
2.7	Patch clamp electrophysiology .....	91
2.7.1	DRG neuron isolation and culture .....	91
2.7.2	Cell culture and transfection .....	91
2.7.3	Electrophysiology recordings.....	91
2.7.4	Mechanical Stimulation and analysis .....	92
2.8	Statistical analysis .....	93
<b>3</b>	<b>The role of Aqp1 in the generation of mechanically activated currents and mechanical pain .....</b>	<b>94</b>
3.1	Summary .....	94
3.2	Introduction.....	95
3.2.1	Aqp1 mRNA is downregulated in the DRG of mice lacking Nav1.8+ sensory neurons .....	95
3.2.2	The structure and electrophysiological properties of Aqp1 .....	97
3.2.3	The role of Aqp1 in pain.....	99
3.2.4	Breeding strategy for Aqp1 <sup>KO</sup> mice .....	101
3.3	Aims.....	102
3.4	Results.....	103
3.4.1	Aqp1 regulates Piezo2 activity in HEK293T cells .....	103
3.4.2	Aqp1-expressing ND-C cells produce MA currents .....	105
3.4.3	MA currents are altered in the small DRG neurons of Aqp1 <sup>KO</sup> mice ..	107
3.4.4	Aqp1 <sup>KO</sup> mice have reduced sensitivity to noxious mechanical stimuli	110
3.4.5	Aqp1 <sup>KO</sup> mice show no evoked behavioural differences in comparison to WT mice after intraplantar CFA injection.....	112
3.4.6	Aqp1 mRNA is significantly upregulated in the DRG of WT mice after intraplantar CFA injection .....	115
3.5	Discussion .....	117
3.5.1	The role of Aqp1 in acute noxious mechanosensation .....	117
3.5.2	Could there still be a role for Aqp1 in inflammation? .....	118
3.5.3	Should a role for Aqp1 in neuropathic pain be explored?.....	119
3.5.4	Is there a possible role for Aqp1 in regulating the MA currents produced by Piezo2 <i>in vivo</i> ? .....	121
3.5.5	The contribution of other aquaporins to nociception.....	122
3.6	Future directions.....	124

<b>4</b>	<b>Investigating the role of Piezo2 in noxious mechanosensation</b>	<b>126</b>
4.1	Summary	126
4.2	Introduction	127
4.2.1	The structure and electrophysiological properties of Piezo2	127
4.2.2	The role of Piezo2 in pain	129
4.2.3	Piezo2 human mutations	132
4.2.4	Breeding strategy for Piezo2 <sup>fl/fl</sup> ;Nav <sub>v</sub> 1.8-Cre;tdTomato;GCaMP3 mice	134
4.3	Aims	137
4.4	Results	138
4.4.1	Genetic deletion of Piezo2 in Nav <sub>v</sub> 1.8+ sensory neurons does not significantly alter the repertoire of mechanically activated currents that they produce, but does potentiate current amplitude	138
4.4.2	Piezo2 <sup>Nav<sub>v</sub>1.8</sup> animals have normal mechanical sensitivity <i>in vivo</i>	140
4.4.3	Imaging in Piezo2 <sup>Nav<sub>v</sub>1.8</sup> mice reveals a possible means of sensory compensation within the Nav <sub>v</sub> 1.8-negative population of DRG neurons under basal conditions	142
4.4.4	Peak fluorescence of responding GCaMP3 neurons in the DRG validates previous findings in WT animals, and indicates that the activity of Piezo2 <sup>Nav<sub>v</sub>1.8</sup> Nav <sub>v</sub> 1.8+ and negative neurons may be increased in comparison to the WT	148
4.4.5	Piezo2 expression is predominantly restricted to the Nav <sub>v</sub> 1.8-negative population of sensory neurons in WT animals, and Piezo1 to the Nav <sub>v</sub> 1.8+ population	150
4.5	Discussion	152
4.5.1	Is Nav <sub>v</sub> 1.8-Cre an appropriate choice for this study?	152
4.5.2	Are Piezo2 and/or Piezo1 required for the mechanically activated currents produced by Nav <sub>v</sub> 1.8-expressing DRG neurons?	153
4.5.3	A role for Piezo2 in acute noxious mechanical pain can be ruled out	154
4.5.4	Is there a role for Piezo2 in Nav <sub>v</sub> 1.8 sensory neurons in inflammatory allodynia?	155
4.5.5	Is there a role for Piezo1 in noxious mechanosensation <i>in vivo</i> ?	156
4.6	Future directions	158
<b>5</b>	<b>The role of peripheral Parvalbumin-positive neurons in pain</b>	<b>160</b>
5.1	Summary	160
5.2	Introduction	161
5.2.1	Breeding strategies	162
5.3	Aims	165
5.4	Results	166
5.4.1	<i>Ex vivo</i> characterisation of peripheral Parvalbumin neurons	166
5.4.2	Crossing PV-Cre mice with Advillin-loxP-tdTomato-Stop-loxP-DTA mice causes significant PV+ neuron ablation in the DRG of progeny	168

5.4.3	Peripheral PV+ neurons are necessary for normal motor function in mice .....	170
5.4.4	<i>In vivo</i> GCaMP imaging is a useful tool for examining the sensitivity of peripheral sensory neurons to innocuous and noxious stimuli pre and post inflammation.....	172
5.4.5	The neuron response profiles of PV <sup>DTA</sup> mice are comparable to WT mice .....	175
5.4.6	The activity of responding neurons is increased in PV <sup>DTA</sup> mice in comparison to the WT, under basal conditions.....	177
5.4.7	PV <sup>DTA</sup> mice are hypersensitive to noxious cold.....	180
5.4.8	Stimulus-independent pain is dramatically increased in PV <sup>DTA</sup> animals in comparison to WT animals following induction of acute inflammation .....	183
5.4.9	Evidence for peripheral sensory neuron hypersensitivity is observed in the spinal cord of PV <sup>DTA</sup> animals as determined by <i>in vivo</i> electrophysiology .	186
5.4.10	Peripheral cutaneous PV+ neurons respond to a range of stimuli including noxious mechanical and thermal stimuli pre and post PGE <sub>2</sub> injection ....	189
5.5	Discussion .....	193
5.5.1	Is this means of targeted peripheral PV+ neuron ablation an appropriate choice for the experiments I set out to perform? .....	193
5.5.2	The contribution of peripheral PV+ neurons to mechanical nociception and the gate control theory of pain.....	195
5.5.3	Is there a role for peripheral PV+ neurons in gating noxious thermal stimuli? .....	197
5.5.4	The contribution of peripheral PV+ neurons to gating acute inflammatory pain.....	200
5.5.5	Could these observations aid our understanding of current non-pharmaceutical approaches to pain management? .....	201
5.6	Future directions.....	204
<b>6</b>	<b>Discussion .....</b>	<b>207</b>
<b>7</b>	<b>Summary.....</b>	<b>210</b>
<b>8</b>	<b>References.....</b>	<b>211</b>
<b>9</b>	<b>Appendices.....</b>	<b>231</b>
9.1	Appendix A: Additional methods and results for chapter 5 .....	231
9.1.1	<i>In vitro</i> GCaMP imaging.....	231
9.1.2	Cold plate .....	231
9.1.3	GCaMP3 is poorly expressed in the PV+ neurons of PV <sup>tdTom</sup> ; <i>Pirt</i> -GCaMP3 mice.....	232
9.1.4	Global GCaMP6s mice are behaviourally normal .....	235

## **List of figures**

Figure 1.1. The phases of an action potential .....	21
Figure 1.2. Transduction and transmission in nociceptors .....	23
Figure 1.3. A summary of cutaneous mechanoreceptor subtypes .....	25
Figure 1.4. Sensory neuron classification according to unbiased full RNA transcriptome analysis .....	27
Figure 1.5. The termination pattern of peripheral sensory neurons in the dorsal horn of the spinal cord.....	31
Figure 1.6. The neurochemical markers of non-overlapping populations of Lamina I-II interneurons .....	33
Figure 1.7. The gate control theory of pain, and the dorsal horn circuitry associated with mechanical pain.....	36
Figure 1.8. Schematic of supraspinal pain pathways.....	40
Figure 1.9. The updated 2008 IASP definition of hyperalgesia and allodynia.....	41
Figure 1.10. Mechanisms mediating persistent pain following tissue injury/inflammation or nerve injury .....	43
Figure 1.11. The effect of peripheral nerve injury on the excitability on PV+ DH interneurons .....	50
Figure 1.12. The process of noxious mechanotransduction, and recording MA currents in vitro .....	53
Figure 1.13. The proposed gating mechanisms of mechanotransducers .....	60
Figure 1.14. The primary structure of the alpha and beta subunit of voltage gated sodium channels .....	72
Figure 1.15. The proposed contribution of peripheral sensory neuron subtypes to nociceptive gate control in the dorsal horn of the spinal cord.....	74
Figure 3.1. The structure of the Aqp1 monomer, and Aqp1's tetrameric structure in the membrane .....	98
Figure 3.2. Aqp1 potentiates the MA current produced by Piezo2 in HEK293T cells .....	104
Figure 3.3. Aqp1 produces an MA current in ND-C cells.....	106
Figure 3.4. MA currents from total Aqp1 <sup>KO</sup> DRG are unaltered .....	108
Figure 3.5. MA currents in Aqp1 <sup>KO</sup> DRG are altered in small diameter neurons.....	109
Figure 3.6. Noxious mechanical sensitivity is impaired in Aqp1 <sup>KO</sup> mice.....	111
Figure 3.7. Thermal and mechanical sensitivity of Aqp1 <sup>KO</sup> animals after intraplantar injection of CFA.....	114
Figure 3.8. Aqp1 and Piezo2 mRNA expression in the DRG of naïve animals versus those treated with CFA .....	116

Figure 4.1. Diagram of a Piezo2 homotrimer .....	128
Figure 4.2. Example breeding strategy for Piezo2 <sup>fl/fl</sup> ;Nav1.8-Cre;tdTomato;GCaMP3 mice.....	135
Figure 4.3. Electrophysiological characterisation of DRG neurons from Piezo2 <sup>Nav1.8</sup> mice and WT littermate controls .....	139
Figure 4.4. Acute behavioural characterisation of Piezo2 <sup>Nav1.8</sup> mice.....	141
Figure 4.5. <i>In vivo</i> GCaMP3 imaging comparing responses of DRG neurons in Piezo2 <sup>Nav1.8</sup> mice versus WT controls to peripheral stimulation before and after induction of acute inflammatory pain .....	147
Figure 4.6. Peak fluorescence as a measure of the extent of activity of responding DRG neurons in Piezo2 <sup>Nav1.8</sup> mice versus WT controls to peripheral stimulation before and after induction of acute inflammatory pain .....	149
Figure 4.7. RNAScope targeting Piezo1 and Piezo2 mRNA expression in the DRG of Piezo2 <sup>Nav1.8</sup> and WT animals.....	151
Figure 5.1. Breeding strategy for <i>Pvalb</i> ;tdTomato;GCaMP6s (PV <sup>Tom</sup> ;GCaMP6s) mice .....	163
Figure 5.2. Cre expression in <i>PV</i> -Cre mice is predominantly restricted to PV+ sensory neurons, which innervate the glabrous skin in mice.....	167
Figure 5.3. PV <sup>DTA</sup> mice express significantly lower levels of PV mRNA and protein in the DRG .....	169
Figure 5.4. PV <sup>DTA</sup> mice have significant deficits in motor function and coordination	171
Figure 5.5. <i>In vivo</i> GCaMP imaging used to compare responses of WT DRG neurons to peripheral stimulation before and after induction of acute inflammatory pain .....	174
Figure 5.6. Comparative responses of PV <sup>DTA</sup> DRG neurons to peripheral stimulation before and after induction of acute inflammatory pain .....	176
Figure 5.7. Peak fluorescence as a measure of activity of responding DRG neurons in PV <sup>DTA</sup> mice versus WT controls to peripheral stimulation before and after induction of acute inflammatory pain.....	179
Figure 5.8. Acute behavioural characterisation of PV <sup>DTA</sup> mice .....	182
Figure 5.9. Stimulus-independent and stimulus-dependent behaviours observed in WT versus PVDTA animals in response to intraplantar PGE2 injection .....	185
Figure 5.10. <i>In vivo</i> electrophysiology in WDR neurons of the dorsal horn of the spinal cord in WT versus PV <sup>DTA</sup> animals .....	188
Figure 5.11. <i>In vivo</i> GCaMP6s imaging comparing responses of PV+ and PV-negative neurons to peripheral stimulation before and after induction of acute inflammatory pain in PV <sup>Tom</sup> ;GCaMP6s mice .....	192
Figure 5.12. Transcriptional profiles of putative thermosensors within two distinct PV populations of sensory neurons reveal overlapping expression of noxious thermosensors and PV .....	199

Figure 9.1. GCaMP3-expressing PV+ neurons do not fluoresce as readily as the non-PV population in the presence of high concentration potassium solution, but do after incubation with the calcium indicator Fluo4-AM.....234

Figure 9.2. There is no significant behavioural difference between WT and global GCaMP6 mice.....236

### **List of tables**

Table 1.1. A summary of mammalian noxious mechanotransducer candidates according to the qualifications of a bona fide mechanotransducer.....	61
Table 1.2. The role of aquaporins in nociception .....	65
Table 2.1. Ear lysis buffer .....	76
Table 2.2. 10X GB .....	76
Table 2.3. Typical PCR components per reaction .....	77
Table 2.4. Typical PCR thermal cycling protocol .....	77
Table 2.5. cDNA synthesis components per reaction .....	78
Table 2.6. qPCR components per reaction .....	79
Table 2.7. qPCR primers .....	79
Table 2.8. qPCR thermal cycling protocol .....	79
Table 2.9. <i>In vivo</i> GCaMP imaging stimulation protocol .....	88
Table 3.1. Dysregulated genes identified by microarray in the DRG of Na <sub>v</sub> 1.8 <sup>DTA</sup> mice .....	96
Table 3.2. Previous pain behavior assays in Aqp1 knockout/knockdown mice .....	100
Table 3.3. Genotyping primers for Aqp1KO animals .....	101
Table 4.1. Summary of murine Piezo2 deletions and resulting phenotype .....	131
Table 4.2. Summary of human Piezo2 GOF and LOF mutations.....	133
Table 4.3. Genotyping primers for Piezo2fl/fl;Na <sub>v</sub> 1.8-Cre;tdTomato;GCaMP3 mice	136
Table 5.1. Genotyping primers for PV <sup>Tom</sup> , PVDTA , GCaMP3, and GCaMP6s mice .....	164

### **Abbreviations**

AD	Alzheimer's disease
ALS	Amyotrophic lateral sclerosis
AM	A mechanonociceptor
AP	Action potential
Aqp1-13	Aquaporin 1-13
ASD	Autism spectrum disorder
ASIC	Acid-sensing ion channels
<i>C. elegans</i>	<i>Caenorhabditis elegans</i>
CCI	Chronic constriction injury
CFA	Complete Freund's adjuvant
CGRP	Calcitonin gene-related peptide
CIP	Congenital insensitivity/indifference to pain
CNS	Central nervous system
COX2	Cyclooxygenase 2
CSF	Cerebral spinal fluid
DH	Dorsal horn
DMEM	Dulbecco's modified Eagle's medium
DRG	Dorsal root ganglia
DTA	Diphtheria toxin fragment A
FEPS	Familial episodic pain syndrome
GABA <sub>A</sub> R	GABA <sub>A</sub> receptor
GAPDH	Glyceraldehyde 3-phosphate dehydrogenase
GECI	Genetically encoded calcium indicator
GFP	Green fluorescent protein
GOF	Gain-of-function
HEK293	Human embryonic kidney 293 cell
HTMR	High threshold mechanoreceptor
IA	Intermediately adapting
IRES	Internal ribosome entry site
ISH	<i>In situ</i> hybridisation
KO	Knockout
LOF	Loss-of-function
LTMR	Low threshold mechanoreceptor
MA	Mechanically activated
MEC-10	Mechanosensory protein 10
MEC-2	Mechanosensory protein 2



MEC-4	Mechanosensory protein 4
MEC-6	Mechanosensory protein 6
ND-C	Neuroblastoma derived cell
NGF	Nerve growth factor
NKCC1	Na–K–2Cl cotransporter
NMB-1	Noxious mechanosensation blocker 1
NMDAR	NMDA receptor
NMO	Neuromyelitis optica
NSAID	Non-steroidal anti-inflammatory drug
OA	Osteoarthritis
OSN	Olfactory sensory neurons
PAD	Primary afferent depolarisation
PCR	Polymerase chain reaction
PGE <sub>2</sub>	Prostaglandin E <sub>2</sub>
Piezo1	Piezo type mechanosensitive ion channel component 1
Piezo2	Piezo type mechanosensitive ion channel component 2
Pirt	Phosphoinositide interacting regulator of TRP
PNS	Peripheral nervous system
PSI	Presynaptic inhibition
PV/Pvalb	Parvalbumin
qPCR	Quantitative PCR
RA	Rapidly adapting
SA	Slowly adapting
SCI	Spinal cord injury
SFN	Small fibre neuropathy
siRNA	Small interfering siRNA
SNI	Spared nerve injury
SNL	Spinal nerve ligation
STOML3	Stomatin-like protein 3
STZ	Streptozotocin
tdTomato	Tandem dimer tomato fluorescent protein
TENS	Transcutaneous Electrical Nerve Stimulation
TG	Trigeminal ganglia
Tmem150c	Transmembrane protein 150c
TRAAK	TWIK-related arachidonic acid-stimulated K <sup>+</sup> channel
TREK-1	TWIK-1 related K <sup>+</sup> channel
TRPA1	Transient receptor potential ankyrin 1

TRPC	Transient receptor potential channel
TRPM8	Transient receptor potential cation channel subfamily M member 8
TRPV1	Transient receptor potential vanilloid 1
TTX-R	Tetrodotoxin-resistant
TTX-S	Tetrodotoxin-sensitive
TWIK-1	Tandem of P domains in a Weak Inward rectifying K <sup>+</sup> channel
VGCC	Voltage gated calcium channels
VGKC	Voltage gated potassium channel
VGLUT3	Vesicular glutamate transporter 3
VGSC	Voltage gated sodium channel
WDR	Wide dynamic range
WT	Wild-type

### ***Acknowledgements***

I would like to thank my supervisor Professor John Wood for providing me with the opportunity to carry out a PhD in his lab, and for all of his invaluable support and guidance throughout.

To those of the Molecular Nociception group (past and present), thank you for making my time in the lab such a friendly and enjoyable experience. Without your time, expertise, and humour, none of this would have been possible. In particular, I want to thank Ana, Ed, Marta, Queeni, and Skip for their endless support, both practically, and emotionally. I am further indebted to Ed and Skip for the time they spent reading and commenting on the contents of this thesis. I would like to thank Andrei, James, and Jing for all of their technical guidance, and Jane, who taught me so much (and with so much patience!) in the beginning stages of my PhD.

Special thanks go to my Mum, Dad, Jacob, and Grandparents, my London family, Mark, Tom and Lea, my oldest friends Aneesah, Tamsin, and Tessa, and to Mika. I am so grateful for all of your support throughout, and for always encouraging me to keep going!

## **1 Introduction**

The International Association for the Study of Pain (IASP) defines pain as ‘an unpleasant sensory and emotional experience associated with actual or potential tissue damage or described in terms of such damage’. Pain serves a protective function, allowing us to withdraw from potentially harmful stimuli, and a heightened sensitivity associated with inflammation facilitates tissue recovery. Whereas nociception refers to the detection of a noxious stimulus by an afferent fibre of the peripheral nervous system (PNS), the actual perception of pain is highly subjective and relies upon complex processing within the central nervous system (CNS) (D’Mello & Dickenson, 2008).

Despite acute pain’s protective role, pain that persists after tissue healing and for longer than three months is deemed chronic, and is a pathologic condition that severely impacts upon quality of life (Raffaelli & Arnaudo, 2017). In the UK alone, it is predicted that one-third to one-half of the adult population suffers from chronic pain (Fayaz et al., 2016). Chronic pain can arise due to persistent nociceptive input; such is the case in prolonged inflammation, or from direct damage to peripheral sensory neurons (e.g. due to diabetic neuropathy or chemotherapeutic neurotoxicity). Pain in this instance often cannot be treated, as such there is an urgent need for novel efficacious therapeutics.

Within the scope of this thesis, I will primarily focus on acute nociceptive pain pathways, as opposed to the mechanisms underpinning chronic pathological pain. However, to understand the latter, it is imperative to understand the former. The aim of the experiments herein will be to determine the contribution of known ion channels to acute mechanical pain, and the role of a subset of Parvalbumin-expressing peripheral sensory neurons in acute pain.

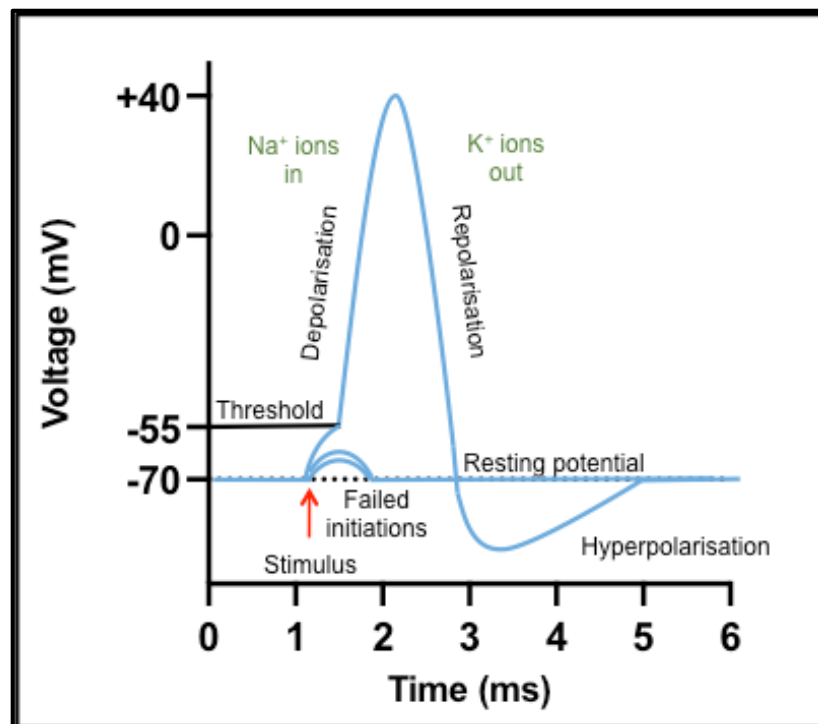
### **1.1 Basic neurophysiology in the peripheral somatosensory system**

The nervous system can be broken into two aforementioned components, the CNS and the PNS. The CNS consists of the brain and spinal cord, and the PNS consists of all neurons outside of these regions. The PNS can be further subdivided into the sensory component which responds to external (or internal) stimuli, and the motor component, which in turn consists of two divisions; the somatic motor division, and the autonomic motor division. The former incorporates motor neurons that connect the brain and the spinal cord to skeletal muscle, which allows for voluntary behaviour. The latter consists of axons that innervate smooth muscle, cardiac muscle, and glands, and mediates involuntary behaviour. Within the autonomic motor division you have the sympathetic, parasympathetic, and enteric divisions. The sympathetic division is responsible for the body's 'fight or flight' response, and the parasympathetic division is responsible for 'housekeeping' during rest. The enteric division consists of neurons that influence gastric motility and secretion. All regions of the nervous system consist of two main types of cell; neurons which are responsible for electrochemical signalling (via the generation of action potentials (APs)), and supporting cells termed glia. Collective bundles of neuronal cell bodies that serve a particular function are known as nuclei within the CNS, and ganglia within the PNS.

The somatosensory system is an essential component of the PNS that enables us to interact with our environment via nociceptive, proprioceptive, mechanical and thermal cues. Somatosensation relies upon the initial perception of these cues via a heterogeneous population of pseudo-unipolar neurons whose cell bodies reside in the dorsal root ganglia (DRG) and the trigeminal ganglia (TG), to provide sensation to the body and the face respectively (Hendry & Hsiao, 2012). The peripheral terminals of these neurons innervate the skin, viscera, muscle and tendons, and their central terminals synapse with second order neurons in the spinal cord or the brainstem of the CNS. These neurons can be broadly subdivided based on their cell body size, axon diameter, extent of myelination, and conduction velocity. They are termed A $\beta$ , A $\delta$  and C fibres, their size, extent of myelination, and conduction velocity decreasing in that order (Abraira & Ginty, 2013).

Somatosensory neurons have a unique role within the nervous system in that they are responsible for producing the 'receptor potential' of a given stimulus, and then propagating this signal in the form of APs along the length of the axon to the CNS. APs are an extremely rapid change in transmembrane electrical potential within neurons, predominantly mediated by the transfer of Na<sup>+</sup> and K<sup>+</sup> ions into and out of the axon

(Figure 1.1). At rest, the membrane potential of a neuron is largely dictated by open 'resting' K<sup>+</sup> channels which allow K<sup>+</sup> ions to move across the membrane to the outside of the cell down their concentration gradient, causing a negative charge on the cytosolic face of the membrane. Consequently, the resting membrane potential (~70mV) is near the equilibrium potential of K<sup>+</sup> ions (E<sub>k</sub>), this is the point at which the movement of K<sup>+</sup> ions stops as the electrical potential attracting ions into the cell balances the ions moving down their concentration gradient. At rest, the concentration of K<sup>+</sup> ions is typically 10 times the concentration found in the extracellular fluid, whereas the concentrations of Na<sup>+</sup> and Cl<sup>-</sup> ions are much higher outside the cell than inside. These concentrations are maintained by Na<sup>+</sup>/K<sup>+</sup> ATPase pumps that actively pump 3 Na<sup>+</sup> ions out of the cell for every 2 K<sup>+</sup> ions pumped in.

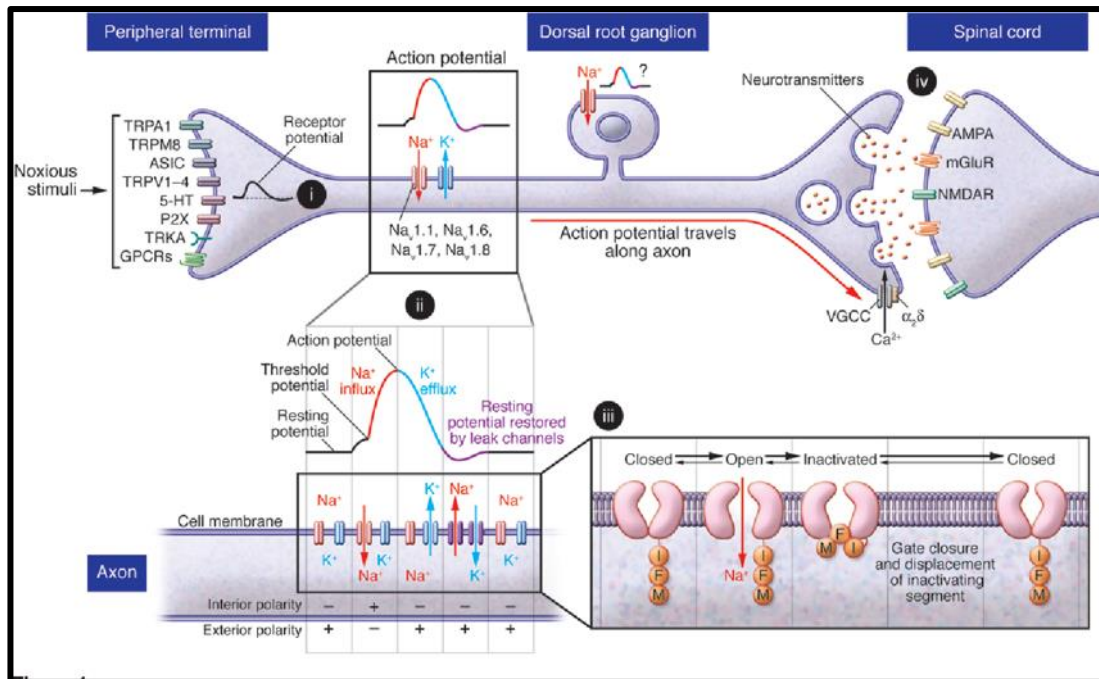


**Figure 1.1. The phases of an action potential**

A stimulus activates the appropriate receptor at the peripheral terminal of the neuron leading to an influx of cations. If the stimulus is strong enough, this influx will cause the neuron membrane to reach the threshold potential for activation. At this point, VGSCs are activated resulting in a large influx of Na<sup>+</sup> ions, and a rapid depolarisation of the membrane. The membrane repolarises as VGSCs inactivate, and as VGKCs activate to cause an efflux of K<sup>+</sup> ions out of the neuron. Hyperpolarisation occurs as a result of continued K<sup>+</sup> efflux, and the membrane gradually returns to the resting potential as VGKCs close (adapted from Molecular Devices, 2020).

APs are initiated in the PNS by the conversion of an external stimulus into electrochemical signals within the body. These signals are generated by a range of receptors that are sensitive to stimuli including thermal and mechanical cues, which

cause these ion channels to open allowing for an influx of cations into the peripheral terminal of the neuron (Figure 1.2). The transducers responsible for producing these 'receptor potentials' include Piezo2, a mechanically gated ion channel essential for innocuous touch sensation and proprioception in mammals (Ranade et al., 2014; Woo et al., 2015), a noxious heat transducer; capsaicin-sensitive Transient receptor potential channel vanilloid 1 (TRPV1) (Cavanaugh et al., 2009), and the noxious cold and menthol-sensitive Transient receptor potential cation channel subfamily M member 8 (TRPM8) (Knowlton et al., 2013). Provided the receptor potential is enough to cause the membrane to depolarise to the point at which the threshold potential is reached i.e. -50mV, an AP is triggered due to the abrupt opening of voltage-gated Na<sup>+</sup> channels (VGSCs). Within the PNS these include the sodium channels Na<sub>v</sub>1.1-1.3 and Na<sub>v</sub>1.6-1.9. The opening of VGSCs allows external Na<sup>+</sup> ions to flood into the neurons causing the membrane to depolarise. This depolarisation leads to the activation of other VGSCs along the length of the axon, triggering further APs accordingly. APs are unable to travel back in the opposite direction due to the 'refractory period' on that portion of the membrane caused by the inactivation of the VGSCs. Another contributing factor to this refractory period is the opening of voltage-gated K<sup>+</sup> channels (VGKCs) which allow for the efflux of K<sup>+</sup> ions and a subsequent hyperpolarisation of the membrane. Assuming the intensity of the stimuli is strong enough, this allows for a further AP to be generated despite the refractory period. Information is transferred not via the amplitude of AP, but rather by the frequency and pattern of APs. The speed of AP generation down the length of the axon can be modified with myelination, which greatly increases this speed. Myelination of the axon of neurons is mediated by myelin-producing glial cells which wrap insulating myelin around the axon it is adjacent to. This myelin sheath is discontinuous, broken by so-called nodes of Ranvier where VGSCs cluster. Thus, the AP jumps from node to node in a process known as saltatory conduction. Once the AP has travelled the length of the axon to the central terminal, it triggers Ca<sup>2+</sup> influx as a consequence of the activation of voltage-gated Ca<sup>2+</sup> channels (VGCCs), and the subsequent release of neurotransmitters such as glutamate at the presynaptic terminal (Hendry & Hsiao, 2012). Glutamate activates receptors on the postsynaptic terminals of neurons in the spinal cord, and the signal is then propagated to supraspinal regions of the CNS. The propagation and transmission of these electrochemical signals, or APs, forms the basis of all neuronal excitability within the nervous system.



**Figure 1.2. Transduction and transmission in nociceptors**

Noxious stimuli impinge upon the peripheral terminal of a nociceptor causing the appropriate channel to open (e.g a thermosensor or chemosensor), allowing for the influx of cations and the generation of a receptor potential, in a process termed transduction (i). Provided this receptor potential depolarises the membrane enough to recruit VGSCs, these channels open and allow for the influx an Na<sup>+</sup> ions down their electrochemical gradient to elicit an action potential (ii). A highly conserved motif (IFM)acts to inactivate VGSCs after opening, and as the AP is propagated along the length of the axon this so called 'refractory period' of VGSCs prevents APs from travelling back to the peripheral terminal (iii). Once an AP has been 'transmitted' the length of the axon, depolarisation at the presynaptic terminal causes the activation of VGCCs, a subsequent influx of Ca<sup>2+</sup> ions, and the release of neurotransmitters (iv). These then activate the appropriate receptor on the postsynaptic terminal of spinal neurons, ultimately leading to the propagation of signal to supraspinal structures in the CNS (Raouf et al., 2010).





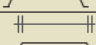

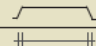


## **1.2 Mechanosensation and pain**

### **1.2.1 Primary afferent neurons and mechanosensory end organs**

Mechanically sensitive neurons dominate the PNS, making up ~90% of all sensory neurons in the DRG, the subtypes of which are summarised in Figure 1.3. Those responsible for innocuous touch sensing are predominantly A $\beta$  afferents which have large diameter, heavily myelinated axons, with a fast conduction velocity of 16 - 100 m/s (Abraira & Ginty, 2013). They are classified as low threshold mechanoreceptors (LTMRs) and can be further subcategorised based on their peripheral end organs and their response to steady indentation of the skin. A $\beta$  afferents that produce high frequency AP firing activity in response to an onset of stimuli, which then silence during the static phase of the stimulus, are termed as rapidly adapting (RA) fibres, and re-fire as the stimulus is removed. This is synonymous with our perceived acclimation to stimuli that remain in contact with our skin, for example clothing. Slowly adapting (SA) A $\beta$  afferents have a sustained pattern of AP firing throughout the duration of stimulation. A $\beta$  LTMR end organs of the glabrous skin include the RA Meissner corpuscles and Pacinian corpuscles, responsible for detecting skin movement and vibration respectively. SA end organs include Merkel cells, which respond to indentation, and Ruffini endings, which sense skin stretch (Abraira & Ginty, 2013). These different end organs enable us to distinguish between a milieu of touch sensations ranging from the brush of a feather to the feeling of something held in the hand. A $\beta$  central projections terminate in laminae III to V of the dorsal horn of the spinal cord (Lallemend & Ernfors, 2012). An additional group of A $\beta$  afferents are termed proprioceptors; their peripheral projections innervate the muscle and tendons and terminate either as Golgi tendon organs or muscle spindles. These end organs respond to muscle stretch and contraction and are essential for fine motor coordination and movement (Medici & Shortland, 2015).

Fibres that detect noxious force are high threshold mechanonociceptors (HTMRs) and make up most of the thinly myelinated A $\delta$  and unmyelinated C fibre populations, which conduct at 5-30 m/s and 0.5-2.0 m/s, respectively (Delmas et al., 2018). The faster conducting A $\delta$  fibres are responsible for the initial 'first-pain' often described as a stabbing, pricking sensation, followed by a 'second-pain', which is more aching and diffuse, and is transduced by the slower C fibres (Julius & Basbaum, 2001; Price & Dubner, 1977). The C fibre population can be further characterised as peptidergic or non-peptidergic. The former is identified by the expression of neuropeptides such as the neurotransmitter substance P, or calcitonin gene-related peptide (CGRP), and TrkA, the tyrosine kinase receptor for nerve growth factor (NGF). The non-peptidergic

population can be selectively labelled with the  $\alpha$ -D-galactosyl-binding lectin IB<sub>4</sub> (Julius & Basbaum, 2001). HTMRs terminate in the glabrous and hairy skin as free nerve endings and often exhibit little to no adaptation in response to a sustained stimulus (Delmas et al., 2018). The majority of thinly-myelinated A $\delta$  fibre central projections terminate in lamina I and V of the dorsal horn. Peptidergic and non-peptidergic C fibres terminate in laminae I and II (Lallemend & Ernfors, 2012).

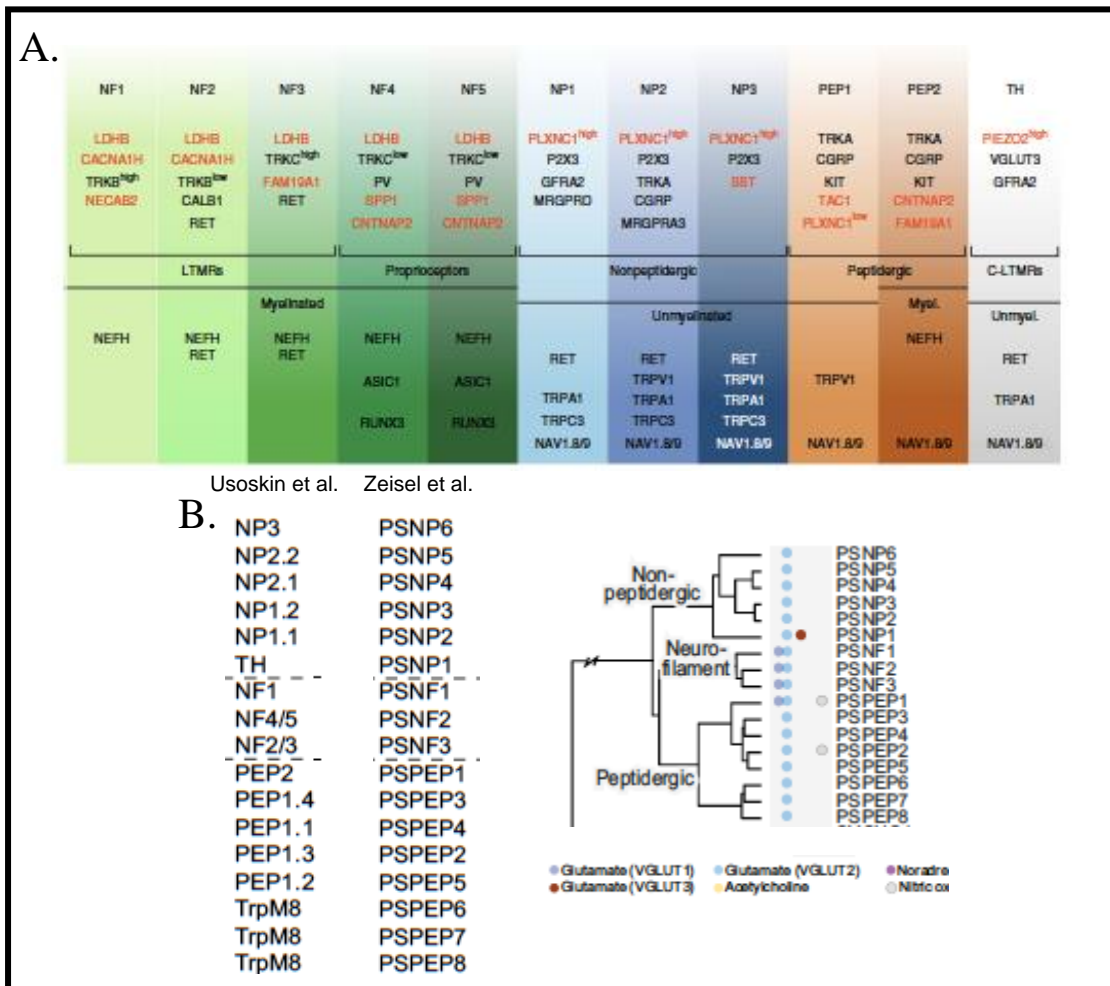
Physiological subtype	Associated fiber (conduction velocity <sup>1</sup> )	Skin type	End organ/ending type	Location	Optimal Stimulus <sup>4</sup>	Response properties
SAI-LTMR	A $\beta$ (16-96m/s)	Glabrous	Merkel cell	Basal Layer of epidermis	Indentation	
		Hairy	Merkel cell (touch dome)	Around Guard hair follicles		
SAII-LTMR	A $\beta$ (20-100m/s)	Glabrous	Ruffini <sup>2</sup>	Dermis <sup>3</sup>	Stretch	
		Hairy	unclear	unclear		
RAI-LTMR	A $\beta$ (26-91m/s)	Glabrous	Meissner corpuscle	Dermal papillae	Skin movement	
		Hairy	Longitudinal lanceolate ending	Guard/Awl-Auchene hair follicles	Hair follicle deflection	
RAII-LTMR	A $\beta$ (30-90m/s)	Glabrous	Pacinian corpuscle	Deep dermis	Vibration	
A $\delta$ -LTMR	A $\delta$ (5-30m/s)	Hairy	Longitudinal lanceolate ending	Awl-Auchene/ Zigzag hair follicles	Hair follicle deflection	
C-LTMR	C (0.2-2m/s)	Hairy	Longitudinal lanceolate ending	Awl-Auchene/ Zigzag hair follicles	Hair follicle deflection	
HTMR	A $\beta$ /A $\delta$ /C (0.5-100m/s)	Glabrous Hairy	Free nerve ending	Epidermis/Dermis	Noxious mechanical	

**Figure 1.3. A summary of cutaneous mechanoreceptor subtypes**

Alongside those found in the glabrous skin, this table also includes the mechanosensory end organs found in the hair follicles of hairy skin in mice, of which there are three, guard, awl/auchene, and zigzag. These follicles are innervated by longitudinal lanceolate endings that are either A $\beta$  RA-LTMRs, A $\delta$ -LTMRs, or C-LTMRs. Circumferential lanceolate endings are also found in each of the hair follicle types, the physiology of which is unknown. Like glabrous skin, noxious touch in the hairy skin is transduced via free nerve endings in the epidermis (Abraira & Ginty, 2013).

Electrophysiological recordings of *ex vivo* skin-nerve preparations, in combination with post-recording intracellular labelling has enabled the broad functional identification of cutaneous somatosensory neurons and the anatomy of their associated end organs or lack thereof, described in Figure 1.3 (Abraira & Ginty, 2013). However, it is with the identification of sensory-specific transducers and subsequent genetic and/or pharmacological targeting of the neurons expressing them, that we are beginning to understand the extent of functional heterogeneity amongst peripheral sensory neurons. Notably, recent unbiased single cell RNA sequencing of DRG neurons in mice has allowed for a more thorough investigation into the molecular markers expressed by distinct sub populations of peripheral sensory neurons, and has identified further functional subtypes (Figure 1.4) (Usoskin et al., 2015; Zeisel et al., 2018). An example of these are the TrkB+ population of peripheral sensory neurons. TrkB is a marker for RA myelinated neurons innervating the hair follicles, and Meissner's corpuscles of the glabrous skin. Their central projections terminate in

laminae III/IV of the dorsal horn. Genetically-mediated TrkB+ afferent ablation in adult animals causes a specific and significantly reduced response to a cotton swab brushed across the hind paw, the lightest of dynamic mechanical stimuli, whilst maintaining all other mechanical sensory modalities (Dhandapani et al., 2018).



**Figure 1.4. Sensory neuron classification according to unbiased full RNA transcriptome analysis**

**A.** Classification of sensory neuron subtypes in the DRG according to Usoskin et al. (2015). The functional groups are titled at the top, followed by previously identified markers in black, and newly proposed markers in red. The genes below correspond to those that are commonly studied in the field. 'NF' corresponds to neurofilament heavy chain expressing neurons, 'NP' to nonpeptidergic nociceptors, 'PEP' to peptidergic nociceptors, and 'TH' to those expressing tyrosine hydroxylase, which make up a distinct subclass of unmyelinated neurons. **B.** Single cell RNA-seq studies have enabled Zeisel et al. (2018) to further subdivide DRG neurons into 18 functional neuron subtypes. On the left, the correlation between the Usoskin et al. (2015) and Zeisel et al. (2018) DRG neuron subpopulation datasets. Note the presence of a previously undefined population of Trpm8-expressing neurons in the Usoskin et al. (2015) data. On the right, the hierarchy of somatosensory populations identified by Zeisel et al. (2018) is depicted, including their corresponding neurotransmitters.

### 1.2.2 Peripheral mechanonociception

Nociceptor activation occurs when afferents are exposed to extreme thermal or mechanical stimuli as long as the depolarisation is sustained. Primary mechanical and thermal hyperalgesia occurs if there is tissue injury and is dependent on C fibre activity. Peptidergic C fibres release inflammatory mediators including substance P and CGRP into the surrounding tissue triggering vasodilation, and an infiltration of white blood cells. These contribute to an 'inflammatory soup' that decreases the activation threshold of nociceptive fibres leading to their hypersensitivity to touch and temperature, and mediates a recruitment of otherwise 'silent' nociceptors (Basbaum et al., 2009). It is worth noting that other types of nociceptor include those that are sensitive to chemical stimuli, and those that are termed 'polymodal' which respond to both thermal and mechanical stimuli. Although a number of receptors responsible for transducing noxious thermal stimuli are known (i.e. TRPM8 and TRPV1), the receptor that transduces acute mechanical pain is for the most part ambiguous. The sodium channels associated with the conduction of nociceptive signals are Na<sub>v</sub>1.7, Na<sub>v</sub>1.8, and Na<sub>v</sub>1.9, and human mutations of these channels are associated with various pain pathologies (Liu & Wood, 2011).

Mechanonociceptive A $\delta$  fibres, also referred to as A mechanonociceptors (AMs), make up most of the HTMRs in the PNS. They are typically lightly myelinated afferents that terminate in the periphery as free nerve endings in the epidermis and dermis. Mechanonociceptors also include a cohort of slow-conducting C nociceptors. Recent research has identified specific subpopulations of touch-sensing A $\beta$  sensory neurons that interact with the mechano-nociceptive pathway to modulate the perception of mechanical pain (Arcourt et al., 2017).

The increase in the identification of sensory-specific molecular markers have lent themselves to the 'labelled line' theory of somatosensation, which posits that individual subsets of peripheral neurons are sensory-specific. This is an idea that is perhaps contradictory to the extent of polymodality previously reported in electrophysiology studies of nociceptors, however, increasing evidence would suggest sensory-specificity under non-pathological conditions (Emery & Wood, 2019). Thermo-specific nociceptor examples include those that express TRPV1, the pharmacological ablation of which significantly and specifically reduces the sensitivity of mice to noxious heat stimuli (Cavanaugh et al., 2009; Mishra & Hoon, 2010). Populations of neurons identified as mechanonociceptor-specific, include the Mrgprd+ population of sensory neurons which encompass ~90% of all cutaneous nonpeptidergic C fibres. Genetic

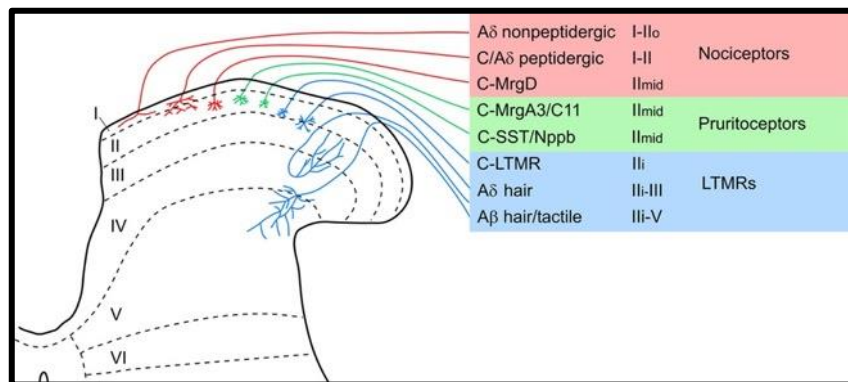
ablation of Mrgprd+ neurons in adult mice causes an increased threshold to punctate mechanical (von Frey) stimulation with no alteration to noxious thermal sensation, contrary to *ex vivo* electrophysiology recordings indicating polymodality amongst the Mrgprd+ population (Cavanaugh et al., 2009). The use of recently developed techniques such as functional *in vivo* calcium imaging has also aided the sensory refinement of known neuronal subpopulations, such as those expressing CGRP. Where CGRP is an inflammatory neuropeptide typically associated with peptidergic C nociceptors (Gibson et al., 1984), Ghitani et al. (2017) identified a subset of lightly myelinated A $\delta$  HTMRs expressing the CGRP transcript *Calca*, the peripheral nerve endings of which terminate in hair follicles. This population of neurons is specifically responsible for the sensation of noxious hair pull in mice.

To add a layer of complexity to the sensory specificity of mechanonociceptors, the labelled line theory is bolstered by a 'population coding' model of sensory perception. This model describes crosstalk likely at the level of the dorsal horn between a combination of noxious and innocuous sensory inputs, that shapes the overall perception of mechanical pain. Evidence for sensory crosstalk can be perceived from the everyday practices of scratching to relieve an itch, cooling to relieve heat, or rubbing an area that has received a mechanical insult. Interestingly, the modulation of mechanonociception by the combinatorial input of labelled HTMRs and LTMRs in the dorsal horn was recently described by Arcourt et al. (2017). In this study the group first isolated a population of A $\delta$  sensory neurons expressing the marker *Npy2r*, previously described in the RNA-seq study by Usoskin et al. (2015). This particular population are heat insensitive (i.e. do not express TRPV1) and do not overlap with peptidergic and non-peptidergic C nociceptors. They also express Na<sub>v</sub>1.8 and terminate as free nerve endings in the hairy and glabrous skin of the hind paw, with central projections predominantly terminating in lamina II. Genetic ablation of peripheral Npy2r+ neurons in mice causes a significantly delayed withdrawal response to a noxious pinprick stimulus on the hind paw, with no effect on thermal or von Frey thresholds. Interestingly, exacerbated nocifensive responses were observed when this population of neurons was optogenetically activated. As part of this study, Arcourt et al. (2017) also describe a LTMR specific marker, *MafA*, which demonstrates no overlap with any markers of A or C fibre nociceptors. MafA+ neurons innervate Meissner's corpuscles in the glabrous skin and lanceolate endings in hairy skin, with central projections terminating in laminae III-IV, typical of A $\beta$  LTMRs. When Npy2r+ and MafA+ neuron populations were simultaneously optogenetically activated, LTMR-derived input

alleviated nociceptor evoked pain, with an effect more pronounced at low frequency stimulation. Thus, LTMRs provide an inhibitory effect on mechanical pain transmission that is blocked as nociceptor activity increases. This is an elegantly executed example of the contribution of specified sensory neuron populations to the so-called 'gate control theory' of pain originally described over 50 years ago (Melzack & Wall, 1965).

### 1.2.3 Mechanical pain pathways/circuits in the dorsal horn

The spinal cord is the first point of nociceptive modulation. It encompasses the integration of innocuous and nociceptive input from primary sensory neurons, post-synaptic inhibition of dorsal horn neurons, presynaptic inhibition of primary sensory neurons, and top-down modulation from supraspinal regions of the CNS, where pain perception ultimately arises. The dorsal horn (DH) is the entry point for peripheral sensory neurons into the spinal cord and is divided into six distinct laminae as described by Rexed (1954), who observed these distinct layers based upon the morphology of cells residing there, and the distribution of grey and white matter. Depending on the type of primary afferent, each central terminal projects to a distinct lamina of the DH (Figure 1.5). Broadly speaking, the superficial DH (laminae I-IIo) is the termination point for nociceptive fibres, with low-threshold fibres predominantly terminating in the deeper laminae (III-V) (Todd, 2010). Here we focus on the interaction between primary DRG neurons and the spinal cord, but it should be noted that the medullary dorsal horn is the region of TG neuron termination.



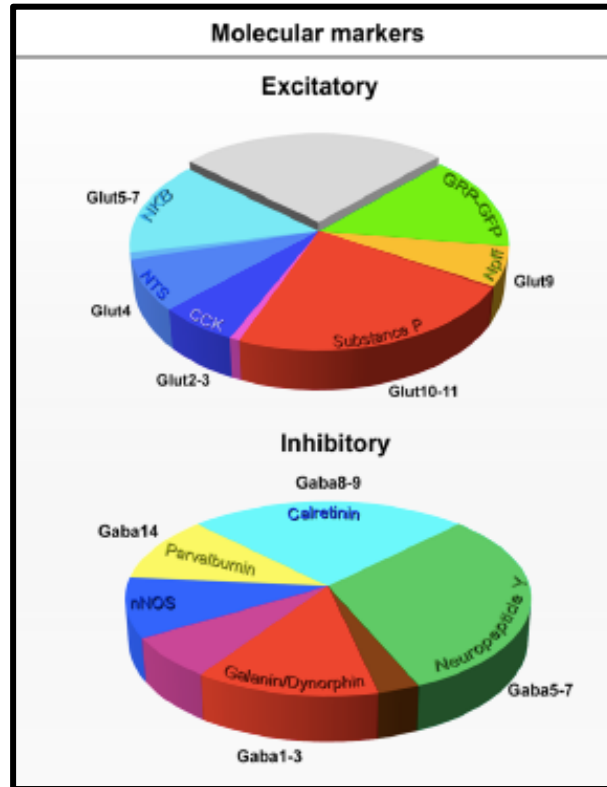
**Figure 1.5. The termination pattern of peripheral sensory neurons in the dorsal horn of the spinal cord**

HTMRs predominantly terminate in the superficial horn, and LTMR termination occurs in lamina II and extends to the deep dorsal horn (Todd, & Wang, 2018).

Neurons of the DH, like the DRG, are exceptionally heterogeneous, and can be characterised according to morphology, electrophysiological traits, and transcriptomic profile. The great majority of all DH neurons are interneurons (~99%), i.e. neurons that project to regions within the spinal cord, mostly intrasegmentally, but there are some that are referred to as propriospinal, that project to other spinal segments (Peirs et al., 2020). The remaining neurons are projection neurons that send axons to supraspinal regions of the CNS, many of which are found in Lamina I and are nociceptor specific. In the deeper dorsal horn in lamina V, so-called wide dynamic range (WDR) neurons are projection neurons that respond to both innocuous and noxious inputs (Braz et al., 2014).



The relative proportion and heterogeneity of interneurons reflects the importance of their role in integrating and modulating sensory information, rather than just relaying information to higher structures. Very broadly speaking DH neurons can be classified as either excitatory, or inhibitory, releasing the neurotransmitters glutamate, and GABA/glycine, respectively. GABAergic interneurons predominantly reside in laminae I-III, and glycinergic interneurons in Laminae III-V and I. The vesicular GABA transporter (VGAT) can be used to identify inhibitory interneurons, and vesicular glutamate transporter 2 (VGLUT2) to identify excitatory neurons. Most investigations of DH neurons have occurred in lamina II, believed to be the core of the gate control theory of pain. The non-overlapping populations of excitatory and inhibitory interneurons found here and in lamina I are summarised in Figure 1.6.



**Figure 1.6. The neurochemical markers of non-overlapping populations of Lamina I-II interneurons**

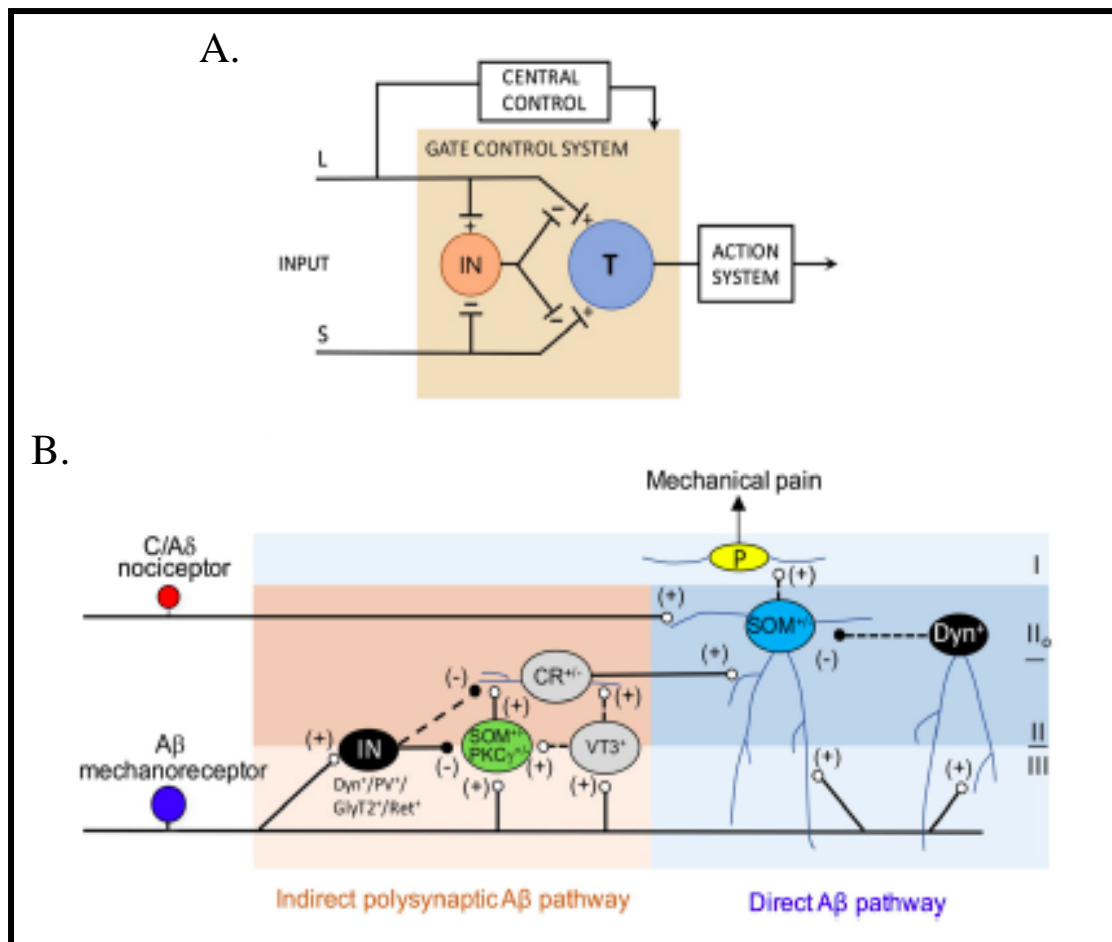
Approximately 75% of all excitatory neurons in these laminae express either of the following; neurotensin (NTS), substance P (SP), neurokinin (NKB), gastrin-releasing peptide (GRP), cholecystokinin (CCK) or neuropeptide FF (NPFF). The remaining 25% are likely to include vertical cells which aren't included in these identified populations. Relatively broad classes of markers for vertical cells include somatostatin (SOM), enkephalin (ENK) or calretinin (CR), which overlap extensively with one another and with the six populations described above. Inhibitory interneurons in this region include five largely non-overlapping populations that express galanin/dynorphin (GAL/DYN), neuropeptide Y (NPY), neuronal nitric oxide synthase (nNOS), Parvalbumin (PV) or CR, which account for nearly all inhibitory interneurons in laminae I-II (Peirs et al., 2020).

Modulation of mechanical nociception by innocuous A $\beta$  fibres is not a novel concept and is broadly described by the gate control theory of pain. Contrary to the specificity/labelled line hypothesis which describes distinct pathways for transmitting specific sensory modalities, the gate control theory of pain, as described by Melzack and Wall (1965) (Figure 1.7.A), is favoured. It describes a means of pain modulation via the interplay of activity between nociceptors and innocuous LTMRs, which converge on spinal transmission (“T”) neurons in the dorsal horn. T neurons then transmit this integrative signal to higher order neurons of the CNS. Where nociceptors provide direct excitatory input to T neurons, LTMRs synapse to inhibitory interneurons (“IN”) in lamina II of the dorsal horn, which in turn provide inhibitory input to T neurons. As such, LTMRs have the ability to close this nociceptive gate, whereas strong nociceptive inputs are responsible for opening it. This so-called pain gate can also be opened and closed by top-down inhibitory or excitatory signals from the brain. It is believed that pathology (e.g. chronic inflammation and nerve damage) associated plasticity is responsible for attenuating the inhibitory signals received by the IN neurons and/or directly sensitising T neurons, such that LTMRs are capable of activating T neurons and evoking allodynia (a painful response to an innocuous stimulus). Over time the gate control theory of pain has become more complex as the contribution of individual spinal neuron subtypes to nociception have been identified (Duan et al., 2018). I will go on to discuss some of these below, some of which are included in a revised version of gate control DH circuitry depicted in Figure 1.7.B, which are specific to mechanical pain.

With specific subpopulations of DH neurons identified, an important component of any investigation into neuron functionality is to investigate their role *in vivo*. Various tactics have been employed to selectively inhibit and/or activate inhibitory and excitatory interneurons within the DH, revealing a plethora of neuron-specific sensory modalities associated with nociception. To investigate the role of inhibitory interneurons (or “IN” interneurons), early rudimentary studies applied GABA<sub>A</sub> and glycine receptor antagonists to the spinal cord, demonstrating that a block of spinal inhibition led to exaggerated pain responses in rats (Sivilotti & Woolf, 1994). Molecular-genetic approaches have since allowed for the targeting of specific populations within the DH giving a greater insight into the functional circuitry here, revealing key players that receive LTMR input and are involved in closing the pain gate. Specific inhibitory interneuron targets have included the PV+ population of interneurons, ablation of which causes the development of mechanical allodynia, and activation an increase in the withdrawal threshold for noxious mechanical (but not thermal) stimuli (Petitjean et

al., 2015). Similarly, ablation of inhibitory DYN+ cells causes a hypersensitivity to noxious mechanical but not thermal insults (Duan et al., 2014). A subject of contention, however, has been the role of DYN+ neurons in itch. Where Duan et al. (2014) found an exacerbation of the itch response as a result of DYN+ neuron ablation, another group reported that chemogenetic activation of these neurons suppresses itch (Huang et al., 2018). In addition, Huang et al. (2018) found that activation of the NNOS+ population increased the threshold for mechanical and heat pain. Others have studied the consequence of the ablation of the RET+ subset of inhibitory interneurons, predominantly located in lamina III, which resulted in mechanical allodynia and increased responses to noxious mechanical and thermal stimuli. Activating them resulted in reduced acute pain and hyperalgesia (Cui et al., 2016).

Similar ablation studies have been performed on excitatory interneurons (or “T” neurons) including those expressing SOM, which comprise of a large population of excitatory neurons found throughout lamina I – II. SOM+ neuron ablation dramatically reduced acute mechanical pain, as well as mechanical allodynia present in neuropathy and inflammatory models (Duan et al., 2014). Similarly, activation results in pain-like behaviour (Christensen et al., 2016), thus these neurons are deemed essential for mechanical pain perception. Deletion of VGLUT3 (found in a large population of lamina III neurons and overlapping with a proportion of PKC $\gamma$  neurons) within neurons results in reduced mechanical pain and reduced mechanical allodynia as a consequence of nerve injury or inflammation. Chemogenic activation results in evoked mechanical allodynia but no change in thermal pain (Peirs et al., 2015).



**Figure 1.7. The gate control theory of pain, and the dorsal horn circuitry associated with mechanical pain**

**A.** The gate control theory of pain proposed in 1965. 'L' refers to large diameter fibres, and 'S' to small diameter fibres. 'T' are transmission neurons, and 'IN' are inhibitory neurons in the substantia gelatinosa (lamina II) of the dorsal horn (Duan et al., 2018; Melzack & Wall, 1965).

**B.** Schematic showing the spinal circuits that transmit mechanical pain in the dorsal horn. 'CR' refers to transient-central cells partly marked by Calb2/calretinin. The 'SOM' neuron in blue is a vertical neuron in lamina II; 'P' refers to a projection neuron in lamina I. 'IN' is an inhibitory interneuron at the II- III border or within lamina III, and includes the Dyn, PV, GlyT2, and Ret lineage neurons (Duan et al., 2018).

Where the circuits described above focus on postsynaptic inhibition of excitatory interneurons mediated by GABAergic inhibitory interneurons, presynaptic inhibition (PSI) of LTMRs and HTMRs driven by sensory neuron input also contributes to gating pain. This phenomenon, also depicted in Figure 1.7.A, is described as the ability of LTMRs to excite IN neurons which in turn presynaptically inhibit sensory input from both large and small fibres (Mendell, 2014). Initially described over 70 years ago, the specific neurons involved in PSI remain relatively undefined. It is believed that PSI is mediated by GABA<sub>A</sub> receptors (GABA<sub>A</sub>Rs) at the central termini of peripheral neurons. More recently and somewhat paradoxically, a role for NMDA receptors (NMDARs) in small diameter afferent induced PSI has also been described (Zimmerman et al.,

2019). Activation of presynaptic GABA<sub>A</sub>Rs via GABAergic interneurons is believed to cause PSI by an efflux of Cl<sup>-</sup> ions, subsequently depolarising the terminal in a process known as primary afferent depolarisation (PAD). This in turn reduces neurotransmitter release from the afferent in a number of hypothesised ways. These are; shunting inhibition causing a diminution of AP height, thus no neurotransmitter release; an inactivation of VGSCs diminishing AP height and therefore neurotransmitter release; and/or, an inactivation of VGCCs in the terminals, again reducing neurotransmitter release (Guo & Hu, 2014; Zimmerman et al., 2019). The strength of GABA-induced PAD is primarily reliant upon the expression of the inwardly directed Na<sup>+</sup>-K<sup>+</sup>-2Cl<sup>-</sup> cotransporter (NKCC1) in peripheral sensory neurons as it is responsible for maintaining intracellular concentrations of Cl<sup>-</sup>, which the strength and polarity of GABA-mediated neurotransmission is largely dependent on. A loss of either GABA<sub>A</sub>R or NMDAR-mediated PSI in mice has been demonstrated to induce a mechanical hypersensitivity in both hairy and glabrous skin. Moreover, a loss of GABA<sub>A</sub>R only also leads to deficits in fine texture discrimination, demonstrating a role for the PSI of A $\beta$ -LTMRs in tactile acuity. Specific populations of interneurons responsible for mediating PSI include the CCK excitatory interneurons via a GABAergic inhibitory mediator, which are responsible for LTMR to LTMR PSI. The VGLUT3 population of excitatory interneurons receive input from nociceptors to mediate NMDA-mediated PSI in LTMRs (Zimmerman et al., 2019).

#### **1.2.4 Supraspinal pain pathways**

The nociceptive projection neurons in the DH responsible for transmitting pain signalling to supraspinal structures are referred to as anterolateral tract (ALT) neurons. They are concentrated in lamina I, largely absent from lamina II, and scattered throughout III-VI. These neurons project predominantly to the contralateral side. The sensation of pain is then processed by a large distributed neuronal network, which has two main processing streams; the spinothalamo-cortical pathway that processes the discriminative aspects of pain, and the spinoparabrachial-limbic pathway that processes the affective-motivational aspects of pain. At all of these stages there are integrative signals, both inhibitory and excitatory, which help to shape the ultimate perception of pain.

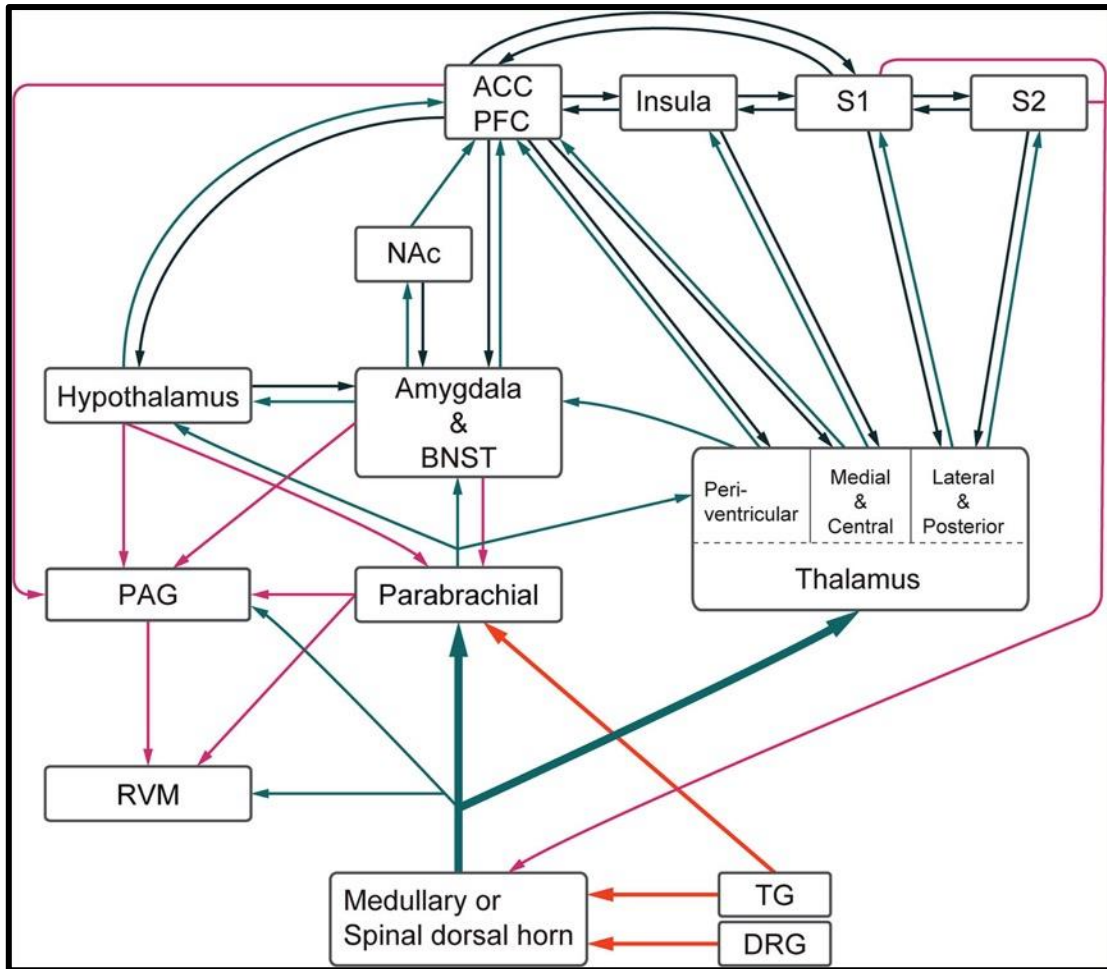
The discriminative aspects of pain refer to discerning the location, type, and intensity of pain. As part of the spinothalamo-cortical pathway, ALT nociceptive projection neurons terminate in multiple nuclei in the thalamus, including the ventral posterior complex, the central nucleus (both centrolateral (CL) or centromedial (CM)), the medial dorsal nucleus (MD), and the posterior nuclear group (Po). Neurons of these thalamic nuclei in turn project to several cortical areas, including the primary somatosensory (S1), the secondary somatosensory (S2), and the insular and the cingulate cortex (Figure 1.8). Sensory specificity, hence discrimination, is retained in the somatosensory cortex. This is demonstrated by the identification of S1 neurons within so-called region 3b/1 as responsible for the sensation of 'fast' pain via A $\delta$  nociceptors, and those located in region 3a mediate the second pain evoked by slowly conducting C fibres (Vierck et al., 2013).

The spinoparabrachial-limbic pathway integrates nociceptive signals of all modalities from all regions of the body, thus does not have the same discriminatory output as the spinothalamic-cortical pain pathway. Instead, it is responsible for the affective-motivational aspects of pain. In this instance, spinal ALT projection neurons make their way to the lateral parabrachial nucleus (LPb) in the brainstem. LPb neurons then send projections to the central nucleus of the amygdala (CeA), the lateral bed nucleus of stria terminalis (BNST), the midline paraventricular nucleus of the thalamus (PVT), and the lateral and periventricular region of the hypothalamus (Hyp) (Figure 1.8). CeA and BNST neurons then project to the nucleus accumbens (NAc) and to the cingulate and prefrontal cortex (PFC). The PVT provides input to the cingulate and insular cortex. The CeA, BNST and the cingulate cortex (particularly the anterior cingulate cortex (ACC)) are known to process affective emotional responses. Some of the specific

neuronal populations involved in this process include CGRP+ neurons from the LPb which terminate in the CeA, the activation of which is sufficient to cause fear/threat learning (Han et al., 2015).

The descending pathways of pain transmission are responsible for integrating top-down (incorporating cognitive and emotional factors that can control pain processing) and bottom-up influences on pain transmission and are either capable of facilitating or inhibiting pain. Evidence for descending control of pain perception from higher centres was originally demonstrated by the electrical stimulation of the PAG and RVM in the brainstem causing analgesia in rodents as a consequence (Mayer & Price, 1976), and similarly with PAG stimulation in humans. The PAG is able to control nociceptive transmission of the spinal cord via a relay in the RVM, furthermore, this network can be recruited with the administration of opioid analgesics (Yaksh et al., 1988). This led to the observation that the PAG/RVM network is susceptible to modulation by the three major groups of endogenous opioids; the enkephalins, endorphins, and dynorphins. RVM outputs terminate in the dorsal horn where they provide inhibition of excitatory interneurons, excitation of inhibitory interneurons, as well as direct post-synaptic inhibition of projection neurons, and inhibition of neurotransmitter release in primary afferents. The RVM regulates facilitation and/or inhibition via functionally distinct populations of neurons. These are ON-cells and OFF-cells. ON-cells are known to promote nociception, whereas the activation of OFF-cells facilitates antinociception, and are necessary for the analgesic action of opioids.



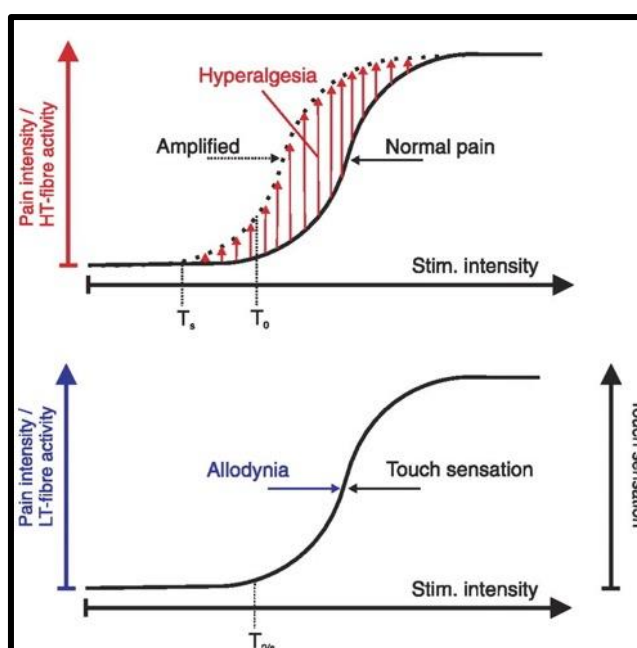


**Figure 1.8. Schematic of supraspinal pain pathways**

Ascending pathways are depicted in green, and the main descending pathways in pink. ACC, anterior cingulate cortex; PFC, prefrontal cortex; S1, primary somatosensory cortex; S2, secondary somatosensory cortex; NAc, nucleus accumbens; BNST, bed nucleus stria terminalis; PAG, periaqueductal grey; RVM, rostroventral medulla; TG, trigeminal ganglion; DRG, dorsal root ganglion. (Todd & Wang, 2020).

### 1.2.5 The transition from acute to chronic pain

Chronic pain can arise due to persistent nociceptive input; such is the case in prolonged inflammation, or from direct damage to peripheral sensory neurons (e.g. due to diabetic neuropathy or chemotherapeutic neurotoxicity). These phenomena cause peripheral sensitisation characterised by increased AP firing and neurotransmitter release into the dorsal horn. A subsequent central sensitisation in the dorsal horn arises as heightened excitability leads to the recruitment of NMDA receptors, an increase in levels of cytosolic calcium ions and ultimately a long-term shift in the activation of nociceptive circuits (Ji et al., 2003). This dysregulation of pain pathways manifests itself as pain in response to innocuous stimuli (allodynia), hypersensitivity to noxious stimuli (hyperalgesia) (Figure 1.9), or as spontaneous pain in neuropathic pain syndromes (Sandkühler, 2009). At present, treatments for chronic pain include non-steroidal anti-inflammatory drugs (NSAIDs) and opioids, both of which are poorly efficacious in treating neuropathic pain (Yekkirala et al., 2017). The anticonvulsant gabapentanoids have given better results in treating pain associated with neuropathy, but like opioids, the propensity for misuse and dependence is high (Wise, 2017). The quantity and severity of side effects associated with current pain treatments is due to the plethora of normal physiological roles their targets have.

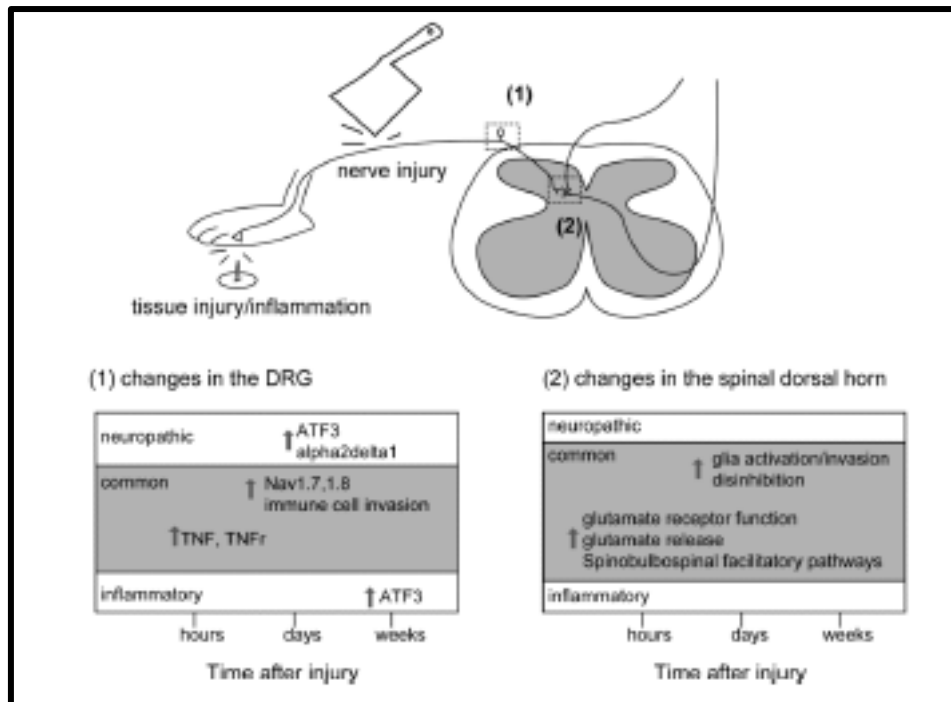


**Figure 1.9. The updated 2008 IASP definition of hyperalgesia and allodynia**

The top graph depicts the definition of hyperalgesia, an enhanced response to normally painful stimuli.  $T_0$  refers to the normal pain threshold, and  $T_s$  to the pain threshold after sensitisation. The graph below depicts allodynia, a pain response to normally innocuous stimuli.  $T_{0/s}$  refers to the normal stimulation threshold for touch response, and is also the threshold for allodynia (Sandkühler, 2009).

### **1.2.6 Animal models of pain**

Many of the experiments described within this thesis use acute nociceptive behavioural assays in transgenic mice, with emphasis on the mechanical component of pain. However, the development of animal models of inflammatory and neuropathic pain have been key to our understanding of the pathological mechanisms underpinning chronic pain states. Inflammatory models of pain in rodents include those that induce acute or chronic inflammation. Of the former, models include intraplantar injection of prostaglandin E<sub>2</sub> (PGE<sub>2</sub>) into the hind paw. PGE<sub>2</sub> is a known inflammatory mediator, with receptors expressed throughout the PNS (Kawabata, 2011), initial injection of which causes transient mechanical and thermal hypersensitivity as a consequence of nociceptor sensitisation (Domenichiello et al., 2017; Kuhn & Willis, 1973). Longer-lasting models of inflammatory pain include injection of Complete Freund's adjuvant (CFA), inducing isolated swelling and hypersensitivity lasting for weeks (Larson et al., 1986). Models of neuropathic pain in rodents comprise of surgical ligation/crush/or transection injuries performed on the sciatic nerve, and disease models include the systemic injection of streptozotocin which induces diabetic neuropathy. The injection of chemotherapeutic agents such as oxaliplatin in rodents, known to induce neuropathic pain in humans, also serves as a translatable model of neuropathy (Jaggi et al., 2011). Where the aetiology of pain as a consequence of tissue versus neuropathic injury in the initial stages are clearly different, as injury/pain persists, common mechanisms in both can contribute to persistent pain (Figure 1.10) (Xu & Yaksh, 2011).



**Figure 1.10. Mechanisms mediating persistent pain following tissue injury/inflammation or nerve injury**

Following tissue injury or nerve injury, pathological changes that might lead to persistent pain in the DRG (1) and the spinal cord dorsal horn (2) are listed. Common mechanisms are shown in the grey boxes and include the upregulation of various pain associated VGSCs and inflammatory mediators. Immune cells are activated and invade nervous tissue, and excitatory neurotransmission is also enhanced. ATF3, activating transcription factor 3; TNF, tumor necrosis factor; TNFr, tumor necrosis factor receptor (Xu & Yaksh, 2011).

### **1.2.7 The contribution of peripheral somatosensory neurons to chronic pain**

Where central sensitisation is key to regulating the spread of pain beyond the site of injury, the emotional aspects of pain, and the chronicity of pain (Woolf & Salter, 2000), it is evident that peripheral input is essential in driving the development of chronic pain and maintaining it (Gold & Gebhart, 2010). For example, appropriate postsurgical pharmacological blockade in the periphery decreases the likelihood of pain transitioning from acute to chronic in human patients (Katz & Seltzer, 2009), and peripheral nerve block in patients with peripheral nerve injury or distal polyneuropathy leads to a complete abolition of ipsilateral pain, irrespective of the extent of central sensitisation (Haroutounian et al., 2014). How peripheral neurons contribute to this phenomena still remains to be fully determined. We do know that hyperalgesia is believed to be produced by sensitisation of nociceptors, but there is little evidence for the involvement of nociceptors in mechanical allodynia (Sandkühler, 2009). This is corroborated by nociceptor ablation studies in mice that exhibit a profound hyposensitivity to acute noxious mechanical stimuli and reduced hyperalgesia after exposure to inflammatory agents, but still develop heightened pain sensitivity to mechanical stimuli after nerve injury (Abrahamsen et al., 2008).

As such, mechanical allodynia is thought to be due to the recruitment of innocuous A $\beta$  fibres. Evidence for this is found in human nerve injury, which causes a selective loss of small but not large diameter DRG neurons, and allows A $\beta$  primary afferent fibres to access spinal cord pain circuits (Sukhotinsky et al., 2004). Furthermore, rodent studies using A $\beta$  fibre specific blockade alleviates pain in models of nerve injury, diabetic neuropathy, and chemotherapy (Xu et al., 2015). The molecular identity of these neurons is gradually being elucidated using novel molecular markers such as those described by Usoskin et al., (2015). For example, targeted ablation of A $\beta$  TrkB+ peripheral neurons that innervate hair follicles, and Meissner corpuscles in the glabrous skin of mice causes a reduction in mechanical allodynia after nerve injury (but not in an inflammatory pain model). Furthermore, their optogenetic activation triggers a nocifensive response (Dhandapani et al., 2018).

Thus, where a recruitment of A $\beta$  fibres may negatively regulate mechanical pain under normal and acute inflammatory conditions, recruitment in a neuropathic setting may serve to positively regulate it. However, non-pharmacological approaches to treating chronic pain (e.g. TENS (Transcutaneous Electrical Nerve Stimulation)) often aim to activate LTMRs (Levin & Hui-Chan, 1993). Perhaps as we continue to functionally

disambiguate individual populations of A $\beta$  sensory neurons, we may identify individual roles for each in their contribution to, or management of chronic pain conditions.

### 1.2.8 *In vivo* GCaMP imaging and the PNS

Calcium imaging is a means of tracking intracellular calcium signalling which has an extensive role within neurons, driving processes such as exocytosis at the presynaptic terminal to gene transcription at the level of the nucleus. At rest, the intracellular concentration of calcium ions ( $\text{Ca}^{2+}$ ) is maintained at approximately 50-100 nM, rising to levels that are 10 to 100 times higher in the activated neuron (Grienberger & Konnerth, 2012). This rise in concentration is predominantly driven by the influx of external  $\text{Ca}^{2+}$ , often as a result of AP activity and the concomitant recruitment of voltage gated calcium channels (VGCCs) allowing for  $\text{Ca}^{2+}$  influx across the membrane. As such, an increase in intracellular  $\text{Ca}^{2+}$  is considered synonymous with AP activity (Tian et al., 2012). Novel calcium imaging techniques using genetically encoded calcium indicators (GECIs) are an exciting addition or even alternative to traditional experimental techniques in neuroscience. Unlike electrophysiology, GECI imaging does not require direct interaction with neurons, thus maintaining their physiological integrity, and allows for simultaneous imaging across an entire population of neurons (Grienberger & Konnerth, 2012).

The GECI, GCaMP, is a single fluorophore GECI consisting of a  $\text{Ca}^{2+}$  binding domain – calmodulin (CaM) - bound to the C-terminus of a circularly permuted eGFP (cpeGFP) molecule. A  $\text{Ca}^{2+}$ /CaM binding myosin light chain kinase domain (M13) is fused to the N-terminus of the cpeGFP, which is poorly fluorescent in the absence of  $\text{Ca}^{2+}$ . However, once CaM binds  $\text{Ca}^{2+}$ , a conformational change allows CaM to bind to the M13 domain. This causes a structural shift within the cpeGFP, eliminating a solvent pathway present in the absence of  $\text{Ca}^{2+}$ , causing de-protonation of the fluorophore and vigorous excitation (Akerboom et al., 2009).

*In vivo* GCaMP imaging of DRG neurons has already proved exceptionally insightful with regard to our understanding of sensory processing at the level of the periphery, demonstrating that thermal sensing by peripheral neurons relies upon a graded coding for heat, and a combinatorial coding for cold sensing (Wang et al., 2018). It has also been used to monitor the responses of somatosensory neurons to acute painful stimuli and during chronic pain pathologies (Kim et al., 2016; Chisholm et al., 2018; Emery et al., 2016; Smith-Edwards et al., 2016). Exciting findings include those of Kim et al. (2016) who describe gap junction-mediated coupling at the soma of DRG neurons after the induction of inflammatory pain and neuropathic pain, thus providing evidence for a novel form of plasticity at the level of the DRG. This technique has also provided an important means to challenge fundamental concepts such as the extent of nociceptor

polymodality (Emery et al., 2016). A recent review has elaborated upon these findings by suggesting that the discrepancies between the extent of polymodality reported with electrophysiological fibre recordings (between 50 and 80%) versus *in vivo* GCaMP imaging of DRG neurons (~7%) is due to the depth of the receptive fields of neurons stimulated in these studies (Lawson et al., 2019). Nociceptors with a superficial receptive field are far more likely to be polymodal than those found in the deeper tissues, the latter of which is extensively stimulated in the aforementioned GCaMP study (Emery et al., 2016). As the use of the technique continues to rapidly grow and evolve, there is no doubt *in vivo* GCaMP imaging will continue to offer invaluable insight into the mechanisms underpinning nociception, and will be used considerably within this thesis.



### **1.3 The function of Parvalbumin-positive neurons in the nervous system**

As part of this study, I aim to investigate the role of cutaneous PV+ sensory neurons in pain. PV is a  $\text{Ca}^{2+}$  binding protein that is expressed broadly throughout the peripheral and central nervous systems. With the combined aid of immunohistochemical, transcriptomic, and functional studies it is established that PV-expressing neurons are responsible for a wide range of essential functions within the body, some of which include the maintenance of normal pain sensation.

#### **1.3.1 PV+ neurons in the brain**

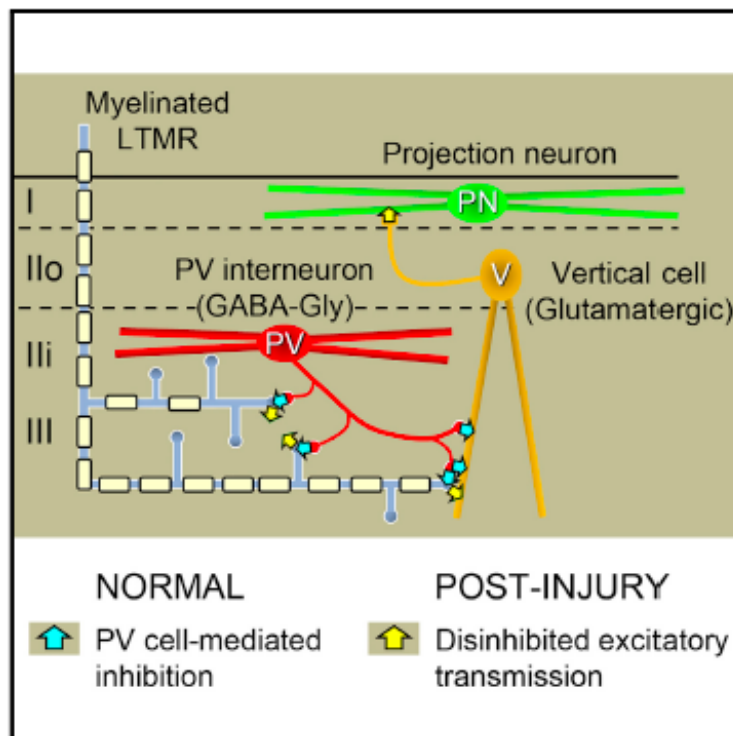
Within the brain, emphasis with respect to pathology has been placed on the expression of PV protein itself. Here, PV+ neurons are GABAergic interneurons which facilitate sensory and cognitive information processing by controlling pyramidal neuron activity and generating gamma oscillation (Hongo et al., 2020). The highest density of PV interneurons are found in the cerebellum, cortex, hippocampus, thalamus, and striatum (Filice et al., 2019). Aberrant function of PV+ neurons within these different regions manifests itself as distinct cognitive and sensory deficits in humans. For example, PV neurons within the cortices contribute to autism spectrum disorders (ASD). Despite no mutations in the *Pvalb* gene ever having been reported in ASD or in any other neurodevelopmental disorder, PV mRNA and protein is downregulated in the ASD brains of patients and mouse models of the disease, as well as schizophrenia and bipolar disorder (Gandal et al., 2012; Wang et al., 2011). Subsequent studies have confirmed that this reduction is not due to a depletion of PV+ interneurons, but due to downregulation of PV protein (Filice et al., 2016). It is believed that in this instance PV protein's ability to sequester  $\text{Ca}^{2+}$  is of particular importance with respect to regulating neurotransmitter release, hence a depletion of PV leads to enhanced inhibition and a subsequent alteration of the excitatory/inhibitory balance within these circuits. In behaving PV global knockout (KO) mice, the loss of PV expression within this circuitry manifests itself as a phenotype resembling that of ASD patients (Wöhr et al., 2015), including impaired social interactions, communication deficits, and the development of repetitive behaviours. Intriguingly these animals also exhibit a reduction in nociceptive and startle responses, and an increase in seizure susceptibility, which are all comorbidities of ASD in humans. As proof of principle, treatment of mice heterozygous for the PV KO gene with 17- $\beta$  estradiol leads to a rescue effect in sociability assays and repetitive behaviours with a concomitant increase in PV expression in the cortices, similar to the levels found in wild type (WT) animals (Filice et al., 2018). There are, however, pathologies associated with a diminution of PV interneurons themselves, for example, a loss of PV neurons within the hippocampus is associated with mouse

models of Alzheimer's disease (AD), and AD patients. Memory deficits associated with this disease are ameliorated with the recovery of PV+ neuron density (Hongo et al., 2020).

### **1.3.2 PV+ neurons in the dorsal horn**

A reduction of PV interneurons within the spinal cord has also been linked to pathology in murine ablation studies. PV+ neurons within the dorsal horn of the spinal cord co-express the inhibitory neurotransmitters GABA and glycine. They reside at the border of lamina II and III, where they receive input from peripheral A $\beta$  fibres and provide PSI to these, as well as postsynaptic inhibition to PKC $\gamma$  excitatory interneurons (Peirs et al., 2020; Petitjean et al., 2015). More recently it was established that PV interneurons also synapse to excitatory vertical cells whose axons span laminae II and III and interact with laminae I projection neurons (Boyle et al., 2019). Despite efforts to describe them 40 years ago (Celio & Heizmann, 1981), the role of PV interneurons within the dorsal horn is only now coming to light. Two recent studies demonstrate the importance of PV+ neurons in the dorsal horn in the maintenance of normal mechanosensation, and their contribution to mechanical allodynia as a consequence of nerve injury. Under normal conditions, inhibitory PV interneurons receive peripheral input from large diameter A $\beta$  fibres, which relay innocuous touch sensation, and are not activated by noxious peripheral input. A study by Petitjean et al. (2015) demonstrated that ablation or silencing of PV+ interneurons causes mechanical allodynia, as does nerve injury (e.g. the spared nerve injury (SNI) model of neuropathic pain), both due to a decrease in the number of synaptic connections between PV+ interneurons and PKC $\gamma$  excitatory interneurons. Pharmacogenetic activation of PV+ interneurons significantly increased withdrawal threshold of awake naïve and neuropathic mice to mechanical stimuli but not to noxious thermal stimuli. The same phenomenon was reported following sub-cutaneous capsaicin injected into the heel (Petitjean et al., 2015). A further study consolidated a portion of these findings by demonstrating again that normal PV+ interneuron function is essential in preventing mechanical allodynia due to nerve injury and that PV+ interneuron expression is not reduced as a consequence (Boyle et al., 2019). However, they found no difference in contacts between PV neurons and PKC $\gamma$  somas and dendrites (Boyle et al., 2019). Instead, Boyle et al. (2019) demonstrate that under normal conditions PV+ interneurons presynaptically suppress LTMR activity whilst simultaneously inhibiting a postsynaptic target of that same afferent input, in this case vertical cells which provide direct input to nociceptive projection neurons in lamina I. They report that peripheral nerve injury causes a reduction in the excitability of PV interneurons which in turn likely

leads to a reduction of PV cell-mediated inhibition of peripheral A $\beta$  neurons and vertical neurons, thus allowing innocuous primary afferents to activate nociceptive circuits (Figure 1.11). This was confirmed by blocking PV interneuron activity, stimulating the hind paw of the same mouse with innocuous stimuli, and observing significant cFos expression throughout the dorsal horn, including lamina I and II which isn't observed in control animals.



**Figure 1.11. The effect of peripheral nerve injury on the excitability on PV+ DH interneurons**

PV+ interneurons mediate presynaptic control of myelinated afferents via axoaxonic inputs. PV interneurons simultaneously mediate postsynaptic inhibition of vertical cells. Allodynic mice show reduced PV cell excitability but no structural plasticity as a consequence of nerve injury (Boyle et al., 2019).

### **1.3.3 PV+ neurons in the PNS**

Research into the contribution of peripheral PV+ neurons to pain has been sparse, especially with respect to those innervating the skin. Peripheral PV+ neurons make up approximately 25 % of L4 and L5 DRG neurons innervating the sciatic nerve. These are predominantly proprioceptors that innervate muscle and terminate either as Golgi tendon organs or muscle spindles (Shortland & Mahns, 2016). However, a small portion of PV+ DRG neurons are cutaneous afferents (Honda, 1995) that terminate as Meissner and Pacinian corpuscles in the glabrous skin (de Nooij et al., 2013). In the periphery, like the spinal cord, work has predominantly focused on the role of PV neurons themselves rather the role of PV protein, as somatosensory phenotypes have not been reported as a consequence of PV deletion in nervous tissues alone. For example, the first PV global KO studies initially aimed to investigate the role of PV protein in the fast-twitch muscle fibres where high concentrations of PV protein are found. PV KO mice exhibited a higher concentration of  $Ca^{2+}$  in muscle fibres which generated a greater force during a single twitch, and a prolonged contraction-relaxation cycle (Schwaller et al., 1999). The group subsequently proposed that PV expression in fast twitch fibres is important in the performance of rapid, phasic movements, and that PV deletion does not cause any significant developmental or breeding differences in mice, nor does it affect behaviour or physical activity. We know from subsequent ASD studies that this is not the case, but the lack of a motor deficit in these animals suggests that within peripheral proprioceptors, PV is either non-essential for their function, or compensatory mechanisms are capable of preserving proprioception. As such, I aimed to investigate the role of peripheral PV+ neurons themselves within this study.

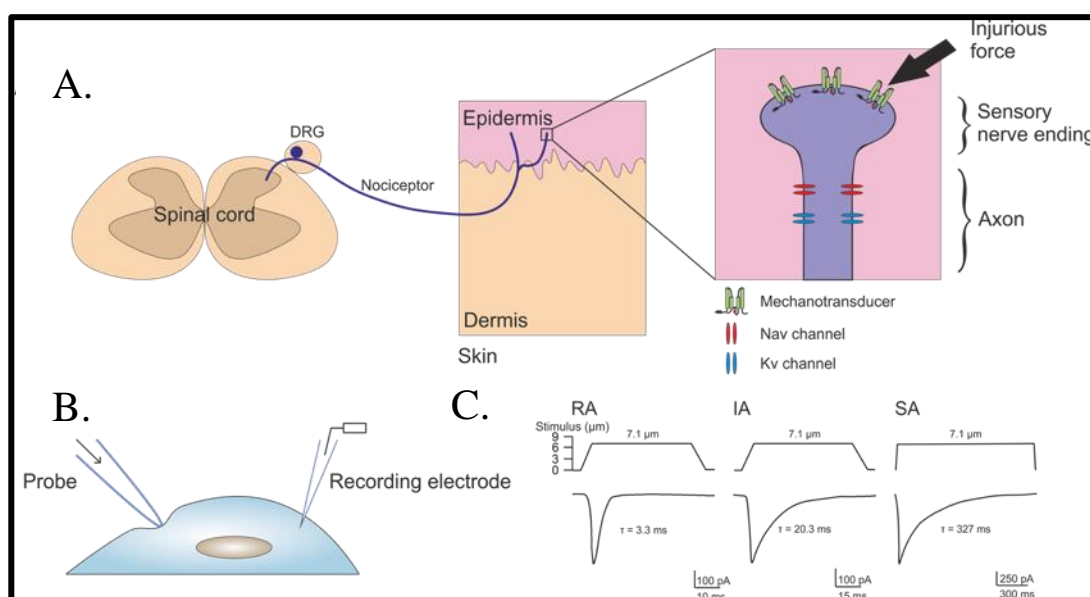
#### **1.4 The mechanotransducers responsible for touch, proprioception, and pain**

In order to perceive the extensive variety of external tactile stimuli the body is exposed to, mechano-sensitive sensory neurons must be endowed with the molecular transducers capable of responding to these forces. This sensitivity is mediated via the activation of mechanotransducer channels expressed at the peripheral terminals of sensory neurons, which are responsible for transforming mechanical force into electrochemical signals by producing cationic, inward, mechanically activated (MA) currents (Delmas et al., 2011). Although we predominantly focus on the mechanisms of mechanosensation in the PNS here, mechano-sensitive tissue and its associated mechanotransducers are found throughout the body, including in the cardiovascular, baroreceptor, vestibular, and hearing systems.

##### **1.4.1 The electrophysiological properties of mechanotransducers**

Whereas other sensory transducers (e.g. rod cells in the retina) are highly enriched within isolated sensory organs, the identification of mechanotransducers has been somewhat harder, due to their limited and diffuse expression within the PNS. As such, much work in identifying them has been based upon genetic screens, and subsequent high-throughput siRNA knockdown in mechanosensitive tissues, rather than standard biochemical approaches. The subsequent study of identified candidate mechanotransducers has relied upon the generation of appropriate mechanical electrophysiology assays. The range of cellular mechanical assays developed reflects the diversity of internal and external mechanical forces exerted upon mechanotransducers throughout the body. Assays include those that induce cell stretch, osmotic challenge, and fluid shear stress. However, the technique that has proven most beneficial to our understanding of tactile mechanosensitivity is the mechano-clamp technique (Figure 1.5.B). The mechano-clamp technique was initially developed by John Levine (McCarter et al., 1999) and has been used to mechanically interrogate the cellular soma or neurites of isolated DRG neurons, by membrane indentation with a glass probe. The cell is held at its resting membrane potential, and the evoked MA currents can be categorised into three groups depending on their threshold of activation and their inactivation kinetics. They are low-threshold rapidly adapting (RA) currents (<20 ms), intermediately adapting (IA) currents (>20 <100 ms), and high-threshold slowly adapting (SA) currents (>100 ms) (Rugiero et al., 2010; Hao and Delmas, 2010). Pharmacological blockade of specific MA currents in sensory neurons has aided our understanding of the subsequent mechanical sensations they contribute to. For example, the pharmacological blockade of SA MA currents by noxious mechanosensation blocker 1 (NMB1) (which has ~30 fold selectivity for SA

over RA currents) *in vivo*, reduces the response of behaving mice to noxious mechanical stimuli, and *in vitro* binds selectively to nociceptive cells (Drew et al., 2007). Thus, SA currents are generally believed to be responsible for noxious mechanical sensation, and low-threshold RA currents are responsible for conveying innocuous mechanical sensation (Drew et al., 2004; Drew et al., 2002). Generic mechanotransducer blockers such as FM1-43 cause a reduction in responses to both light touch, and noxious mechanical stimuli when injected into the hind paw of mice (Drew & Wood, 2007). Examples of MA current recordings from DRG neurons using the mechano-clamp technique can be seen in Figure 1.12.C.



**Figure 1.12. The process of noxious mechanotransduction, and recording MA currents *in vitro***

**A.** The cell bodies of nociceptors are located in the DRG and their long axons project to the periphery where they terminate as free endings. Noxious mechanotransducers are expressed at the membrane of these sensory nerve endings and are responsible for producing MA currents when exposed to injurious force. The MA currents lower the membrane potential to the threshold required for the production of action potentials, which are then propagated down the length of the axon to the laminae of the dorsal horn in the spinal cord by voltage-gated ion channels. From there, these signals are transmitted to higher neurological structures. **B.** Mechano-clamp recording from a cultured cell. Mechano-clamp is a technique used to record MA currents *in vitro*; the cell is voltage-clamped and then prodded with a blunt glass probe at increasing increments and the subsequent MA currents recorded. **C.** Examples of MA currents recorded from the sensory neurons of rats held at a voltage of -60 mV, using the mechano-clamp technique. The traces include the stimulus protocol, which shows the distance the probe depressed the membrane of the cell to produce the corresponding RA, IA or SA currents. Visually, the SA current appears similar to the IA current, but as the scale bar demonstrates, this recording was taken over a much longer period of time. Time constants for the current decay of each trace are given (adapted from Delmas et al. (2011); Hao and Delmas (2010)).

### 1.4.2 Qualities of a *bona fide* mechanotransducer

While there has been some success in identifying mammalian mechanotransducers, as will be discussed, a *bona fide* mechanotransducer responsible for noxious mechanosensation has been harder to identify, as until very recently none have met all of the necessary qualifications. These are; i) the endogenous expression of the candidate in mechanically sensitive tissue, ii) an abolition of MA currents when the gene is deleted in these tissues. lii) When deleted from a model organism a mechanical phenotype should be observed in the behaving animal, iv) the candidate should also be able to confer mechanosensitivity when expressed in naive cells (Árnadóttir & Chalfie, 2010). Noxious mechanotransducer candidates to date are summarised in Table 1.1. Identifying *bona fide* mechanotransducers in invertebrates has proven much more successful than identifying mammalian mechanotransducers thus far.

### 1.4.3 Invertebrate mechanotransducers and their mammalian homologues

As the ability to perceive external mechanical cues is essential to survival, it is not surprising that this sensation is evolutionarily conserved between bacteria, archaea, and eukarya. Organisms as basic as the nematode, *Caenorhabditis elegans* (*C. elegans*), have the ability to distinguish between noxious and non-noxious temperatures, chemicals, pH, and touch. In fact, most mammalian mechanotransducer candidates have previously identified homologues in invertebrates, but few have met the *bona fide* status of their invertebrate counterparts. For example, the mammalian acid-sensing ion channels (ASICs) which belong to the proton-gated subgroup of degenerin-epithelial Na<sup>+</sup> channel (DEG/ENaC) family of cation channels, were initially implicated in mechanosensation as their *C. elegans* homologues, the MEC subunits are responsible touch perception. These include MEC-4 and MEC-10 which generate the pore-forming component of a mechanotransducer required for activity in gentle touch neurons (O'Hagan et al., 2005). Evolutionarily conserved DEG/ENaC genes in *Drosophila* include *Pickpocket* and *Balboa*, however, like MEC-4 and MEC-10, these genes are only capable of producing an MA current when expressed together in a heterologous system (Mauthner et al., 2014). Interestingly, a regulator of mechanotransduction, MEC-2, has a mammalian homologue known as STOML3 (stomatin-like protein 3), which is also responsible for the modulation of mechanosensory signalling, in this instance via the regulation of mammalian Piezo channels (Poole et al., 2014).

The mammalian ASICs 1-3 are expressed in peripheral LTMRs and HTMRs. ASIC KO studies in mice revealed that ASICs may play a role in interoceptive mechanosensation as ASIC2 KO mice exhibit a decreased gain of the baroreflex, and develop

hypertension as a consequence (Lu et al., 2009). The most investigated of the ASICs with respect to tactile mechanosensitivity has been ASIC3. Skin-nerve preparations from global ASIC3 KO mice show deficits in the responses of HTMRs to noxious mechanical stimuli (Price et al., 2001). However, animals transgenically expressing a dominant-negative form of ASIC3 display increased sensitivity to noxious mechanical stimuli (Mogil et al., 2005). Furthermore, expression of ASICs in heterologous cells does not produce MA currents, nor is there any alteration in the repertoire of MA currents produced by dissociated DRG neurons from ASIC2 or ASIC3 KO animals (Drew et al., 2004). Thus, ASICs are not *bona fide* mechanotransducers, but data supports a modulatory role for them in visceral and cutaneous mechanosensory functions.

Transient receptor potential (TRP) channels are another evolutionarily conserved family of ion channels, which can be classified into seven categories based on sequence similarity. They are TRPA, TRPC, TRPM, TRPML, TRPP, TRPN, and TRPV (Christensen & Corey, 2007), some of which are essential for mechanosensation in *Drosophila* and *C. elegans*. For example, the TRPN orthologue, NOMPC, in *Drosophila* is responsible for the sensation of light touch in larvae. NOMPC meets the requirements of a *bona fide* mechanotransducer as is able to confer mechanosensitivity to heterologous cells, and mutations in the putative pore have been demonstrated to alter ion selectivity (Yan et al., 2013). Similarly, the *C. elegans* TRPN orthologue, TRP-4, also has *bona fide* mechanotransducer status and is necessary and sufficient for light touch sensation (Kang et al., 2010). In addition, the TRPA orthologues, *Painless* in *Drosophila*, and TRPA-1 in *C. elegans* are responsible for mechanical nociception, and touch sensation respectively (Kindt et al., 2007; Tracey et al., 2003). Evidence for the role of the mammalian homologue TRPA1 in mechanosensation has been less compelling. Where studies have demonstrated that global TRPA1 KO animals have a reduction in SA MA currents in nociceptors and some deficits in tactile sensation (Kwan et al., 2006; Vilceanu & Stucky, 2010), others have shown that TRPA1 does not produce MA currents when expressed in a heterologous system, nor does its deletion affect mechanonociception in behaving animals exposed to a noxious pinprick stimulus (Vilceanu & Stucky, 2010; Zappia et al., 2017). Further evidence has suggested it may play a modulatory role in noxious mechanosensation as a consequence of inflammation (Lennertz et al., 2012). Other studies investigating the role of mammalian TRP channels in mechanosensation have identified the TRPC family's involvement, including TRPC1, TRPC3, TRPC5, and TRPC6. In the case of these candidates, their role in mechanosensation has been



disputed due to the functional redundancy observed in single, or even double TRPC KO mice, possibly due to the propensity of TRPC channels to form heteromeric complexes (Quick et al., 2012). To address this redundancy the same group found that a global quadruple TRPC KO resulted in a significant diminution of responses to innocuous punctate and dynamic touch (Sexton et al., 2016). When expressed in naïve cells (e.g. HEK293T) either individually or in combination, TRPC3 and TRPC6 do not produce MA currents. However, when expressed in a neuronal cell line, MA currents were produced with the expression of one channel and enhanced with the expression of both (Quick et al., 2012). Without the expression of all four aforementioned TRPC channels in naïve cells it is uncertain whether MA currents would be produced as a consequence. As these TRPC channels can confer mechanosensitivity to neuronal cells when expressed individually, it is likely that their functionality relies upon their ability to form mechanotransducer complexes via an interaction with auxiliary proteins, although it is still debateable that these are MA pore-forming complexes.

#### **1.4.4 Mammalian mechanotransducers**

Where the study of mammalian homologues of *bona fide* invertebrate mechanotransducers has been largely unsuccessful in identifying mammalian pore-forming MA ion channels, genomic screens in mechanosensitive mammalian cell lines have yielded some success, none greater than the Piezo story. The mechanotransducer, Piezo1, originally identified from a screen in the murine N2A neuronal cell line, led to the characterisation of the second member of the Piezo family, Piezo2. It is now widely accepted that the MA non-selective cation channel Piezo2 is responsible for mechanical sensation in mammals. Since its identification 10 years ago (Coste et al., 2010), a vast array of sensory neuron specific Piezo2 deletions in mice have identified a functional role for it in touch sensitive neurons, and also those responsible for proprioception. Animals with temporally-controlled Piezo2 deletion in all peripheral sensory neurons demonstrate significantly decreased responses to innocuous stimuli (Ranade et al., 2014), and those with constitutive Piezo2 deletion in proprioceptors have significantly diminished motor function and coordination (Woo et al., 2015). Alongside this, mechano-clamp recordings in the DRG neurons of Piezo2 KO mice demonstrate a significant reduction of RA MA currents, and Piezo2 is capable of conferring mechanosensitivity to naïve cells. A similar motor and tactile phenotype to those observed in Piezo2 KO mice is observed in humans with loss-of-function (LOF) Piezo2 mutations (Chesler et al., 2016). Furthermore, Advances have been made in recent years to fully elucidate the structure and gating mechanisms of mammalian Piezos, with greater success in Piezo1, which has key roles in vascular

development, baroreceptor reflex, and insulin sensitivity. Although it is undeniable that Piezo2 is essential to innocuous mechanosensing in rodents and humans, there has been much debate regarding its contribution to mechanonociception, as will be discussed at length in chapters to come.

Other recent mammalian candidate mechanotransducers (again identified via high-throughput genomic screens) have included TMEM150c (Tentonin 3), a molecule considered to be responsible for producing an SA MA current associated with proprioceptive function (Hong et al., 2016). Mice with Tentonin 3 deletion exhibit severe proprioceptive deficits and a concomitant reduction in the number of SA currents produced by dissociated DRG neurons. However, Tentonin 3 only sporadically produces SA MA currents when expressed in naïve HEK293T cells (Hong et al., 2016), which have since been proposed to express endogenous Piezo1 (Dubin et al., 2017). For this reason it has been suggested that rather than being a pore-forming ion channel itself, Tentonin 3 is responsible for modulating the currents produced by other mechanotransducers, as it is incapable of producing an MA current when expressed in Piezo 1 KO HEK293T cells (Dubin et al., 2017). Further evidence for a modulatory role for Tentonin 3 has been reported in Piezo1 KO HEK293T cells heterologously expressing known mammalian mechanotransducers such as the potassium-selective inhibitory channel, TREK-1, and Piezo2 (Anderson et al., 2018).

Evidence would suggest that the recently identified TMEM120a (TACAN) contributes to noxious mechanosensitivity. Beaulieu-Laroche et al. (2020) describe TACAN as a novel pore-forming mechanotransducer that produces an SA current when expressed in heterologous cells, and in lipid bilayers, in response to pressure applied to these systems in the cell-attached electrophysiology configuration. When TACAN was knocked-down using siRNA, cultured mouse DRG neurons displayed a decrease in the proportion of SA MA currents they produced when exposed to mechano-clamp electrophysiology, and a concomitant increase in the number of cells that did not respond to mechanical stimulation. Mice with a conditional TACAN deletion in Mrgprd+ neurons demonstrate a reduced sensitivity to suprathreshold von Frey stimuli. However, there is no observable phenotype with respect to the noxious pinprick assay in pan-neuronal TACAN knockdown or KO mice. The authors reconcile this finding by suggesting that TACAN is responsible for mediating C fibre mechanical 'slow' pain and that the noxious mechanotransducer responsible for the 'fast' pain mediated by A $\delta$  fibres remains unidentified (Beaulieu-Laroche et al., 2020). This is a nice example

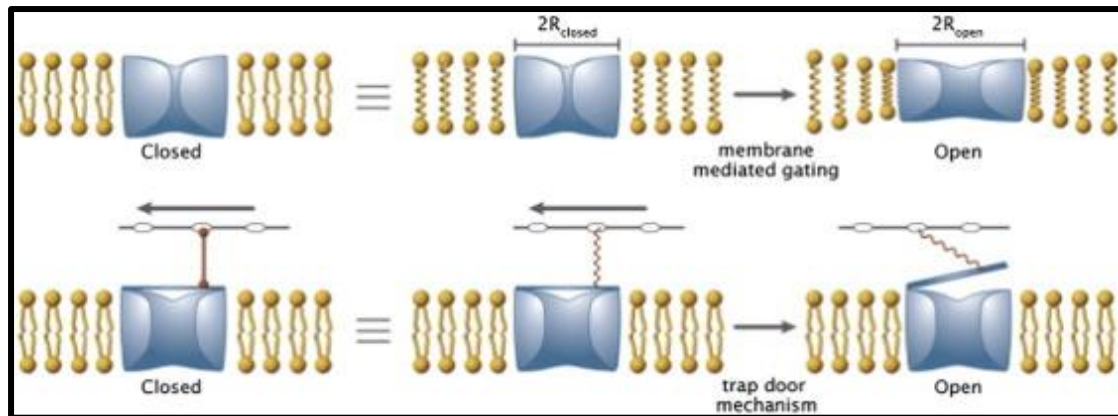
of how our improved understanding of the functional diversity of sensory neurons has allowed for the direct identification of transducers specific to those populations.

In addition to depolarising mechanotransducers, mechanically-sensitive hyperpolarising K<sup>+</sup> channels are also present throughout the PNS, aiding the modulation of mechanosensory signalling. Of the three classes of potassium channels it is the 'two pore domain' class of channels (K<sub>2</sub>P) that are inherently mechanosensitive, with TWIK-1 (Tandem of P domains in a Weak Inward rectifying K<sup>+</sup> channel) being one of the first identified mammalian mechanotransducers (Lesage et al., 1996). Three other K<sub>2</sub>P channels are also mechanically activated, these are TREK-1 (TWIK-1 related K<sup>+</sup> channel) (Fink et al., 1996), TREK-2 (Bang et al., 2000), and TRAAK (TWIK-related arachidonic acid-stimulated K<sup>+</sup> channel) (Fink et al., 1998). They are polymodal (i.e. they activate in response to multiple sensory modalities) and fine-tune the responses of peripheral sensory neurons to thermal and mechanical stimuli. TREK-1 is expressed in the CNS and PNS, in the latter it is predominantly restricted to small diameter sensory neurons, including those that are peptidergic and non-peptidergic, and extensively colocalises with heat-sensing TRPV1 (Alloui et al., 2006). TREK-1 KO mice have a significantly increased sensitivity to punctate mechanical force (von Frey) but not to noxious pinch (Randall-Selitto) applied to the hind paw. TREK-1 is also responsible for negatively regulating painful heat perception in mice. Confirmation of TREK-1's *bona fide* mechanotransducer status comes from its ability to produce MA currents in response to membrane stretch, osmotic swelling, and laminar shear stress, when expressed in a heterologous system (Patel et al., 1998). Similarly, TREK-2 and TRAAK are also capable of producing MA currents when expressed in naïve cells (Bang et al., 2000; Florian Lesage et al., 2000), and a mechanical hypersensitivity in response to von Frey stimulation of the hind paw is observed in mice with these channels deleted (Noël et al., 2009). Interestingly, this mechanical hypersensitivity in response to von Frey stimuli is not exacerbated in TREK-1, TREK-2, and TRAAK triple KO animals, excluding compensatory mechanisms in single KOs. Furthermore, TREK-1 and TREK-2 (but not TRAAK) are involved in osmotic pain hyperalgesia in the presence of inflammation (Pereira et al., 2014). With respect to heat sensing, TREK-2 is required for the discrimination of warm perception and aversive noxious heat by responding to temperatures between 40°C and 46°C, and TREK-1 and TRAAK respond to noxious temperatures between 46°C and 50°C (Pereira et al., 2014). As will shortly be discussed, the identification of mechanosensitive K<sub>2</sub>P channels has also aided our understanding of the gating mechanisms exhibited by mammalian mechanotransducers.

#### **1.4.5 Gating mechanisms of mechanotransducers**

There are two basic models of gating mechanisms for mechanically sensitive ion channels. These are the 'force-from-lipid' model, and the 'tethered' model (Figure 1.13). For the former, forces directly impinging upon the lipid bilayer are responsible for opening an MA channel, whereas the tethered model requires the recruitment of auxiliary structures such as the extracellular matrix, and/or intracellular cytoplasm in order for an MA channel to open (Kung, 2005). The force-from-lipid model was proposed as a consequence of our understanding of prokaryotic mechanotransducers. Cloning of the bacterial MscL and MscS channels and their functional reconstitution into lipid membranes demonstrated that they were capable of retaining mechanosensitivity in the absence of tethering and/or auxiliary units, thus making them inherently mechanosensitive (Kung, 2005). The reconstitution of candidates into liposomes has thus become the gold standard for documenting inherent mechanosensitivity in candidates (Martinac et al., 2010). It is now evident that eukaryotic mechanotransducers are also capable of conforming to this model of gating, where it was previously believed they relied upon auxiliary units due to the complexity of the extracellular and cytoplasmic networks. These include TREK-1 and TRAAK, as demonstrated by their retained mechanosensitivity when purified channels are expressed in proteoliposomes containing only channel and lipid (Berrier et al., 2013; Brohawn et al., 2014). Similar findings have recently been reported with Piezo1 (Cox et al., 2016; Syeda et al., 2016), but not with Piezo2.

Evidence for the tethered model comes not just from the inactivity of known mechanotransducers reconstituted into bilayers, but a recent investigation into NOMPC revealed the presence of N-terminal ankyrin repeats (ARs) which are required to tether the channel to microtubules, which in turn convey force to the channel. NOMPC channels with truncated ARs cannot function as force sensors (Zhang et al., 2015). With the continued advancement of single-particle cryogenic electron microscopy (cryo-EM) technology, there is opportunity to determine the structures of ion channels in various states within their native environment, which will undoubtedly yield important answers to gating questions (Autzen et al., 2019).



**Figure 1.13. The proposed gating mechanisms of mechanotransducers**

The top portion of the figure represents the ‘force-from-lipid’ gating mechanism and the bottom portion represents the tethered model (Soattin et al., 2016).

While Piezo channels are responsible for transducing innocuous mechanical stimuli, a mammalian noxious mechanotransducer has proven harder to identify. The candidates put forward are summarised in Table 1.1, and whether or not they meet the qualifications of a *bona fide* mechanotransducer. To date, TACAN is the only candidate to meet all qualifications, however, it only contributes to one component of noxious mechanosensation, i.e. ‘slow’ mechanical pain. As such, I attempt to investigate the role of Aquaporin1, a water and non-selective cation channel, in pain, that is specifically expressed in the  $\text{Na}_v1.8+$  population of sensory neurons known to be responsible for noxious mechanical sensation, including ‘fast’ mechanical pain.

Candidate	Produces MA currents in a heterologous system		MA currents altered in DRG/skin-nerve prep		Noxious mechanosensation altered <i>in vivo</i>		References
			Mode of Inhibition/activation	Phenotype	Mode of Inhibition/activation	Phenotype	
Piezo2	+	✓	<i>Advil</i> -CreERT <sup>2</sup> -mediated deletion	✓	<i>HoxB8</i> -Cre-mediated deletion	Decreased sensitivity to noxious mechanical pinprick and tail-clip assays	(Coste et al., 2010; Murthy et al., 2018; Ranade et al., 2014)
	-	-	-	-	<i>Advil</i> -Cre-mediated deletion	Increased sensitivity to noxious mechanical Randall-Selitto assay	(Zhang, et al., 2019)
TACAN (Tmem120a)	+	✓*	siRNA knock-down in DRG	✓	shRNA knock-down in sciatic nerve	Decreased sensitivity to high intensity von Frey stimulus	(Beaulieu-Laroche et al., 2020)
	-	-	-	-	shRNA knock-down in sciatic nerve	No difference observed with pinprick assay	(Beaulieu-Laroche et al., 2020)
ASIC3	+	-	Global KO	✓ (skin nerve prep)	-	-	(M. P. Price et al., 2001)
	-	X	Global KO	X (DRG neurons)	Transgenic expression of dominant-negative ASIC3	Increased sensitivity to von Frey and tail-clip assays	(Drew et al., 2004; Mogil et al., 2005)
TRPA1	+	-	Global KO/pharmacological inhibition	✓	Global KO	Decreased sensitivity to high intensity von Frey stimulus	(Kwan et al., 2006; Vilceanu & Stucky, 2010)
	-	X	-	-	<i>Advil</i> -Cre-mediated deletion	No difference observed with pinprick assay	(Vilceanu & Stucky, 2010; Zappia et al., 2017)
Piezo1	+	✓	<i>Advil</i> -Cre-mediated ectopic expression	✓	Agonist (Yoda1)-mediated activation	Increased sensitivity to von Frey assay	(Coste et al., 2010; Wang et al., 2019; Zhang et al., 2019)
	-	-	-	-	<i>Advil</i> -Cre-mediated ectopic expression	Increased sensitivity to von Frey and brush, and a decreased sensitivity to Randall-Selitto	(Zhang et al., 2019)

**Table 1.1. A summary of mammalian noxious mechanotransducer candidates according to the qualifications of a *bona fide* mechanotransducer**  
All candidates are expressed in mechanically-sensitive tissues. The '+' corresponds to a positive argument for the candidate's contribution to noxious mechanosensation, whereas the '-' denotes a negative finding. Only TACAN meets all requirements of a *bona fide* noxious mechanotransducer, however, as discussed in-text, it is not responsible for the noxious mechanosensitivity of A $\delta$  fibres.

### **1.5 Aquaporins and pain**

Aquaporins are homotetrameric water channels that facilitate the bi-directional transport of water in cells. Since the discovery and identification of the first aquaporin, Aquaporin1 (Aqp1), in erythrocytes (Preston & Agre, 1991), a further 13 have been identified in mammals (Aqp0 – Aqp13). These are expressed throughout the body, including the nervous system, with little overlap between homologues (Verkman, 2012). Their ubiquitous expression reflects their myriad of functions, ranging from urine concentration in the kidney (Ma et al., 1998), to regulating water permeability of lung vasculature (Bai et al., 1999), and maintaining intra-ocular fluid levels and pressure in the eye (Hamann et al., 1998). As such, dysregulation of these proteins has been associated with a number of pathologies in humans and rodents, often due to a tissue-specific imbalance of water homeostasis (King et al., 2004).

However, aquaporins are not just responsible for water transport across cell plasma membranes, there are those that also transport the small molecule glycerol (aiding adipocyte metabolism as one functional example) and are referred to as aquaglyceroporins. These include Aqp3, Aqp7, and Aqp9 (Verkman, 2012). Furthermore, there is evidence to show that Aqp1 can be permeated by cations (Boassa et al., 2006), Aqp6 by anions (Yasul et al., 1999), and Aqp7 and Aqp9 by urea (Litman et al., 2017). These differing permeability traits are dictated by structure. All aquaporins consist of four aquaporin monomers which are made up of six tilted transmembrane helices surrounding a central water and solute pore cavity which contains two helix-forming loops that enter and exit from the same side of the membrane. These two loops contain highly conserved asparagine-proline-alanine (NPA) motifs. These motifs are believed to enable water transport by providing hydrogen bonds to water molecules via the asparagine (N) residue, which lowers the energy required to remove a water molecule from bulk solution. For aquaglyceroporins, this residue is believed to do the same with glycerol thus also facilitating the transport of this small molecule. The less conserved regions of aquaporins are the N and C termini which vary in length; however, their structure has been difficult to determine using x-ray crystallography.

Of those that are expressed in the mammalian nervous system, Aqp1, Aqp4, and Aqp9 are present in the brain and the spinal cord (Papadopoulos & Verkman, 2013), and Aqp1, Aqp2, and Aqp4 in the PNS (Ma et al., 2011). Their expression has been reported in neurons and supporting cells, and for some, has been associated with the regulation of normal pain perception. These are summarised in Table 1.2. Of these

aquaporins, Aqp4 is the most abundantly expressed within the CNS and is found in the optic nerve, the SC and the brain. In these regions it is responsible for a variety of functions including water transport into and out of the brain, astrocyte migration, and neural signal transduction. Dysregulation of Aqp4 has been linked to various pathologies including the development of brain oedema in response to injury, altered seizure thresholds in epilepsy, and it also has a major role in neuroinflammatory diseases such as neuromyelitis optica (NMO). NMO occurs as a consequence of astrocyte damage mediated by Aqp4-specific antibodies, which ultimately negatively affects the myelin in the spinal cord and optic nerve (Verkman et al., 2017). Aqp4 expression is also found in the supporting cells of the PNS to a much lesser extent, the function of which has yet to be determined (Kato et al., 2014). Those that argue a role for Aqp4 in pain report that Aqp4 KO (Aqp4<sup>KO</sup>) mice have an increased threshold to noxious heat, and a reduced hypersensitivity to acute inflammation (Bao et al., 2010). Furthermore, Aqp4 expression in spinal astrocytes is upregulated as a consequence of spinal or peripheral neuropathy, which are both associated with chronic pain (Mulligan & MacVicar, 2006; Nestic et al., 2005; Oklinski et al., 2015). These studies predict that Aqp4 contributes to pain by regulating glutamate release from astrocytes, and the subsequent impact this has on neighbouring neuronal excitability. There is, however, conflicting evidence for a role of Aqp4 in pain. In the study by Kato et al. (2014), they demonstrate that Aqp4<sup>KO</sup> mice have no alteration in sensitivity to cold and mechanical stimuli in the presence or absence of peripheral neuropathic pain. It is clear that further investigation is needed in order to confirm a role for CNS and/or PNS Aqp4 in pain.

A possible role for Aqp2 and Aqp3 in pain is based upon their overexpression in response to various pain pathologies. Aqp2 expression is upregulated in small diameter sensory neurons (nociceptors) as a consequence of inflammatory and neuropathic pain, but a functional role has not been ascribed to it (Borsani et al., 2009; Buffoli et al., 2009). Aqp3's role in pain is more tenuous and does not rely upon its expression within the nervous system, instead, it is known to be overexpressed in the cartilage of osteoarthritis (OA) sufferers, a disease typically associated with localised mechanical pain, again with no prediction of a functional mechanism (Meng et al., 2007). Interestingly, Aqp3 expression is also found in the nucleus pulposus cells of the spinal cord which make up the gelatinous core of the shock-absorbing intervertebral disks. Dehydration of these can lead to disk degeneration and back pain (Richardson et al., 2008). With the use of specific antagonists, and/or knockouts/knockdowns, it



would be interesting to see if pain sensation is altered in any way with the inhibition of either Aqp2 or Aqp3.

Aqp1 expression in the CNS is predominantly restricted to the choroid plexus of the brain where it is responsible for CSF production, and regulates this via cation conductance within the central pore of its homotetrameric structure (Boassa et al., 2006). However, its contribution to pain sensation is believed to be due to its expression in the TG and DRG of the PNS, where it is restricted to small-diameter sensory neurons typically associated with nociception (Oshio et al., 2006). Aqp1's contribution to nociception will be discussed in detail in paragraphs to follow, but like Aqp4, Aqp1<sup>KO</sup> mice have proven to be exceptionally useful in establishing the role of Aqp1 in pain. For example, mice lacking Aqp1 demonstrate a deficit in sensing acute cold, heat, and inflammatory pain (Oshio et al., 2006; Zhang & Verkman, 2010). Others have demonstrated that an upregulation of Aqp1 is observed in both the PNS and CNS of rats as a consequence of spinal cord injury (SCI) which is also correlated with mechanical allodynia (Nesic et al., 2008). The contribution of Aqp1 to nociception is in part proposed to be due to the regulation of AP generation in nociceptors via a direct interaction with the voltage gated sodium channel, Na<sub>v</sub>1.8 (Zhang & Verkman, 2010). Although evidence for Aqp1's role in pain perception is the most extensive of any aquaporin to date, it is important to note that conflicting studies have also been reported. Despite Shields et al. (2007) further confirming the expression of Aqp1 in nociceptors, their pain behaviour investigations in Aqp1<sup>KO</sup> mice did not reveal any pain phenotype.

Thus far, the generation of aquaporin KO mice has been exceptionally insightful in determining a role for aquaporins in pain, although in every instance further investigation is needed to confirm and ascribe a functional role. As part of the studies herein I hope to do so with the use of the Aqp1<sup>KO</sup> mouse, to explore the contribution of Aqp1 to noxious mechanosensation.

Aquaporin	Expression pattern in the nervous system		Evidence for a role in nociception	Nociceptive mechanism
Aqp1	PNS	Small diameter neurons in the DRG (M), medium diameter neurons in the TG (R) and nodose ganglia (M) (Ma et al., 2011)	Aqp1 <sup>KO</sup> mice have a reduced sensitivity to heat and cooling under basal conditions, and a reduction in spontaneous pain and thermal hyperalgesia caused by acute inflammation. Melatonin-induced Aqp1 downregulation causes a reduction in mechanical allodynia after SCI (R) (Nesic et al., 2008; Oshio et al., 2006; Zhang & Verkman, 2010)	An Aqp1-Na <sub>v</sub> 1.8 interaction in nociceptors is responsible for regulating action potential firing. In Aqp1 <sup>KO</sup> animals Na <sub>v</sub> 1.8 channel inactivation is accelerated (Zhang & Verkman, 2010)
	CNS	Schwann cells of the enteric nervous system (H) (Gao et al., 2006) Ependymal cells of the ventricular choroid plexus (M) (Boassa et al., 2006) Astrocytes and ependymal cells in the SC (R) (Nesic et al., 2008)		
Aqp2	PNS	Neurons in the TG (M) (Borsani et al., 2009)	Elevated expression in small diameter TG neurons and Schwann cells after formalin injection (M) (Borsani et al., 2009)  <i>De novo</i> expression in small diameter DRG neurons after CCI surgery (R) (Buffoli et al., 2009)	Not known
	CNS	SC, subcortical white matter, hippocampus. Cell type not known (H) (Mobasheri et al., 2005)		
Aqp3	PNS	Not known	Elevated expression in osteoarthritic cartilage (R) (Meng et al., 2007)	Not known
	CNS	Not known		
Aqp4	PNS	Satellite glial cells in the DRG and TG (M) (Kato et al., 2014)	Not known  Aqp4 <sup>KO</sup> mice had increased thresholds to noxious heat (Hargreaves, hot plate, tail flick) and chemical (formalin) stimuli. Mechanical (von Frey) threshold was unchanged (Bao et al., 2010)  Elevated expression in spinal astrocytes after spinal cord injury and peripheral nerve injury (CCI and SNI) (R) (Mulligan & MacVicar, 2006; Nesic et al., 2005; Oklinski et al., 2015)	? Impaired extracellular K <sup>+</sup> buffering by astrocytes ? Concomitant downregulation of connexin 43 in astrocytes leading to their decreased glutamate release  ? Swelling-induced release of glutamate from astrocytes that can induce hyperexcitability in pain processing neurons as a consequence of Aqp4 upregulation
	CNS	Spinal astrocytes (M, R, H) (Nesic et al., 2010)		

**Table 1.2. The role of aquaporins in nociception**

Aquaporins 1, 2 and 4 are expressed throughout the peripheral and central nervous system in both neurons and supporting cells. Roles for them in both normal nociceptive processing and under pathological conditions have been described in rodents, and abnormal expression patterns have also been reported in humans with neuropathic pain. It should be noted, however, that to date, no human aquaporin mutation has been associated with altered nociception. This table does not include evidence against a role in pain for the aquaporins which are discussed in text. 'M' – mouse, 'R' – rat, 'H' – human.

### **1.6 The role of voltage gated sodium channels in nociception**

VGSCs are expressed throughout the PNS, in the terminals, axons, and somas of primary sensory neurons. They are permeable to sodium ions as a consequence of membrane depolarisation (i.e. in the presence of generator potentials) and are essential to AP electrogenesis and neurotransmitter release at the central terminals of these neurons. There are nine mammalian VGSCs,  $Na_v1.1-1.9$ , which consist of a large pore-forming alpha subunit, and smaller associated beta-subunits (Figure 1.14). The alpha subunit consists of approximately 2000 amino acids arranged into four domains (DI-DIV), with each domain consisting of six transmembrane segments (S1-S6). S1-S4 contain positively charged amino acids which are key to their role as a voltage sensor, and S5 and S6 form the sodium ion selective pore. These channels exist in three different states; open, closed, and inactive. When the membrane is depolarised, the voltage sensor of the channel moves outwards, opening the pore for a period of  $<1$  ms. The channel then enters its inactivated state mediated by a cytoplasmic inactivation 'gate' located between DIII and DIV. This gate has a conserved isoleucine, phenylalanine and methionine (IFM) motif, flanked by glycine and proline residues which act as hinges, allowing the IFM motif to swing over and cover the intracellular mouth of the pore. Broadly speaking, large diameter neurons (e.g. LTMRs) express the tetrodotoxin-sensitive (TTX-S) VGSCs  $Na_v1.1$ ,  $Na_v1.6$ , and  $Na_v1.7$  (Bennett et al., 2019) and a subset of these also express the tetrodotoxin-resistant (TTX-R) VGSC  $Na_v1.8$  (Shields et al., 2012). Small diameter neurons (nociceptors) however, express high levels of the TTX-R channels  $Na_v1.8$  and  $Na_v1.9$ , but also  $Na_v1.6$  and  $Na_v1.7$  (Black et al., 2008).

$Na_v1.7$  is encoded by the *SCN9A* gene and produces a TTX-S current that is fast activating and inactivating, but slow to recover from fast-inactivation. Its expression is largely localised to the PNS, but it is also found in olfactory sensory neurons (OSNs) which synapse to the mitral cells of the olfactory bulb (Firestein, 2001). Although expressed ubiquitously in peripheral sensory neurons, greatest  $Na_v1.7$  expression is found in nociceptors, with a role for  $Na_v1.7$  in nociception initially noted by the observation that  $Na_v1.7$  is upregulated in painful versus non-painful neuromas in humans (Kretschmer et al., 2002). Shortly after this, the first human gain-of-function (GOF) *SCN9A* mutation was reported in patients with erythromelalgia (Yang et al., 2004), a disease characterised by burning pain in the extremities (predominantly in the feet) which is exacerbated by warmth and relieved by cooling (Drenth et al., 2007). More GOF mutations associated with erythromelalgia have been described since and cause a hyperpolarising shift in the voltage dependence of activation of  $Na_v1.7$ , and

increased discharge in response to slow depolarisations. In the DRG this manifests itself as a lowered threshold for AP generation and a higher frequency of repetitive firing (Dib-Hajj et al., 2005). This discovery was closely followed by rodent Na<sub>v</sub>1.7 KO studies using the Cre-lox system to selectively ablate Na<sub>v</sub>1.7 from nociceptors by crossing Na<sub>v</sub>1.8-Cre mice to Na<sub>v</sub>1.7 floxed mice (Nassar et al., 2004). These progeny had a reduced sensitivity to noxious thermal (although no obvious insensitivity to the hot plate assay) and mechanical insults, as well as reduced nociceptive responses to inflammatory pain. This group also demonstrated that global Na<sub>v</sub>1.7 KO is neonatally lethal in mice as it causes anosmia, preventing pups from feeding. It was later demonstrated that Na<sub>v</sub>1.7 expression in OSNs is essential to presynaptic neurotransmitter release at the olfactory glomerulus, hence essential to the sense of smell (Weiss et al., 2011). Subsequent validation of the importance of Na<sub>v</sub>1.7's contribution to pain sensing in humans was confirmed with the discovery of consanguineous families suffering from congenital insensitivity/indifference to pain (CIP) due to LOF mutations in the *SCN9A* gene (Cox et al., 2006). These individuals are also anosmic, with all other sensory modalities intact (Goldberg et al., 2007). These studies highlight the protective function of pain, as CIP individuals suffer from self-mutilating oral and finger injuries due to biting from infancy, and will often develop secondary orthopaedic problems as adults due to unnoticed and untreated fractures (Goldberg et al., 2007).

Understandably, these findings have made Na<sub>v</sub>1.7 an appealing target for the development of novel analgesics. Current non-selective VGSC antagonists include lidocaine and carbamazepine, however, their activity against sodium channels present in the heart and the brain is dose limiting. Recent drug trials have included the development of Na<sub>v</sub>1.7 monoclonal antibodies, and small molecule inhibitors targeting less homologous regions of the Na<sub>v</sub>1.7 channel, with limited success (Bennett et al., 2019). This may be in part explained by the more recent observation that a lack of functioning Na<sub>v</sub>1.7 from birth synergistically upregulates the body's endogenous opioid system (Minett et al., 2015). Careful hand-rearing of pups enabled Gingras et al. (2014) to generate global Na<sub>v</sub>1.7 KO mice, fully recapitulating the CIP phenotype of patients (mutant mice reached maximum latency on the hot plate assay in this instance). However, this study also demonstrated that axonal transmission in nociceptors was not completely abolished in the absence of Na<sub>v</sub>1.7, indicative of an additional mechanism behind the fully pain insensitive phenotype. This mechanism was uncovered with the identification of an upregulation of *Penk* mRNA in whole DRG samples from Na<sub>v</sub>1.7<sup>Advil</sup> mice, which had undergone conditional sensory neuron

Na<sub>v</sub>1.7 deletion (Minett et al., 2015). Penk is the precursor of endogenous opioids Leu- and Met-enkephalin, leading to the hypothesis that CIP sufferers and Na<sub>v</sub>1.7 null mice do not feel pain as a combined consequence of Na<sub>v</sub>1.7 LOF and enkephalin-mediated analgesia. The same study went on to demonstrate a pain rescue effect in Na<sub>v</sub>1.7<sup>Advil</sup> mice treated with the opioid antagonist naloxone, and in a CIP individual which enabled them to essentially feel pain for the first time.

Unlike Na<sub>v</sub>1.7, the majority of our understanding of Na<sub>v</sub>1.8's contribution to pain comes from animal studies, rather than human mutations. Na<sub>v</sub>1.8 is encoded for by the *SCN10A* gene and its expression is restricted to the PNS, preferentially to nociceptors (Akopian et al., 1996; Sangameswaran et al., 1996). Na<sub>v</sub>1.8 produces a slow activating and inactivating TTX-R current, with an activation threshold that is significantly more depolarised than most VGSCs, including Na<sub>v</sub>1.7. This allows Na<sub>v</sub>1.8 to activate even when neurons are depolarised to a membrane potential that inactivates other VGSCs. Na<sub>v</sub>1.8 contributes most of the sodium current underlying the upstroke of the action potential in nociceptors, thus its modulation can significantly alter the excitability of neurons (Akopian et al., 1996). Na<sub>v</sub>1.8 null mice are viable and are demonstrated to have reduced sensitivity to noxious mechanical, heat, and inflammatory stimuli (Akopian et al., 1999), with concomitant upregulation of TTX-S currents in sensory neurons. This compensatory upregulation may provide an explanation as to why we do not see reduced sensitivity to chronic inflammatory and neuropathic insults in Na<sub>v</sub>1.8 null mice, versus rodents that have undergone Na<sub>v</sub>1.8-selective blockade (Jarvis et al., 2007).

A key feature of Na<sub>v</sub>1.8 is that, compared to other VGSCs, its inactivation kinetics are far less affected by cold. As such, Na<sub>v</sub>1.8 is essential to sensing sustained freezing temperatures, and noxious mechanical stimuli at freezing temperatures. This has been demonstrated both electrophysiologically and behaviourally in mice. Zimmermann et al. (2007) showed that cooling enhances the voltage-dependent slow inactivation of TTX-S VGSCs, but that the inactivation properties of Na<sub>v</sub>1.8 are cold-resistant. Cooling was also found to decrease the activation threshold of TTX-R currents. Na<sub>v</sub>1.8 null mice had negligible nocifensive responses to noxious cold in comparison to WT littermate controls. Similarly, mice that have undergone genetically-mediated Na<sub>v</sub>1.8 sensory neuron ablation (Na<sub>v</sub>1.8<sup>DTA</sup>) have significantly reduced sensitivity to freezing temperatures (Abrahamsen et al., 2008). These findings were recently elaborated upon with the combined use of *in vivo* GCaMP imaging of the DRG neurons of Na<sub>v</sub>1.8 null mice, and further behavioural assays in these animals (Luiz et al., 2019). This

study confirmed that Na<sub>v</sub>1.8+ sensory neurons were in fact only responsible for noxious cold sensing at prolonged freezing temperatures, and that responses to cooling >1°C were provided by a population of Na<sub>v</sub>1.8 negative sensory neurons. As such, the behavioural sensitivity of Na<sub>v</sub>1.8 null, and Na<sub>v</sub>1.8<sup>DTA</sup> mice to cooling temperatures above 1°C were either unchanged, or enhanced, respectively.

Although our knowledge of Na<sub>v</sub>1.8 human mutations is limited in comparison to Na<sub>v</sub>1.7, several reports have highlighted a role for Na<sub>v</sub>1.8 in painful inherited small fibre neuropathy (SFN). In these instances, GOF mutations in *SCN10A* cause hyperexcitability of nociceptors by either hyperpolarising Na<sub>v</sub>1.8 activation, accelerating its recovery from inactivation near resting membrane potential, or enhancing slow-ramp currents. This causes increased firing frequency of APs in response to suprathreshold stimuli in the nociceptor, and also triples the proportion of spontaneously firing neurons (Faber et al., 2012). More recently, a Na<sub>v</sub>1.8 SNP has been identified that confers reduced sensitivity to noxious mechanical stimuli in humans due to accelerated inactivation of Na<sub>v</sub>1.8 (Duan et al., 2016). These studies confirm a role for Na<sub>v</sub>1.8 in human nociception, making it an appealing target for novel analgesics. While therapeutics targeting Na<sub>v</sub>1.8 GOF mutations may prove beneficial to these patients, growing evidence supports a role for Na<sub>v</sub>1.8 in cardiac function, likely to hinder attempts to therapeutically target it in normal Na<sub>v</sub>1.8-expressing patients (Bennett et al., 2019).

Na<sub>v</sub>1.9 is encoded for by the *SCN11A* gene with expression predominantly restricted to small diameter DRG and TG sensory neurons. Na<sub>v</sub>1.9 produces a TTX-R current which activates at hyperpolarised voltages, and inactivates with 'ultra-slow' kinetics, resulting in a persistent sodium current after activation. As such, it is believed to act as a 'threshold' channel, in other words, it is responsible for the amplification of subthreshold stimuli in order to generate an AP (Bennett et al., 2019; Cummins et al., 1999). Evidence for a role for Na<sub>v</sub>1.9 in nociception has been established more recently than Na<sub>v</sub>1.7, and Na<sub>v</sub>1.8. The development of Na<sub>v</sub>1.9 null mutant mice revealed that Na<sub>v</sub>1.9 is required for normal responses to noxious mechanical and thermal stimuli, although only when presented as slow ramps as opposed to a step-like application (Minett et al., 2014). This was interpreted to reflect the slow kinetics of the channel. Additional murine studies have highlighted a role for Na<sub>v</sub>1.9 in pathological pain states, including inflammatory pain (Amaya et al., 2006), bone cancer pain (Qiu et al., 2012), and cold allodynia (Lolignier et al., 2015). Thus far it remains to be determined if Na<sub>v</sub>1.9 contributes to neuropathic pain (Bennett et al., 2019).

There are three known types of clinical manifestation with regard to  $\text{Na}_v1.9$  human mutations. These include painful SFN, Familial Episodic Pain Syndrome (FEPS) (Okuda et al., 2016), and a loss of pain (Leipold et al., 2013). All of these mutations are associated with autonomic comorbidities such as gastrointestinal dysfunction. Interestingly, GOF mutations in  $\text{Na}_v1.9$  are responsible for the loss of pain phenotype. These mutations cause an increase in the basal activity of  $\text{Nav}1.9$ , leading to excess sodium ion influx and subsequent cell depolarisation. This is likely to cause other pain-associated VGSCs such as  $\text{Na}_v1.7$  and  $\text{Na}_v1.8$  to undergo progressive inactivation, resulting in a conduction block, thus preventing transmission of pain signals (Leipold et al., 2013). This is in stark contrast to the LOF mutations in  $\text{Na}_v1.7$  responsible for CIP.

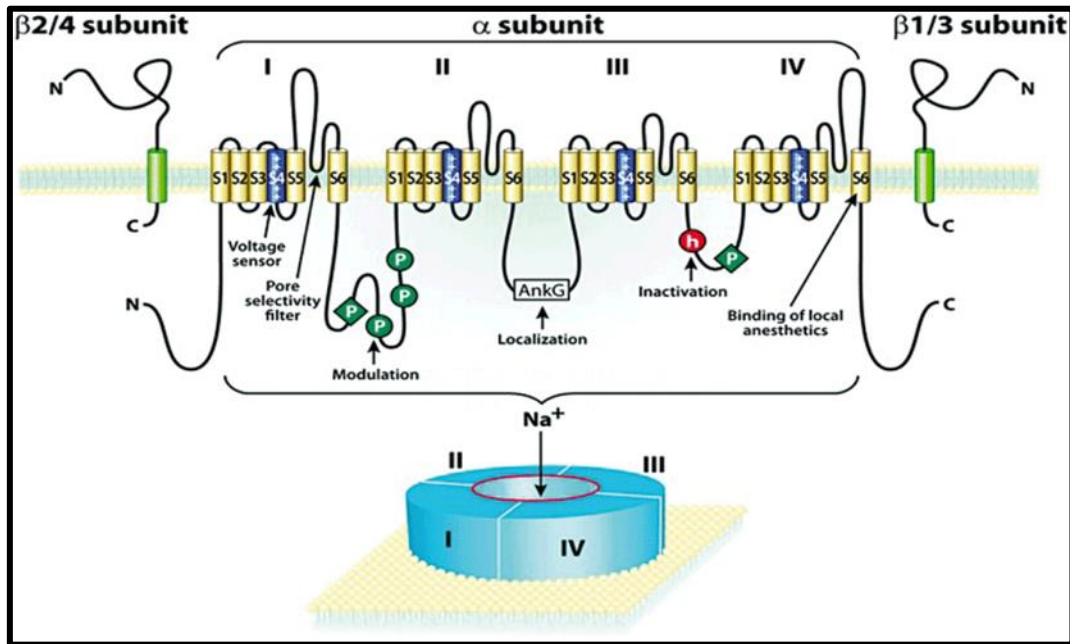
$\text{Na}_v1.3$  is encoded for by the *SCN3A* gene and produces a TTX-S current that is fast inactivating and rapidly repriming. It is expressed in the brain and the peripheral sensory neurons during development but is almost undetectable in these regions in the adult rodent, where  $\text{Na}_v1.3$  expression is instead restricted to sympathetic neurons (Rush et al., 2006). However, there is evidence for  $\text{Na}_v1.3$  re-expression in adult rat sensory neurons as a consequence of sensory neuron injury. Black et al. (1999) reported an accumulation of  $\text{Na}_v1.3$  in transected and ligated sciatic nerves both distal and proximal to the ligature. The group surmised that  $\text{Na}_v1.3$  is responsible for the rapidly repriming TTX-S current that is produced in small diameter neurons after axotomy, thus contributing to the abnormal hyperexcitability and ectopic firing observed in injured axons of sensory neurons that make up painful neuromas. This same observation has not been confirmed in humans.

$\text{Na}_v1.3$  KO mice studies have provided a somewhat contradictory insight into the contribution of  $\text{Na}_v1.3$  to neuropathic pain. As expected,  $\text{Na}_v1.3$  KO animals have normal responses to both acute noxious and inflammatory stimuli, but still develop mechanical allodynia after nerve injury (Nassar et al., 2006). Black et al. (1999) had previously demonstrated that the transection of DRG central projections does not increase  $\text{Na}_v1.3$  expression nor significantly alter the TTX-S current kinetics of small diameter neurons after this. This may explain why Nassar et al. (2006) reported no amelioration of neuropathic pain in their  $\text{Na}_v1.3$  KO animals as central projections of sensory neurons were targeted in their nerve injury model. Injection of  $\text{Na}_v1.3$  shRNA directly into L4 DRG of rats on the same day as SNI surgery (a model that targets peripheral projections), caused a significant recovery of mechanical sensitivity by day

10-20 in these animals in comparison to animals who had not undergone  $\text{Na}_v1.3$  shRNA knockdown (Samad et al., 2013). A similar observation was made in the streptozotocin (STZ) induced diabetic model of neuropathic pain, by injecting the same  $\text{Na}_v1.3$  shRNA construct, this time intrathecally, causing a significant reversal of mechanical allodynia at 3 weeks post injection in these animals (Tan et al., 2015). Levels of  $\text{Na}_v1.3$  expression had previously been demonstrated to increase in the DRG neurons of rats who have undergone STZ-induced models of diabetic neuropathic pain (Craner et al., 2002). There is also some evidence to suggest that  $\text{Na}_v1.3$  expression is upregulated in the spinal cord and in supraspinal structures as a consequence of both peripheral and central neuropathy. Overall, these findings suggest a possible role for  $\text{Na}_v1.3$  in the generation of neuropathic pain. However, unlike the VGSCs discussed above, there have been no reports of pain-associated  $\text{Na}_v1.3$  human mutations. A further caveat to  $\text{Na}_v1.3$ 's potential as a therapeutic target lies with its significant homology with other VGSCs including  $\text{Na}_v1.2$ , mutations of which have been associated with seizure disorders in humans (Theile & Cummins, 2011).

Within the context of this thesis, a particular area of interest with regard to the contribution of VGSCs to pain is  $\text{Na}_v1.8$ . This particular channel is a marker for neurons that are sensitive to noxious mechanical stimuli under normal conditions, as evidenced in the  $\text{Na}_v1.8+$  sensory neuron ablation study (Abrahamsen et al., 2008). As such, I target the  $\text{Na}_v1.8+$  population of sensory neurons as a means of identifying a candidate noxious mechanotransducer, and to investigate the role of a known innocuous mechanotransducer in mechanical pain.



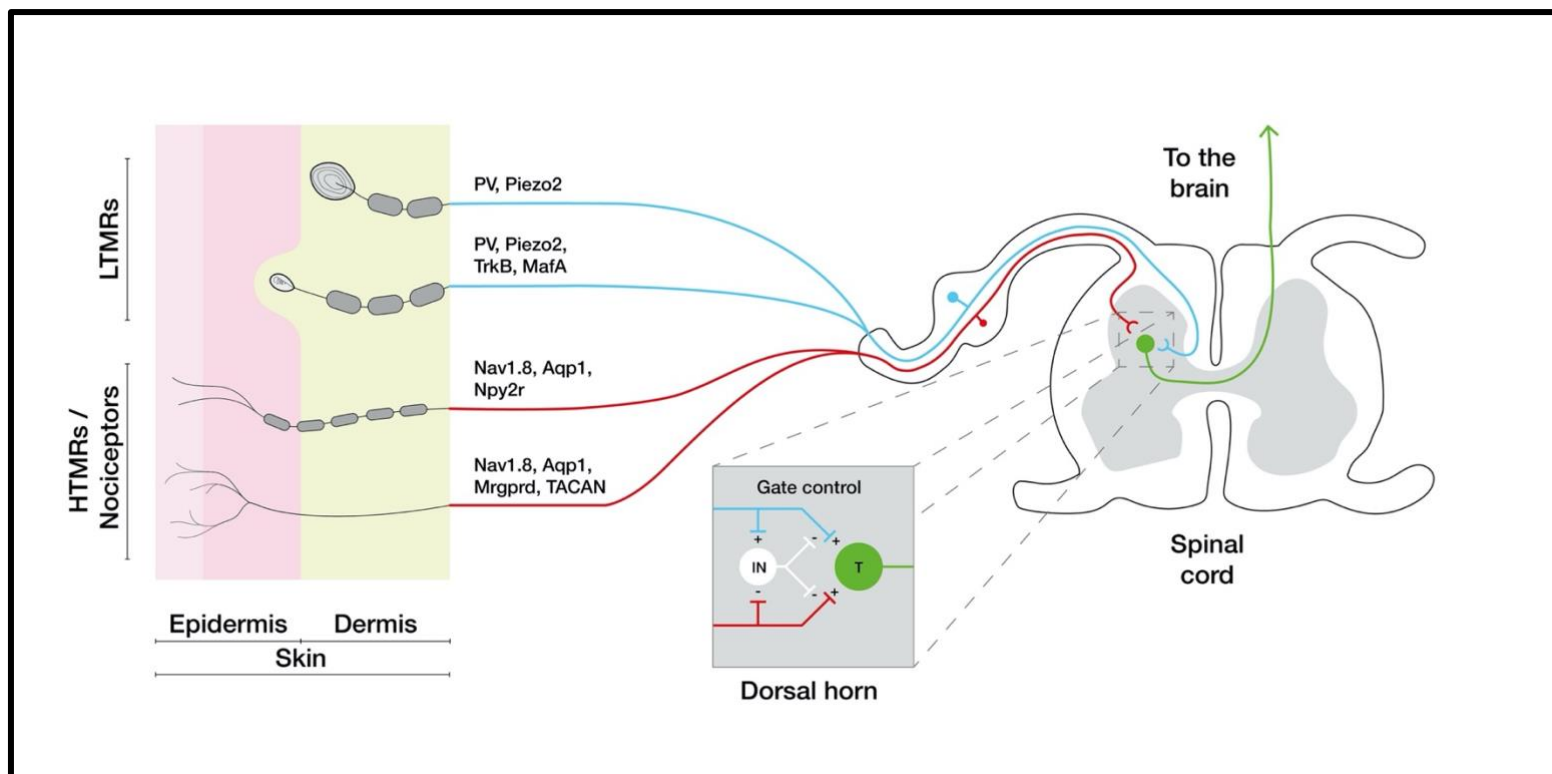


**Figure 1.14. The primary structure of the alpha and beta subunit of voltage gated sodium channels**

The alpha subunits of VGSCs are formed of domains I-IV (shown at bottom of figure), which are in turn each made up of six transmembrane helices (S1-6). S1-4 form the voltage sensor, and the linker connecting S5 and S6 creates the sodium selective pore. Residues in S6 of domains I, III, and IV are the binding sites for some local anaesthetics, e.g. lidocaine. P denotes areas of protein phosphorylation by PKA (circles) and PKC (pentagon), and h refers to the 'hinged lid' which incorporates the IFM inactivation motif (Benarroch, 2007).

**1.7 The proposed contribution of mechanosensitive peripheral sensory neuron subtypes to gating pain in the dorsal horn**

Figure 1.15 depicts the proposed contribution of specific mechanosensitive neuron subpopulations to the regulation of pain within the dorsal horn via gate control, in accordance with current literature. The contribution of Aqp1, Piezo2, and PV to mechanical pain sensing will be studied extensively within this thesis.



**Figure 1.15. The proposed contribution of peripheral sensory neuron subtypes to nociceptive gate control in the dorsal horn of the spinal cord**

Innocuous mechanical stimuli are detected in the glabrous skin by A $\beta$  fibre low threshold mechanoreceptors (LTMRs). The end organs of these include vibration-sensing Pacinian corpuscles, which express PV and the mechanotransducer Piezo2, as well as Meissner corpuscles which sense skin movement, subsets of which express the molecular markers TrkB and MafA. Noxious mechanical stimuli impinge upon the free nerve endings of lightly myelinated A $\delta$  fibres and non-myelinated C fibres, which are also referred to as high threshold mechanoreceptors (HTMRs). HTMRs include those that express Nav1.8 and Aqp1, a subset of A $\delta$  fibres that express Npy2r, and subsets of nonpeptidergic C fibres that express Mrgprd and TACAN. These mechanical signals are transmitted to the dorsal horn of the spinal cord where LTMRs indirectly negatively regulate nociceptive signalling by activating inhibitory 'IN' interneurons in the dorsal horn. These IN neurons provide inhibitory input to transmission 'T' neurons, which receive direct excitatory input from nociceptors and are responsible for transmitting the pain signal to higher structures of the CNS. Thus, LTMRs close the nociceptive gate, and strong nociceptive inputs are responsible for opening it.

### **1.8 Cre-lox DNA recombination**

Cre-lox genetic recombination is employed within this study to control the inactivation or expression of genes in targeted tissue. This system relies upon the 38 kDa enzyme, Cre recombinase, to catalyse DNA recombination between sites known as loxP sequences. The loxP sequence consists of 34 bp containing two 13 bp inverted repeats flanking an 8 bp core region where recombination takes place. Two loxP sites in the same orientation mediate the excision of the intervening DNA, leaving one loxP site remaining. Both the Cre enzyme and the loxP sequence are derived from bacteriophage P1 (Sauer & Henderson, 1988). As these sites are not native to the mouse genome, they have to be introduced by transgenic (ES cell) technology. Cre and loxP strains are typically developed separately and then crossed to generate a Cre-lox strain. Cre-dependent gene KO is achieved by placing loxP sites either side of a gene (floxing), or flanking exons within a gene, leading to permanent gene disruption. Unless Cre is present, expression of the gene will occur as normal, resulting in a normal phenotype. Cre-dependent gene expression occurs as a consequence of placing a stop codon flanked by loxP sites upstream of a gene of interest. The expression of the Cre enzyme can be controlled by a tissue specific promoter, and in certain instances can be controlled with the administration of chemicals. In this way, the Cre-lox strategy allows for the spatial and temporal control of genes (Sosa et al., 2010).

## 2 Methods

### 2.1 *Molecular Biology*

#### 2.1.1 Genotyping

##### 2.1.1.1 DNA extraction

Ear tissue samples were collected from mice and placed into 0.5 ml Eppendorf tubes with 30  $\mu$ l lysis buffer (Table 2.1 and 2.2) and 1  $\mu$ l of 19.7 mg/ml Proteinase K (Roche) in 499  $\mu$ l PCR lysis buffer. Samples were then incubated at 55°C for 1 h, then at 95°C for 5 minutes, to deactivate proteinase K. Samples were vortexed then spun down and stored at -20°C.

Reagent	Volume (ml)
10X GB (see table below)	22.35
25% TritonX-100	8.30
b-mercaptoethanol	3.35
H <sub>2</sub> O	16
Total Volume	50

**Table 2.1. Ear lysis buffer**

Reagent	Volume (ml)
1.5 M Tris pH8.8	4.47
1.0 M (NH <sub>4</sub> ) <sub>2</sub> SO <sub>4</sub>	1.66
1.0 M MgCl <sub>2</sub>	0.67
H <sub>2</sub> O	3.2
Total Volume	10

**Table 2.2. 10X GB**

##### 2.1.1.2 Polymerase chain reaction

To check for genes of interest, a PCR reaction was set up in 0.2 ml tubes containing ear DNA sample, appropriate primers, and PCR reagents according to Table 2.3. DreamTaq green PCR master mix (2X) (Thermo Scientific) contained DreamTaq DNA polymerase, 2X DreamTaq Green buffer, 0.4 mM of dATP, dCTP, dGTP and dTTP, and 4 mM MgCl<sub>2</sub>. Samples were gently vortexed and spun down prior to performing the PCR reaction. A typical PCR cycle is depicted in Table 2.4 and was adapted according to the requirements of each primer set.

Reagent	Volume ( $\mu$ l)
DreamTaq Master Mix	10
Forward Primer (10 $\mu$ M)	1
Reverse Primer (10 $\mu$ M)	1
DNA Template	1.5
Nuclease-Free Water	6.5

**Table 2.3. Typical PCR components per reaction**

Step	Temperature ( $^{\circ}$ C)	Duration	Cycles
Initial Denaturation	95	1-3 min	1
Denaturation	95	30 s	25-40
Annealing	Tm of primers -5	30 s	
Extension	72	1 min	
Final Extension	72	5-15 min	1
Hold	4	$\infty$	1

**Table 2.4. Typical PCR thermal cycling protocol**

### 2.1.1.3 Gel electrophoresis

Samples underwent gel electrophoresis to separate PCR products by size. To prepare a 1% agarose gel, a 0.5 g agarose pellet (Bioline) was added to 50 ml 1X TAE electrophoresis buffer (40mM Tris-acetate, 1mM EDTA, pH~8.5) and heated to a rolling boil. Once slightly cooled, ethidium bromide was added (0.5  $\mu$ g/ml), and the gel poured and set with the appropriate number of wells. 10  $\mu$ l of an appropriate weight molecular marker was run alongside samples in each gel. The samples were run at 120 volts for 30 minutes to separate bands (PowerPac, Bio-Rad), which were then visualised on an UPV BioDoc-It™ system.

## 2.1.2 Quantitative RT-PCR

*Pvalb* RNA expression study performed by Dr. Jane Sexton, WIBR, UCL

### 2.1.2.1 RNA extraction from DRG

Mice were culled in accordance with the Animals (Scientific Procedures) Act 1986. DRG were freshly harvested from adult mice and submerged in RNA/later™ (Invitrogen) solution for up to 48 h at 4°C before RNA isolation. RNA from the DRG of a single animal was extracted using 0.8 ml TRIzol® (Invitrogen) reagent and homogenized using a Minilys® homogenizer (Peqlab) for 3 x 10 seconds. RNA was purified with the RNeasy® MinElute® Cleanup Kit (QIAGEN), according to manufacturer's instructions. RNA concentration (ng/μl) was checked using a Nanodrop spectrophotometer (Thermo Scientific) and stored at -80°C.

### 2.1.2.2 cDNA synthesis

cDNA was synthesised from approximately 1 μg of isolated RNA, using the iScript™ reverse transcription supermix for RT-qPCR kit (Bio-Rad). The supermix contained reverse transcriptase, RNase inhibitor, dNTPs, random primers, buffer, MgCl<sub>2</sub> and stabilisers. The volumes of reagents used are summarised in Table 2.5. These were incubated in single steps of 25 °C for 5 min, 42 °C for 30 min, 85 °C for 5 min and 4 °C ∞. cDNA was stored at -20°C

Reagent	Volume μl
iScript RT Supermix	4
RNA Template	1 μg
Nuclease-Free Water	Variable
Total Volume	20

**Table 2.5. cDNA synthesis components per reaction**

### 2.1.2.3 qPCR analysis

To detect relative expression levels of genes in the DRG, qPCR reactions were set up using SYBR Green Supermix (Bio-Rad) according to Table 2.6. The target genes and primer pairs are listed in Table 2.7. All primers were designed using the NCBI Primer Blast Tool and purchased from Sigma. Each reaction (20 μl total volume) was plated in triplicate and read in a 96-well optical plate using the Bio-Rad CFX Connect™ Real-Time PCR Detection System (Bio-Rad). The thermal cycling conditions are summarised in Table 2.8. The  $2^{-\Delta\Delta C_t}$  method (Livak & Schmittgen, 2001) was used to analyse the threshold cycle (Ct) values obtained for each primer pair normalised to the values obtained from GAPDH primer pairs, to give a relative expression level.

Reagent	Volume (µl)
SYBR Green Supermix	10
Forward Primer (10 µM)	1
Reverse Primer (10 µM)	1
cDNA Template	1.5
Nuclease-Free Water	6.5

**Table 2.6. qPCR components per reaction**

Species	Gene	Target	Sequence (5'-3')
Mouse	<i>Aqp1</i>	Aqp1 – Forward	CTGGTCCAGGACAACGTGAA
		Aqp1 - Reverse	GCCAGTGTAGTCAATCGCCA
	<i>Fam38b</i>	Piezo2 - Forward	GCCTTGTACCAGGTGCACTA
		Piezo2 – Reverse	CACGCGACCATTGACTTTGG
	<i>Pvalb</i>	PV - Forward	CCCGCTCAAACAGTTGCAGG
		PV - Reverse	TCAGAATGGACCCCAGCTCAT
	<i>GAPDH</i>	GAPDH - Forward	TGCGACTTCAACAGCAACTC
		GAPDH - Reverse	CTTGCTCAGTGTCTTGCTG

**Table 2.7. qPCR primers**

Step	Temperature °C	Duration	Cycles
Initial Denaturation	95	3 min	1
Denaturation	95	30 s	40
Annealing	60	30 s	
Extension	72	30 s	
Melting Curve	-	-	1
Hold	4	∞	1

**Table 2.8. qPCR thermal cycling protocol**



## **2.2 Immunohistochemistry**

*DRG Immunohistochemistry performed by Dr. Jane Sexton, WIBR, UCL*

### **2.2.1 Tissue Collection**

Mice were terminally anaesthetised via intraperitoneal (i.p) sodium pentobarbital injection at a dose of 150 mg/kg to induce terminal anaesthesia. They were transcardially perfused with heparinised saline (0.1 M phosphate buffered saline (1X PBS) with 0.01 µl/1000 ml heparin) followed by 4% PFA in 1 X PBS for 5-10 minutes. Tissues were dissected and post-fixed in 4% PFA at 4°C for 2 h followed by 30% w/v sucrose in PBS at 4°C overnight before being mounted in OCT medium, snap-frozen on dry ice, then stored at -80°C

### **2.2.2 Sectioning**

Sections of 10 µm were cut using a Cryostat and mounted onto Ultrafrost slides (Thermo Scientific). Slides were then stored at -80°C

### **2.2.3 Immunostaining and analysis**

Slides were removed from -80°C and airdried for 30 minutes at 4°C then for 120 minutes at room temperature (RT). Slides were washed for 3 x 5 minutes in 1X PBS containing 0.3% Triton-X (PBST) before being blocked with blocking buffer (PBST with 10% goat serum) for 60 minutes at RT. Tissue was incubated with anti-Parvalbumin antibody (Abcam, ab11427) diluted in blocking buffer (1:700), at 4°C overnight. The next day slides were washed for 3 x 10 minutes in PBST and incubated with Alexa-fluor goat anti-rabbit secondary antibody (Invitrogen, A11008) diluted in blocking buffer (1:1000) for 2 hs at RT. A further 3 x 10 minute washes in PBST were performed to remove secondary antibody and the slides were then dried at RT. Slides were mounted with Vectashield® hardset mounting medium containing DAPI (Vector Laboratories). Images were taken on an upright Leica confocal microscope (SP8). LASX software (Leica) was used for cell counts.

### **2.3 In-situ hybridisation (RNAScope® technology)**

*Performed in collaboration with Dr. Andrei Okorokov, WIBR, UCL*

Tissue collection and sectioning was performed as described for immunohistochemistry experiments. For optimum signal, tissue was prepared for RNAScope® technology according to the manufacturer's 'Fresh frozen sample preparation and pre-treatment protocol'. As such, slides were removed from -80°C and post-fixed in 4% PFA at 4°C for 1 h. Slides were washed for 2 x 3 minutes in 1X PBS at RT, then dehydrated in ascending concentrations of EtOH (50, 70, 100%) for 5 minutes at a time. The 100% EtOH step was repeated. Slides were airdried, treated for 10 minutes at RT with RNAScope® Hydrogen Peroxide, then washed twice in 1X PBS for 3 minutes at RT. RNAScope® Protease IV was applied to the slides for 20 minutes at RT. Slides were again washed twice in 1X PBS for 3 minutes at RT. The RNAScope® assay was then performed according to manufacturer's instructions using the RNAScope® Multiplex Fluorescent Reagent Kit V2 kit (ACDBio, Cat. No. 323100). RNA targeting probes used were the channel 2 mm-Piezo1 probe (ACDBio, Cat. No. 500511), and the channel 1 mm-Piezo2Δ probe (targeting region 7487-7977) (ACDBio, Cat. No. 500501). TSA 405 (Akoya Biosciences, Cat. No. NEL703001KT) and Opal 520 (Perkin Elmer, Cat. No. NEL811001KT) dyes were used. Images were taken on an upright Zeiss LSM880 Airyscan microscope.

## **2.4 Behavioural assays**

### **2.4.1 Motor co-ordination tests in PV<sup>DTA</sup> mice**

*Performed by Dr. Jane Sexton, WIBR, UCL*

#### **2.4.1.1 Beam test**

Mice were placed at one end of a beam of ~1 cm<sup>2</sup> cross sectional surface area, which was above a box containing soft bedding. A white light, which was designed to deter the mice, was placed at the start of the beam walk, while food was placed at the end of the beam to attract them. After at least 3 training attempts, mice were filmed walking along the beam from one side to the other. WT mice are able to use their tail for balance and grip the beam without issue. Mice with motor and coordination deficits are typically unable to grasp or balance on the beam and can fall from it.

#### **2.4.1.2 Set speed rotarod**

The rotarod (IITC Life Science) apparatus was set such that WT mice were able to stay on the rod for the entire duration of the test. The rod rotated at 5 rpm for a period of 60 seconds. The latency of the animal to fall from the rod was recorded; if mice held onto the rod for 3 consecutive revolutions this also counted as a fall. The test was repeated 3 times per mouse and an average taken.

#### **2.4.1.3 Accelerating Rotarod**

Mice were trained on the apparatus (IITC Life Science) the day before the experiment whilst it ran at a constant speed of 4 rpm for a minimum of 5 minutes. On the day of the experiment mice were placed on the rod whilst it was running at a speed of 4 rpm. The max speed was then set to 40 rpm to accelerate over the course of 3 minutes. The latency of the animal to fall from the rod was recorded; if mice held onto the rod for 3 consecutive revolutions this also counted as a fall. The test was repeated 3 times per mouse and an average taken.

#### **2.4.1.4 Activity test**

Mice were placed in an open field enclosure and video recording software was used to assess activity and rearing of mice when in a novel environment for a period of 5 minutes. The total distance travelled as well as the number of rearings were monitored using automated software for this period.

#### **2.4.1.5 Grip force**

The automated Grip-Strength Meter (Ugo Basile) was used to assess the grip strength and duration of grip in mice. Mice were placed on a plastic grate with all four paws in contact with the grate. They were then gently pulled by the tail until they released the grate from their grip. The duration mice held onto the grate and the maximum force which was applied to the grate was recorded. The test was repeated 3 times per mouse and an average taken.

#### **2.4.1.6 Reaching score**

Each animal was held in the air by the tail, 5 cm away from a horizontal surface for 5 seconds. A wild type mouse should demonstrate a reaching movement towards the horizontal surface, whereas animals with proprioceptive deficits are inclined to curl towards the abdomen. A scoring system was used to quantify this; if the mouse reached its forelimbs towards the surface, it received a score of 1. If the mouse curled towards the abdomen, it received a score of 0. A partial curl received a score of 0.5.

### **2.4.2 Mechanical sensitivity tests**

#### **2.4.2.1 Cotton swab test**

The cotton swab test was used as a measure of innocuous dynamic sensitivity (Garrison et al., 2012). Mice were habituated in modular enclosures placed on a mesh platform for a minimum of 1 hr prior to testing. A cotton swab was “puffed out” so that the head was approximately 3 times the normal size. This was stroked across the plantar surface of the paw in a ~1 second sweep 5 times with a minimum of a minute between each stroke. A response was counted if either a withdrawal from the cotton swab was observed or a flutter or shake of the paw.

#### **2.4.2.2 Up-down von Frey**

Tactile punctate sensitivity was assessed using von Frey hairs (Bioseb) applied to the plantar surface of the paw using the up-down method for obtaining the 50% paw withdrawal threshold (Chaplan et al., 1994). Animals were habituated to von Frey chambers (modular enclosures placed on a mesh platform) for a minimum of 1 hr before the experiment. Von Frey filaments were then applied perpendicularly to the paw, until buckling, always beginning with the filament that provides 0.4 g of force. If a response (i.e. a lift, flick, or shake of the paw) was observed during or immediately after filament application, the next filament down (in this case 0.16 g) was applied in the following round of testing, and if there was no response, the next filament up (0.6 g) was applied and so on until a minimum of 6 recordings had been made.

#### **2.4.2.3 Percentage von Frey**

In this von Frey testing paradigm (Kim & Chung, 1992), the animals are acclimated as above, but paws were stimulated with the following filament forces (g); 0.07, 0.16, 0.4, 0.6, 1, 1.4, 2. Filaments were applied in that order for a total of 5 times each, and the subsequent response to each trial was recorded. This allowed me to then express the number of positive responses as a percentage of total trials for each filament.

#### **2.4.2.4 Dynamic plantar aesthesiometer (electronic von Frey)**

As another means of assessing mechanical threshold, a dynamic plantar aesthesiometer was used (Ugo Basile). In this instance a single unbending filament was applied to the hind paw with increasing force until the paw was withdrawn. A major benefit to using the electronic von Frey apparatus over manual von Frey filaments is that this method produces less variability between datasets. It should be noted that the electronic von Frey assay produces paw withdrawal thresholds that are much higher than with manual von filaments, a typical threshold for C57BL/6 mice being ~5-6 g (Deuis et al., 2017).

Mice were habituated in modular enclosures placed on a mesh platform for a minimum of 1 hr prior to testing. The touch stimulator unit was positioned under the target area of the paw and the protocol initiated. This drove a movable force actuator (a metal 0.5 mm filament) set to apply a maximum weight of 10 g over a period of 20 s (ramp speed 0.5 g/s) (Emery et al., 2011). The force at which the animal withdrew its paw from the stimulus was automatically recorded by the machine. This was repeated on each hind paw 3 times and an average taken (Deuis & Vetter, 2016).

#### **2.4.2.5 Randall-Selitto (tail and hind paw)**

Noxious mechanical sensitivity was assessed using the Randall-Selitto assay (Randall & Selitto, 1957). In this test a blunt force is applied to either the tail or the paw until a nocifensive response is evoked. In this instance a bench-top, as opposed to a hand-held device, was used (Ugo Basile). For those receiving tail testing, mice were restrained in a clear plastic tube and acclimatised for 5 minutes. A blunt force was then applied to the tail with increasing pressure until a pain response was evoked (Minett et al., 2014). For those undergoing hind paw testing, mice were gently held by the scruff and habituated to the equipment the day before testing. On the day of the experiment, mice were gently scruffed and a blunt force was then applied to the paw with increasing pressure until a pain response was evoked. For both assays, a pain response was considered to be either a vocalisation, or an escape reaction. The experiment was then stopped, and the force recorded. This was repeated on each animal 3 times and an average taken.

### **2.4.3 Thermal sensitivity tests**

#### **2.4.3.1 Hargreaves**

The Hargreaves test was used to assess spinal reflex responses to noxious thermal stimulation (Hargreaves et al., 1988). Mice were habituated on a glass base in perspex modular enclosures for a minimum of 1 hr prior to testing. A radiant heat source was then placed under the plantar surface of the paw with a cut-off time of 30 s to prevent tissue damage. Stimulation was stopped at the point at which a nocifensive response was seen (withdrawal, shaking, licking of the paw) and the time was recorded. This was repeated on each animal 3 times and an average taken.

#### **2.4.3.2 Hot plate**

Unlike the Hargreaves assay, the hot plate assay is a means of assessing heat sensitivity believed to be reliant on supraspinal processing (Giglio et al., 2006; Woolfe & Macdonald, 1944). A hot/cold plate (Ugo Basile) was used for this experiment. Mice were habituated to the apparatus at room temperature for 2 minutes the day before testing. On the day of testing, a mirror was placed behind the plate in order to observe the animal from all angles, and the plate was heated and held at  $50 \pm 0.2^{\circ}\text{C}$ . The mouse was placed on the plate and the timer started. The time at which the mouse exhibited a nocifensive behaviour (hind paw licking, shaking, and jumping etc.) was recorded and the mouse immediately removed from the plate. This was repeated at  $55 \pm 0.2^{\circ}\text{C}$  on the following day.

#### **2.4.3.3 Thermal place preference**

In this instance, the thermal place preference test was used to assess noxious cold sensitivity. Two adjacent plates (a test plate and a second plate) were both held at  $20^{\circ}\text{C}$ . Mice were then placed on the plates and allowed to explore for 120 seconds for habituation purposes. The temperature of the test plate was then set to  $25^{\circ}\text{C}$  and the mice allowed to explore for a further 120 seconds (to accommodate for any anomalies observed in the following assay) and the time spent on the test plate recorded. The test plate was then set to  $4^{\circ}\text{C}$  and the assay repeated. In all instances, the mice were placed on the test plate at the beginning of the experiment to ensure that they were exposed to the set temperature. In each instance the test plate and the second plate were switched to ensure that environmental factors did not bias the amount of time the mice spent on the test plate.

#### **2.4.3.4 Dry ice**

As first described by Brenner et al. (2012), the dry ice assay was used to assess sensitivity to cooling of the hind paw. Mice were habituated on a glass base (6 mm thickness) in perspex modular enclosures for a minimum of 1 hr prior to testing. A pellet of compacted dry ice power

was applied to the glass underneath the hind paw, which provides a ramping cooling stimulus, with temperature ranges between 5–12°C (Brenner et al., 2012). The latency of the mouse to withdraw their hind paw from the stimulus was measured. This was repeated on each animal 3 times and an average taken.

#### **2.4.3.5 Acetone**

As an additional means of assessing sensitivity to cooling I used the acetone assay (Carlton et al., 1994; Colburn et al., 2007). This elicits a cooling of the skin to innocuous temperatures of 15-21°C (Colburn et al., 2007; Leith et al., 2010). Mice were habituated in modular enclosures placed on a mesh platform for a minimum of 1 hr prior to testing. Using a modified syringe, a drop of acetone was applied to the plantar surface of the hind paw. A stop-watch timer was used to record the amount of time animals spent shaking and licking their paw within a 60 s timeframe, directly after acetone application.

### **2.4.4 Inflammatory pain models**

#### **2.4.4.1 CFA administration and behavioural testing**

Administration of Complete Freund's adjuvant (CFA) is a model of chronic inflammation, resulting in thermal and mechanical hypersensitivity in the region of administration, lasting for up to two weeks in rodents (Larson et al., 1986). It is a water-in-oil emulsion containing killed *Mycobacterium*. Two baseline recordings of mechanical and thermal sensitivity were made using the up-down von Frey and Hargreaves methods, respectively, prior to CFA administration. Each animal then received a single subcutaneous injection of 20 µl of 100% CFA (Thermo Scientific) into the ventral aspect of the ipsilateral hind paw. Animals were returned to their home cage and subsequent up-down von Frey and Hargreaves testing was performed for up to 14 days after injection to measure subsequent hypersensitivity.

#### **2.4.4.2 PGE<sub>2</sub> administration and behavioural testing**

Administration of prostaglandin E<sub>2</sub> (PGE<sub>2</sub>) is a model of acute inflammation, resulting in thermal and mechanical hypersensitivity in the region of administration (Domenichiello et al., 2017; Kuhn & Willis, 1973). Mice were habituated in transparent modular enclosures placed on a mesh platform for a minimum of 1 hr. A baseline recording of mechanical sensitivity was then performed on both ipsi- and contralateral hind paws, using the dynamic plantar aesthesiometer equipment prior to PGE<sub>2</sub> administration. Each mouse then received a single subcutaneous injection of 20 µl of 500 µM PGE<sub>2</sub> (Sigma) into the ventral aspect of the ipsilateral hind paw. Mice were placed immediately back into their modular enclosures and their activity recorded for 20 minutes. After 20 minutes I performed another round of the electronic von Frey assay on both hind paws, and repeated this again at 60 minutes, to

measure mechanical hypersensitivity. Activity recordings were analysed after the assay for incidences of paw lifts as an indicator of non-stimulus evoked nocifensive responses.



## 2.5 GCaMP Imaging

### 2.5.1 *In vivo* GCaMP imaging

Mice either expressing GCaMP3 (PV<sup>DTA</sup>;GCaMP3) or GCaMP6 (PV<sup>tdTom</sup>;GCaMP6s) were used for *in vivo* studies. They were anaesthetised using ketamine (120 mg/kg) and medetomidine (1.2 mg/kg) and placed on a heated mat (VetTech) to maintain body temperature. Ocular lubricant was applied to the eyes to prevent drying. Once the paw-pinch reflex was no longer observed the back was shaved, the overlying skin and muscle gently removed, and a dorsal laminectomy performed to expose the DRG at spinal level L4, all the while perfusing the area with artificial cerebrospinal fluid (aCSF) containing (in mM): 120 NaCl, 3 KCl, 1.1 CaCl<sub>2</sub>, 10 glucose, 0.6 NaH<sub>2</sub>PO<sub>4</sub>, 0.8 MgSO<sub>4</sub>, 18 NaHCO<sub>3</sub> (adjusted to pH 7.4 with NaOH). Once the DRG was exposed, the mouse was clamped in position at the vertebral column rostral to the laminectomy using custom made clamps, under an upright Leica confocal microscope (SP8). The ipsilateral hind paw was secured to allow for application of stimuli. GCaMP was excited using a laser wavelength of 488 nm. All images were acquired using a dry 10x objective. The following stimulation protocol was used:

Time	Stimulus	Duration
00:30	Cotton Swab	10 s
01:00	Brush	
01:30	Vibrate (128 Hz)	
02:00	von Frey 1.0 g	10 Applications
02:30	von Frey 2.0 g	
03:00	Prod 100 g/cm <sup>2</sup>	10 s
03:30	Prod 150 g/cm <sup>2</sup>	
04:00	Pinch	
04:30	55 °C Water	10 s
05:00	0 °C Water	
Intraplantar injection of 20 µl 500 µM PGE <sub>2</sub> , wait 5 minutes then repeat protocol		

**Table 2.9. *In vivo* GCaMP imaging stimulation protocol**

The Stimulation protocol began with the most innocuous stimuli and gradually increased in intensity, ending in the most noxious in order to limit sensitisation throughout the duration of the protocol (the gradual increase in intensity is depicted as the transition from green to red). The protocol was designed to encompass as many mechanical modalities as possible, including dynamic stimuli such as cotton swab and bush, which were swept over the hind paw for a duration of 10 s. Unlike the other stimuli that maintained contact with the skin for 10 s, von Frey filaments were applied to the hind paw 10 times in 10 different regions to ensure as much of the paw was stimulated as possible, thus increasing the chance of visualising activated neurons at the DRG. Pinch (using curved forceps to avoid tissue damage), and 55°C and 0 °C water were considered noxious.

### 2.5.2 Analysis

All *in vivo* and *in vitro* data was acquired using LASX software (Leica). Videos were converted into TIFF format and analysed using ImageJ software. The TIFF videos were first stabilised using the Turboreg ImageJ plugin, and ROIs were manually drawn within the cytoplasm of identified neurons. Raw data was extracted in the form of averaged pixels per ROI per frame and analysed in Microsoft Excel. To determine whether a neuron was responsive to a given stimulus, the raw traces were first smoothed by averaging the preceding four frames of any test frame to reduce noise. Then the derivative of each frame was taken as  $\Delta F/\Delta t$  (change from one frame to the next), where F is fluorescence and t is time. A neuron was included as a responder to a given stimulus if the following was true:  $\Delta F_{stim}/\Delta t > [(\Delta F_{basal}/\Delta t) + 4s_{basal}]$ , where  $F_{stim}$  is the maximum derivative value within a given stimulus application window.  $F_{basal}$  is the average derivative baseline value (average of four frames preceding stimulus), and  $s_{basal}$  is the SD of the baseline derivative values. Peak fluorescence of a given neuron was determined by calculating  $\Delta F/F_0$  in smoothed traces, where  $\Delta F/F_0 = (F_t - F_0)/F_0$ .  $F_t$  is the fluorescence at time t, and  $F_0$  the minimum fluorescence over the entire baseline and stimulation period.

## **2.6 *In vivo* electrophysiology of the dorsal horn**

*Performed in collaboration with Dr. Shafaq Sikandar, WHRI, QMUL*

### **2.6.1 Electrophysiology recordings**

Mice were anaesthetised with 4 % isoflurane delivered in a gaseous mix of 0.5 l/min N<sub>2</sub>O and 1.5 l/min O<sub>2</sub>; they were then secured in a stereotaxic frame and maintained under anaesthesia with 1.5 %-1.7 % isoflurane for the duration of the experiment. A laminectomy was performed to expose the L3-5 region of the spinal cord. WDR neurons in the deep dorsal horn (lamina III-V at ~200 – 600 µm depth) were selected for recording using a parylene-coated tungsten electrode (A-M Systems Inc.). Neuronal activity was visualised using an oscilloscope. The sampling rate was 20000 Hz, and data was analysed on a spike amplitude and waveform basis using a CED 1401 interface coupled to Spike2 software (Cambridge Electronic Design Ltd., Cambridge, UK). Once an appropriate neuron was isolated a 5 minute recording was taken prior to stimulation to record baseline spontaneous activity. To assess evoked activity the same stimuli used for the *in vivo* imaging experiments were applied to the ipsilateral glabrous skin of the hind paw (Table 2.9). This stimulation protocol also included 8 g and 26 g von Frey filaments. Ethyl chloride was applied for a duration of 1 second as a further measure of noxious cooling, and the evoked activity measured over a duration of 10 s. This particular cooling assay cools skin to noxious temperatures of 5°C or below (Leith et al., 2010). Spontaneous activity to ethyl chloride was also recorded for a duration of 60 s after the initial 10 s recording. Unless otherwise stated, all other stimuli were applied to the hind paw for a duration of 10 s. Once this protocol was completed, the animals were injected in the same hind paw with 20 µl of 500 mM PGE<sub>2</sub>, and another 5 minute recording was made to assess the extent of non-stimulus evoked activity. The stimulation protocol was then repeated.

### **2.6.2 Analysis**

When analysing the data, neurons were discarded if they did not produce a minimum of 100 spikes to a brush stimulus, a minimum of 50 spikes for an 8 g von Frey stimulus, and a response to noxious heat. A response to noxious cold was not deemed essential to this experiment. To count as a response, a minimum of 10% change from baseline was required.

## **2.7 Patch clamp electrophysiology**

### **2.7.1 DRG neuron isolation and culture**

Immediately after CO<sub>2</sub> euthanasia, DRG were removed from 8-16 week old mice and digested for 45 min at 37°C in Ca<sup>2+</sup>- and Mg<sup>2+</sup>-free Hanks' balanced salt solution (HBSS) containing 5 mM 4-(2-hydroxyethyl)-1-piperazineethanesulfonic acid (HEPES), 10 mM glucose, 5 mg/ml collagenase and 10 mg/ml dispase. DRG were then triturated in Dulbecco's modified Eagle's medium (DMEM) containing 10% foetal bovine serum (FBS) using fire-polished glass pipettes. Cells were plated on poly-L-lysine and laminin coated 35 mm dishes in DMEM containing 10% FBS and 125 ng/ml nerve growth factor (NGF). Neurons were kept at 37°C in 5% CO<sub>2</sub> and used for patch clamp studies 24-72 hours after culturing.

### **2.7.2 Cell culture and transfection**

HEK293T and ND-C cells were cultured in DMEM containing 4.5 mg.ml<sup>-1</sup> glucose and 10% FBS on 35 mm dishes and kept at 37°C in 5% CO<sub>2</sub>. Both cell lines were passaged twice a week. For transfection, cells were plated onto 35 mm dishes and transiently transfected with the appropriate constructs using lipofectamine 2000 reagent (Invitrogen), over 4-8 h. Approximately 1 µg of each construct and 10 µl of lipofectamine was used per transfection. Constructs used were: *Aqp1-IRES-tdTomato*, *Piezo2-IRES-GFP*, and *IRES-tdTomato*, generated by Dr Stephane Lollignier, Dr James Cox, and Dr Yury Bogdanov, of the Molecular Nociception Group, respectively. Patch clamp experiments were carried out 24–72 hours post transfection

### **2.7.3 Electrophysiology recordings**

DRG neurons whose cell bodies were not in contact with those of other neurons, and HEK and ND-C cells expressing fluorescent proteins were selected for recording. Patch-clamp recordings were performed in the whole-cell configuration with the cells held at a voltage approximately equivalent to their resting membrane potential, which was -50 mV for HEK293T cells, -60 mV for ND-C cells, and -70 mV for DRG neurons. For an approximation of the resting membrane potential of each cell type, voltage clamp mode was briefly switched to current clamp ( $I = 0$ ) as soon as the whole-cell configuration was achieved. Experiments were carried out at room temperature, with cells bathed in a standard extracellular solution, containing (in mM): 140 NaCl, 4 KCl, 1.8 CaCl<sub>2</sub>, 1 MgCl<sub>2</sub>, 10 HEPES and 5 glucose (adjusted to pH 7.4 using NaOH).

Patch pipettes were pulled from borosilicate glass capillaries using a PC-10 puller (Narishige) and fire-polished to a resistance of 2.0 – 4.5 MΩ. The intracellular solution contained (in mM): 140 KCl, 1.6 MgCl<sub>2</sub>, 2.5 MgATP, 0.5 NaGTP, 2 EGTA, 10 HEPES (adjusted to pH 7.3 with

KOH). Capacitive transients were cancelled and series resistances were not compensated. Recordings were low-pass filtered at 5 kHz and sampled at 20 kHz. Electrophysiological data was acquired using an AxoPatch 200B amplifier (Molecular Devices) and digitised using a 1440 Digidata (Molecular Devices). Data was recorded using Clampfit 10.6 software (Molecular Devices).

#### **2.7.4 Mechanical Stimulation and analysis**

Mechanical stimulation of cell bodies was achieved using a heat-polished glass pipette (tip diameter of approximately 2  $\mu\text{m}$ ) controlled by a piezo-electric crystal drive (Burleigh LSS-3000) and placed at an angle of 70° to the surface of the dish. The probe was positioned so that a 10  $\mu\text{m}$  movement did not visibly contact the cell but that an 11  $\mu\text{m}$  movement (a 1  $\mu\text{m}$  displacement stimulus) produced an observable membrane deflection. The probe was moved at a speed of 1  $\mu\text{m}/\text{ms}$ . 250 ms mechanical steps were applied every 10 s in 1  $\mu\text{m}$  increments.

Current types were classified according to their adaptation kinetics using the following criteria; rapidly adapting currents showed >80% decay over the course of the 250 ms stimulation, slowly adapting currents showed <20% decay and intermediately adapting currents showed >20%, <80% decay (Raouf et al., 2018). Currents were also classified according to exponential fit and tau decay values; RA currents were best described by a bi-exponential fit, IA and SA currents were best described by a mono-exponential fit (Eijkelkamp et al., 2013). Cells which did not produce a current of at least 20 pA were considered mechanically insensitive. Analysis and fits were performed using Clampfit 10.6 (Molecular Devices), with the Chebyshev fitting method.

## **2.8 Statistical analysis**

Statistical analysis was performed where appropriate using a combination of GraphPad Prism 7 and 8 Software. The mean  $\pm$  SEM was calculated for all data where applicable. To compare groups Student's unpaired t tests, Student's paired t tests, regular two-way ANOVA with Tukey's multiple comparison test, and regular one-way ANOVA with Dunnet's multiple comparison test, were performed. Mann-Whitney test was used for comparisons within discrete datasets. Data are presented as Mean  $\pm$  SEM. \* $p < 0.05$ ; \*\* $p < 0.01$ ; \*\*\* $p < 0.001$ ; \*\*\*\* $p < 0.0001$ .

### **3 The role of Aqp1 in the generation of mechanically activated currents and mechanical pain**

#### **3.1 Summary**

The search for the mechanotransducer responsible for the perception of mechanical pain has, until recently, proven relatively unsuccessful. The recent identification and characterisation of TACAN has implicated this protein in the transduction of the 'slow' mechanical pain transmitted by a population non-peptidergic C fibres. However, the mechanotransducer responsible for transducing 'fast' mechanical pain associated with A $\delta$  fibres has yet to be identified. As such, we studied a list of novel candidates generated as a consequence of the ablation of the Nav1.8+ population of sensory neurons that are known to be essential for noxious mechanosensation. Identified mRNAs that were significantly downregulated included the water channel Aqp1, which is also known to function as a non-selective cation channel in the CNS and has been previously implicated in pain. Using the gold-standard approach to assessing the validity of mechanotransducer candidates I heterologously expressed Aqp1 in HEK293T cells and performed mechano-clamp electrophysiology to determine if Aqp1 can produce mechanically activated (MA) currents in naïve cells *in vitro*. Aqp1 failed to produce MA currents in HEK293T cells, suggesting that it is unlikely to be a *bona fide* mechanotransducer. However, it positively regulated the currents produced by the innocuous mechanotransducer Piezo2 when co-transfected in HEK293T cells, and produced MA currents by itself when expressed in the neuronal ND-C cell line. Therefore, Aqp1 may contribute to mechanosensation by acting as a regulator and/or component of a mechanotransducer complex. I also performed mechano-clamp electrophysiology on dissociated DRG neurons from Aqp1<sup>KO</sup> mice, and *in vivo* behavioural assays in these animals to determine if Aqp1 is essential to noxious mechanical sensitivity. Although there was no significant diminution of slowly adapting (SA) currents produced by small DRG neurons in Aqp1<sup>KO</sup> mice, Aqp1's contribution to mechanosensing is confirmed by impairments in noxious mechanosensation in the behaving animals. I also performed a model of chronic inflammatory pain but found no phenotypic differences in the Aqp1<sup>KO</sup> versus the WT animals suggesting that Aqp1 does not have a role in inflammatory hyperalgesia. Previous work suggests that Aqp1 may contribute to chronic pain as a consequence of peripheral neuropathy. Unfortunately, this was not investigated within our study but it is interesting to note that prior studies have indicated that Aqp1's contribution to neuropathic pain is via its water channel rather than its central ion channel pore. As such, more investigation is needed to determine what component of Aqp1 is required for acute noxious mechanosensation, and how Aqp1 contributes to pathological pain.

## 3.2 Introduction

### 3.2.1 Aqp1 mRNA is downregulated in the DRG of mice lacking Na<sub>v</sub>1.8+ sensory neurons

In an effort to identify novel noxious mechanotransducers and modulatory proteins our group has previously compiled a list of genes that are dysregulated in mice with toxin-mediated ablation of Na<sub>v</sub>1.8-expressing neurons (Table 3.1) (unpublished data). It is well established that this subset of sensory neurons is critical for acute noxious mechanosensitivity (Abrahamsen et al., 2008) and genes identified in this list have, in the past, proved to be implicated in mechanosensory processes, including TRPC3 and TRPC6 (Quick et al., 2012). Aqp1 mRNA is downregulated 6.7 fold in mice with DTA-ablated Na<sub>v</sub>1.8+ neurons (Na<sub>v</sub>1.8<sup>DTA</sup> mice), and Aqp1 has previously been the subject of nociceptive studies. Thus, I aimed to investigate the direct role of Aqp1 in noxious mechanosensation. This study began at a point in which we had little to no understanding as to which ion channel was responsible for mediating mechanical pain, however, recent evidence would suggest the involvement of the novel mechanotransducer, TACAN (Beaulieu-Laroche et al., 2020). Whilst this is an important finding, Beaulieu-Laroche et al. (2020) isolated TACAN's activity to the Mrgprd+ population of nonpeptidergic C fibres, and surmise it's contribution to mechanical pain sensing constitutes the 'slow' pain mediated by these fibres. This leaves the A $\delta$  'fast' pain mechanotransducer ambiguous. A $\delta$  neurons within the Na<sub>v</sub>1.8 population that are responsible for noxious mechanical sensation include those expressing the molecular marker *Npy2r* (Arcourt et al., 2017). Therefore, we continue to consider the Na<sub>v</sub>1.8 population of sensory neurons as exceptionally relevant in attempting to identify novel noxious mechanotransducers.



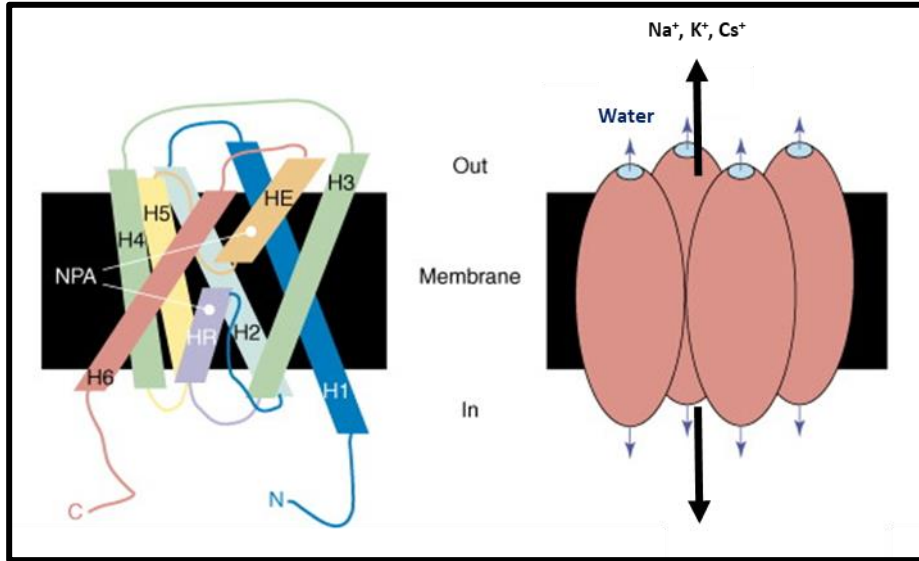
Gene symbol	Gene name	Fold-change	p-value
<b>Scn10a</b>	Nav1.8 alpha subunit	-37.59423	8.22E-05
<b>Scn11a</b>	Nav1.9 alpha subunit	-23.321207	1.99E-05
<b>Npy2r</b>	Neuropeptide Y receptor Y2	-20.93179	2.74E-05
<b>Mrgpra3</b>	MAS-related GPR, family member A3	-18.031508	0.00028773
<b>Trpa1</b>	Transient receptor potential cation channel, subfamily A, member 1	-13.50676	0.00118605
<b>P2rx3</b>	Purinergic receptor P2X 3	-11.931453	3.56E-06
<b>Mrgpra2</b>	MAS-related GPR, member A2	-10.771561	5.06E-05
<b>Th</b>	Tyrosine hydroxylase	-10.488062	0.00148609
<b>Trpc6</b>	transient receptor potential cation channel, subfamily C, member 6	-8.6587071	9.05E-06
<b>Ntrk1</b>	Neurotrophic receptor tyrosine kinase 1 (TrkA)	-8.2925748	0.00041884
<b>Plxnc1</b>	Plexin C1	-6.8878104	5.71E-06
<b>Aqp1</b>	Aquaporin 1	-6.7295054	0.00023255
<b>Trpc3</b>	Transient receptor potential cation channel, subfamily C, member 3	-6.3598173	9.33E-06
<b>Gfra2</b>	GDNF family receptor alpha 2	-4.8827962	5.14E-06
<b>Sst</b>	Somatostatin	-4.6948472	6.54E-05
<b>Calcb</b>	Calcitonin related polypeptide beta (CGRP2)	-3.6206742	2.81E-05
<b>Trpv1</b>	Transient receptor potential cation channel, subfamily V, member 1	-3.5498856	0.00026312
<b>Tac1</b>	Tachykinin precursor 1	-2.8717656	0.00037814
<b>Kit</b>	KIT proto-oncogene, receptor tyrosine kinase	-2.4635485	0.00019588
<b>Scn9a</b>	Nav1.7 alpha subunit	-2.2007306	0.00067279
<b>Trpc4</b>	Transient receptor potential cation channel, subfamily C, member 4	-1.805635	0.00090946
<b>Ret</b>	Ret proto-oncogene	-1.4735996	0.00063507
<b>Ntrk2</b>	Neurotrophic receptor tyrosine kinase 2 (TrkB)	1.2498714	0.00926151
<b>Nefh</b>	Neurofilament Heavy Chain	1.28468287	0.00529469
<b>Ntrk3</b>	Neurotrophic receptor tyrosine kinase 2 (TrkC)	1.30052042	0.04661856
<b>Cntnap2</b>	Contactin associated protein 2	1.61820058	0.0007237
<b>Ldhb</b>	Lactate dehydrogenase B	1.73125438	0.00018618
<b>Spp1</b>	Secreted phosphoprotein 1	1.86012136	0.00022637
<b>Calb1</b>	Calbindin 1	1.87157766	0.00092461
<b>Pvalb</b>	Parvalbumin	2.26621644	0.00013246
<b>Runx3</b>	Runt-related transcription factor 3	2.37437258	0.00014645

**Table 3.1. Dysregulated genes identified by microarray in the DRG of Nav1.8<sup>DTA</sup> mice**

A selection of dysregulated genes from a microarray study in mice that have undergone peripheral Nav1.8+ neuron ablation. Only dysregulated genes with a p-value <0.05 were considered. The example genes shown include those identified in the Usoskin et al. (2015) study and encompass a broad range of genes specific to innocuous and noxious sensory neurons. Those associated with LTMRs are included in the lower portion of the table and demonstrate a significant upregulation, whereas those specific to the Nav1.8+ population of sensory neurons exhibit a significant downregulation and are located in the top portion of the table.

### **3.2.2 The structure and electrophysiological properties of Aqp1**

Aqp1 is a homotetrameric water channel formed from small hydrophobic membrane proteins approximately 30kDa in size, which consist of six  $\alpha$ -helical domains surrounding a water pore, as depicted in Figure 3.1 (Tait et al., 2007). It is responsible for bidirectional osmotically driven water transport in various structures of the body including the vascular system, kidneys, and the nervous system (Verkman et al., 2000). Aqp1 KO (Aqp1<sup>KO</sup>) mice demonstrate Aqp1's importance for urinary concentration (Ma et al., 1998), which is also true of humans (King et al., 2001), due to its role in increasing osmotic reabsorption of water from renal collecting ducts. However, Aqp1 also functions as a cGMP-gated non-selective cation channel via a central pore within its tetrameric structure. This ion channel function can be observed in the CNS where Aqp1 is expressed in the ventricular-facing membrane of the choroid plexus epithelium of the brain. It is this non-selective cation channel property that modulates cerebral spinal fluid (CSF) production (Boassa et al., 2006; Oshio et al., 2004; Yu et al., 2006). Activation of the Aqp1 ion channel in the choroid plexus epithelium (by atrial natriuretic peptide (ANP) which binds to a guanylate cyclase receptor and causes the generation of cGMP) decreases basal-to-apical fluid transport. Conversely, Aqp1 block with Cd<sup>2+</sup> restores fluid transport. The properties of the Aqp1 ion channel current include a permeability to Na<sup>+</sup>, K<sup>+</sup>, TEA<sup>+</sup>, and Cs<sup>+</sup>, a voltage insensitivity, and a dependence on cGMP (Boassa et al., 2006). Consequently, Aqp1<sup>KO</sup> mice exhibit reduced intracranial pressure and increased survival in response to cold injury brain trauma due to a reduction in CSF production (Oshio et al., 2005). This data indicates that Aqp1 inhibition may have a protective role in human disorders of increased intracranial pressure.



**Figure 3.1. The structure of the Aqp1 monomer, and Aqp1's tetrameric structure in the membrane**

**A.** Structure of the Aqp1 monomer that consists of six  $\alpha$ -helical domains and two conserved NPA motifs.  
**B.** Four Aqp1 monomers come together in the membrane of various tissues within the body to form a homotetrameric structure. Each monomer consists of a water pore. The central pore of the homotetramer acts as a non-selective cation channel (adapted from Tait et al. (2007))

### **3.2.3 The role of Aqp1 in pain**

Within the PNS, Aqp1 expression is found in the mechanosensitive periodontal Ruffini endings, and terminal Schwann cells (Nandasena et al., 2007). Importantly, Aqp1 is also expressed in the sensory neurons of the nodose ganglia, the TG, and the DRG (Shields et al., 2007). In the DRG, it is restricted to the small diameter neurons innervating the superficial layers of the dorsal horn (Solenov et al., 2002), which are responsible for nociception. This observation has already made Aqp1 the subject of nociceptive investigation (Table 3.2). Prior characterisation of Aqp1<sup>KO</sup> mice has provided evidence for a role of Aqp1 in inflammatory and cold pain perception (Oshio et al., 2006; Zhang & Verkman, 2010), nociceptive modalities typically associated with Na<sub>v</sub>1.8 expressing neurons. Dysregulated Aqp1 expression has also been linked to mechanical allodynia after spinal cord injury (Nesic et al., 2008). Our group has previously demonstrated a downregulation of Aqp1 mRNA in the DRG of mice as a consequence of Na<sub>v</sub>1.8+ peripheral neuron ablation (Table 3.1). This population of sensory neurons is also essential to acute mechanical pain perception, yet no group has published data on the sensitivity of Aqp1<sup>KO</sup> mice to acute mechanical pain. This, in conjunction with a known endogenous role for Aqp1 as a non-selective cation channel has led me to assess the role of Aqp1 in mechanotransduction and noxious mechanosensitivity.

Behavioural Assay		Reference			
		Oshio et al., 2006	Shields, et al, 2007	Nesic et al., 2008	Zhang & Verkman, 2010
Acute	Von Frey	X	X	-	-
	Hargreaves	-	X	-	-
	Tail flick	✓	X	-	-
	Hot plate	-	X	-	X
	Cold plate	-	-	-	✓
Acute inflammation	Tail clip	X (unpublished)	-	-	-
	Capsaicin	✓	X	-	✓(Spontaneous)
	Formalin	X	X	-	X
	PGE <sub>2</sub>	-	X	-	✓(Thermal)
Chronic inflammation	Bradykinin	-	-	-	✓(Spontaneous)
	CFA	-	X	-	-
Neuropathic	SCI	-	-	✓(mechanical)	-
	SNI	-	X	-	-

**Table 3.2. Previous pain behavior assays in Aqp1 knockout/knockdown mice**

'X' refers to no change in behaviour in comparison to WT controls. '✓' denotes a decrease in sensitivity to the assay performed, and '-' indicates where the assay was not performed. Inflammatory and neuropathic pain models include a description of the stimuli (or if the behaviour was stimulus independent i.e. spontaneous) that the knockout/knockdown animal demonstrates a reduction in hypersensitivity to.

### 3.2.4 Breeding strategy for Aqp1<sup>KO</sup> mice

As part of this study, I used Aqp1 KO mice which were kindly provided by Olivier Devuyst and Yvette Cnops; the knockout design was as previously described (Ma et al., 1998). Mice heterozygous for the mutant Aqp1 allele were bred to one another to produce progeny that were either Aqp1 WT (Aqp1<sup>wt/wt</sup>), Aqp1 heterozygotes (Aqp1<sup>mut/wt</sup>), and Aqp1<sup>KO</sup> (Aqp1<sup>mut/mut</sup>). Only Aqp1 WT (littermate controls), and Aqp1<sup>KO</sup> mice were used for experiments. Mice were genotyped before and after behavioral assays using the genotyping primers in Table 3.3.

Gene	Primer	Sequence	WT band	KO band
<i>Aqp1</i>	WT Fwd	AAGTCAACCTCTGCTCAGCTGGG	500 bp	430 bp
	Mut Fwd	CTCTATGGCTTCTGAGGCGGAAAG		
	Common Rev	ACTCAGTGGCTAACAACAAACAGG		

**Table 3.3. Genotyping primers for Aqp1<sup>KO</sup> animals**

### 3.3 Aims

- To assess the mechanosensitivity of Aqp1 *in vitro* by performing mechano-clamp electrophysiology (an established electrophysiological technique for characterising MA currents (Dubin et al., 2017)) on cell lines heterologously expressing Aqp1
- To repeat the above assay using the cultured DRG neurons of Aqp1<sup>KO</sup> mice to determine the contribution of Aqp1 to mechanosensitivity in these cells
- To determine the extent to which Aqp1 contributes to noxious mechanosensitivity *in vivo* by implementing behavioural assays in Aqp1<sup>KO</sup> mice

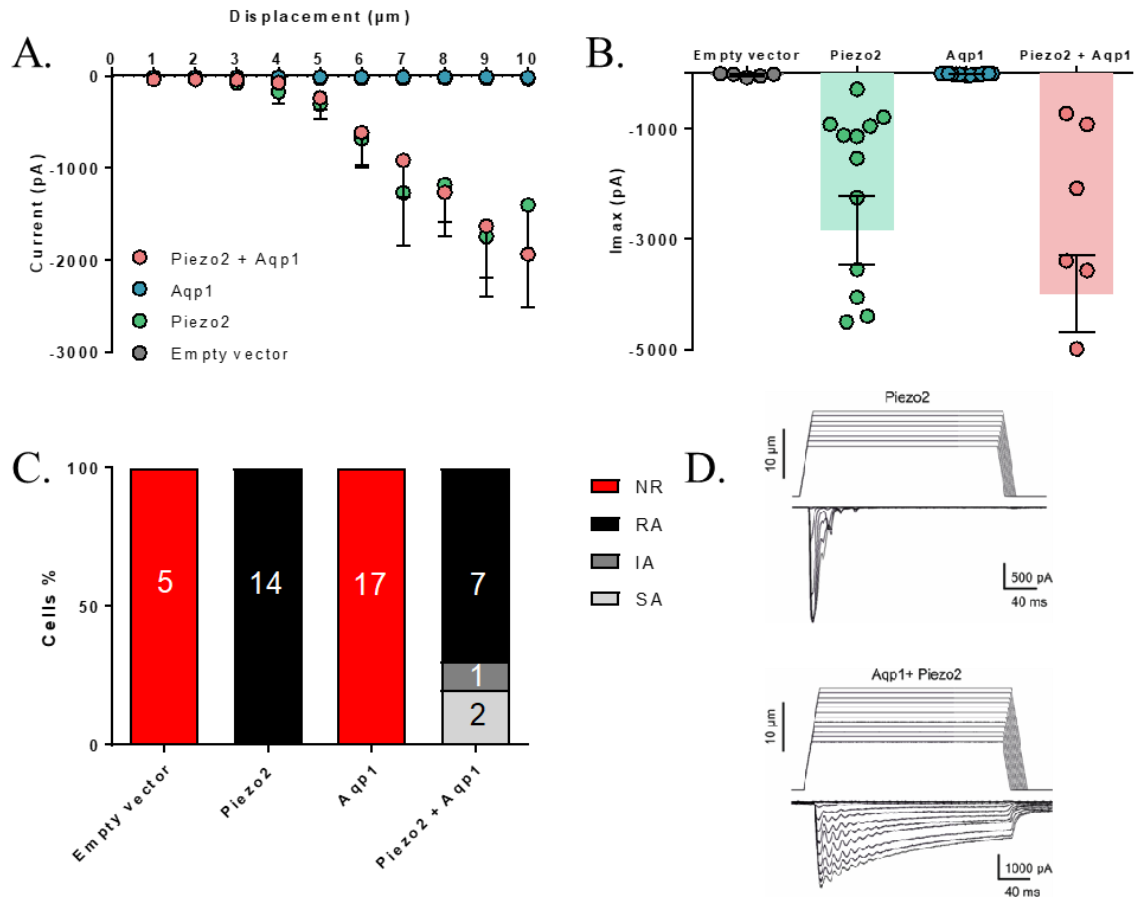
### 3.4 Results

#### 3.4.1 Aqp1 regulates Piezo2 activity in HEK293T cells

The gold-standard approach to characterising MA currents is to express candidate ion channels in naïve cells and record the MA currents they produce (Dubin et al., 2017). I expressed Aqp1 in naïve HEK293T cells by transfecting them with an *Aqp1-IRES-tdTomato* construct. To record MA currents, I employed the mechano-clamp assay, which aims to mimic mechanical stimulation by prodding the cell membrane with a blunt fire-polished glass pipette. In sensory neurons, this assay produces well-characterised MA currents that can be classified according to their decay kinetics. For reference, MA current kinetics have been previously defined with time constants ( $\tau$ ) of < 20 ms for rapidly adapting (RA) currents and > 100 ms for slowly adapting (SA) currents, currents that fall between these values are considered intermediately adapting (IA) (Hao & Delmas, 2010; Rugiero et al., 2010).

As expected, Piezo2 expression in HEK293T cells produces significant RA MA currents that increase in amplitude with increasing displacement. Aqp1 alone produces no discernible current (Figure 3.2.A-B), however, Piezo2 and Aqp1 co-expression produces a significant MA current with an average  $I_{max}$  of  $-3985.36 \pm 701.4916$  pA ( $p= 0.0005$ ) (mean  $\pm$  SEM) when compared to the empty vector control. The mean percentage decay is also 34% slower than cells expressing Piezo2 only (Figure 3.2.C-D). A trend towards an increase in amplitude can also be observed. Of note there is no discernible difference in the displacement depth required to produce these different current types, despite it being widely accepted that SA currents have higher thresholds of activation than RA currents. It is likely that Aqp1 is in some way positively regulating the current produced by Piezo2 in this instance.





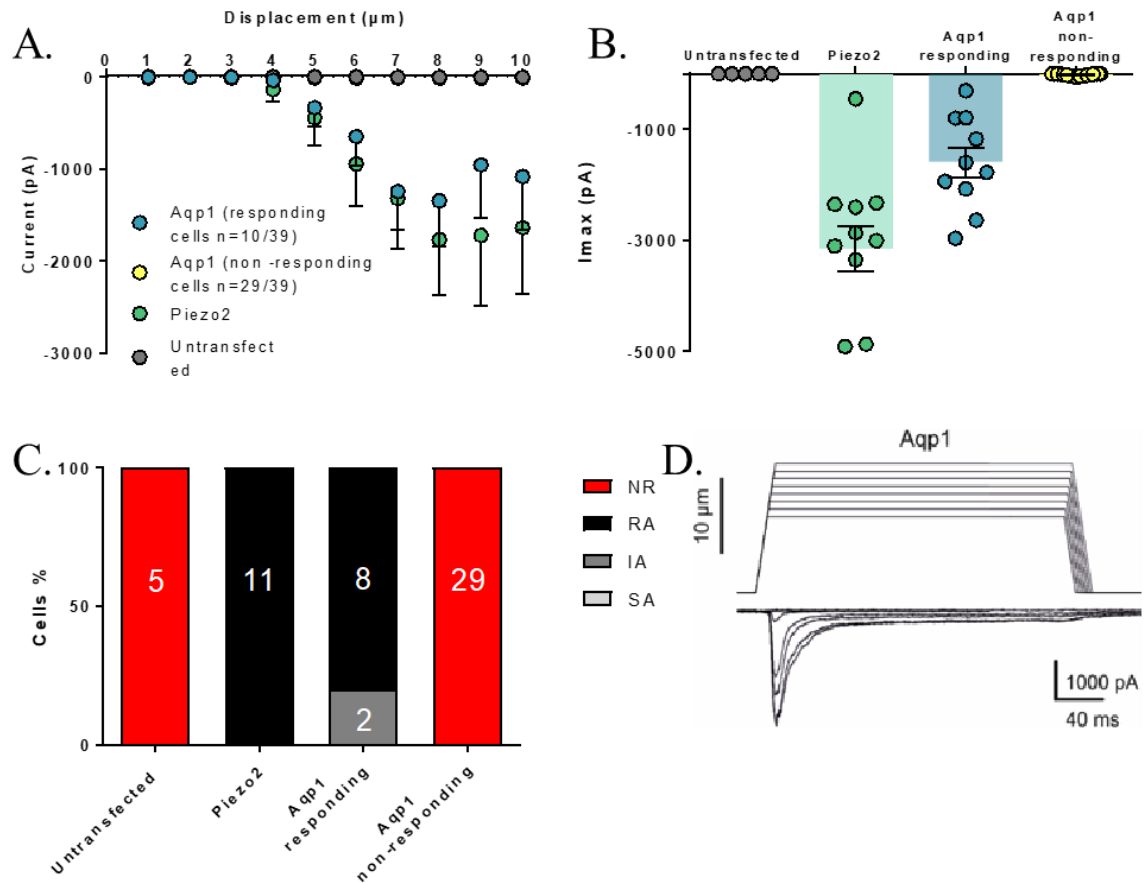
**Figure 3.2. Aqp1 potentiates the MA current produced by Piezo2 in HEK293T cells**

**A.** Average amplitude of MA currents produced by Aqp1-IRES-tdTomato, Piezo2-IRES-GFP, IRES-tdTomato expressing HEK293T cells, and Aqp1-IRES-tdTomato and Piezo2-IRES-GFP co-expressing HEK293T cells at increasing depths of displacement. **B.** The average maximal current amplitude of each transfected HEK293T cell before the recording was lost. **C.** The proportion of MA current types produced by transfected HEK293T cells. Currents are defined as non-responsive (NR), rapidly adapting (RA), intermediately adapting (IA), and slowly adapting (SA). **D.** Representative trace from a Piezo2-expressing HEK293T cell, and an Aqp1 and Piezo2 co-expressing HEK293T cell. Unpaired student's t-test. Data are shown as Mean  $\pm$  SEM. (Empty vector n =5; Piezo2 n =14; Aqp1 n =17; Piezo2 + Aqp1 n =10).

### **3.4.2 Aqp1-expressing ND-C cells produce MA currents**

Aqp1 is expressed in different tissues, including the kidney and the lung, where it functions as a water channel (Verkman et al. 2000), and structures of the brain where it functions as an ion channel (Boassa et al., 2006). Thus, it is highly likely that Aqp1's environment dictates its functionality. For a clearer indication of its role within sensory neurons I chose to express Aqp1 in the ND-C neuronal cell line, a neonatal rat DRG neuron and mouse neuroblastoma hybrid (J. N. Wood et al., 1990). When differentiated, ND-C cells possess the machinery required to produce endogenous MA currents (Rugiero & Wood, 2009).

In this cell line, Piezo2 produces a robust RA current again, but in this case, Aqp1 expression alone was enough to produce an MA current in ~ 26% of transfected ND-C cells with an average  $I_{max}$  of  $-1605.66 \pm 268.26$  pA ( $p= 0.0004$ ) (Figure 3.3.B). The observation that Aqp1 transfection in ND-C cells is sufficient to produce MA currents in the absence of Piezo2 is strong evidence in support of a role for Aqp1 in mechanotransduction. Whether this is due to a positive regulation of endogenous MA currents remains to be determined.

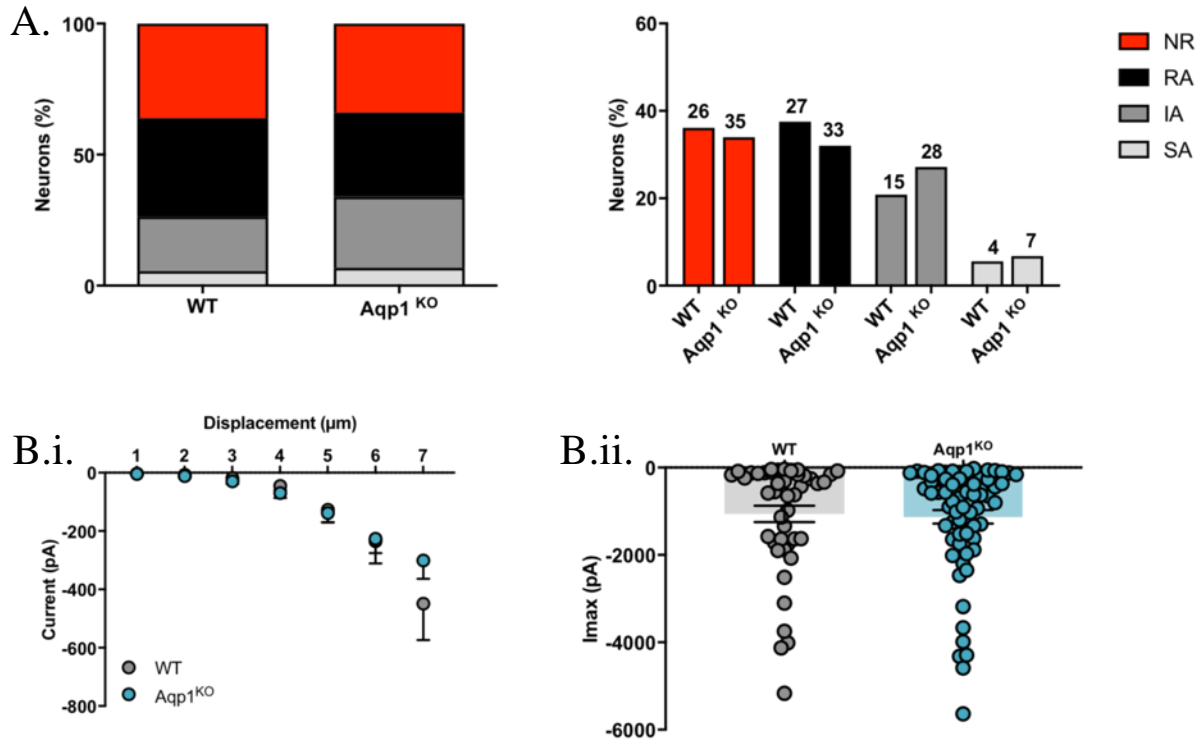


**Figure 3.3. Aqp1 produces an MA current in ND-C cells**

**A.** Average amplitude of MA currents produced by responding and non-responding Aqp1-IRES-tdTomato expressing ND-C cells, Piezo2-IRES-GFP expressing ND-C cells, and untransfected ND-C cells. **B.** The average maximal current amplitude of each transfected and untransfected ND-C cell before the recording was lost. **C.** The proportion of MA current types produced by transfected ND-C cells. **D.** Representative trace from an Aqp1 expressing ND-C cell. Unpaired student's t-test. Data are shown as Mean  $\pm$  SEM. (Untransfected n =5; Piezo2 n =11; Aqp1 n =39).

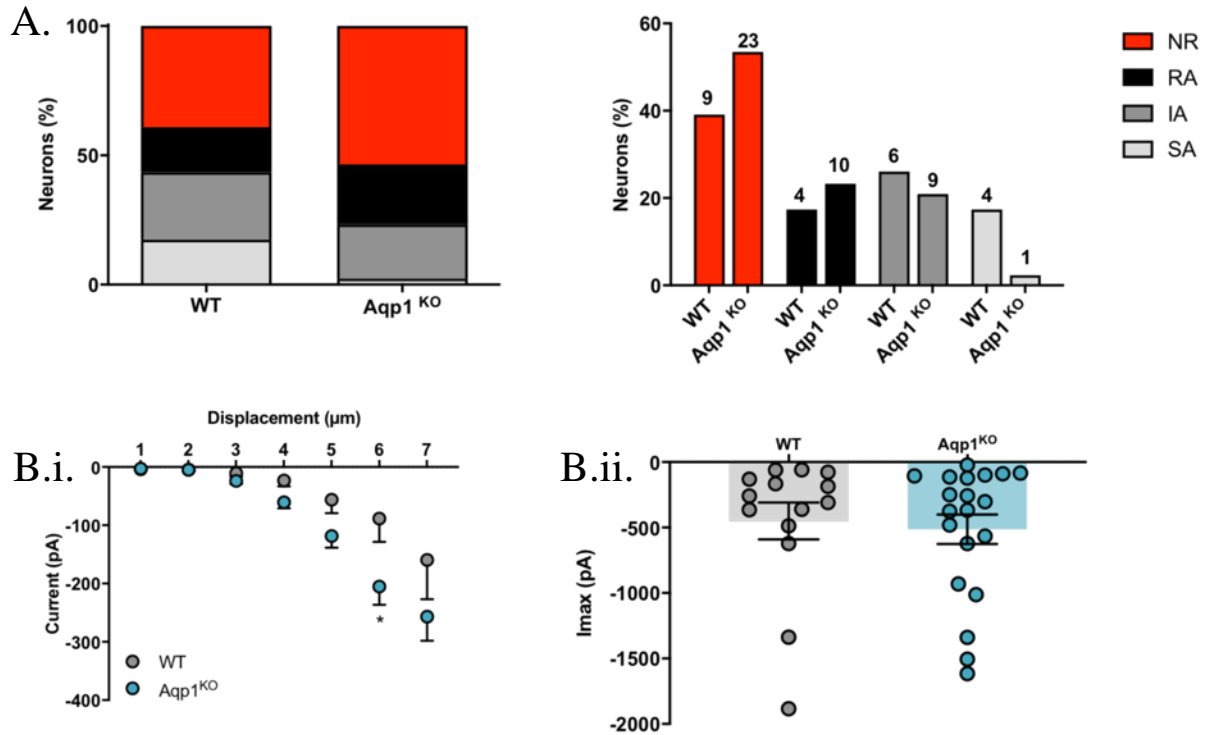
### 3.4.3 MA currents are altered in the small DRG neurons of Aqp1<sup>KO</sup> mice

Having established that Aqp1 can contribute to the production of SA MA currents in cell lines, I compared the mechanosensitivity of murine Aqp1<sup>KO</sup> and WT DRG neurons *in vitro*. Using mechano-clamp electrophysiology I found that the proportions of rapidly, intermediately, and slowly adapting currents were comparable between genotypes (Figure 3.4.A). There was no significant difference in the average amplitude of MA currents produced at membrane displacements between 1-7  $\mu\text{m}$  (7  $\mu\text{m}$  being the maximum displacement before the first recording was lost) (Figure 3.4.B.i), or the maximum current produced at any displacement before the recording was lost (Figure 3.4.B.ii). Given that Aqp1 is expressed in small diameter sensory neurons, I next looked exclusively at currents recorded in neurons with a capacitance of less than 20 pF. In this population, which is akin to small diameter nociceptive fibres, I also observed no significant differences in the repertoire of MA currents produced between genotypes (Figure 3.5.A). However, I did observe a significant increase in the average amplitude of MA currents produced between 1-7  $\mu\text{m}$  displacement in the Aqp1<sup>KO</sup> small DRG neurons (WT =  $-88.43 \pm 40.06$  pA; Aqp1<sup>KO</sup> =  $-205.09 \pm 31.46$  pA;  $p=0.0114$ ) (Figure 3.5.B.i). This is perhaps a consequence of an increase in the proportion of RA currents produced by the Aqp1<sup>KO</sup> small DRG neurons (and concomitant decrease in SA currents), which require less displacement depth to be produced. More recordings are required to determine if this interpretation is true. I observed no significant differences between the maximum amplitude of MA currents produced (Figure 3.5.B.ii).



**Figure 3.4. MA currents from total Aqp1<sup>KO</sup> DRG are unaltered**

Electrophysiological characterisation of DRG neurons from Aqp1<sup>KO</sup> mice and WT littermate controls. **A.** The proportion of MA currents produced by DRG neurons of Aqp1<sup>KO</sup> and WT mice. No significant difference between genotypes. Ordinary two-way ANOVA with Sidak's multiple comparisons test. **B.i.** Average amplitude of MA currents produced by responding Aqp1<sup>KO</sup> and WT DRG neurons in response to increasing membrane displacement. 7 μm was the depth at which the first recording was lost. Ordinary two-way ANOVA with Sidak's multiple comparisons test. **B.ii.** The average maximal current amplitude of all responding DRG neurons before each recording was lost. Unpaired student's t-test. Data are shown as Mean ± SEM. (WT DRG neurons n =72; Aqp1<sup>KO</sup> n=103).

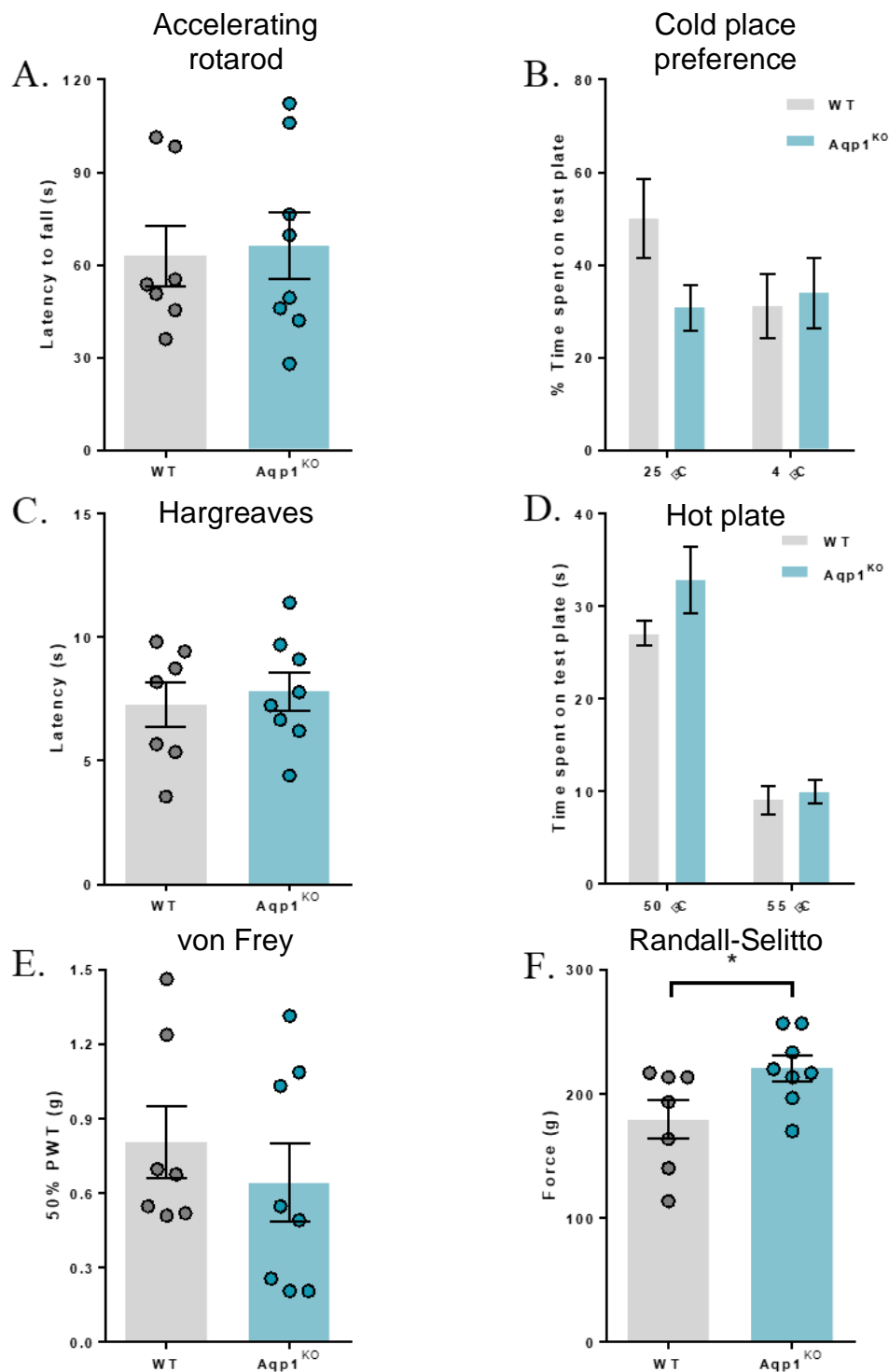


**Figure 3.5. MA currents in Aqp1<sup>KO</sup> DRG are altered in small diameter neurons**

Electrophysiological characterisation of small DRG neurons from Aqp1<sup>KO</sup> mice and WT littermate controls. **A.** The proportion of MA currents produced by small DRG neurons of Aqp1<sup>KO</sup> and WT mice. No significant difference between genotypes. Ordinary two-way ANOVA with Sidak's multiple comparisons test. **B.i.** Average amplitude of MA currents produced by responding Aqp1<sup>KO</sup> and WT DRG neurons in response to increasing membrane displacement. 7  $\mu$ m was the depth at which the first recording was lost. Ordinary two-way ANOVA with Sidak's multiple comparisons test. **B.ii.** The average maximal current amplitude of all responding DRG neurons before each recording was lost. Unpaired student's t-test. Data are shown as Mean  $\pm$  SEM. (WT DRG neurons n =23; Aqp1<sup>KO</sup> n=44).

#### **3.4.4 Aqp1<sup>KO</sup> mice have reduced sensitivity to noxious mechanical stimuli**

I next examined the response of Aqp1<sup>KO</sup> mice to various innocuous and noxious stimuli. It has been previously reported that these animals have unimpaired responses to stimulation of the hind paw with von Frey hairs, and to noxious heat stimuli (Oshio et al., 2006; Shields et al., 2007). My findings were consistent with this (Figure 3.6.E and C). Additionally, I found no impairments in the motor coordination of Aqp1<sup>KO</sup> mice (Figure 3.6.F). These prior studies, however, did not use the Randall-Selitto assay to assess sensitivity of these animals to acute noxious mechanical stimuli. I found that Aqp1<sup>KO</sup> mice displayed significantly impaired responses to noxious mechanical pressure applied to the tail when compared to WT mice (WT =  $179 \pm 15.48\text{g}$ ; Aqp1<sup>KO</sup> =  $220.4 \pm 10.32\text{g}$ ;  $p = 0.04$ ). These findings suggest that while Aqp1 may not alone be a slowly adapting mechanotransducer, it is at least necessary for normal mechanosensory function.



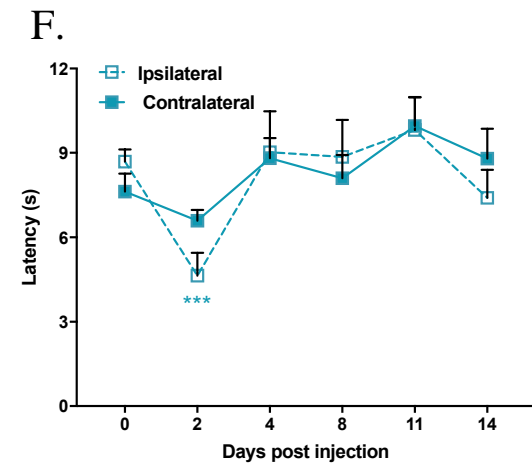
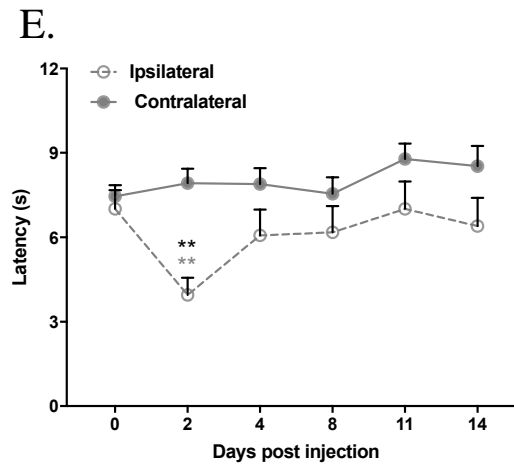
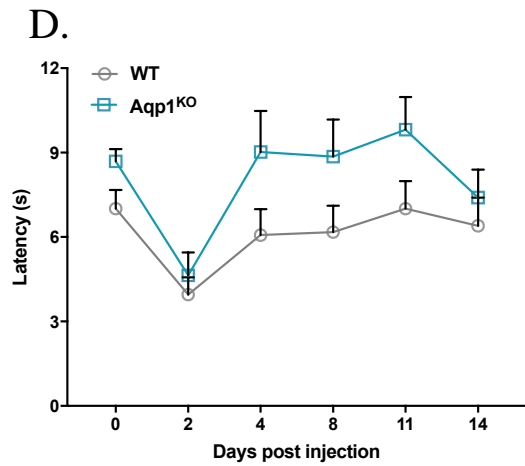
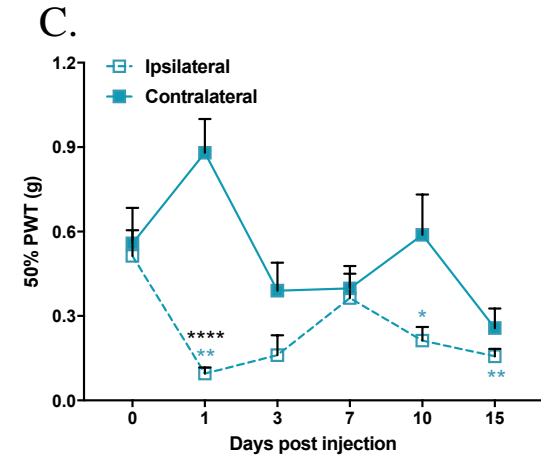
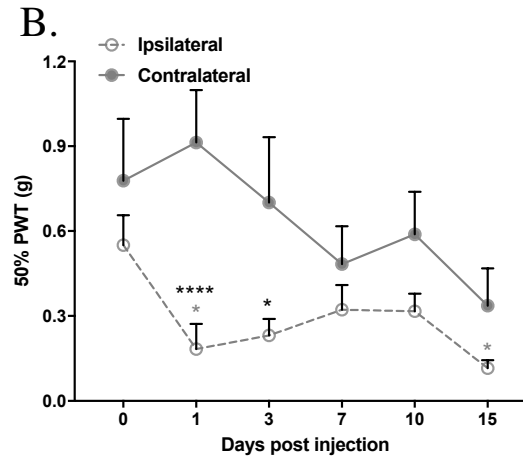
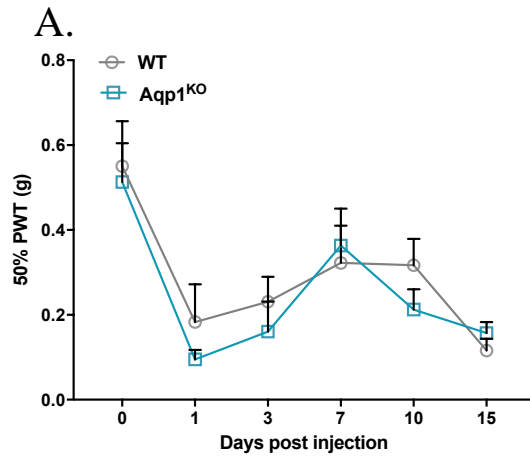
**Figure 3.6. Noxious mechanical sensitivity is impaired in Aqp1<sup>KO</sup> mice**

Acute behavioural characterisation of Aqp1<sup>KO</sup> mice, including noxious thermal and mechanical assays. **A.** Motor coordination measured as time spent on an accelerating rotarod before falling. **B.** Noxious cold place preference assay **C.** Hargreaves assay assessing latency to remove hind paw from a noxious heat stimulus. **D.** Hot plate assay quantified as the amount of time spent on test plate until a nocifensive response was observed. **E.** Innocuous von Frey hairs applied to the hind paw. Bars represent the force required to produce a withdrawal response 50% of the time (up/down method). **F.** Noxious Randall-Selitto assay applied to the base of the tail demonstrates the force required to elicit a nocifensive response. Data are shown as Mean  $\pm$  SEM. Statistical analysis was performed using the unpaired Student's t test. (WT n=7; Aqp1<sup>KO</sup> n=8).



### **3.4.5 Aqp1<sup>KO</sup> mice show no evoked behavioural differences in comparison to WT mice after intraplantar CFA injection**

Previous work has investigated the role of Aqp1 in inflammatory pain, again with conflicting results (Oshio et al., 2006; Shields et al., 2007; Zhang & Verkman, 2010). Assays that have thus far yielded abnormal phenotypes in Aqp1<sup>KO</sup> animals have been those using acute inflammatory agents such as capsaicin, PGE<sub>2</sub>, and bradykinin, however, for the former two, contradictory findings have been published. Within this study I chose to assess the contribution of Aqp1 to inflammatory pain using an intraplantar injection of CFA. This is a chronic model of inflammation and is typically characterised by a local mechanical and thermal hyperalgesia that lasts for two to three weeks, with associated oedema in the ipsilateral hind paw. A comparison between the evoked responses (up/down von Frey and Hargreaves assay) seen in the WT and Aqp1<sup>KO</sup> mice after CFA administration demonstrates that both cohorts develop a significant mechanical hypersensitivity from day 1 after CFA administration, that lasts for the duration of the study (>2 weeks), with an apparent contralateral mechanical hypersensitivity from day 7 (Figure 3.7.A-C). A hypersensitivity to the Hargreaves assay in both genotypes peaks at day 2 post-injection, and appears to resolve itself in both cohorts from day 4 (Figure 3.7.D-F).

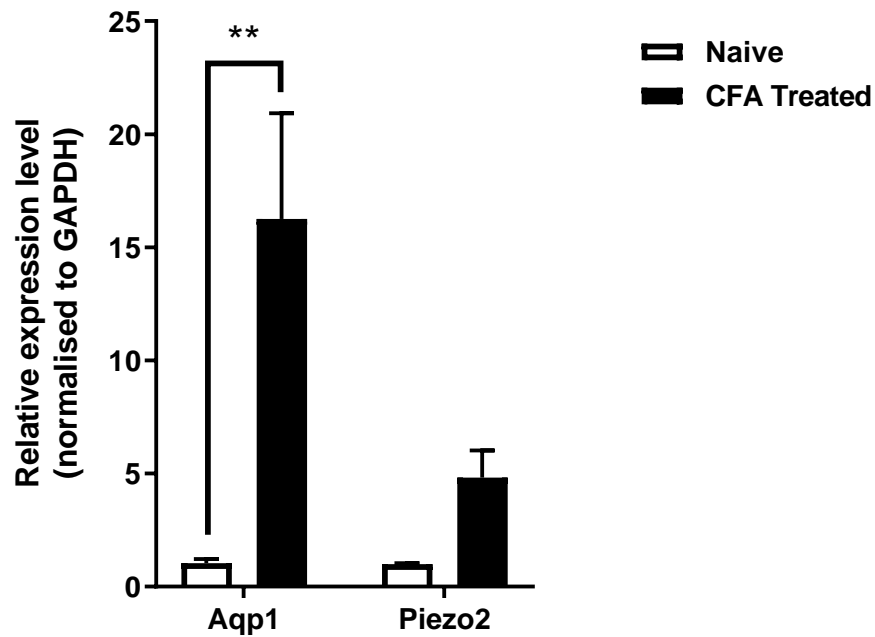


**Figure 3.7. Thermal and mechanical sensitivity of Aqp1<sup>KO</sup> animals after intraplantar injection of CFA**

**A.** Up/down von Frey of the ipsilateral hind paw of WT and Aqp1<sup>KO</sup> mice after intraplantar injection of 20  $\mu$ l CFA. **B.** Comparative responses of WT ipsilateral and contralateral hind paws to up/down von Frey stimulation. **C.** Comparative responses of Aqp1<sup>KO</sup> ipsilateral and contralateral hind paws to up/down von Frey stimulation. **D.** Hargreaves assay (radiant heat stimulus) applied to the ipsilateral hind paw of WT and Aqp1<sup>KO</sup> mice. **E.** comparative responses of WT ipsilateral and contralateral hind paws to the Hargreaves assay. **F.** Comparative responses of Aqp1<sup>KO</sup> ipsilateral and contralateral hind paws to the Hargreaves assay. Data are shown as Mean  $\pm$  SEM. Statistical analysis was performed using RM one-way ANOVA with Dunnett's multiple comparisons test to compare subsequent recordings to the baseline, and RM two-way ANOVA with Tukey's multiple comparison test to compare ipsilateral and contralateral hind paws, and WT and Aqp1<sup>KO</sup> ipsilateral hind paws. Black stars represent significance in comparison to contralateral hind paw, and grey and blue stars represent significance in comparison to the baseline. (WT n=8; Aqp1<sup>KO</sup> n=8).

### **3.4.6 Aqp1 mRNA is significantly upregulated in the DRG of WT mice after intraplantar CFA injection**

To assess if Aqp1 has a role in the CFA model of chronic inflammatory pain, I chose to extract the DRG of WT animals that were exposed to CFA as part of the behavioural assay, and also three WT littermate animals that had been injected with a single 20 µl injection of saline into the hind paw at the same time as those that were treated with CFA. As an aside, I also assessed the expression of Piezo2 mRNA in this model, to gain insight into whether Piezo2 contributes to mechanical hyperalgesia/allodynia in these animals. Surprisingly, although the behavioural phenotype of the animals remained the same, I found a significant increase in the expression of Aqp1 mRNA in the DRG of animals in comparison to their saline-injected counterparts (Figure 3.8). No significant increase in Piezo2 mRNA expression was observed.



**Figure 3.8. Aqp1 and Piezo2 mRNA expression in the DRG of naïve animals versus those treated with CFA**

Animals were treated with intraplantar injections of either saline (naïve) or CFA, and all DRG harvested on day 15. RT-qPCR revealed a significant increase in Aqp1 mRNA expression in the DRG of animals treated with CFA when compared to their saline-treated counterparts. No significant increase in Piezo2 mRNA expression was observed. Unpaired student's t-test. Data are shown as Mean ± SEM. (n = 3 per group).

### **3.5 Discussion**

A role for Aqp1 in peripheral nociception became the source of debate some years ago. The current work agrees with the findings made by two groups who demonstrate that Aqp1 does not appear to be important for the majority of acute pain modalities (Oshio et al., 2006; Shields et al., 2007; Zhang & Verkman, 2010). Instead, I find Aqp1 has a specific ability to contribute to mechanically activated currents and that it is required for normal acute noxious mechanical sensitivity.

In an attempt to describe novel noxious mechanotransducers we used a combination of molecular analyses and a knowledge of current literature to identify our candidate, Aqp1, a water channel expressed in Na<sub>v</sub>1.8+ sensory neurons. I cross-examined Aqp1 and found that expression of Aqp1 alone does not confer mechanosensitivity to HEK293T cells, but does to neuronal ND-C cells. This may be explained by the notion that Aqp1's ion channel capability is dependent upon specific regulatory mechanisms or interactions that vary within expression systems (Boassa et al., 2006). Indeed, ion channel activity has been reported as undetectable in Aqp1-transfected HEK cells (Tsunoda et al., 2004). Therefore it is likely that the PNS, like the CNS, provides the appropriate environment for Aqp1 to form ion channel complexes that are mechanosensitive in this instance.

#### **3.5.1 The role of Aqp1 in acute noxious mechanosensation**

Although I report that Aqp1 does not significantly contribute to the production of SA MA currents in small diameter DRG neurons, more electrophysiological recordings are required, as Aqp1 is necessary for normal noxious mechanosensitivity. As Aqp1 does not produce an MA current in naïve cells, it is debatable as to whether it makes up the pore-forming component of a mechanotransducer. My findings are similar to those of studies on another mammalian noxious mechanotransducer candidate, TRPA1, the orthologue of which confers mechanosensitivity in *C.elegans*. DRG neurons from TRPA1 KO mice have been shown to produce significantly fewer SA MA currents (Vilceanu & Stucky, 2010) and KO mice are desensitised to noxious mechanical stimuli applied to the hind paw (Andersson et al., 2009; Kwan et al., 2006). Despite these findings, interest in TRPA1 has declined as, like Aqp1, it also fails to produce an MA current when expressed in a heterologous system (Vilceanu & Stucky, 2010). However, human GOF mutations

in TRPA1 are responsible for Familial Episodic Pain Syndrome (FEPS) a disorder characterised by episodic mechanical pain in the upper body (Kremeyer et al., 2010), clearly demonstrating a fundamental role for TRPA1 in normal human nociceptive function. My findings and those relating to TRPA1 indicate that noxious mechanosensory systems are complex, and likely to feature auxiliary proteins necessary for tethering, gating, and regulating the channels in question, which are not found in naïve systems. This should not lessen the importance of these channel's contributions to mechanosensation. Evidence for such mechanotransducer complexes has been described in much simpler invertebrate systems. For example the 'degenerin' proteins MEC-4 and MEC-10 are believed to be pore-forming subunits of an ion-channel complex essential for touch-sensing neurons in *C. elegans*, that can only confer mechanosensitivity to a naïve cell when co-expressed (O'Hagan et al., 2005). Furthermore, they are regulated by the associated proteins MEC-2 (Goodman et al., 2002) and MEC-6 (Chelur et al., 2002). Similarly, in vertebrates TRPC3 and TRPC6 contribute to MA currents in mice, but it is only when both TRPC3 and TRPC6 are knocked out do the animals exhibit a mechanosensory deficit (Quick et al., 2012). This deficit is exacerbated in TRPC1, 3, 5 and 6 quadruple null mice (Sexton et al., 2016). Thus, Aqp1 contributes to acute noxious mechanosensation, most likely by regulating and/or interacting with a still unidentified mechanotransducer expressed by small diameter, Na<sub>v</sub>1.8+ sensory neurons. Observations made of other members of the aquaporin channel family support a role for aquaporins in regulating sensory transduction processes. Aqp4 is expressed in supporting cells in the inner ear and the retina and it is proposed that in these contexts it contributes to extracellular K<sup>+</sup> homeostasis thus allowing sensory transduction to occur in nearby excitable cells (Li, 2001; Li et al., 2002; Lu et al., 2008). As such, this newly identified regulatory role for Aqp1 in mechanotransduction aligns with current understanding of the function of this family of channels. Of note, a novel subpopulation of cutaneous Schwann cells have been recently identified that are closely associated with small diameter, mechanosensitive, unmyelinated fibres, and are required for detecting noxious mechanical stimuli in glabrous and hairy skin (Abdo et al., 2019). These end organs are highly enriched with Aqp1, contributing to the argument that Aqp1 contributes to normal acute noxious mechanosensation.

### **3.5.2 Could there still be a role for Aqp1 in inflammation?**

Despite the lack of a behavioural pain phenotype in Aqp1<sup>KO</sup> animals after CFA administration, we cannot ignore the significant upregulation of Aqp1 mRNA in the DRG of WT animals as a consequence. This suggests a role for Aqp1 in the PNS during inflammation, even if it is not contributing to inflammatory pain. This same upregulation is observed in neuropathological

conditions including Alzheimer's disease, traumatic brain injury, and also spinal cord injury (Halsey et al., 2018). In the latter, an upregulation of Aqp1 in the tissues surrounding the lesion site, including astrocytes, is observed (Nesic et al., 2008). It is hypothesised that in this instance Aqp1's function is to coordinate and promote astrocyte migration to the lesion. As my qPCR was performed on whole DRG, we cannot exclude the possibility that the upregulation of Aqp1 mRNA I observe is as a consequence of increased expression in the supporting cells rather than in the neurons. Indeed, Aqp1 expression in human glia of the PNS has been observed even under basal conditions (Gao et al., 2006). An upregulation of Aqp1 mRNA has been reported in other tissues in response to chronic osmotic challenge, and injury. These include the renal medullary (kidney) cells, where it is suggested that hypertonicity results in an upregulation of Aqp1 downstream of the activation of extracellular MAPK (mitogen-activated protein kinases) pathways such as ERK, p38 kinase, and JNK (Umenishi & Schrier, 2003). These kinases regulate the activation of the osmotic response element (ORE) located in the promoter region of Aqp1, which leads to gene transcription and Aqp1 upregulation. An upregulation of Aqp1 in this instance is thought to enhance the urinary concentrating mechanism. MAPK-dependent upregulation of Aqp1 has also been reported in astrocytes following a cortical stab wound assay (Mccoy & Sontheimer, 2010). This group proposed that in this setting, Aqp1 upregulation contributes to astrocyte migration, and may also contribute to cortical oedema associated with brain injury. It may be of interest to investigate the possible upregulation of Aqp1 in peripheral supporting cells further, as satellite glial cells in the DRG have been implicated in enhanced pain sensitivity as a consequence of inflammation and peripheral nerve injury (Ji et al., 2013; Kim et al., 2016). Perhaps I don't observe any phenotypic differences in WT versus Aqp1<sup>KO</sup> animals in response to inflammation as other members of the aquaporin family are able to compensate for the loss of Aqp1 in glia.

Of note, the upregulation of Aqp1 mRNA I observe in the DRG as a consequence of CFA exposure, contradicts the findings of Borsani et al. (2009) who report unaltered Aqp1 protein expression in the trigeminal ganglia (TG) of their formalin-treated mice. This particular study performed tissue extraction for immunohistochemical and western blot analysis only four hours after exposure to the inflammatory agent, and may reconcile my contradictory findings at day 15. It is also possible that my observed Aqp1 mRNA upregulation does not reflect that of Aqp1 protein expression.

### **3.5.3 Should a role for Aqp1 in neuropathic pain be explored?**

Interestingly, the migratory phenotype observed in astrocytes as a consequence of Aqp1



upregulation may also hold true in injured Aqp1-expressing peripheral neurons. By performing a spinal cord injury (SCI) model of neuropathic pain in rats, Nesic et al. (2008) found that peripheral Aqp1+ neurons (near to the spinal cord lesion site), which usually terminate in laminae I and II of the dorsal horn, exhibited excessive sprouting and were penetrating into deeper areas of the dorsal horn as a consequence of Aqp1 upregulation. This dorsal horn sprouting has previously been associated with mechanical and thermal allodynia in mice (Macias et al., 2006). Nesic et al. (2008) hypothesised that this sensory neuron migration was due to Aqp1's ability to promote axonal elongation in much the same way as it stimulates astrocyte migration, by allowing for the intake of water into the cells/axons. Furthermore, daily intraperitoneal administration of the antioxidant, melatonin in these animals led to a diminution in Aqp1 expression in the injured spinal cord and a subsequent reduction in the development of neuropathic pain, as measured by applying von Frey filaments to the surrounding dermatomes of the trunk region. Thus, Aqp1+ sensory neurons contribute to pain associated with neuropathy-induced hypoxia.

Another argument for Aqp1's role in migration and elongation of sensory neurons has been described by Zhang & Verkman (2015) who demonstrated that Aqp1 promotes nerve regeneration in animals that have been subjected to a sciatic nerve compression injury. This group observed an upregulation of Aqp1 mRNA and protein in the DRG after a crush injury that was significant at day 7. By studying DRG cultures of Aqp1-deficient mice this group also found that axonal growth was impaired but could be rescued by transfection with Aqp1 or with an alternate water-transporting aquaporin, such as Aqp4. Transfection with non water-transporting Aqp1 mutants could not rescue the diminution of axonal extension. Thus, Aqp1 is essential to water transport facilitated extension of axonal outgrowths after injury.

Although peripheral axonal regeneration is an essential process for reinnervation of target tissues after injury, this process does not always lead to successful reinnervation and in fact may drive chronic pain (Xie et al., 2017). When neuropathic pain is initiated in rats by performing the spinal nerve ligation (SNL) model, the injured nerves regenerate and successfully reinnervate target tissue. However, if exposed to the SNI model which targets the sciatic nerve, a regenerative phenotype occurs in the injured axons but does not lead to successful reinnervation, instead resulting in the development of a neuroma and tangled neural processes at the site of injury, which contribute to chronic pain (Xie et al., 2017). By directly injecting the neuroma with an anti-regenerative compound the group found that chronic pain was attenuated. As such, long lasting chronic pain may reflect an anatomical inability for the regenerating nerves to successfully

reinnervate target tissues. Aqp1 antagonists directly applied to neuromas may be an effective treatment for chronic pain in instances that do not lend themselves to successful regeneration, i.e. limb amputation. This treatment would have to be exercised with caution where axonal regeneration is beneficial and leads to successful reinnervation of the target tissue.

The argument for not pursuing the role of Aqp1 in the development and maintenance of neuropathic pain as part of this study, is that previous work from our group has suggested that the Na<sub>v</sub>1.8+ population of neurons is not responsible for neuropathic pain (Abrahamsen et al., 2008). However, studies using the Na<sub>v</sub>1.8-Cre line (generated in our lab) to create conditional knockouts of specific genes believed to be responsible for the generation and maintenance of chronic pain argue against this. For example, much work has been done on the hyperpolarization-activated cyclic nucleotide-gated ion channel 2 (HCN2), which when conditionally deleted in the Na<sub>v</sub>1.8+ population of sensory neurons rescues mechanical hypersensitivity in mice which have undergone sciatic nerve chronic constriction injury (CCI) (Emery et al., 2011). The same can also be said of a model of diabetic neuropathy (Tsantoulas et al., 2017). Thus, constitutively ablating such a large portion of sensory neurons is likely to induce compensation within the affected animals to ensure survival. This may explain why Na<sub>v</sub>1.8<sup>DTA</sup> mice retain peripheral hypersensitivity similar to their WT counterparts as a consequence of neuropathic injury. For completeness it would be prudent to perform a study of the role of Aqp1 in neuropathic pain in Aqp1<sup>KO</sup> mice, however, where Aqp1's contribution to acute mechanical pain may be due to its ion channel function, Aqp1 likely promotes chronic pain via its water pores.

#### **3.5.4 Is there a possible role for Aqp1 in regulating the MA currents produced by Piezo2 *in vivo*?**

Interestingly, like Tentonin 3 (Anderson et al., 2018), the present study demonstrates that Aqp1 is capable of regulating the current produced by Piezo2 in HEK293T cells. Other such Piezo2 regulatory proteins have already been identified and include the mammalian MEC-2 orthologue, STOML3. STOML3 is able to reduce Piezo2 threshold of activation (Poole et al., 2014) by altering membrane stiffness (Qi et al., 2015). I propose that similarly to the *Xenopus* oocytes in which Aqp1's water channel function was discovered, Aqp1 expression in HEK293T exacerbates water transport leading to osmotically-induced cell swelling, and potentiates Piezo2 function in this manner (i.e. via its water channels). It was recently demonstrated that membrane stretch caused by osmotic swelling in the neurons of the rat DRG and also Piezo2-expressing HEK293 cells potentiates the MA current produced by Piezo2, and also alters its kinetics from rapidly adapting to slowly adapting. Furthermore, injecting a hypotonic solution into the paw of the rat caused a

reduction in the rat's withdrawal threshold to mechanical stimuli (Jia et al., 2016). Although a role for Piezo2 in acute mechanical pain has generally been excluded, a pathological role for it in mechanical allodynia and hyperalgesia has been identified (Eijkelkamp et al., 2013; Ferrari et al., 2015; Murthy et al., 2018; Szczot et al., 2018). Therefore, one may surmise that Aqp1's ability to potentiate Piezo2 activity may be relevant in pathological scenarios of cell damage and inflammation whereby Aqp1 exacerbates osmotically induced cell-swelling leading to enhanced noxious mechanosensitivity in these neurons. Unfortunately, my CFA findings do not support this hypothesis at least in a chronic inflammatory setting, as Aqp1<sup>KO</sup> animals did not exhibit a significant reduction in mechanical (or thermal) hypersensitivity after CFA injection in comparison to WT littermate controls. This is in line with the findings of Shields et al. (2007), although they did not publish their CFA von Frey data. Despite this, Piezo2 has been described as responsible for mediating tactile sensitisation under inflammatory conditions induced by CFA administration in mice, and capsaicin-mediated inflammation in humans (Szczot et al., 2018). Perhaps I do not observe a diminution of mechanical hypersensitivity in Aqp1<sup>KO</sup> mice as there is only a partial overlap between Piezo2 and Na<sub>v</sub>1.8-expressing sensory neurons, the latter of which Aqp1 expression is predominantly restricted to. Maybe there is a role for other aquaporins that are restricted to neuron subpopulations (such as the medium to large diameter neurons) that do express Piezo2, in inflammatory pain. Consequently, proteins that cause aberrant Piezo2 function under pathological conditions may be considerably effective therapeutic targets for treating pain

### **3.5.5 The contribution of other aquaporins to nociception**

Although Aqp1 has arguably been the main focus within the aquaporin family regarding PNS contribution to pain, there have been reports of other aquaporins also expressed in the PNS that are aberrantly regulated as a consequence of inflammation or neuropathy. Borsani, et al., (2009) report a significant upregulation of Aqp2 protein expression in the small-diameter neurons of the TG within four hours of formalin treatment, but also an increase in Aqp2 expression in the neuronal membrane of medium and large diameter TG neurons. This finding has been extended to an upregulation of Aqp2 in the DRG after chronic constriction injury (CCI) of the sciatic nerve (Buffoli et al., 2009). Interestingly, treatment of mice with NSAIDs, which inhibit PGE<sub>2</sub> synthesis, known to cause inflammatory hyperalgesia, has been demonstrated to reduce Aqp2 protein abundance in the renal medulla in normal and water-restricted rats (Ren et al., 2015). Could this perhaps be extrapolated to a reduction of aberrant Aqp2 expression in the PNS, in turn suggesting a role for Aqp2 in pathological pain states? Further work using conditional Aqp2 KO animals, as global Aqp2 deletion is lethal (Rojek et al., 2006), Aqp2 knockdown, or pharmaceutical targeting of Aqp2 would

be beneficial in teasing out any role that Aqp2 may have in behaving animals with respect to pain. As there is an upregulation of Aqp2 in the PNS due to inflammation one may predict that this is able to compensate for the loss of Aqp1 in the Aqp1<sup>KO</sup> mice, and thus hyperalgesia is retained in response to CFA injection in these animals.

Previous groups have stipulated that Aqp1's contribution to pain is due to indirect or direct interactions with well-characterised 'pain' ion channels such as TRPV1 and Na<sub>v</sub>1.8. I am the first to demonstrate a role for Aqp1 in mechanotransduction, my findings implicating Aqp1 in the production of slowly adapting mechanically activated currents in small diameter DRG neurons, and normal acute noxious mechanosensitivity in mice. My data also suggests that the role of Aqp1 in pain may be two-fold. Firstly, as a mechanosensitive ion channel responsible for acute mechanical sensing, and secondly as a water channel that may contribute to aberrant mechanical pain by exacerbating cell swelling and potentiating the current produced by innocuous mechanosensors, such as Piezo2.

### **3.6 Future directions**

Here I describe a novel role for Aqp1 in acute mechanical pain, an important addition to our understanding of the basis and complexity of noxious mechanosensitivity. However, this study also generates further questions, an important one being which component of Aqp1 contributes to acute noxious mechanosensation? Although I predict that it is the contribution of the ion channel, to definitively address this question, future work may also include the use of Aqp1-specific antagonists that either target the water channel or ion channel components of this protein. These include Bacopasode II, and AqB011, respectively (De Ieso et al., 2019). A combination of pharmacological treatment during mechano-clamp electrophysiology of cultured DRG neurons, in conjunction with administration to behaving animals would be just some of the ways that we could go about investigating this, and certainly would be an essential tool to deciphering the most efficacious means of targeting Aqp1 in pain patients. Not only that, the use of pharmacological compounds is an important tool for targeting proteins in the adult mice as opposed to genetic manipulations that delete a protein during development, which may lead to developmental compensation. Consequently, it may also be of interest to study the expression patterns of other relevant members of the aquaporin family (for example Aqp2 and Aqp4) in the PNS of Aqp1<sup>KO</sup> animals to determine if there is indeed an element of compensation, under basal and pathological conditions.

As mentioned, there is also clear scope for investigating the role of Aqp1 in neuropathic pain, however, like the acute pain studies; previous investigations have been relatively contradictory. Aqp1 has previously been demonstrated to contribute to mechanical allodynia in a SCI model of neuropathic pain (Nesic et al., 2008), however, studies using a model of peripheral neuropathic pain (SNI) indicate that Aqp1 may not play a role in this pathology (Shields et al., 2007). The latter study also found no phenotypic differences between animals with respect to acute pain sensing, although they did not perform a noxious mechanical assay, like the Randall-Selitto test I performed here. Considering Aqp1's potential to contribute to peripheral axonal elongation in response to nerve injury, it would certainly be interesting to explore, more so with respect to treating chronic pain, as acute pain sensing is essential to human survival, and caution must be taken when targeting proteins that have a role in this component of pain.

As is the case of all basic science, translation to humans is the most important aspect of this research. Published human Aqp1 mutation studies have yet to address a role for Aqp1 in pain

(Preston et al., 1994), that is not to say that it doesn't contribute, but there is an obvious requirement to establish this, which is understandably out of the scope of this research. This study and other studies before it argue a clear need to investigate these human mutations further.

The present study brings us another step closer to understanding the intricate processes that underlie acute mechanical pain. It emphasises the necessity of multiple proteins and protein complexes in noxious mechanosensation and offers an exciting novel insight into Piezo2 regulation. That Aqp1 does not produce a current in naïve HEK293T cells should not lessen the importance of its contribution to this process. Excitingly, my findings still leave scope for the discovery of a *bona fide* noxious mechanotransducer.

## **4 Investigating the role of Piezo2 in noxious mechanosensation**

### **4.1 Summary**

Recent publications have alluded to a role for the innocuous mechanosensor, Piezo2, in acute mechanical pain. The data described in the previous chapter indicates that Piezo2 may be susceptible to positive regulation within the Na<sub>v</sub>1.8+ population of sensory neurons by the water/ion channel Aqp1, causing a slowing in the kinetics of the MA current produced by Piezo2, which is associated with mechanical nociception. To probe the role of Piezo2 in acute noxious mechanosensing I deleted its expression in the Na<sub>v</sub>1.8+ cohort of sensory neurons in mice, those which are known to be responsible for transducing and transmitting this sensation. In doing so I also maintained the integrity of neurons responsible for proprioception, thus rendering the resulting animals with intact motor coordination. In generating these mice (using a Cre-lox mediated form of targeted Piezo2 deletion) I was able to probe the DRG neurons of these animals *in vitro* using mechano-clamp electrophysiology to determine the extent, if any, of changes to the repertoire of MA currents produced. I also interrogated the contribution of Piezo2 within the Na<sub>v</sub>1.8+ population of sensory neurons to acute innocuous and noxious sensation in the behaving animals. Recent advances in *in vivo* GCaMP imaging enabled me to explore the responses of DRG neurons (both Na<sub>v</sub>1.8+ and negative) to a host of stimuli in the intact, anaesthetised animal as a means of validating my electrophysiology and behavioural findings, and offering us an insight into Piezo2's role within the Na<sub>v</sub>1.8+ population of DRG neurons in contributing to acute inflammatory pain.

I report that Piezo2 does not contribute to acute mechanical pain in mice. Published conflicting evidence may be explained by defects in proprioception brought about by a more widespread DRG neuron Piezo2 deletion. However, my imaging data would suggest that within the Na<sub>v</sub>1.8+ sensory neuron population, Piezo2 may be responsible for mechanical allodynia/hyperalgesia as a consequence of acute inflammation, a phenomenon that requires further investigation. Prior publications have reported similar findings in response to inflammation, but the properties of the sensory neurons responsible have yet to be described. Similarly to the previous chapter, my findings suggest that there remains an as yet unidentified mechanotransducer(s) responsible for acute mechanical pain.

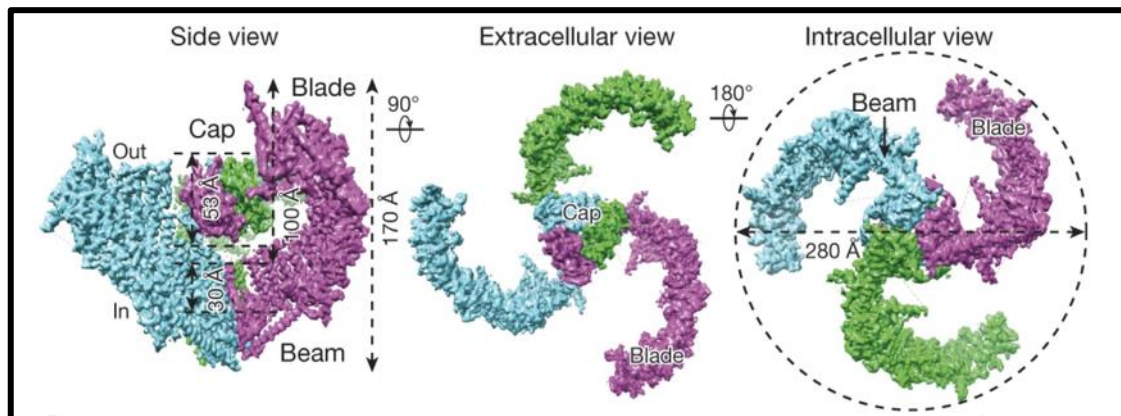
## **4.2 Introduction**

Piezo2 was identified as a *bona fide* mammalian mechanotransducer in 2010 by the group of Ardem Patapoutian after cloning its homologue, Piezo1 from the mouse neuroblastoma cell line, Neuro2A (N2A), and subsequent cloning of Piezo2 from mouse DRG neurons (Coste et al., 2010). Both Piezo proteins are evolutionarily conserved and produce excitatory mechanically activated non-selective cationic currents, but have differing expression patterns and thus functions within the body. Piezo1 expression is primarily restricted to non-neuronal cells, including vascular endothelial cells, bladder urothelial cells, erythrocytes, and chondrocytes. It responds to a range of physiological mechanical stimuli including cell stretch and shear stress (Wu et al., 2016). Piezo2 is expressed in cutaneous sensory end organs and within the sensory neurons of the PNS where it is responsible for detecting innocuous touch (Ranade et al., 2014; Woo et al., 2014), some elements of tactile pain (Murthy et al., 2018; Szczot et al., 2018), and conveying mammalian proprioception (Woo et al., 2015). Piezo2 is also expressed in the nodose ganglia where it is required for normal lung volume regulation in adult mice, and also in the neurons of neural crest origin where it is essential for efficient respiration in new born mice (Nonomura et al., 2017). The joint function of Piezo1 and Piezo2 in the nodose and petrosal sensory ganglia of mice is also required for normal arterial baroreceptor activity and function, critical to maintaining short-term blood pressure homeostasis in mammals (Zeng et al., 2018). Many of these observations in murine studies are recapitulated in human Piezo2 LOF mutations, which will be discussed shortly.

### **4.2.1 The structure and electrophysiological properties of Piezo2**

Piezo1 and Piezo2 proteins are exceptionally large, consisting of approximately 2500 and 2800 amino acid residues, respectively, with both proteins sharing approximately 42% homology. Recent cryo-electron microscopy studies have enabled researchers to establish the 3D structure of Piezo1 (Zhao et al., 2018), and Piezo2 (Wang et al., 2019), which both form homotrimeric non-planar propeller-like structures in the membrane (Figure 4.1). The blades of each Piezo2 protomer come together to create a curved dome within the membrane, with an extracellular cap structure at the homotrimer's centre formed from the C-terminal extracellular domains (CED) of each protomer. An intracellular beam connects and supports the central region and the proximal transmembrane helices of each blade. Each Piezo2 protomer consists of 38 transmembrane helices to create a channel complex comprised of 114 transmembrane helices in total, the largest number identified of any mammalian membrane protein.





**Figure 4.1. Diagram of a Piezo2 homotrimer**

Three Piezo2 protomers come together to form a homotrimer in the cell membrane. Each protomer creates a 'blade', and forms an extracellular cap with their extracellular C-terminal domains at the centre of the Piezo2 complex (Adapted from Wang et al. (2019)).

Despite these recent advances in determining piezo protein structure, their gating mechanisms have proved difficult to elucidate, much more so than transmembrane proteins gated by either voltage or ligands. Nevertheless, there are two key predicted models of mechanotransducer activation. The first is the 'force-from-lipid' model, which describes a mechanism by which a mechanotransducer is directly activated by force transmission from lipid to the channel (Ranade et al., 2015). This is likely to be the means by which Piezo1 is activated, as studies have demonstrated Piezo1 is capable of activation when expressed in lipid bilayers only, making this channel inherently mechanosensitive. This observation does not rule out the impact of the cytoskeleton and/or accessory proteins in regulating the mechanically activated current produced by Piezo1, especially since its kinetics, when expressed in a lipid membrane only, are much slower than those observed when it is expressed in cells (Syeda et al., 2016). Other inherently mechanosensitive channels include bacterial MscS and MscL channels, and mammalian TRAAK and TREK channels (Syeda et al., 2016). The second gating model posits that an extracellular or intracellular tether is required to link the mechanosensitive channel with the extracellular matrix and cytoskeleton of the cell to confer mechanosensitivity (Ranade et al., 2015). This model has been proposed for Piezo2 as Piezo2 activity has not been recorded in excised membrane patches or in artificial lipid bilayers (Moroni et al., 2018). Mechanotransducers gated by this mechanism also have the capacity to be regulated by additional auxiliary subunits, lipid rafts, or small molecules that are released during mechanical stimulation. An example of a Piezo2 regulator (as mentioned in the previous chapter) includes the MEC-2 homologue, STOML3, which is responsible for recruiting and binding cholesterol at the membrane, creating lipid raft complexes,

and causing an increase in membrane stiffness and subsequently Piezo2 sensitisation (Qi et al., 2015). An upregulation of STOML3 has been reported in mouse models of neuropathic pain, and small molecule inhibition of STOML3 reduces tactile allodynia in these animals (Wetzel et al., 2017).

Initial electrophysiological characterisation of Piezo2 was performed in the whole-cell mechano-clamp configuration in Piezo2-expressing HEK293T and N2A cells, and revealed a cation selectivity sequence of  $\text{Ca}^{2+} > \text{K}^+ > \text{Na}^+ > \text{Mg}^{2+}$ . The current-voltage relationship of Piezo2 is linear between -80 and +80 mV, and the MA currents it produces demonstrates a fast time constant for inactivation at <10 ms (Coste et al., 2010). However, work by Szczot et al. (2017) has since revealed that there are as many as 17 isoforms of Piezo2 found in mouse sensory neurons, with distinct rates of inactivation, ion permeability, and modulation by intracellular calcium. These isoforms appear essential to mechanosensory specialisation, examples of which include Piezo2 isoforms that express exon 35, which causes an increased rate of inactivation kinetics. Exon 35 isoforms are expressed in proprioceptors and LTMRs, and are undetectable in nociceptors such as those expressing the molecular marker, *Mrgprd* (Cavanaugh et al., 2009). It is proposed that conditions promoting mechanical allodynia or hyperalgesia might lead to changes in the expression of Piezo2 splice variants, resulting in altered mechanical sensitivity.

#### **4.2.2 The role of Piezo2 in pain**

Piezo2 conditional KO studies in mice using Cre-Lox recombinase have utilised the *Piezo2<sup>fl/fl</sup>* mouse generated by Ardem Patapoutian and colleagues (Ranade et al., 2014) to elucidate Piezo2's diverse functions within the body. These *Piezo2<sup>fl/fl</sup>* animals have been bred with mice expressing Cre recombinase in various tissue types, thus generating progeny with tissue-specific deletions of Piezo2, the phenotypes of which are summarised in Table 4.1. Using the inducible pan-neuronal Advillin-CreERT2 mouse (*Advil-CreERT2*), it was initially reported that Piezo2 is responsible for transducing light touch sensation, and with a Parvalbumin-Cre mouse (*PV-Cre*), proprioceptive cues. A topic of debate, however, is the extent to which (if any) Piezo2 is required for acute noxious mechanosensation, a key question that I will be addressing within this chapter.

The use of Piezo2 conditional KO mice, as well as Piezo2 antisense oligonucleotides, (either administered systemically or locally) have previously indicated that Piezo2 contributes to pathological mechanical pain. The first example of this described a significant attenuation of mechanical allodynia in two models of neuropathic pain in mice, after intrathecal injection of

Piezo2 antisense ODNs (oligodeoxynucleotides) (Eijkelkamp et al., 2013). Piezo2's ability to contribute to mechanical hyperalgesia was demonstrated by Ferrari et al. (2015) who showed an elimination of stimulus-dependent mechanical hyperalgesia caused by an injection of the pronociceptive mediators endothelin-1 and oxaliplatin, after injection of Piezo2 antisense ODNs in the area of nociceptive testing (hind paw). However, conflicting evidence using a Cre-Lox approach indicated that Piezo2 does not contribute to either acute mechanical pain, or to CFA or Bradykinin-induced inflammatory mechanical hyperalgesia (Murthy et al., 2018; Ranade et al., 2014; Woo et al., 2015). These particular examples used *Advil-CreERT2*, and may be the reason as to why more extreme phenotypes are observed in the non-inducible versions of these Cres, some of which have proven to be perinatally lethal (Nonomura et al., 2017; Ranade et al., 2014; Zhang et al., 2019). Such non-inducible Cres include the *HoxB8-Cre* that targets Piezo2 expression in the DRG and spinal cord (Murthy et al., 2018; Woo et al., 2015). In this instance animals had severe proprioceptive deficits in their hind limbs, as well as a deficit in innocuous mechanical sensing. However, contrary to the same group's initial findings using the *Advil-CreERT2* mouse (Ranade et al., 2014), Murthy et al. (2018) found that *Piezo2<sup>fl/fl</sup>;HoxB8-Cre* (*Piezo2<sup>HoxB8</sup>*) animals also had a deficit in acute noxious mechanosensing as evidenced using the pinprick and tail clip assays. They also found no reduction in mechanical threshold in *Piezo2<sup>HoxB8</sup>* animals injected with capsaicin, and no development of mechanical allodynia after the spared SNI model of neuropathic pain was performed on these mice. A reduction in hyperalgesia was also observed at week 1 but not at 2 and 3. In a complete contradiction, the use of a non-inducible *Advil-Cre* crossed with *Piezo2<sup>fl/fl</sup>* animals by a separate group resulted in progeny that were sensitised as opposed to desensitised to noxious mechanical stimuli (Zhang et al., 2019).

Method of Piezo2 deletion	Cre/antisense	Targeted region	Phenotype	Additional notes	Reference
Cre/Lox using Piezo2 <sup>fl/fl</sup> animal	<i>Advil-Cre</i>	All DRG neurons	<ul style="list-style-type: none"> <li>Perinatal lethality</li> </ul>		(Ranade et al., 2014)
	<i>Advil-CreERT2</i> (tamoxifen administered in adult mice)	All DRG neurons	<ul style="list-style-type: none"> <li>Deficits in innocuous tactile sensation (hairy and glabrous skin)</li> <li>Unstable gait</li> <li><b>Capsaicin – only slight lowering of mechanical threshold (vF)</b></li> <li>RS and TC normal</li> <li>CFA and Bradykinin normal</li> </ul>	~90% deletion of Piezo2 transcripts in DRG	(Murthy et al., 2018; Ranade et al., 2014; Woo et al., 2015)
	<i>Krt14-Cre</i>	All epithelial cells including Merkel cells	<ul style="list-style-type: none"> <li>Deficits in innocuous tactile sensation (automated vF)</li> </ul>		(Woo et al., 2014)
	<i>HoxB8-Cre</i>	Caudal spinal cord/all DRG neurons	<ul style="list-style-type: none"> <li>Severe proprioceptive deficits in hind limbs</li> <li>Severe deficit in innocuous mechanical sensation</li> <li><b>Some deficits in noxious mechanosensation (PP and TC)</b></li> <li><b>Capsaicin - no lowering of mechanical threshold</b></li> <li><b>SNI - no punctate (vF) or dynamic (brush) mechanical allodynia</b></li> <li><b>Reduced hyperalgesia (PP) at 1 week</b> but not at 2 or 3 weeks after injury</li> </ul>		(Murthy et al., 2018; Woo et al., 2015)
	<i>PV-Cre</i>	Proprioceptors and some cutaneous mechanoreceptors	<ul style="list-style-type: none"> <li>Severe proprioceptive deficits in all four limbs</li> </ul>		(Woo et al., 2015)
	<i>Advil-Cre1</i> (Heppenstall)	All DRG neurons	<ul style="list-style-type: none"> <li>Deficits in gentle touch and proprioception</li> <li><b>Sensitised mechanical pain response (RS)</b></li> </ul>	Cre activity in 75% DRG neurons Deletion in ~ 40-60% of LTMRs Near complete deletion in IB4 +ve neurons	(Zhang et al., 2019)
	<i>Advil-Cre2</i> (Wang)	All DRG neurons	<ul style="list-style-type: none"> <li>Lethal</li> </ul>	Cre activity in 95% of DRG neurons	(Zhang et al., 2019)
Antisense oligonucleotides	Piezo2 antisense ODN intrathecal injection daily (during chronic neuropathic pain models)	DRG neurons (and spinal cord)	<ul style="list-style-type: none"> <li>Deficits in innocuous touch (vF)</li> <li>Noxious heat and mechanical stimulation unchanged</li> <li><b>Mechanical allodynia significantly attenuated in L5 SNT, and CCI</b></li> </ul>	~35% - 50% reduction in mRNA expression in L2-L6 DRG	(Eijkelkamp et al., 2013)
	Piezo2 antisense ODN injection in area of nociceptive testing (hind paw)  Piezo2 antisense ODN intrathecal injection		<ul style="list-style-type: none"> <li><b>Stimulus-dependent mechanical hyperalgesia eliminated</b> (after injection of pronociceptive mediator endothelin-1, and intravenous injection of oxaliplatin)</li> <li>Hyperalgesia not eliminated when injected intrathecally</li> </ul>	In rats	(Ferrari et al., 2015)

**Table 4.1. Summary of murine Piezo2 deletions and resulting phenotype**

All experiments are in mice unless otherwise stated. Those phenotypes relating to mechanical pain are highlighted in bold.

### **4.2.3 Piezo2 human mutations**

How do we reconcile such contradictory findings? Where genetic manipulation and subsequent phenotypic characterisation of mice may be insightful, it can be conflicting, as such, it is always exceptionally informative if there are human mutations to turn to. A number of rare GOF and LOF human Piezo2 mutations have been reported since Piezo2's identification and are summarised in Table 4.2. Interestingly, a key characteristic of both Piezo2 GOF and LOF mutations is distal arthrogyriposis, i.e. contractures in the joints of the lower arms and lower legs. In LOF patients, a lack of proprioceptive feedback in utero likely leads to this pathology. GOF mutations are typically autosomal dominant, often occur spontaneously, and have been identified in exons 15 up to and including exon 52. Electrophysiological studies on cells heterologously expressing some of these mutated variants of Piezo2 (Glu2727del and Ile802Phe) reveal a faster recovery from inactivation, as well as a slowing of inactivation (Coste et al., 2013). Piezo2 LOF mutations are autosomal recessive, requiring two copies of the defective Piezo2 gene in order to generate pathophysiological symptoms. As well as arthrogyriposis, patients with LOF mutations suffer from symptoms including proprioceptive and motor deficits, and impaired touch perception. In some cases, this has also included spontaneously resolving respiratory insufficiency at birth (Delle Vedove et al., 2016). Somewhat reassuringly, these are all symptoms that have been described in Piezo2 KO mice to some varying degree. Importantly, in the context of this study, pain phenotyping of these patients demonstrates that acute mechano-nociception remains intact (Chesler et al., 2016). However, functional Piezo2 is deemed essential for the generation and maintenance of inflammation-induced mechanical allodynia (Szczot et al., 2018).

	Piezo2 Mutation	Exon	Inheritance	Phenotype	Additional notes	Reference
Gain-of-function	p.Glu2727del p.Ile802Phe	52 17	Autosomal dominant	DA5* DA5*  *With ophthalmoplegia, ptosis, and restrictive lung disease	Both mutations cause MA currents to recover faster from inactivation, p.Glu2727del also causes a slowing of inactivation	(Coste et al., 2013)
	p.Trp2746* p.Ser2739Pro p.Tyr2727Ilefs*7 p.Glu2727del p.Arg2718Pro p.Arg2718Leu p.Arg2686His p.Arg2686Cys p.Thr2356Met p.Ser2223Leu p.Thr2221Ile p.Met998Thr p.Met712Val	52 52 52 52 52 52 52 52 45 45 43 20 15	Autosomal dominant	GS DA5 DA5 DA5 DA5 DA5 DA5 MWS DA5 DA5 DA5 DA5 DA5	Eleven of these mutations believed to alter amino acids in the intracellular C-terminal domain	(McMillin et al., 2014)
	p.Ala1486Pro	30	Autosomal dominant	DA5		(Okubo et al., 2015)
	p.Arg1575* p.Arg1685* p.Arg1685Pro	32 35 35	Two compound heterozygous autosomal recessive mutations	A,b,d, e Loss of vibration detection, touch discrimination (glabrous skin), and joint proprioception	Mutations believed to be prior to the pore-forming region	(Chesler et al., 2016)
Loss-of-function	p.Pro1007Leufs*3 p.Ser517Thrfs*48 p.Leu1874Argfs*5 del exons 6-7	20 13 37	Three homozygous autosomal recessive mutations, and one homozygous deletion of two exons	A, b, e Spontaneously resolving respiratory insufficiency at birth, muscular atrophy and mild distal sensory involvement	Mutations localised to the N-terminal and central region	(Delle Vedove et al., 2016)
	p.Ser903*	18	Three homozygous autosomal recessive mutations	A,b, c, e Impaired proprioception and touch		(Mahmud et al., 2017)
	p.Arg462*	12	Homozygous autosomal recessive mutation	A, b Sensory ataxia, proprioception defect, myopathy, and progressive respiratory failure		(Haliloglu et al., 2017)
	p.Arg1710* p.Gln362* p.His2002fs p.Tyr426X p.R462* p.Ser2602* c.7515+1G>A	43 7 38 9 12 49 46	Three compound heterozygous autosomal recessive mutations and and homozygous autosomal recessive	A,b,e, Loss of touch discrimination, loss of inflammatory tactile allodynia, but normal acute mechanical pain sensing		(Nagi et al., 2019; Szczot et al., 2018)
	p.Val1391Lysfs*39	27	Homozygous autosomal recessive	A,b,c areflexia		(Yamaguchi et al., 2019)

**Table 4.2. Summary of human Piezo2 GOF and LOF mutations**

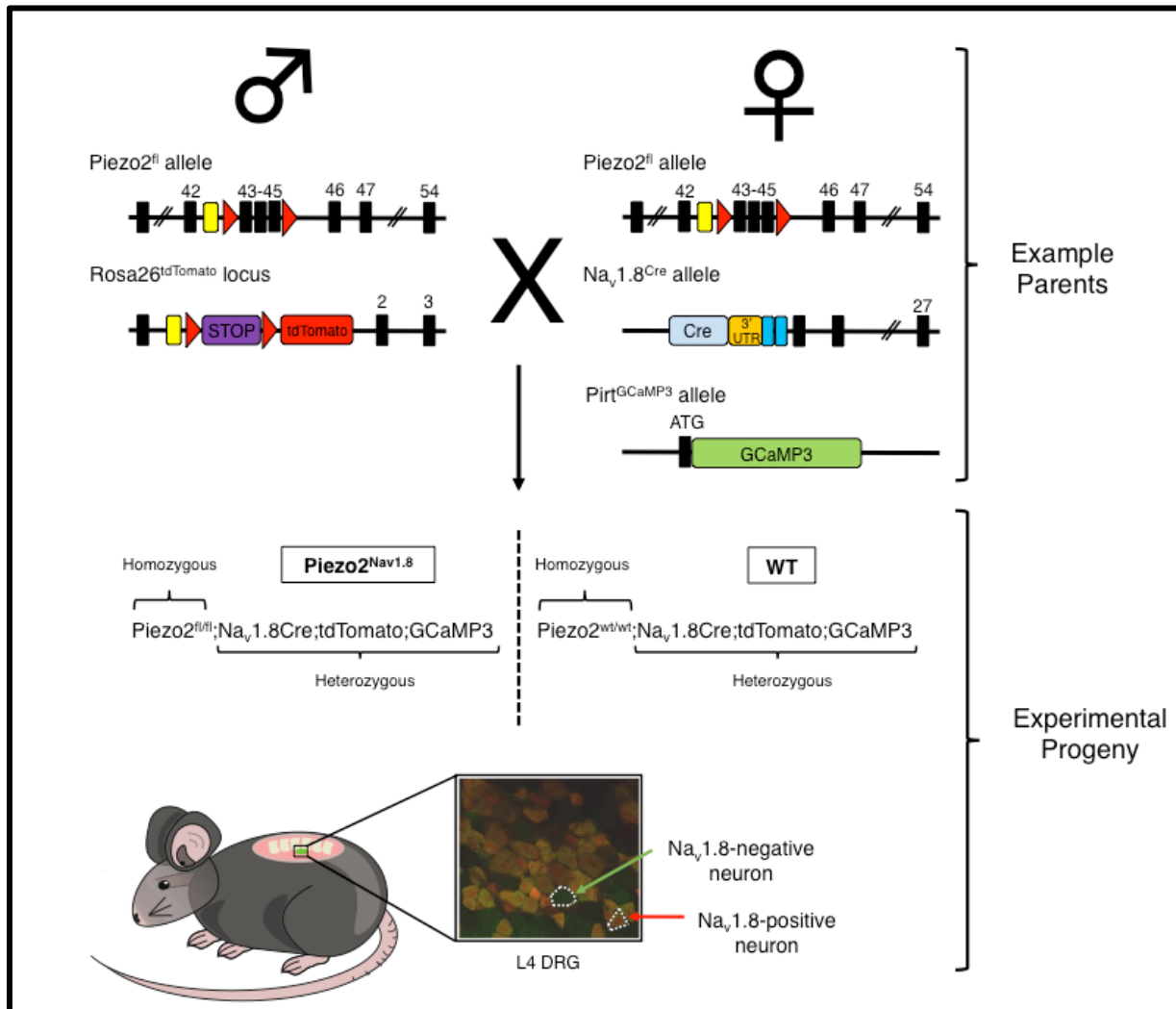
DA5, distal arthrogyposis 5; GS, Gordon syndrome; MWS, Marden-Walker syndrome; A, congenital arthrogyposis; B, progressive scoliosis; C, growth impairment; D, hip dysplasia at birth; E, motor impairment.

To address the conflicting data published on Piezo2 conditional KO mice with regard to mechanical pain sensitivity, I bred Piezo2<sup>fl/fl</sup> animals with Na<sub>v</sub>1.8-Cre mice (generated in our lab (Nassar et al., 2004)) creating Piezo2<sup>fl/fl</sup>;Na<sub>v</sub>1.8-Cre (Piezo2<sup>Nav1.8</sup>) progeny, where Piezo2 is deleted in the peripheral Na<sub>v</sub>1.8+ neurons only. Na<sub>v</sub>1.8 is a VGSC alpha subunit encoded for by the gene *SCN10A*. As described previously, its expression is restricted to a population of peripheral sensory neurons that are essential for acute cold pain, inflammatory pain, and importantly, acute mechanical pain (Abrahamsen et al., 2008). Another key feature of these sensory neurons is that there is no predicted overlap with those expressing Parvalbumin, i.e. proprioceptors (Shields et al., 2012). In this way I hoped to tease out any role that Piezo2 may have in acute mechanical pain *in vivo*, by generating animals that had no deficits in motor coordination that may have consequently compounded the results of our pain behaviour assays, and perhaps those of which have already been published.

#### **4.2.4 Breeding strategy for Piezo2<sup>fl/fl</sup>;Na<sub>v</sub>1.8-Cre;tdTomato;GCaMP3 mice**

Unless otherwise stated, mice were acquired from The Jackson Laboratory. Mice heterozygous for the Piezo2<sup>fl</sup> allele (kindly donated by Ardem Patapoutian, The Scripps Research Institute, Jackson Laboratory stock no. 027720) and the Rosa26-LSL-tdTomato (tdTomato) allele (stock no. 007909) were bred to animals also heterozygous for the Piezo2<sup>fl</sup> allele, the Na<sub>v</sub>1.8-Cre allele (generated as described in Nassar et al., (2004)), and the *Pirt*-GCaMP3 (GCaMP3) allele (generated by Xinzhong Dong, Johns Hopkins University) (Figure 4.2). Experimental electrophysiology and imaging animals were homozygous for Piezo2<sup>fl</sup> and heterozygous for Na<sub>v</sub>1.8-Cre;tdTomato;GCaMP3 (Piezo2<sup>Nav1.8</sup>), and WT animals were Piezo2<sup>wt/wt</sup> but also heterozygous for Na<sub>v</sub>1.8-Cre;tdTomato;GCaMP3 (WT). Those used for behavioural experiments were either Piezo2<sup>fl/fl</sup> and heterozygous for Na<sub>v</sub>1.8-Cre (Piezo2<sup>Nav1.8</sup>), or Piezo2<sup>wt/wt</sup> and

heterozygous or WT for the  $Na_v1.8$ -Cre allele (WT). The primers used for genotyping are shown in Table 4.3.



**Figure 4.2. Example breeding strategy for  $Piezo2^{fl/fl};Na_v1.8$ -Cre;tdTomato;GCaMP3 mice**

The red arrowheads denote loxP sites. These flank exons 43-45 in the  $Piezo2^{fl}$  allele, which when excised results in a frameshift mutation and the introduction of an early stop codon. Male mice heterozygous for the  $Piezo2^{fl}$  allele and for the Rosa26-LSL-tdTomato allele were bred to female mice heterozygous for the  $Piezo2^{fl}$  allele, the  $Na_v1.8$ -Cre allele, and the  $Pirt$ -GCaMP3 allele, to produce experimental progeny that were homozygous for  $Piezo2^{fl}$  and heterozygous for  $Na_v1.8$ -Cre;tdTomato;GCaMP3. Animals that were WT for the  $Piezo2^{fl}$  allele but heterozygous for  $Na_v1.8$ -Cre;tdTomato;GCaMP3 were used as WT controls. The DRG neurons of both genotypes expressed the fluorescent reporter tdTomato in  $Na_v1.8$ -positive peripheral neurons on a background of GCaMP3 expression.



Gene	Primer	Sequence	WT band	Mutant band
Piezo2	WT Fwd	GAAAGTAAGTCTGAATCTCTC	367 bp	509 bp
	Mut Fwd	GTCGACGGTATCGATAAGCT		
	Common Rev	TCCTTTCTGGCTACTGTTCC		
GCaMP3	Common Fwd	TCCCCTCTACTGAGAGCCAG	400 bp	300 bp
	WT Rev	GGCCCTATCATCCTGAGCAC		
	Mut Rev	ATAGCTCTGACTGCGTGACC		
Nav1.8-Cre	WT Fwd	CAGTGGTCAGGCTGTCACCA	258 bp	346 bp
	Mut Fwd	AAATGTTGCTGGATAGTTTTACTGCC		
	Common Rev	ACAGGCCTTCAAGTCCAAGTCC		
tdTomato	WT Fwd	AAGGGAGCTGCAGTGGAGTA	297 bp	196 bp
	WT Rev	CCGAAAATCTGTGGGAAGTC		
	Mut Fwd	GGCATTAAAGCAGCGTATCC		
	Mut Rev	CTGTTCCCTGTACGGCATGG		

**Table 4.3. Genotyping primers for Piezo2<sup>fl/fl</sup>;Nav1.8-Cre;tdTomato;GCaMP3 mice**

### 4.3 **Aims**

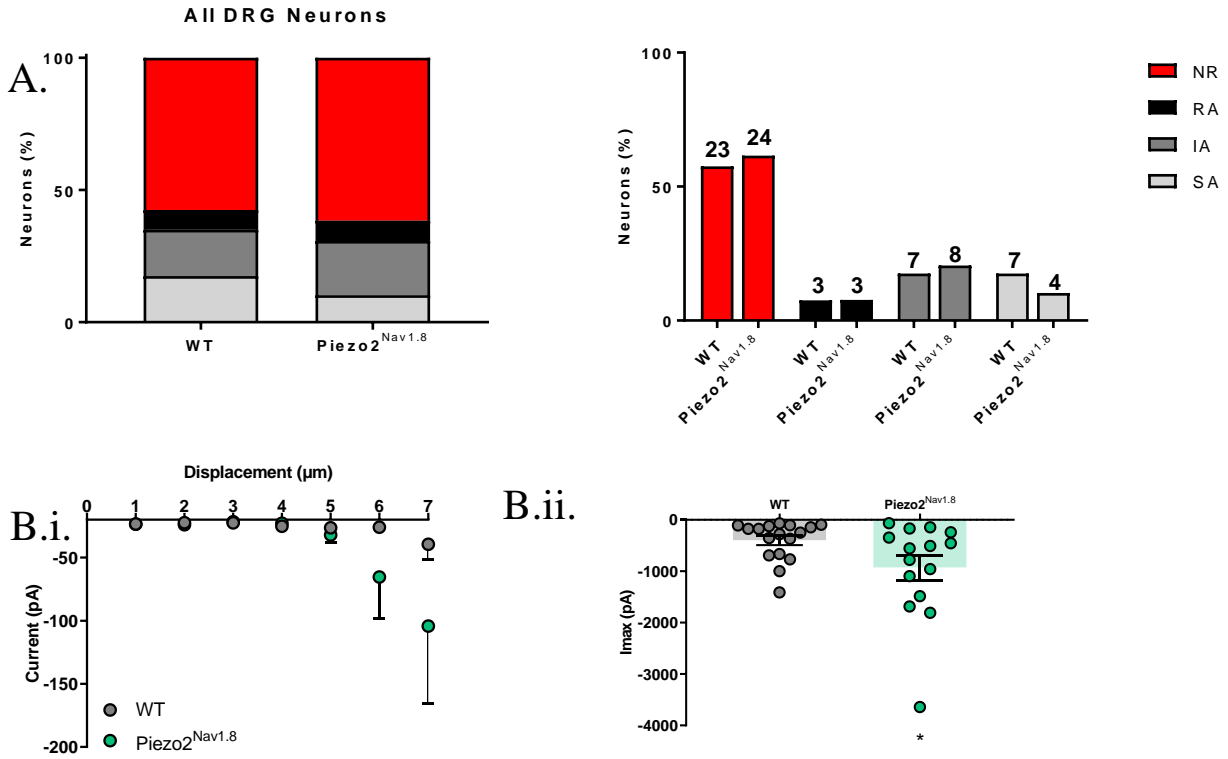
- To assess the role of Piezo2 *in vitro* by performing mechano-clamp electrophysiology on the cultured DRG neurons of Piezo2<sup>Nav1.8</sup> mice
- To investigate the role of Piezo2 *in vivo* in both anaesthetised mice, using GCaMP imaging of the DRG, and in awake mice using behavioural assays
- We will also briefly look at the expression pattern of Piezo2 and Piezo1 with regard to Nav1.8-expressing peripheral sensory neurons using RNAScope *in situ* hybridisation

## 4.4 Results

### 4.4.1 Genetic deletion of Piezo2 in Nav1.8+ sensory neurons does not significantly alter the repertoire of mechanically activated currents that they produce, but does potentiate current amplitude

As demonstrated in the previous chapter, when heterologously expressed in HEK293T cells, Piezo2 consistently produces an RA MA current when these cells are exposed to mechano-clamp electrophysiology. Piezo2 is also required for the production of RA currents in the cultured sensory neurons of mice (Ranade et al., 2014). In this experiment I aimed to assess the difference in the repertoire (i.e. the number of SA, IA, and RA) of MA currents produced by Nav1.8+ DRG neurons in Piezo2<sup>Nav1.8</sup> mice versus WT mice. In order to identify Nav1.8+ neurons I used mice expressing a Cre-driven reporter, Rosa26-LSL-tdTomato, so as to restrict tomato expression to the Nav1.8+ population only. As has been described elsewhere, I found that approximately 75% of cultured DRG neurons were Nav1.8+ (Shields et al., 2012). When probed electrophysiologically I observed a small reduction in the number of RA and SA currents produced by Piezo2<sup>Nav1.8</sup> Nav1.8+ neurons in comparison to Nav1.8+ WT neurons, but not enough for this finding to be significant (Figure 4.3.A). What is quite striking is the number of non-responding cells in both cohorts. Reassuringly we see a similar proportion of non-responding small DRG neurons (those with a capacitance of <20 pF) in the Aqp1 study. For comparison, the average membrane capacitance of the cells I recorded from in this study was 19.9 (SD = 7.9) pF and 25.1 (SD = 15.1) pF for WT and Piezo2<sup>Nav1.8</sup> DRG neurons, respectively, and is not surprising considering that Nav1.8+ DRG neurons are predominantly small-diameter. These capacitances are substantially smaller than the 42.3 (SD = 20.1) pF, and 30.3 (SD = 22.6) pF pooled average capacitance of all DRG neurons recorded from in WT and Aqp1<sup>KO</sup> DRG, again in the Aqp1 study. This is likely a characteristic of small-diameter neurons, and has been described elsewhere (Drew et al., 2004).

Another interesting observation is the significantly increased I<sub>max</sub> in Piezo2<sup>Nav1.8</sup> DRG neurons versus WT neurons (WT = -398.8 ± 92.64 pA; Piezo2<sup>Nav1.8</sup> = -929.5 ± 242.5 pA; p = 0.0405) (Figure 4.3.B.ii). This is reflected in the increased activity I observe in Piezo2<sup>Nav1.8</sup> DRG neurons in response to noxious mechanical stimuli applied to the hind paw of these animals during the *in vivo* calcium imaging experiments I will shortly discuss.



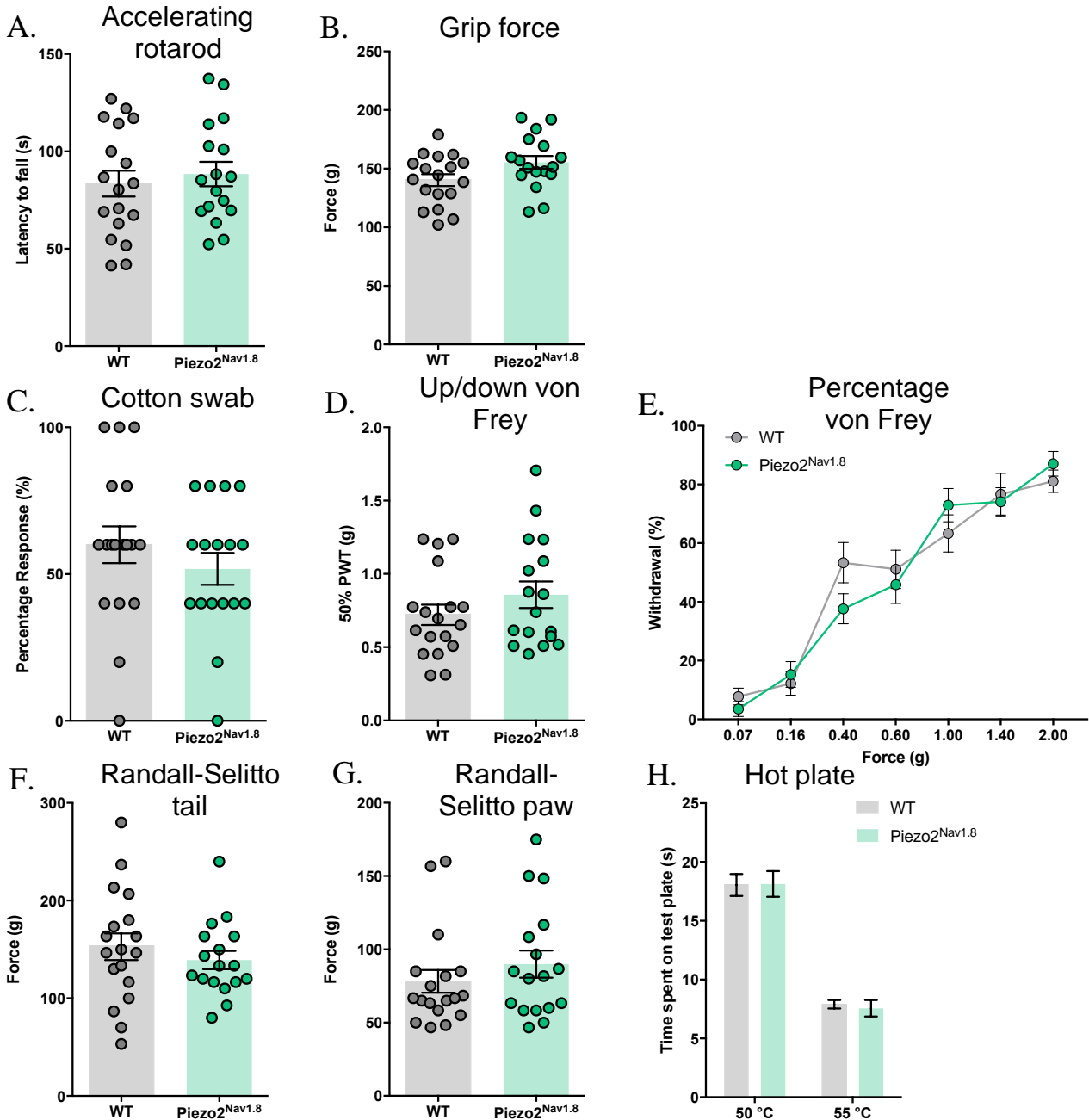
**Figure 4.3. Electrophysiological characterisation of DRG neurons from Piezo2<sup>Nav1.8</sup> mice and WT littermate controls**

**A.** The proportion of MA currents produced by all DRG neurons of Piezo2<sup>Nav1.8</sup> and WT mice. No significant difference between genotypes. Ordinary two-way ANOVA with Sidak's multiple comparisons test **B.i.** Average amplitude of MA currents produced by responding Piezo2<sup>Nav1.8</sup> and WT DRG neurons in response to increasing membrane displacement. 7 μm was the depth at which the first recording was lost. **B.ii.** The average maximal current amplitude of all responding DRG neurons before each recording was lost. Unpaired student's t-test. Data are shown as Mean ± SEM. (WT DRG neurons n=43; Piezo2<sup>Nav1.8</sup> n=39)

#### 4.4.2 Piezo2<sup>Nav1.8</sup> animals have normal mechanical sensitivity *in vivo*

In order to determine the effect of knocking-out Piezo2 in the Na<sub>v</sub>1.8+ population of sensory neurons *in vivo*, I performed a range of behavioural assays on these mice, again, including those that either apply an innocuous dynamic or punctate mechanical stimulus to the hind paw, as well as noxious mechanical, and noxious thermal tests. To first determine that these animals had no motor or proprioceptive deficits (as is the case in animals in which Piezo2 is conditionally knocked-out of Advillin, HoxB8, and Parvalbumin-expressing sensory neurons) I performed the accelerating rotarod assay (Figure 4.4.A), and a grip-force assay assessing all four limbs (Figure 4.4.B). There were no significant differences observed in the performance of the Piezo2<sup>Nav1.8</sup> mice versus their WT littermates. Thus, subsequent behavioural phenotypes could not be deemed a consequence of motor impairment.

As the Na<sub>v</sub>1.8+ population of neurons is reported essential for acute noxious mechanical pain but not for innocuous touch sensation (Abrahamsen et al., 2008), one would expect Piezo2<sup>Nav1.8</sup> mice to respond in the same way as their WT littermates to innocuous mechanical stimulation of the hind paw. This was found to be the case both in the dynamic cotton swab assay where the percentage of withdrawals from the cotton swab was not statistically different (WT = 60 ± 6.262%; Piezo2<sup>Nav1.8</sup> = 51.76 ± 5.439%; p= 0.3304) (Figure 4.4.C), and in the punctate up/down (WT = 0.7206 ± 0.06993g; Piezo2<sup>Nav1.8</sup> = 0.8578 ± 0.09028g; p= 0.2351) and percentage von Frey assays (Figure 4.4.D and E). Any involvement of Piezo2 within the Na<sub>v</sub>1.8+ population in acute noxious mechanosensing should have been observed with the noxious Randall-Selitto assay, which was applied to both the tail and the hind paw in this instance. The response of Piezo2<sup>Nav1.8</sup> mice to this assay was not significantly different to those of the WT animals in the tail (WT = 152.8 ± 13.69g; Piezo2<sup>Nav1.8</sup> = 139.2 ± 9.277g; p= 0.4221) or the hind paw (WT = 78.15 ± 7.78g; Piezo2<sup>Nav1.8</sup> = 89.9 ± 9.261g; p= 0.3362) suggesting that Piezo2 expression in this population of neurons is not responsible for acute noxious mechanosensation. Na<sub>v</sub>1.8+ neurons are also deemed essential to acute and chronic inflammatory pain, both stimulus-independent, and in the presence of mechanical and thermal stimuli. It would be prudent to examine the role of Piezo2 in this population of neurons when exposed to inflammatory mediators *in vivo*, but unfortunately this was outside the scope of this thesis. A further argument to perform these experiments may also be demonstrated in the following imaging data.



**Figure 4.4. Acute behavioural characterisation of Piezo2<sup>Nav1.8</sup> mice**

**A.** Accelerating rotarod. **B.** Grip-force assay. This measures the maximum force applied by all four paws to a plastic grid as they are gently pulled from it. **C.** Cotton swab test assessing innocuous dynamic mechanical sensitivity. Statistical analysis performed using the Mann-Whitney test **D.** Up/down von Frey. **E.** Percentage von Frey. The same filament was applied to the hind paw five times and the number of times the animal withdrew from the stimulus was recorded. **F.** Randall-Selitto assay applied to the base of the tail. **G.** Randall-Selitto assay applied to the hind paw. **H.** Hot plate assay. Data are shown as Mean ± SEM. Statistical analysis was performed using the unpaired Student's t test unless stated otherwise. (WT n=18; Piezo2<sup>Nav1.8</sup> n=17).

#### **4.4.3 Imaging in Piezo2<sup>Nav1.8</sup> mice reveals a possible means of sensory compensation within the Na<sub>v</sub>1.8-negative population of DRG neurons under basal conditions**

*In vivo* GCaMP imaging at the level of the DRG has recently gained traction, a key benefit of which is that the physiology of the animal including sensory pathways remain intact throughout testing. This technique also allows for a large population of cells to be interrogated at any one time, as opposed to traditional electrophysiological techniques that typically target a single cell. By again using the reporter tdTomato to genetically label Na<sub>v</sub>1.8-expressing neurons, on a background of pan-neuronally expressed GCaMP3 (see Figure 4.2 for details on the experimental progeny), I was able to analyse the response of Na<sub>v</sub>1.8+ and negative cells to a range of stimuli applied to the hind paw of anaesthetised WT and Piezo2<sup>Nav1.8</sup> mice. All imaging was performed on the left DRG at lumbar level 4 (L4), and the stimuli applied (see main methods for stimulus protocol) were predominantly mechanical, encompassing as broad a range of discrete mechanical sensations as possible. Noxious heat and noxious cold stimuli were used as modality controls and as a means of determining the extent of polymodality within the DRG neurons. I injected the inflammatory agent PGE<sub>2</sub> (20 µl of a 500 µM concentration) into the hind paw of the animal after performing an initial round of the stimulus protocol. I then repeated the protocol 5 minutes after administration of PGE<sub>2</sub> to see if/how neuron responses differed. PGE<sub>2</sub> is a proalgesic produced by inflammatory cells as a consequence of tissue damage and damage to peripheral neurons, the levels of which are up-regulated in the injured nerves of rats. Perineural injection of COX2 (Cyclooxygenase 2) (an upstream regulator of PGE<sub>2</sub>) inhibitor into the injured nerve attenuates neuropathic pain in rats. PGE<sub>2</sub> is thus considered to contribute to the maintenance of chronic pain (Ma et al., 2010). The benefit of using PGE<sub>2</sub> in this study is that it is also a robust model of acute inflammatory pain; pain behaviour is observed in awake rodents in as little as 5 minutes after injection into the hind paw (Kassuya et al., 2007). The short timeframe with which it takes effect allows for the imaging of the same animal before and after PGE<sub>2</sub> administration, shedding light on the peripheral mechanisms that underpin acute inflammation, and potentially those that drive the generation of chronic pain.

A WT control proved exceptionally beneficial as a means of confirming consistency between my data and that which is already published, and not just as a comparison for my Piezo2<sup>Nav1.8</sup> mice. Under basal conditions the majority of responding DRG neurons in the WT mice respond to the most noxious stimuli, i.e. pinch and 55 °C (Figure 4.5.A.i), this is consistent with a publication also comparing the response profile of neurons to thermal and mechanical stimuli (Wang et al., 2018). I also find that a much larger proportion of Na<sub>v</sub>1.8-negative sensory neurons respond to a noxious cold stimulus than any other modality, this was also reported by Luiz et al., (2019), in which they

effectively used the same WT mice as I describe here (i.e. animals heterozygous for *Pirt*-GCaMP3,  $\text{Na}_v1.8$ -Cre, and a Cre-dependent tdTomato reporter). Prior to their 2019 study, the same group also published their findings on DRG neuron responses to noxious mechanical and thermal stimuli in the presence and absence of  $\text{PGE}_2$ , finding an increase in fluorescence, hence activity, of neurons responding to noxious thermal stimuli after localised injection of  $\text{PGE}_2$  (Emery et al., 2016). I also find this to be the case in my WT animals (Figure 4.6.A.i). One of the primary focuses of the Emery et al. (2016) study was to investigate the extent of polymodality within DRG neurons. My data describes polymodality that is marginally greater than that reported by Emery et al., (2016) under basal conditions (~15% of DRG neurons in WT animals (Figure 4.5.B)) but may be reconciled by the increased number of mechanical modalities assessed within this study. This percentage then jumps to ~17% after injection of  $\text{PGE}_2$  in my WT animals, a modest increase that is also observed by Emery et al. (2016).

Reassuringly, I observe fewer  $\text{Na}_v1.8+$  neurons responding to innocuous dynamic stimuli in the  $\text{Piezo2}^{\text{Nav1.8}}$  animals pre and post  $\text{PGE}_2$  application (Figure 4.5.D.i), which is in-keeping with previous reports looking at the response of  $\text{Piezo2}$  KO TG neurons to a brush stimulus applied to the cheek pre and post exposure to capsaicin (Szczot et al., 2018). This also may reflect the slight diminution in sensitivity I observe in the behaving animals to innocuous tactile sensation. Considering  $\text{Piezo2}$  is known to transduce innocuous tactile sensation, and is expressed in a portion of  $\text{Na}_v1.8+$  neurons, some of which are also known to be LTMRs, this is as you would expect. I find some  $\text{Na}_v1.8+$  neurons do respond to these stimuli in the WT animals. Despite this, it is important to draw attention to the few responses I see here in both genotypes as a consequence of innocuous mechanical stimulation when compared to more noxious mechanical and thermal stimuli. This is something that will be discussed in the following chapter, but I find that the use of *Pirt* (Phosphoinositide interacting regulator of TRP) as a promoter does not result in pan-neuronal DRG GCaMP3 expression. Overlap between *Pirt* and a portion of LTMRs is minimal, and true pan-neuronal GCaMP expression results in a greater proportion of observed neurons responding to innocuous stimuli. We know that the behaving animals (both WT and  $\text{Piezo2}^{\text{Nav1.8}}$ ) do respond to this form of stimulation.

Interestingly, a similar number of cells respond to a vibration stimulus in both genotypes, however, a greater proportion of  $\text{Na}_v1.8$ -negative neurons respond in the  $\text{Piezo2}^{\text{Nav1.8}}$  animals (Figure 4.5.A.i and D.i). Whether or not this alludes to a form of compensation remains to be fully determined as I did not have the means to perform the equivalent vibration behavioural assay.



The argument for compensation is increased with the observation that the  $\text{Na}_v1.8$ -negative neurons responding to vibration in  $\text{Piezo2}^{\text{Nav1.8}}$  animals do not respond to any other stimuli before and after the addition of  $\text{PGE}_2$  (Figure 4.5.D.ii) which is not the case in the WT mice (Figure 4.5.A.ii), the vast majority of which do respond to multiple stimuli, and after the addition of  $\text{PGE}_2$ , all do. This indicates that vibration-sensitive neurons have differing characteristics between genotypes.

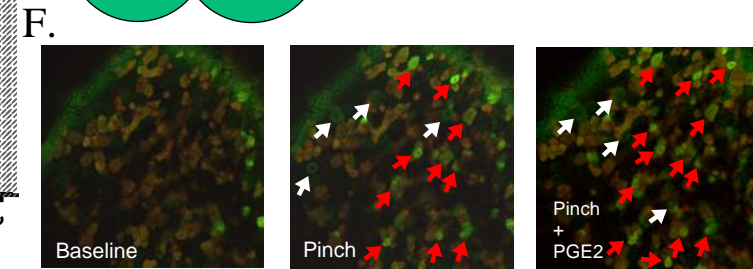
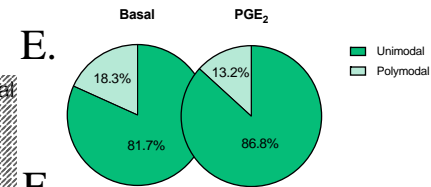
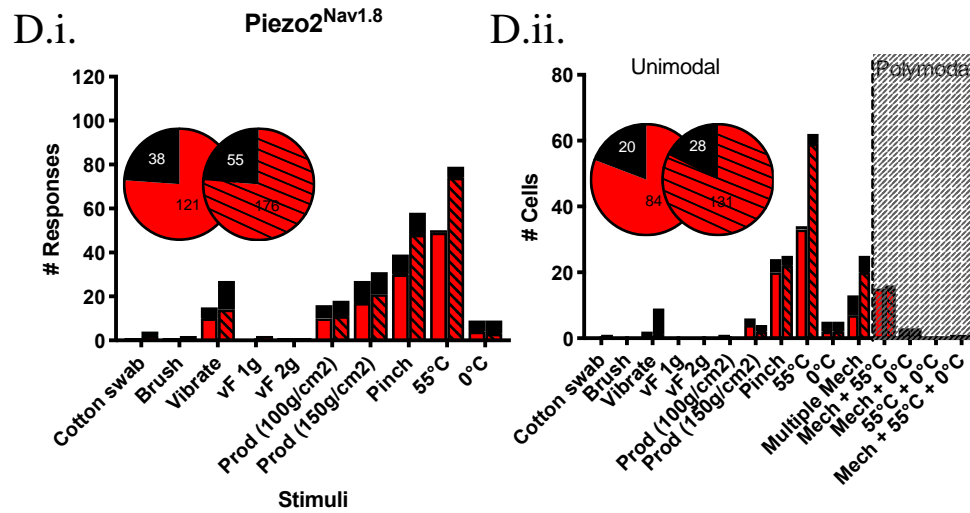
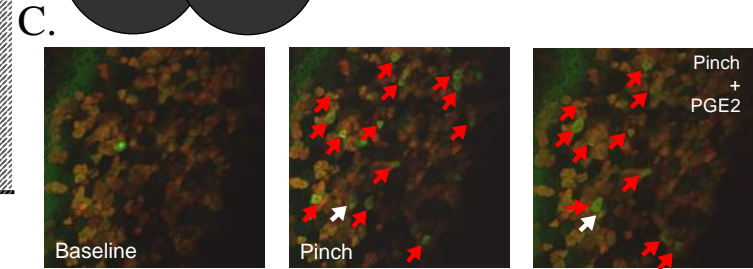
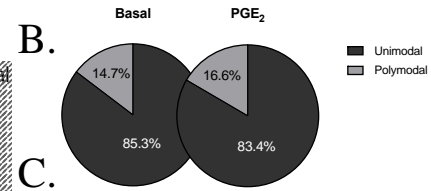
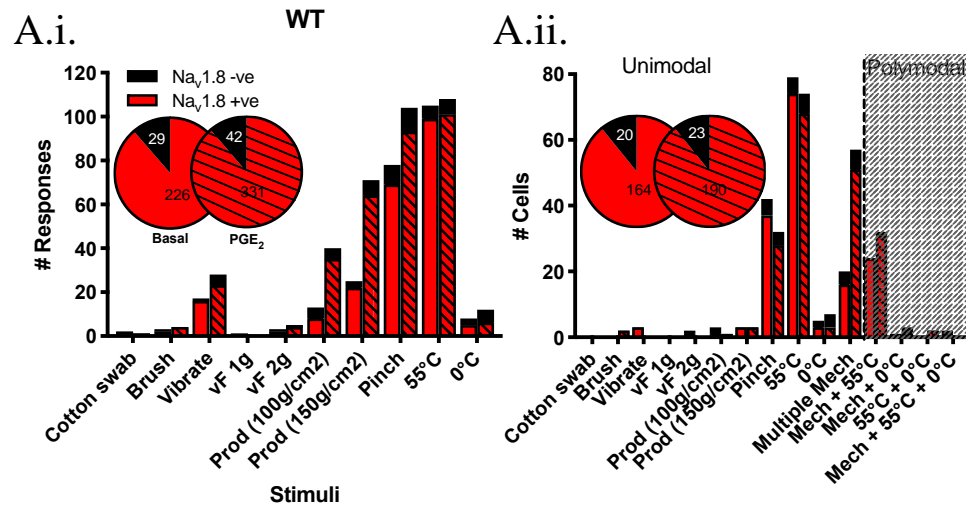
When reflecting on the imaging findings as a whole, a comparison between the responding DRG neurons of WT animals versus  $\text{Piezo2}^{\text{Nav1.8}}$  animals under basal conditions reveals that responses are more evenly distributed between mechanical stimuli (vibration,  $100\text{g}/\text{cm}^2$  and  $150\text{g}/\text{cm}^2$  prod, and pinch) and  $55^\circ\text{C}$  heat in the  $\text{Piezo2}^{\text{Nav1.8}}$  animals (as opposed to WT DRG neurons, the vast proportion of which respond to hind paw pinch and  $55^\circ\text{C}$  water). An observation that is perhaps more striking still is the apparent increase in the proportion of  $\text{Na}_v1.8$ -negative neurons responding to all mechanical stimuli, not just vibration, in  $\text{Piezo2}^{\text{Nav1.8}}$  animals ( $\sim 11\%$  in WT animals versus  $\sim 24\%$  in  $\text{Piezo2}^{\text{Nav1.8}}$  animals) which remains consistent after the application of  $\text{PGE}_2$  (Figure 4.5.A.i and 4.5.D.i). An example of this can be seen when comparing Figure 4.5.C and Figure 4.5.F where a greater proportion of  $\text{Na}_v1.8$ -negative neurons respond to a pinch stimulus than in the WT animal. Again, perhaps alluding to sensory compensation within the  $\text{Na}_v1.8$ -negative neuron population of the  $\text{Piezo2}^{\text{Nav1.8}}$  animals.

Another intriguing observation is the number of cells that respond to multiple types of mechanical stimulation in the WT animals versus the  $\text{Piezo2}^{\text{Nav1.8}}$  animals. Where I first see  $\sim 11\%$  of all responding neurons responding to multiple mechanical modalities in the WT, versus  $\sim 13\%$  in  $\text{Piezo2}^{\text{Nav1.8}}$  neurons under basal conditions, I observe a jump to  $\sim 28\%$  in WT animals with a comparatively modest increase to  $\sim 17\%$  in the  $\text{Piezo2}^{\text{Nav1.8}}$  neurons after the addition of  $\text{PGE}_2$  (Figure 4.5.A.ii and 4.5.D.ii). Could this be an indication that cells that were once responding to noxious mechanical stimuli, now also respond to innocuous mechanical stimulation, or vice versa? Perhaps silent nociceptors were unmasked in the presence of  $\text{PGE}_2$  that respond to both. Either one of these occurrences may explain the mechanical allodynia/hyperalgesia experienced in behaving WT animals exposed to  $\text{PGE}_2$ . Perhaps this behaviour would not be observed in  $\text{Piezo2}^{\text{Nav1.8}}$  mice. This may be a consequence of the extent of recruitment of additional responses to mechanical stimuli observed in the WT animal (e.g. to  $100\text{g}/\text{cm}^2$  and  $150\text{g}/\text{cm}^2$  prod). However, this finding should be approached with some caution, as I do not observe the same substantial

increase in neurons responding to multiple mechanical stimuli after PGE<sub>2</sub> injection in WT GCaMP3-expressing mice in a subsequent chapter.

The most prominent of increases in responding neurons to a particular stimulus after PGE<sub>2</sub> injection in Piezo2<sup>Nav1.8</sup> mice is the recruitment of neurons responding only to 55°C heat. This is reassuring for one, in that I observe a PGE<sub>2</sub>-mediated effect, and for another in that I would not expect this particular modality to be affected with Piezo2 deletion. Perhaps in the behaving Piezo2<sup>Nav1.8</sup> animal I would observe an increased thermal hyperalgesia in comparison to their WT counterparts after PGE<sub>2</sub> injection, indeed, with the genetically targeted diminution of one modality in mice (in this case mechanical sensation), another is often heightened (McCoy et al., 2013).

Finally, I do not observe the same proportions of polymodal neurons in Piezo2<sup>Nav1.8</sup> versus WT animals before and after the addition of PGE<sub>2</sub>. Where I see a greater proportion of polymodal neurons under basal conditions in the Piezo2<sup>Nav1.8</sup> mice, I report a reduction in polymodality in response to PGE<sub>2</sub>, the opposite of my findings in WT animals (Figure 4.5.B and 4.5.D). This is likely a consequence of fewer Na<sub>v</sub>1.8+ unimodal neurons responding to mechanical stimulation due to Piezo2 deletion, and a subsequent recruitment of Na<sub>v</sub>1.8-positive unimodal heat-sensitive neurons (or “silent” nociceptors) after PGE<sub>2</sub> injection which results in a dilution of the basal responding polymodal neurons.



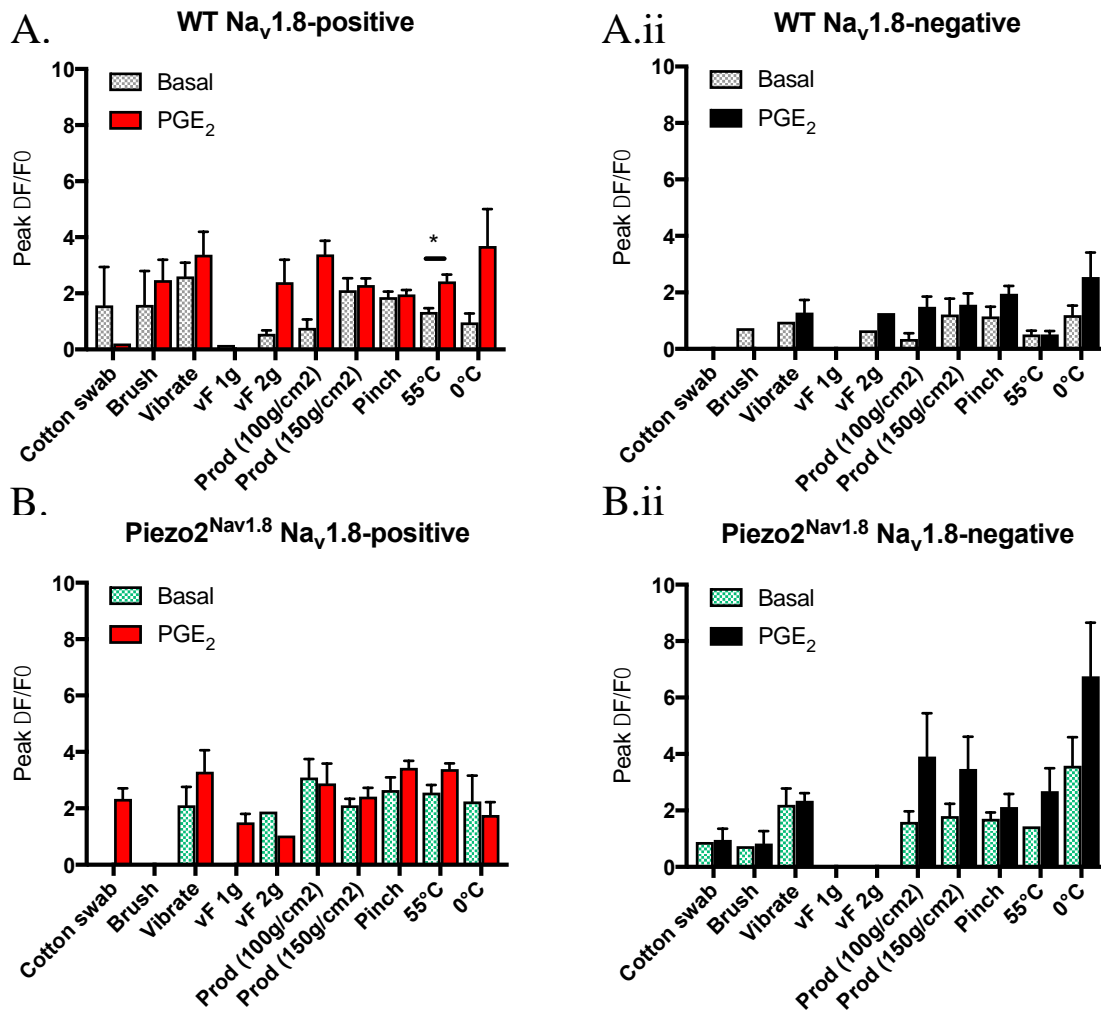
**Figure 4.5. *In vivo* GCaMP3 imaging comparing responses of DRG neurons in Piezo2<sup>Nav1.8</sup> mice versus WT controls to peripheral stimulation before and after induction of acute inflammatory pain**

Red represents tdTomato-expressing Nav1.8 positive neurons, black represents non-tdTomato-expressing Nav1.8-negative neurons. **A.i.** The number of total neuron responses in the DRG of WT animals to stimuli applied to the hind paw, either pre intraplantar injection of PGE<sub>2</sub> or 5 minutes after. Pie charts represent the total number of responses of both Nav1.8+ and Nav1.8-negative neurons pre and post PGE<sub>2</sub>. **A.ii.** The number of total cells responding to either one type of stimuli, modality ('Multiple Mech' refers to neurons responding to multiple types of mechanical stimulation including pinch, and are deemed as unimodal within this study), or as polymodal i.e those responding to more than one modality in the case of 'Mech + 55°C', 'Mech + 0°C', '55°C + 0°C', and 'Mech + 55°C + 0°C'. Pie charts represent the total number of responding cells pre and post PGE<sub>2</sub>. **B.** The percentage of polymodal versus unimodal responding neurons of WT animals pre and post PGE<sub>2</sub>. **C.** Representative images of WT neurons responding to a pinch stimulus pre and post PGE<sub>2</sub>. White arrows represent responding Nav1.8-negative neurons and red arrows represent responding Nav1.8+ neurons. **D.i** The number of total responses in the DRG of Piezo2<sup>Nav1.8</sup> mice to stimuli applied to the hind paw. **D.ii.** The number of total cells responding. **E.** The percentage of polymodal versus unimodal responding neurons of Piezo2<sup>Nav1.8</sup> animals pre and post PGE<sub>2</sub>. **F.** Representative images of Piezo2<sup>Nav1.8</sup> neurons responding to a pinch stimulus pre and post PGE<sub>2</sub> (WT n=3; Piezo2<sup>Nav1.8</sup> n=3).

#### **4.4.4 Peak fluorescence of responding GCaMP3 neurons in the DRG validates previous findings in WT animals, and indicates that the activity of Piezo2<sup>Nav1.8</sup> Nav1.8+ and negative neurons may be increased in comparison to the WT**

Data that can be gleaned from *in vivo* GCaMP imaging studies also includes the peak fluorescence of the responding neurons, and is deemed equivalent to the extent of their activation. Past papers have indicated that peak fluorescence in response to a noxious stimulus increases after PGE<sub>2</sub> application (Emery et al., 2016). As previously discussed I also observe a significant increase in peak fluorescence in Na<sub>v</sub>1.8+ neurons in response to noxious heat in the WT animals after the application of PGE<sub>2</sub> ( $1.340 \pm 0.131 \Delta F/F_0$  pre-PGE<sub>2</sub>;  $2.433 \pm 0.242 \Delta F/F_0$  post-PGE<sub>2</sub>;  $p=0.0009$ ) (Figure 4.6.A.i). This same trend can be observed in the responses to the majority of remaining stimuli in both the Na<sub>v</sub>1.8+ and negative populations of neurons in the WT animals (Figure 4.6.A.i and A.ii).

I do not report any significant increases in fluorescence in the Piezo2<sup>Nav1.8</sup> mice after the addition of PGE<sub>2</sub> in either Na<sub>v</sub>1.8+ or negative populations although a trend is again observed in response to most stimuli (Figure 4.6.B.i and B.ii). Interestingly, one could almost infer increased activity in Piezo2<sup>Nav1.8</sup> neurons under basal conditions in the Na<sub>v</sub>1.8+ population, and after the addition of PGE<sub>2</sub> in the Na<sub>v</sub>1.8-negative population. Again, this is perhaps indicative of compensatory mechanisms within the sensory neurons of these animals due to Piezo2 deletion in the Na<sub>v</sub>1.8+ population.



**Figure 4.6. Peak fluorescence as a measure of the extent of activity of responding DRG neurons in Piezo2<sup>Nav1.8</sup> mice versus WT controls to peripheral stimulation before and after induction of acute inflammatory pain**

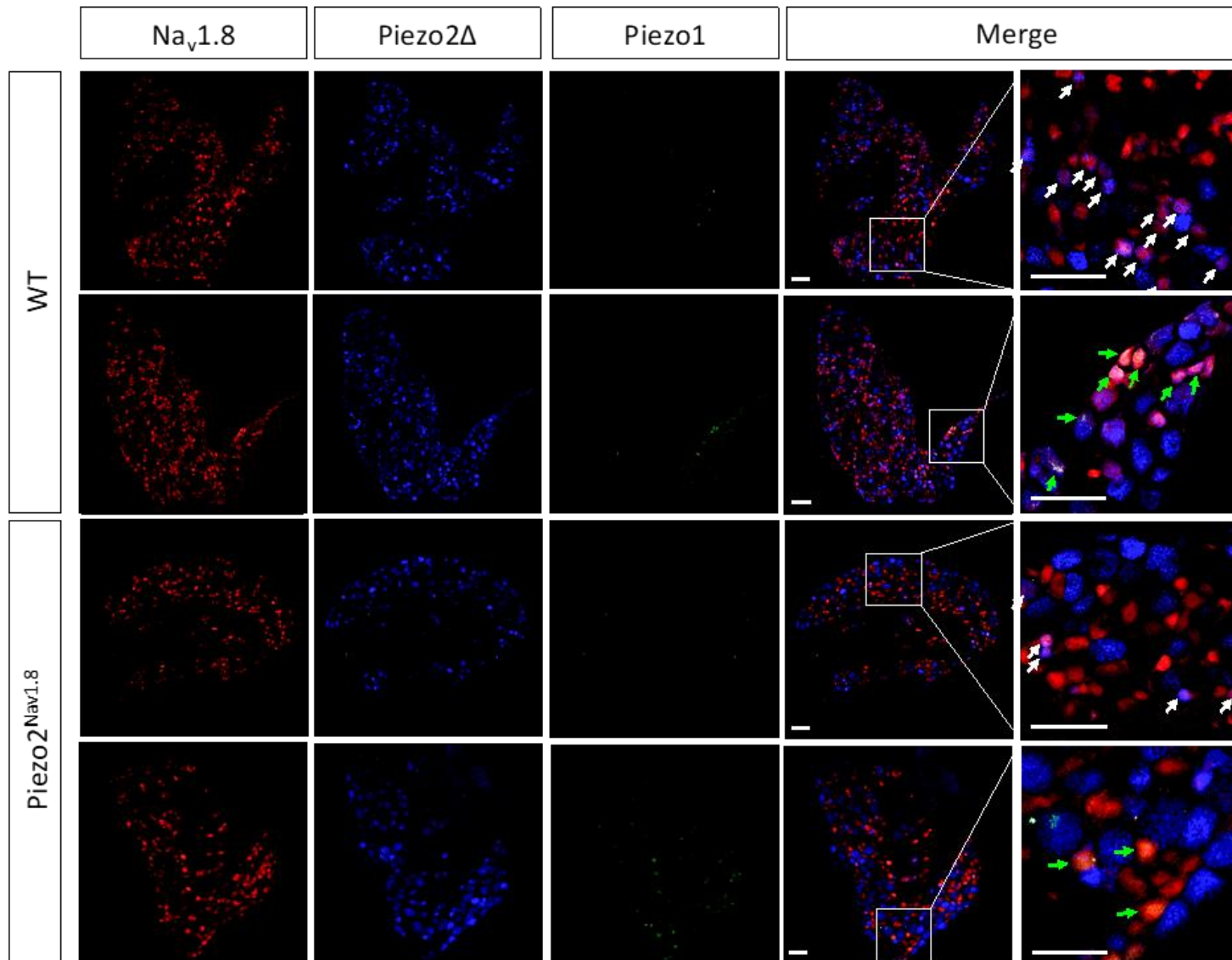
**A.i.** Peak fluorescence of  $Na_v1.8$ + neurons in WT animals, for most stimuli an increase in activity is observed after PGE<sub>2</sub>. A similar trend is seen in **A.ii.** which shows the extent of fluorescence in the  $Na_v1.8$ -negative population. **B.i.** Peak fluorescence of  $Na_v1.8$ + neurons in Piezo2<sup>Nav1.8</sup> mice, for most stimuli an increase in activity is observed after PGE<sub>2</sub>, however, under basal conditions it appears as though fluorescence is increased in Piezo2<sup>Nav1.8</sup> mice in comparison to WT animals. A similar finding is observed in **B.ii.** which shows the extent of fluorescence in the  $Na_v1.8$ -negative population. Data are shown as Mean  $\pm$  SEM. Statistical analysis was performed using the multiple unpaired Student's t test. (WT n=3; Piezo2<sup>Nav1.8</sup> n=3).

#### **4.4.5 Piezo2 expression is predominantly restricted to the Na<sub>v</sub>1.8-negative population of sensory neurons in WT animals, and Piezo1 to the Na<sub>v</sub>1.8+ population**

*Performed in collaboration with Dr. Andrei Okorokov, WIBR, UCL*

As Piezo2 antibody efficacy is notoriously poor, I chose to interrogate Piezo2 transcript expression using a form of fluorescence *in situ* hybridisation (ISH) termed RNAScope. This was to ensure the outlined breeding strategy led to the abolition of Piezo2 expression in the Na<sub>v</sub>1.8+ population of sensory neurons. Interestingly, although Piezo2 expression is believed to broadly span the sensory neuron sub-populations (Coste et al., 2010), our data would suggest that little Piezo2 transcript is found in the Na<sub>v</sub>1.8+ population to begin with, although this is not to suggest that Piezo2 within these cells is any less physiologically relevant (Figure 4.7). As part of these experiments we used a custom Piezo2 probe designed to target the deleted exons in Piezo2<sup>Nav1.8</sup> animals in the event that exon 43-45 deletion still led to transcript synthesis and false-positive results, despite a lack of Piezo2 translation in the KO animals. This probe was termed Piezo2 $\Delta$ . As a consequence of the small target region, signal was poorer than other commercial Piezo2 probes, but still clear. Our data indicates a reduction in Piezo2 transcript expression in the Na<sub>v</sub>1.8+ population of Piezo2<sup>Nav1.8</sup> animals, yet Piezo2 transcript in the Na<sub>v</sub>1.8-negative population retained its high expression (Figure 4.7).

Interestingly, and contrasting to recently published ISH data (Wang et al., 2019), our findings corroborate those initially published by Coste et al., (2010), in that we find limited Piezo1 expression in the DRG, which persists in the Piezo2<sup>Nav1.8</sup> animals, i.e. there is no upregulation of Piezo1 to compensate for the loss of Piezo2 in the Na<sub>v</sub>1.8+ neuron population. Recent work has demonstrated that ectopic Piezo1 expression within the DRG is capable of rescuing the lack of MA currents produced in Piezo2 KO animals, and also the behavioural phenotype. Our images would suggest that an endogenous upregulation of Piezo1 is unlikely to occur in the Piezo2<sup>Nav1.8</sup> mice.



**Figure 4.7. RNAScope targeting Piezo1 and Piezo2 mRNA expression in the DRG of Piezo2<sup>Nav1.8</sup> and WT animals**  
 tdTomato represents Nav1.8+ neurons. White arrows denote overlapping Nav1.8+ and Piezo2-expressing neurons. Green arrows represent Piezo1-expressing neurons. (WT n=1; Piezo2<sup>Nav1.8</sup> n=1)



## 4.5 Discussion

A role for Piezo2 in noxious mechanosensation has been debated since its discovery by the Patapoutian group in 2010. This is mainly compounded by the fact that no other *bona fide* mechanotransducer present in the peripheral nervous system of mammals has been discovered since (with the exception of the very recently identified TACAN). I investigated the role of Piezo2 in the Na<sub>v</sub>1.8+ population of sensory neurons as this population has been deemed essential for acute noxious mechanosensation. Furthermore, these neurons do not overlap with proprioceptors, thus retaining normal motor function in Piezo2<sup>Nav1.8</sup> animals, where previous conditional Piezo2 KOs have failed to. Conveniently, Na<sub>v</sub>1.8+ cells are also the population of sensory neurons that are known to express Aqp1, aiding the study of whether Aqp1 may be responsible for regulating Piezo2 during mechanical pain sensing.

### 4.5.1 Is Na<sub>v</sub>1.8-Cre an appropriate choice for this study?

An important consideration for any study using Cre-Lox transgenic mice is the efficacy of the Cre recombinase used. In this instance it was the previously described Na<sub>v</sub>1.8-Cre (Nassar et al., 2004), which has also been utilised by other groups for various targeted mutations. Reassuringly, work published by Shields et al. (2012) reports that 100% of labelled neurons from Na<sub>v</sub>1.8-Cre reporter mice displayed functional Na<sub>v</sub>1.8-like currents, arguing against transient early expression or a switch in the expression profile of Na<sub>v</sub>1.8 during development. However, it is important to note that not all Na<sub>v</sub>1.8+ neurons are nociceptors. The study by Shields et al. (2012) demonstrates that ~40% of large-diameter A $\beta$  fibres express Na<sub>v</sub>1.8, and that a proportion of Na<sub>v</sub>1.8+ neurons terminate peripherally in Meissner corpuscles and longitudinal lanceolate endings associated with RA A $\beta$  afferents. This is perhaps not surprising considering that ~75% of all peripheral sensory neurons are Na<sub>v</sub>1.8+. As a consequence, we have to consider the likelihood of off-target (non-nociceptor) Piezo2 deletion, which may manifest itself as the mild (and insignificant) hyposensitivity to innocuous mechanical stimuli that I observe in the behaving Piezo2<sup>Nav1.8</sup> mice. Shields et al. (2012) posit that the remaining 60% of Na<sub>v</sub>1.8-negative A $\beta$  afferents are proprioceptors, which fits nicely with my finding that Piezo2<sup>Nav1.8</sup> mice do not have any proprioceptive deficits.

Considering the proportion of peripheral sensory neurons expressing Na<sub>v</sub>1.8, the comparatively mild phenotype of mice which have undergone Na<sub>v</sub>1.8+ sensory neuron ablation (Na<sub>v</sub>1.8<sup>DTA</sup>) is striking (Abrahamsen et al., 2008). For example, as I demonstrate in my *in vivo* GCaMP imaging experiments, the overwhelming majority of neurons responding to noxious heat stimuli are Na<sub>v</sub>1.8+, yet ablating this particular subset does nothing to the resulting behavioural phenotype

in response to noxious heat stimulus in awake animals. Furthermore, the  $\text{Na}_v1.8+$  population of sensory neurons overlaps with VGLUT3 expression, which labels neurons that are C-LTMRs and are responsible for gentle touch sensation and injury-induced mechanical hypersensitivity (Shields et al., 2012). Again, these sensations do not appear to differ in the  $\text{Na}_v1.8^{\text{DTA}}$  mice in comparison to WT animals (Abrahamsen et al., 2008). As such, it can be assumed that compensatory plasticity does indeed occur in  $\text{Na}_v1.8^{\text{DTA}}$  animals. Whether or not the same is true for Piezo2 deletion in these neurons may only fully be determined with either an inducible Cre, or a viral or siRNA knock-down of Piezo2 performed in the adult animal. Since noxious mechanical sensitivity is one phenotype not compensated for in the  $\text{Na}_v1.8^{\text{DTA}}$  mice, one would hope that any role for Piezo2 in noxious mechanosensation would be observed within this study. As such, utilising the  $\text{Na}_v1.8\text{-Cre}$  mouse is an appropriate means of investigating this.

#### **4.5.2 Are Piezo2 and/or Piezo1 required for the mechanically activated currents produced by $\text{Na}_v1.8$ -expressing DRG neurons?**

I performed mechano-clamp electrophysiology recordings in the cultured DRG neurons of WT mice versus  $\text{Piezo2}^{\text{Nav1.8}}$  neurons. In doing so I found a proportionally smaller number of cultured sensory neurons responding to mechanical stimulation within both WT and  $\text{Piezo2}^{\text{Nav1.8}}$   $\text{Na}_v1.8+$  populations in comparison to previously published DRG mechano-clamp datasets (Coste et al., 2010; Ranade et al., 2014). I propose this to be a consequence of the size (and subsequently phenotype) of the neurons targeted. Where you might expect an abolition of RA currents in the  $\text{Na}_v1.8+$  neurons of  $\text{Piezo2}^{\text{Nav1.8}}$  mice, I still observe these. It was initially for this reason that we used ISH RNAScope technology to probe the expression pattern of Piezo1 transcript in the DRG for any Piezo1-mediated compensation within the  $\text{Piezo2}^{\text{Nav1.8}}$  DRG neurons. In agreement with initial publications looking at Piezo1 expression patterns (Coste et al., 2010; Ranade et al., 2014) including the single cell RNA-seq study performed by Usoskin et al. (2015), we find that there is minimal expression of Piezo1 mRNA in the DRG of both WT and  $\text{Piezo2}^{\text{Nav1.8}}$  animals, and that the little transcript present is restricted to the  $\text{Na}_v1.8+$  population. Emerging evidence now suggests that Piezo1 is more present in the DRG than initially believed, and that it may even contribute to mechano-nociception in sensory neurons (Wang et al., 2019). This group also used RNAScope to examine the expression pattern of Piezo1 and Piezo2 transcripts in the DRG, as well as TRPV1, which is expressed in small-diameter heat sensing neurons. They report widespread expression of Piezo2 transcript predominantly in large-diameter neurons, but also describe definitive Piezo1 transcript expression in small diameter neurons distinct from those expressing TRPV1. Approximately 60% of neurons expressing Piezo1 co-expressed Piezo2 in this instance. As a consequence, this group propose that there is an element of functional

redundancy with regard to the two homologues, allowing for compensation mediated by one in the absence of the other. This may explain why we retain RA MA currents in the Nav1.8-population of sensory neurons in Piezo2<sup>Nav1.8</sup> mice. This finding is perhaps also not so surprising given that some RA currents are retained in mice that have undergone more widespread conditional Piezo2 deletion (Ranade et al., 2014).

#### **4.5.3 A role for Piezo2 in acute noxious mechanical pain can be ruled out**

A recent study, using Piezo2<sup>HoxB8</sup> animals, in which Piezo2 was deleted from all sensory neurons and the caudal spinal cord, has implicated Piezo2 in acute noxious mechanosensation (Murthy et al., 2018). It was reported that these mice were significantly hyposensitive to the acute noxious pinprick assay (applied to the hind paw), and tail clip assay. At the same time, a collaborating group also published their data on human Piezo2 mutation patients, who were conflictingly found to have normal responses to acute mechanical pain, but deficits in inflammation-induced mechanical allodynia (Szczot et al., 2018). Thus, Szczot et al. (2018) surmised that Piezo2 had little, if any involvement in acute mechanical pain sensing in humans. My study goes so far as to suggest that the latter is also true in mice.

An essential component of any pain behaviour assay in mice is to first determine if the animals have proprioceptive deficits that may confound their response to noxious stimuli. It is already well-established that Piezo2 is responsible for normal proprioception in mice, as ablating Piezo2 expression in proprioceptors (the Parvalbumin+ population of somatosensory neurons) causes a significant impairment in motor coordination in the behaving animals (Woo et al., 2015). A key observation of Murthy et al. (2018) is that Piezo2<sup>HoxB8</sup> animals also have severe proprioceptive deficits, and although proprioceptive behavioural assays are not reported, representative images of Piezo2<sup>HoxB8</sup> animals are published in their earlier work, depicting them as severely uncoordinated (Woo et al., 2015). The Piezo2<sup>Nav1.8</sup> mice have no observable proprioceptive deficits as ruled out using both the accelerating rotarod assay, and the grip force assay. Importantly, these animals also do not have a deficit in noxious mechanosensation, as demonstrated using the noxious mechanical Randal-Selitto assay, categorically ruling out Piezo2's involvement in acute noxious mechanical sensing. Indeed, my *in vivo* GCaMP imaging of the DRG in these animals also suggests that this is likely to be the case as I continue to observe responses of Nav1.8+ neurons to noxious mechanical stimulation of the hind paw in Piezo2<sup>Nav1.8</sup> animals. Interestingly, a recent Piezo2 conditional KO study using an Advillin-Cre causing Piezo2 deletion in approximately 75% of DRG neurons (including almost all IB4+ mechano-nociceptors),

showed that this loss of Piezo2 actually leads to a sensitisation to noxious mechanical stimuli in mice (Zhang et al., 2019). This supports the idea that Piezo2-mediated innocuous tactile sensing may even contribute to mechanical pain inhibition.

#### **4.5.4 Is there a role for Piezo2 in Na<sub>v</sub>1.8 sensory neurons in inflammatory allodynia?**

The initial study by Ranade et al., (2014) investigating the role of Piezo2 *in vivo* not only reported no deficit in noxious mechanosensation in *Advil-CreERT2* Piezo2 conditional knockout mice, it also described a normal inflammatory pain response to the CFA model of chronic inflammation (at 24hrs), and the Bradykinin model of acute inflammation. This is contradictory to the group's latest findings in which they use a non-inducible *HoxB8-Cre* to conditionally ablate Piezo2 (Murthy et al., 2018), subsequently finding a role for Piezo2 in mice in capsaicin-mediated inflammatory mechanical allodynia. In tandem with Murthy et al. (2018), Szczot et al. (2018) generated conditional Piezo2 knockout animals by introducing a viral vector encoding Cre recombinase into Piezo2<sup>fl/fl</sup>/GCaMP6f<sup>+/+</sup> mice at P0-2. They then performed *in vivo* GCaMP imaging in the TG of the adult mice and observed that a loss of Piezo2 in these animals prevents any response to brush of the cheek, but not to noxious pinch. This response to brush is also absent after injection of capsaicin. It is this absence of response to innocuous tactile stimulation post-inflammation that the same group deemed responsible for the loss of capsaicin-mediated mechanical allodynia observed in human Piezo2 LOF patients. Szczot et al. (2018) also observed a lack of response to brush in their Piezo2 KO mice 24 to 36 hours after administering CFA, suggesting that Piezo2 is required for touch sensing and mechanical allodynia under acute and chronic inflammatory conditions.

Unfortunately, these two studies were published at a time in which mine had drawn to a close, so I did not have the opportunity to replicate these findings behaviourally in Piezo2<sup>Nav1.8</sup> mice. However, I did extensively study the role of Piezo2 within the Na<sub>v</sub>1.8+ population of sensory neurons in response to acute innocuous and noxious mechanical stimulation, using *in vivo* GCaMP imaging in conjunction with intraplantar injection of the acute inflammatory agent PGE<sub>2</sub>. Capsaicin administration is known to cause localised PGE<sub>2</sub> upregulation after application (Saadé et al., 2002) so PGE<sub>2</sub> administration should be an effective means of comparison with Szczot et al.'s (2018) capsaicin findings during their imaging experiments.

PGE<sub>2</sub> is known to cause localised hyperalgesia/allodynia within 5 minutes of application, allowing for the study of its effects within the same animal during *in vivo* GCaMP imaging as the integrity

of the imaged DRG is maintained. I report a number of interesting observations in Piezo2<sup>Nav1.8</sup> animals that may hint at a role for Piezo2 in Nav1.8+ neurons during acute inflammation. These observations include a decrease in the proportion of neurons that are polymodal and also an increase in the number of neurons that are responsive to noxious heat stimuli only in the Piezo2<sup>Nav1.8</sup> mice versus WT animals after intraplantar injection of PGE<sub>2</sub>. As Piezo2 expression is known to overlap with cutaneous TRPV1-expressing neurons (CGRP+ peptidergic nociceptors which mainly mediate noxious heat response) (Zhang et al., 2019), my imaging findings may suggest a sensitisation of heat-responding nociceptors to mechanical stimuli mediated by Piezo2 under acute inflammatory conditions. This sensitisation may, in turn, be absent in Piezo2<sup>Nav1.8</sup> mice, thus why I observe a reduction in the proportion of polymodal neurons after PGE<sub>2</sub> injection. A similar finding has been reported where Piezo2 was deemed responsible for the NGF-induced mechanical sensitisation observed in “silent” nociceptors that are CHRNA3+ and innervate the visceral organs, muscles, and joints (Prato et al., 2017). Further investigations would need to be performed in the behaving animals, but since Nav1.8+ neurons are required for CFA-induced mechanical hyperalgesia/allodynia (Abrahamsen et al., 2008), it is reasonable to assume that Piezo2 may have a role in this.

#### **4.5.5 Is there a role for Piezo1 in noxious mechanosensation *in vivo*?**

As previously mentioned, Piezo1 expression within the DRG is likely much more extensive than originally reported. I propose here that it is this overlap with normally Piezo2-expressing neurons that is likely to compensate for, and maintain the MA currents in the absence of Piezo2 that we observe in the cultured DRG neurons of Piezo2<sup>Nav1.8</sup> mice. The same group that proposed the expression of Piezo1 specifically in small-diameter neurons of the DRG (Wang et al., 2019) also investigated Piezo1's role *in vivo* using behavioural assays in mice. As constitutive deletion of Piezo1 is embryonically lethal, Wang et al. (2019) did so by intradermally injecting the Piezo1 agonist Yoda1 into the hind paw of mice and performing subsequent assessments of nocifensive responses. They found that mice developed a prolonged mechanical hyperalgesia from 30 minutes up to 72 hrs after injection of Yoda1, thus implicating Piezo1 in mechano-nociception. These observations are further supported by another recent study describing Piezo1's contribution to migraine by causing CGRP release in the nociceptive neurons of the TG after activation either by mechanical stimuli or Yoda1 (Mikhailov et al., 2019).

An intriguing study looking at ectopic expression of Piezo1 in the DRG of mice (the same one to report a noxious mechanical hypersensitivity in Piezo2 conditional KO mice) found that ectopic

Piezo1 expression across all DRG sensory neurons sensitises gentle-touch behaviour, and suppresses mechanical pain in these animals (Zhang et al., 2019). They surmised that the latter observation is due to an increase in innocuous mechanical sensing which inhibits noxious mechanosensation. They also went on to demonstrate that simultaneous conditional Piezo2 deletion and ectopic Piezo1 expression in the DRG rescued touch and proprioceptive deficits of Piezo2 knockout mice. Thus, Piezo1 is capable of contributing to mechanical sensitivity *in vivo*, and it is important to note that under normal conditions, Piezo1 expression is restricted to small-diameter sensory neurons that are typically associated with mechano-nociception, where it may contribute to this sensory modality.

Where previous assumptions have stipulated that Piezo1 and Piezo2 mediate distinct functions within the body, emerging evidence suggests that their roles may be more functionally intertwined than initially thought. *Phox2b*-Cre (Cre recombinase expression is restricted to the nodose and petrosal ganglia) Piezo1 and Piezo2 double KO mice have an abolition of drug-induced baroreflex and aortic depressor nerve activity. Thus, Piezo1 and Piezo2 are essential baroreceptor mechanosensors, responsible for acute blood pressure control (Zeng et al., 2018). This observation is a definitive example of the functional redundancy between the two proteins, as separate Piezo1 or Piezo2 KO animals do not have the same baroreceptor deficits. Although we observe no upregulation of Piezo1 in Piezo2<sup>Nav1.8</sup> mice, we surmise that there is also a level of redundancy within the mechanosensitive sensory neurons of the DRG, as such, Piezo1 already residing within these neurons is likely responsible for maintaining the mechanically activated currents that we observe in the DRG of Piezo2<sup>Nav1.8</sup> animals. Invertebrates have one piezo homologue that is responsible for mechano-nociception, it is therefore likely that mammals evolved to have two piezo proteins for fine-tuning somatosensory responses.

#### **4.6 Future directions**

This study describes evidence for an unidentified mechanotransducer responsible for acute mechanical pain that is not Piezo2. I demonstrate that in WT animals there is limited overlap between Nav1.8 and Piezo2-expressing neurons. Interestingly, our electrophysiology data in the DRG neurons of Piezo2<sup>Nav1.8</sup> mice suggests that mechanotransducers alternate to Piezo2 are also capable of producing RA MA currents. Recent studies suggest that Piezo1 may indeed be responsible for producing MA currents in DRG neurons that contribute to tactile sensation, and possibly nociception. It would be intriguing to perform the same electrophysiology, imaging, and behavioural experiments described above using the Piezo1<sup>fl/fl</sup> mouse, also designed by the Patapoutian group, to elucidate a role (if any) for Piezo1 in acute mechano-nociception.

Despite the lack of a contribution of Piezo2 to acute mechanical pain sensing, recent reports have suggested a role for Piezo2 in inflammatory-mediated mechanical allodynia in mice and humans. The GCaMP imaging data here supports these hypotheses, however, a major caveat of the technique is the low number of cells recruited/activated during innocuous mechanical stimulation. This is particularly detrimental considering I am studying Piezo2, a mechanotransducer known to be responsible for tactile sensation. As will be discussed in later imaging experiments within this thesis, I observe that the *Pirt*-GCaMP3 driver used is in fact not specific to all sensory neurons, and that there are a proportion of which (those responsible for light touch and proprioceptive sensing) that do not express *Pirt* and hence do not express GCaMP3. This is also evident when looking at the Usoskin et al. (2015) single-cell RNA-seq data which shows that *Pirt* expression is low in the NF1, NF4, and NF5 populations, those associated with innocuous tactile sensation. Considering that the Nav1.8+ population of sensory neurons is deemed essential for mechanical allodynia under inflammatory conditions, it would be very wise to explore this phenomenon in Piezo2<sup>Nav1.8</sup> mice using a behavioural model of acute and/or chronic inflammation. This, in combination with *in vivo* imaging of Piezo2<sup>Nav1.8</sup> mice expressing GCaMP driven by a true pan-neuronal promoter would be very informative and give us a clear indication of whether this is the case.

As we find that Piezo2 is not required for noxious mechanosensation in nociceptors under basal conditions, it is reasonable to assume that Aqp1 expression in this population of sensory neurons is not responsible for regulating the MA current produced by Piezo2 under normal conditions. This data is exciting as it still suggests that there is an additional mechanotransducer out there responsible for transducing acute mechanical pain, whether it is Piezo1 remains to be determined.

Of great benefit will be a strategy to identify a novel list of noxious mechanotransducer candidates so that we may continue to investigate the role and contribution of various and perhaps unidentified proteins to acute mechanical pain.



## **5 The role of peripheral Parvalbumin-positive neurons in pain**

### **5.1 Summary**

Recent advances in large-scale single cell RNA-sequencing and analyses have identified novel DRG neuron-specific genetic markers, leading to a significant refinement of DRG subpopulations. These findings have paved the way for further studies investigating the contribution of these peripheral neuron subsets in pain, with particular emphasis on those outside of the traditional nociceptive populations. Parvalbumin (PV) has long been established as a marker for proprioceptive afferents, and these novel RNA-seq datasets have emphasised this, yet no group has gone as far as to investigate the functional role of the lesser-known cutaneous PV+ neurons in pain states. The study described here uses complex genetic approaches to ablate or label the peripheral population of PV+ neurons in mice, in combination with the expression of the GECI, GCaMP, in all peripheral neurons. Doing so enabled me to use a combined approach of *in vivo* DRG GCaMP imaging and pain behaviour assays to investigate the role of this cutaneous subset in pain under basal and acute inflammatory conditions, whilst circumventing the proprioceptive deficits mediated by peripheral PV neuron ablation in behaving animals. Where previous studies have hinted at a role for the PV+ population of sensory neurons in chronic pain, this is the first to report an inhibitory role for them in acute pain sensing. Subsequent *in vivo* electrophysiology in the dorsal horn of animals without peripheral PV neurons substantiated these findings by revealing an increased excitability of WDR neurons.

Since Melzack and Wall published their seminal 'Gate Control Theory of Pain' in 1965, the peripheral neurons responsible for closing the so-called 'pain gate' in the spinal cord have for the most part remained unidentified A $\beta$  afferents. Here I propose that cutaneous PV afferents contribute to this integrative nociceptive pathway by activating in response to both noxious mechanical and thermal stimuli, in turn providing inhibitory input to spinal nociceptive transmission neurons. The implications of these findings are great, as we further not only our understanding of the complex circuitry associated with acute pain sensing, but also our understanding of the non-pharmacological approaches to pain management that are already in use (e.g. TENS), that aim to harness this endogenous mechanism of analgesia.

## 5.2 Introduction

Within the PNS, PV is expressed in proprioceptors, and a population of vibration-sensing LTMRs that terminate in the glabrous skin (de Nooij et al., 2013). However, little characterisation has been performed in the latter. Interest in the role of cutaneous PV+ neurons in pain stems from a number of interesting observations. Firstly, PV-expressing neurons have a propensity for survival after nerve injury. This is demonstrated in human studies where PV is expressed in motor neuron groups that are resistant to amyotrophic lateral sclerosis (ALS) (Medici & Shortland, 2015), and in murine studies where an over-expression of PV in motor neurons prevents excitotoxic and injury-induced cell death (Dekkers et al., 2004; Van Den Bosch et al., 2002), presumably due to PV's  $\text{Ca}^{2+}$  buffering properties. Secondly, there is evidence for an upregulation of nociceptive  $\text{Na}_v1.7$  mRNA in the axons of injured proprioceptors in a mouse model of neuropathic pain (Fukuoka et al., 2015). A clustering of sodium channels at the damaged axon of DRG neurons has previously been shown to be responsible for ongoing ectopic activity, synonymous with spontaneous neuropathic pain (Roza et al., 2003), that is primarily carried by A $\beta$  fibres (Devor, 2009). More recently it was established that the mechanotransducer Piezo2 is responsible for proprioception in PV+ neurons (Woo et al., 2015), it has since been demonstrated that Piezo2 is also responsible for mechanical allodynia driven by LTMRs in mice and humans (Murthy et al., 2018b; Szczot et al., 2018), although the specific population of neurons is yet to be determined. Whilst these findings focus on the contribution of PV+ neurons to pathological pain states, my focus will be to investigate the role of cutaneous PV neurons in pain under basal and acute inflammatory conditions, for reasons explained below.

Traditional methods of delineating the contribution of a neuron subtype in pain is to genetically or chemically ablate it in a model organism, and behaviourally assess the resulting phenotype. This experimental paradigm has been advanced with the generation of large DRG single cell RNA-seq datasets, subsequently identifying more refined neuron subsets, hence genetic markers/targets, within the sensory neuron population (Usoskin et al., 2015; Zeisel et al., 2018). A PNS-specific PV+ neuron ablation was executed in this study, using genetically targeted diphtheria toxin fragment A (DTA) expression that has previously been demonstrated to kill targeted cells, purportedly with no extracellular toxic effects (Abrahamsen et al., 2008; Ivanova et al., 2005). The pitfalls of ablating peripheral PV+ neurons in mice (now referred to as PV<sup>DTA</sup> mice) will be highlighted in this study, the phenotype of which bears resemblance to motor deficiencies already described elsewhere (Akay et al., 2014; Murthy et al., 2018; Szczot et al., 2018). Their proprioceptive deficits render pain behaviour assays difficult to interpret, therefore a combinatorial

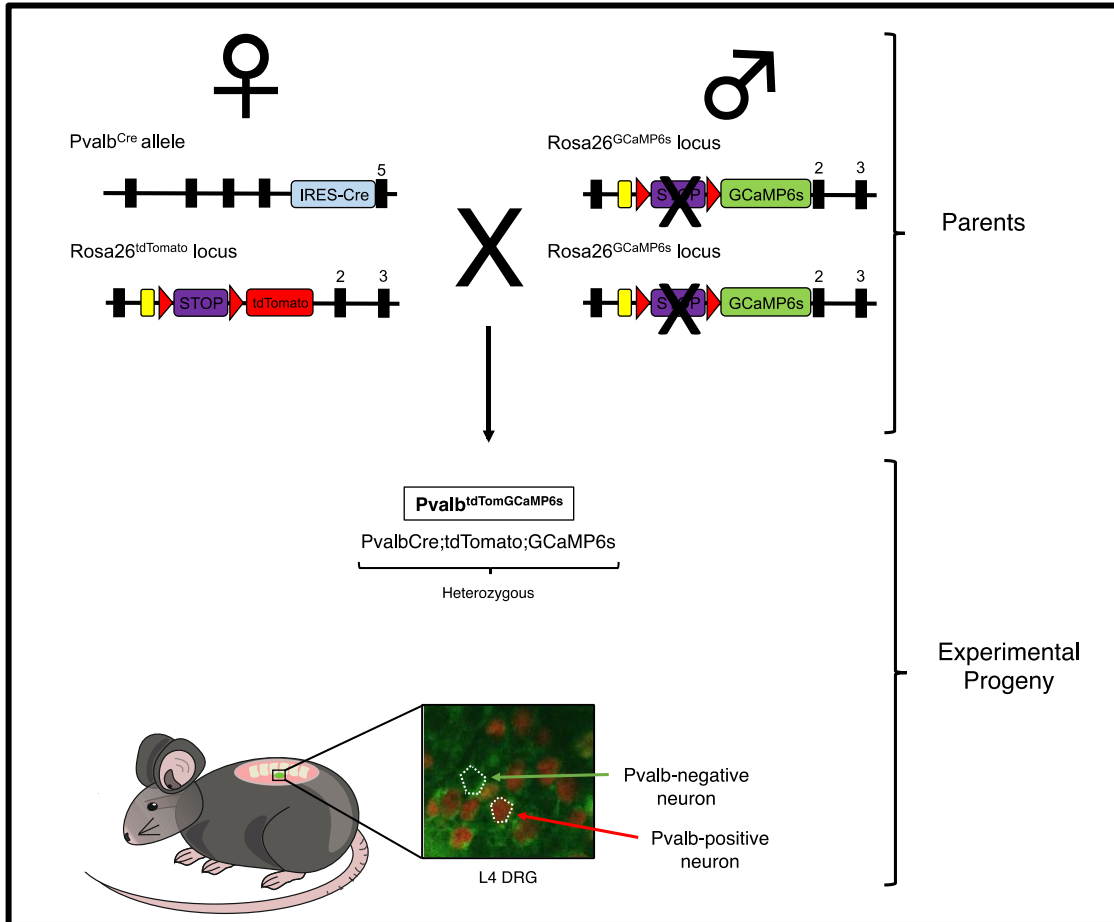
approach to characterising the role of cutaneous PV+ neurons in pain was employed in the form of both DRG *in vivo* GCaMP imaging, and behavioural assays. I had anticipated ruling-out a role for peripheral PV neurons in acute pain sensing, with a hope to pursuing neuropathic pain models after this. Instead, DRG *in vivo* GCaMP imaging identified an increase in activity in the remaining neurons of PV<sup>DTA</sup> mice in comparison to WT littermates, in response to a range of noxious stimuli applied to the hind paw under basal conditions. This led me to postulate that this increased excitability may be perceived as a hypersensitivity in the awake behaving animal.

In order to fully investigate the contribution of cutaneous PV+ neurons to acute, and acute inflammatory pain I have used two strains of mice, one with all peripheral PV+ neurons ablated (PV<sup>DTA</sup>), and the other expressing a fluorescent reporter in all PV+ neurons (PV<sup>Tom</sup>), both on a background of GCaMP expression. This, in combination with *in vivo* electrophysiology in the dorsal horn of PV<sup>DTA</sup> animals, has enabled me to probe the activity of DRG and dorsal horn neurons in the absence of peripheral PV+ neurons, confidently assess the behavioural phenotype of PV<sup>DTA</sup> animals, and to directly observe the activity of PV+ neurons in PV<sup>Tom</sup> mice, all in response to both innocuous and noxious mechanical and thermal cues applied the glabrous skin of the hind paw.

### 5.2.1 Breeding strategies

All animal procedures were performed by licenced individuals and conformed to U.K home office regulations in accordance with the Animals (Scientific Procedures) Act 1986. Unless otherwise stated, animals were acquired from The Jackson Laboratory. Parvalbumin-Cre (PV-Cre) mice (Courtesy of Prof. Michael Hausser, UCL, JAX stock no. 017320) were crossed with Rosa26-LSL-tdTomato reporter mice (JAX stock no. 007909.), or to Advillin-loxP-tdTomato-Stop-loxP-DTA mice (BAC transgenic strain generated by Dr Yury Bogdanov, UCL) to generate heterozygous (where applicable) progeny termed PV<sup>Tom</sup> and PV<sup>DTA</sup> respectively. Progeny were bred to *Pirt*-GCaMP3-expressing mice (generated by Xinzhong Dong, Johns Hopkins University) for GCaMP imaging experiments. Test mice used for *in vivo* imaging experiments were PV<sup>DTA</sup>;GCaMP3, and PV<sup>tdTom</sup>;GCaMP3 mice were used for the *in vitro* assay described in the appendices. All experiments were performed on adult mice (male and female) heterozygous for each genotype, again, where applicable. For further *in vivo* imaging assays, PV<sup>Tom</sup> mice were also bred to homozygous global GCaMP6s mice, originally Rosa26-LSL-GCaMP6s mice (JAX stock no. 024106) whose off-target GCaMP6s expression in the germline led to global GCaMP6s expression. Test mice used for imaging experiments were PV<sup>tdTom</sup>;GCaMP6s. All experiments

were performed on adult mice (male and female) heterozygous for each genotype, again, where applicable. An example breeding strategy can be seen in Figure 5.1, and the primers used for genotyping are listed in Table 5.1.



**Figure 5.1. Breeding strategy for *Pvalb*;tdTomato;GCaMP6s ( $PV^{Tom};GCaMP6s$ ) mice**

The red arrowheads denote loxP sites. A cross over the Stop codon of the *Rosa26*<sup>GCaMP6s</sup> locus indicates its deletion and subsequent constituent global expression of GCaMP6s. Female mice heterozygous for the *Pvalb*-Cre allele and for the *Rosa26*-LSL-tdTomato allele were bred to male mice homozygous for global GCaMP6s, to produce experimental progeny that were heterozygous for *Pvalb*-Cre;*Rosa26*-LSL-tdTomato;GCaMP6s ( $PV^{Tom};GCaMP6s$  mice). The DRG neurons of these mice expressed the red fluorescent reporter tdTomato in PV+ neurons on a background of green GCaMP6s expression.

Gene	Primer	Sequence	WT band	Mutant band
<i>Pvalb</i>	WT Fwd	CAGAGCAGGCATGGTGACTA	500 bp	~100 bp
	WT Rev	AGTACCAAGCAGGCAGGAGA		
	Mut Fwd	GCGGTCTGGCAGTAAAACTATC		
	Mut Rev	GTGAAACAGCATTGCTGTCACTT		
GCaMP6s	WT Fwd	AAGGGAGCTGCAGTGGAGTA	297 bp	450 bp
	Mut Fwd	ACGAGTCGGATCTCCCTTTG		
	Common Rev	CCGAAAATCTGTGGGAAGTC		
DTA	WT Fwd	AAAGTCGCTCTGAGTTGTTAT	602 bp	133 bp
	WT Rev	GGAGCGGGAGAAATGGATATG		
	Mut Fwd	GCGTGGTCAAAGTGACGTAT		
	Mut Rev	AACTCTTCCGTTCCGACTTG		
tdTomato	WT Fwd	AAGGGAGCTGCAGTGGAGTA	297 bp	196 bp
	WT Rev	CCGAAAATCTGTGGGAAGTC		
	Mut Fwd	GGCATTAAAGCAGCGTATCC		
	Mut Rev	CTGTTCTGTACGGCATGG		
GCaMP3	Common Fwd	TCCCCTCTACTGAGAGCCAG	400 bp	300 bp
	WT Rev	GGCCCTATCATCCTGAGCAC		
	Mut Rev	ATAGCTCTGACTGCGTGACC		

**Table 5.1. Genotyping primers for PV<sup>Tom</sup>, PVDTA , GCaMP3, and GCaMP6s mice**

### 5.3 Aims

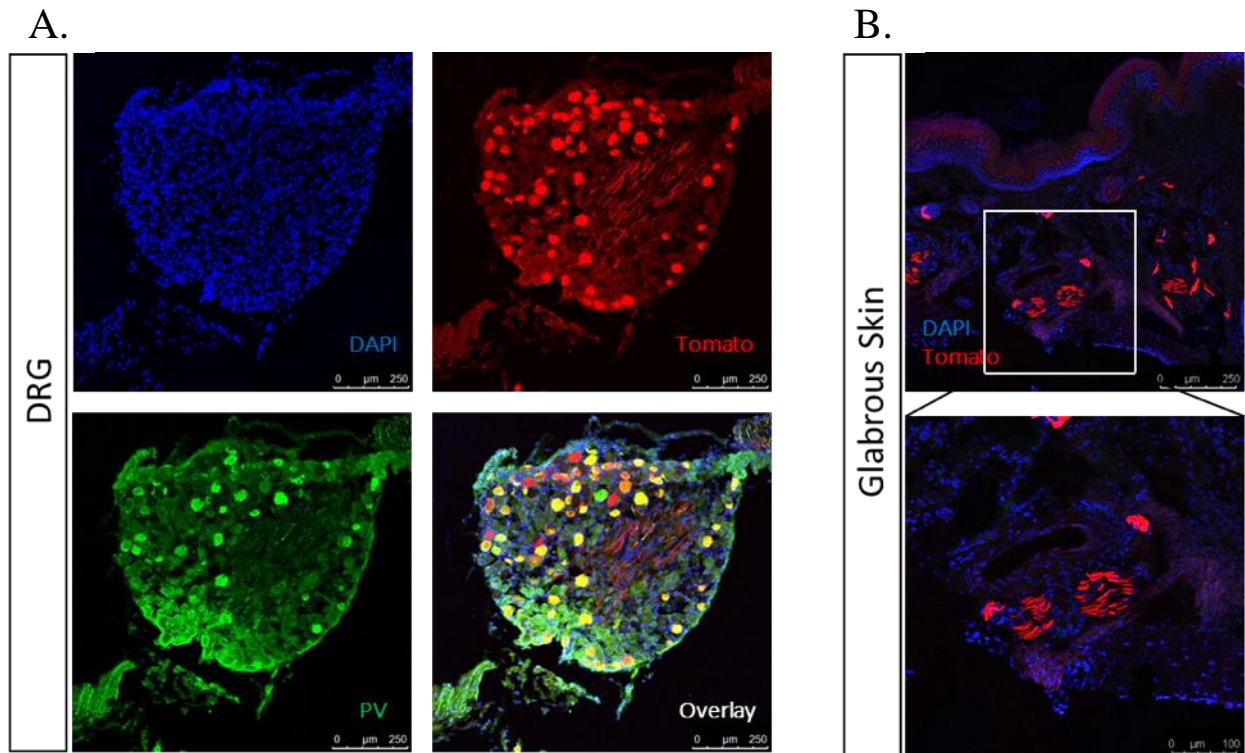
- Characterise the molecular profile of peripheral PV+ neurons *ex vivo* and *in vitro* using a combination of quantitative real time PCR (qRT-PCR) and immunohistochemistry techniques
- Characterise the proprioceptive role of peripheral PV+ neurons *in vivo* using robust behavioural assays in PV<sup>DTA</sup> mice
- Utilise DRG *in vivo* GCaMP imaging techniques in PV<sup>DTA</sup> mice as a preliminary means of determining what role, if any, cutaneous PV+ neurons have in acute pain processing and inflammation
- Perform pain behaviour assays in PV<sup>DTA</sup> mice to determine if these results correlate with those obtained in the *in vivo* GCaMP imaging study
- Use dorsal horn *in vivo* electrophysiology in PV<sup>DTA</sup> animals to link changes in the PNS at the level of the soma with central changes at the level of the dorsal horn
- Repeat DRG *in vivo* imaging experiments using labelled PV+ neurons (as opposed to ablating them) to observe how they directly respond to natural stimuli under basal and acute inflammatory conditions

## 5.4 Results

### 5.4.1 *Ex vivo* characterisation of peripheral Parvalbumin neurons

*DRG Immunohistochemistry performed by Dr. Jane Sexton, WIBR, UCL*

The PV<sup>Tom</sup> mice described above were used here to allow for examination of the expression pattern of Cre in the DRG (Figure 5.2.A). This is an important first step to any Cre-mediated neuron ablation study that aims to minimise the risk of cell death outside of the target population. An average of 8 sections of left and right L4 and L5 DRG of PV<sup>Tom</sup> mice were co-stained with anti-Parvalbumin (anti-PV) antibody, and cells were counted to determine the extent of off-target expression of Cre.  $80.71 \pm 1.60$  % of tdTomato-expressing cells were stained with PV antibody, and  $99.84 \pm 0.14$  % of anti-PV stained cells were tdTomato-expressing neurons. To ensure that PV+ neurons also innervate the glabrous skin of the hind paw (the region stimulated during pain behaviour assays) I examined sections of skin taken from the ventral aspect of the hind paw of PV<sup>Tom</sup> mice (Figure 5.2.B) and found tdTomato expression patterns resembling the cutaneous A $\beta$  afferent endings, Meissner corpuscles (Zimmerman et al., 2014). Further co-staining using antibodies specific to ending types will corroborate this finding.

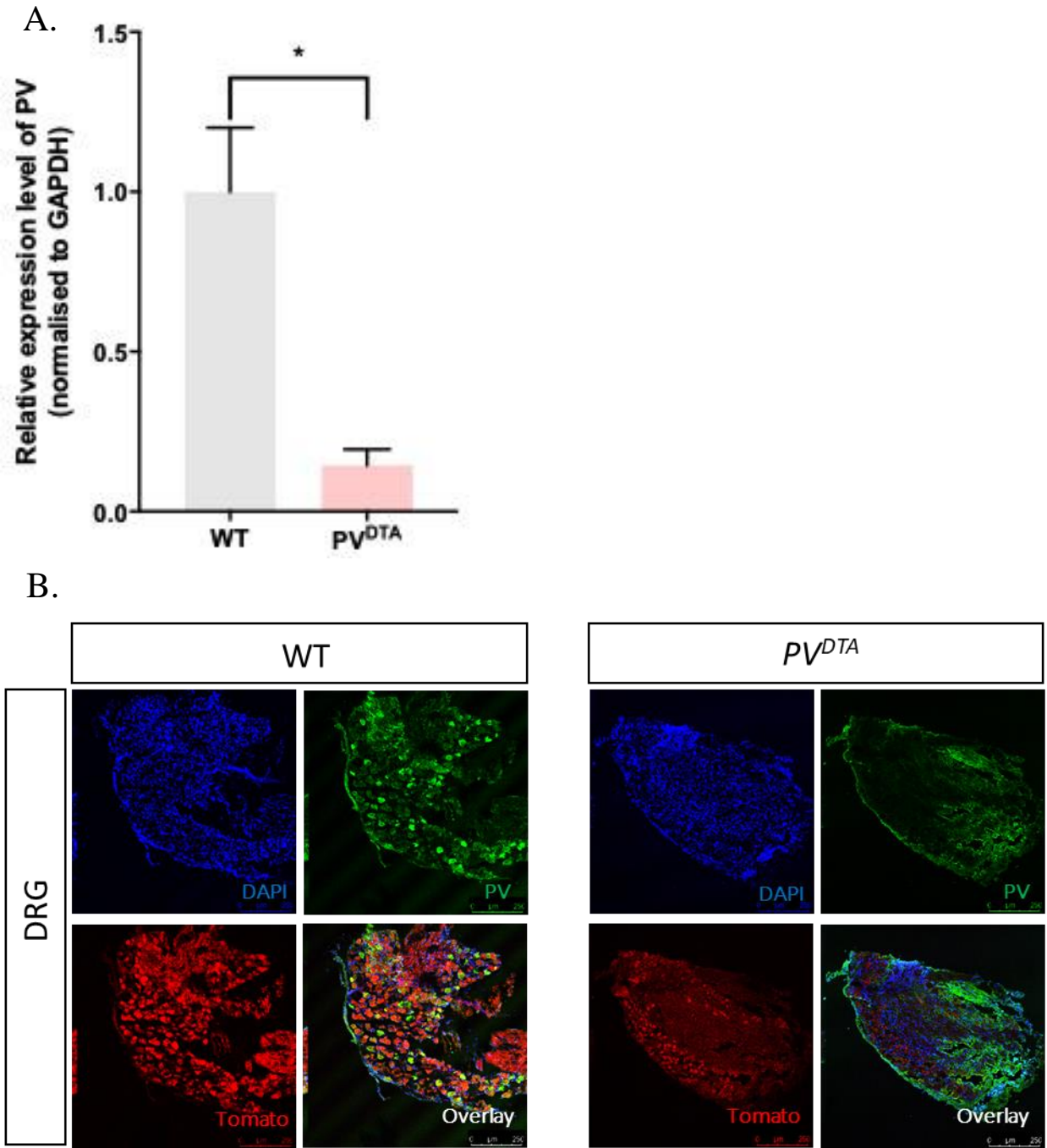




#### **5.4.2 Crossing PV-Cre mice with Advillin-loxP-tdTomato-Stop-loxP-DTA mice causes significant PV+ neuron ablation in the DRG of progeny**

*Performed by Dr. Jane Sexton, WIBR, UCL*

PV-Cre mice were crossed with Advillin-loxP-tdTomato-Stop-loxP-DTA mice to produce offspring with Cre-mediated DTA-ablation of the peripheral PV neurons (PV<sup>DTA</sup>). In the absence of Cre the Advillin-loxP-tdTomato-Stop-loxP-DTA mice express tdTomato in all Advillin+ neurons. Advillin expression is restricted to the PNS only, thus only peripheral PV- positive neurons were ablated. As a means of verifying PV neuron ablation, qRT-PCR was performed on DRG extracted from all levels of the spinal cord. A significant reduction of PV mRNA expression was observed in PV<sup>DTA</sup> mice in comparison to WT littermate controls (Figure 5.3.A). To determine if there was a concomitant reduction of PV protein, immunohistochemistry was performed on an average of 7 sections of left and right L4 and L5 DRG taken from PV<sup>DTA</sup> mice and WT littermate controls (Figure 5.3.B). Quantification of anti-PV stained cells revealed  $21.80 \pm 1.65$  % of WT neurons were PV positive compared to  $6.91 \pm 1.31$  % of PV<sup>DTA</sup> DRG neurons ( $p = <0.0021$ ), indicative of a significant reduction of PV protein expression in PV<sup>DTA</sup> DRG.



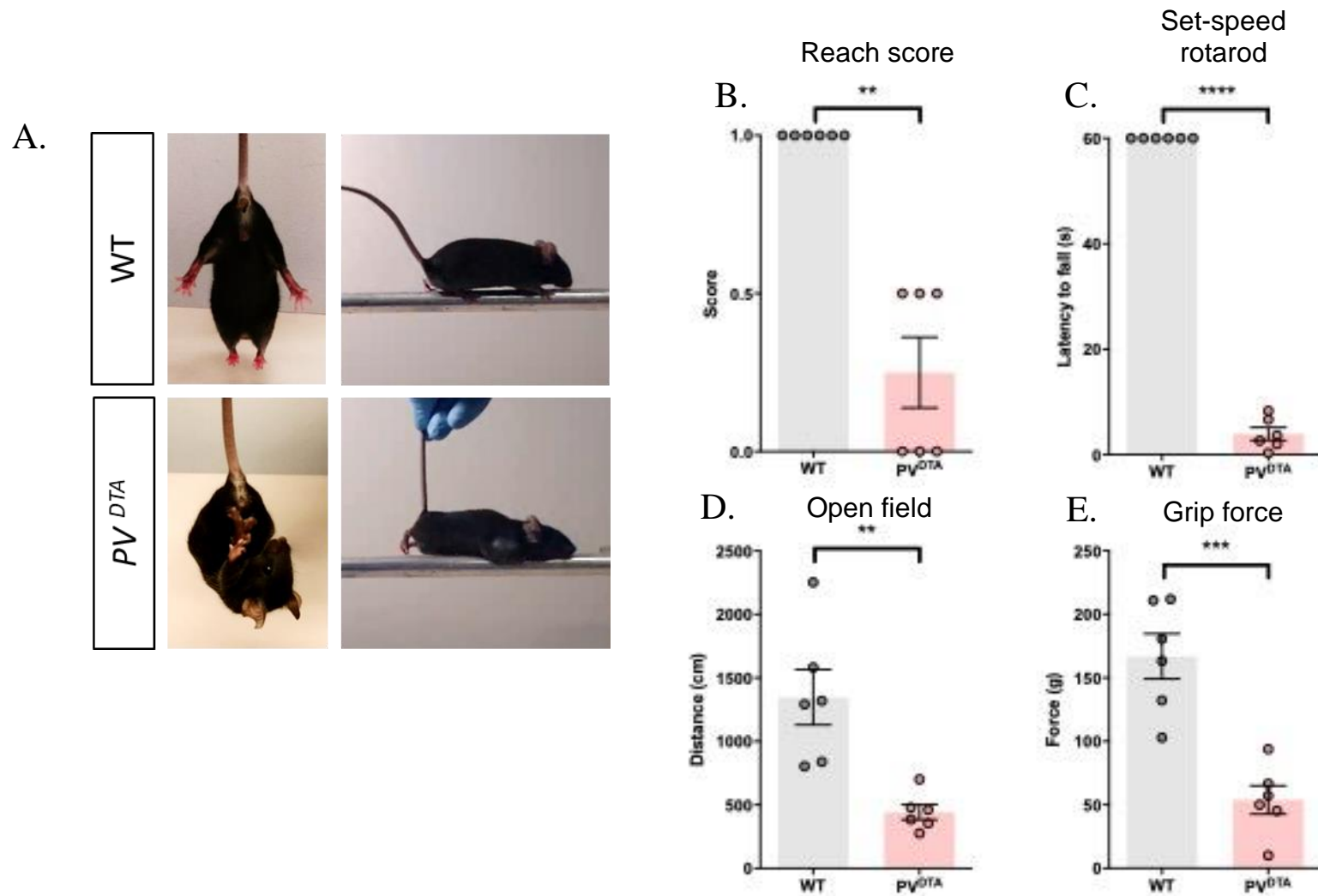
**Figure 5.3. PV<sup>DTA</sup> mice express significantly lower levels of PV mRNA and protein in the DRG**

**A.** qRT-PCR showing PV mRNA expression in the DRG of PV<sup>DTA</sup> mice is significantly reduced versus WT littermate controls, relative to GAPDH expression (n= 3 per group). Data presented as Mean ± SEM with unpaired Student's t test. **B.** Immunohistochemistry sections of DRG staining with anti-PV antibody and DAPI. TdTomato represents the Advillin-expressing neuronal population (n= 3 per group).

### 5.4.3 Peripheral PV+ neurons are necessary for normal motor function in mice

Performed by Dr. Jane Sexton, WIBR, UCL

As mentioned, peripheral PV+ neurons are predominantly proprioceptors. Unsurprisingly, ablating these neurons in mice causes significant deficits in motor coordination. WT mice will walk unaided from one side of a raised beam to the other, whereas PV<sup>DTA</sup> mice cannot support themselves on a beam unaided (Figure 5.4.A). When gently held by the tail, WT mice will typically reach towards the ground, however, PV<sup>DTA</sup> mice will curl their limbs towards their abdomen in an uncoordinated fashion (Figure 5.4.A). This observation was quantified by assigning a score of 1 for an obvious reach towards the ground within a 5 second window, 0.5 for a partial curl towards the abdomen, and a score of 0 for a total curl towards the abdomen. WT mice achieved a score of  $1 \pm 0$  verses PV<sup>DTA</sup> mice that scored an average of  $0.25 \pm 0.1118$  ( $p= 0.0022$ ) (Figure 5.4.B). Mice were observed on the rotarod apparatus (Figure 5.4.C), which was maintained at a constant speed of 5 rpm for a period of 60 seconds. PV<sup>DTA</sup> mice fell off almost instantly with an average time spent on the apparatus of  $3.945 \pm 1.228$  s, in comparison to the WT mice which remained on the rod for the entire test period ( $p= <0.0001$ ). Distance of travel within an open field chamber over a period of 5 minutes revealed PV<sup>DTA</sup> mice travelled a significantly shorter distance ( $442.8 \pm 59.72$  cm) than their WT littermates ( $1348 \pm 218.6$  cm) ( $p= 0.0025$ ) (Figure 5.4.D). Grip force exerted when all limbs were placed on a grid attachment was recorded as  $166.9 \pm 17.75$  g for the WT and  $53.85 \pm 11.22$  g for PV<sup>DTA</sup> mice ( $p= 0.0003$ ) (Figure 5.4.E). Again, this difference was statistically significant. The severe motor deficit of PV<sup>DTA</sup> mice rendered pain behaviour assays challenging to interpret as they rely upon a coordinated withdrawal response. As such, an alternate means of probing their sensitivity to noxious stimuli had to be adopted. I initially turned to *in vivo* GCaMP imaging at the level of the DRG as a surrogate for pain behavioural testing.



**Figure 5.4. PV<sup>DTA</sup> mice have significant deficits in motor function and coordination**

**A.** Representative images of age-matched adult PV<sup>DTA</sup> mouse versus WT littermate control showing reach and beam tests. **B.** Reach score assigned according to ability of mouse to reach towards the ground while held by the tail. Data displayed as Mean ± SEM with Mann-Whitney test. **C.** Time spent on rotarod apparatus set at a constant speed of 5 rpm with a maximum test time of 60 s. **D.** Distance travelled in 5 minutes in an open field chamber. **E.** Total force exerted by all four limbs on grip force grid attachment. (n = 6 per group) Data are shown as Mean ± SEM with unpaired Student's t test unless specified otherwise.

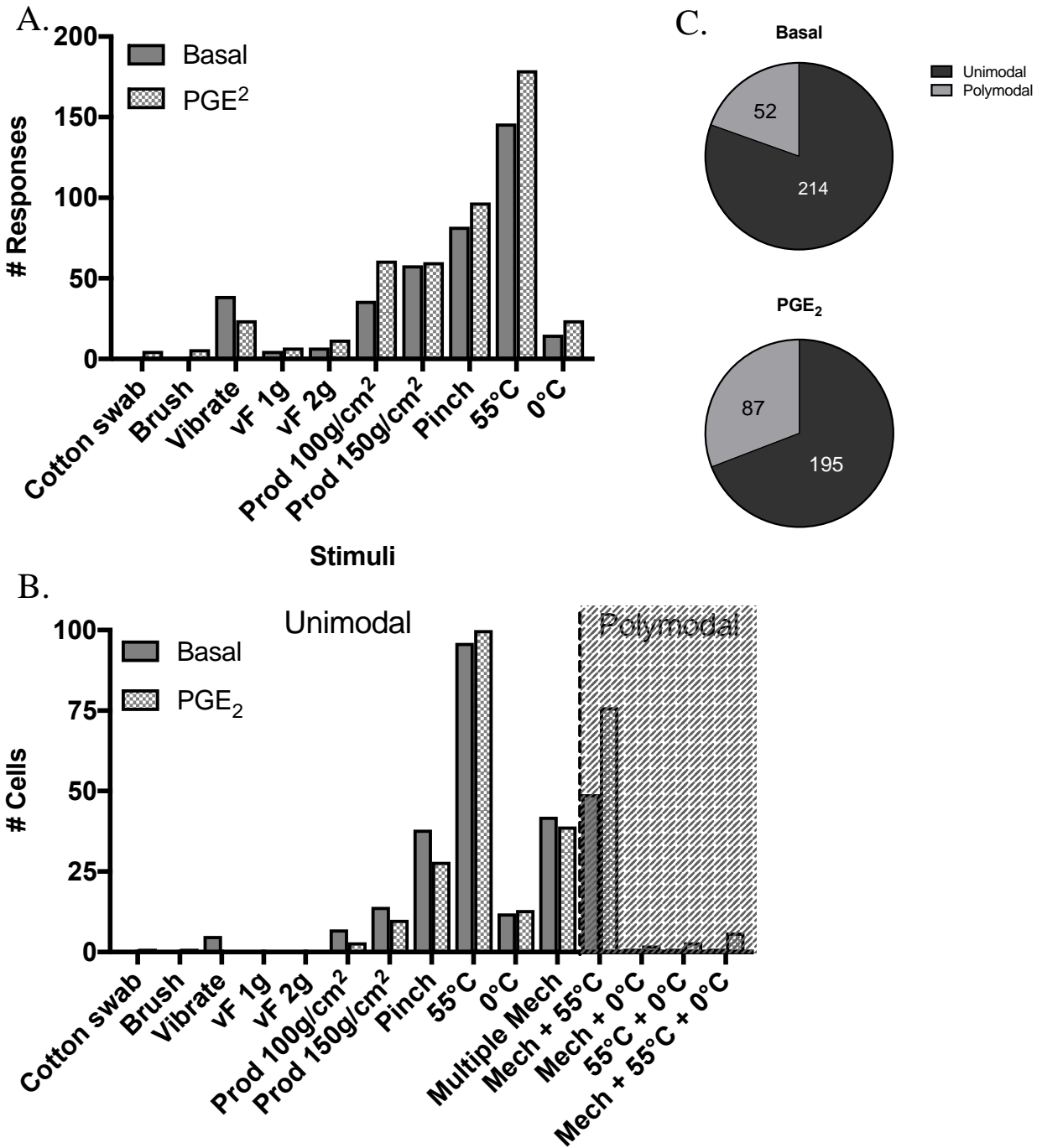
#### 5.4.4 *In vivo* GCaMP imaging is a useful tool for examining the sensitivity of peripheral sensory neurons to innocuous and noxious stimuli pre and post inflammation

To perform *in vivo* GCaMP imaging in the DRG of PV<sup>DTA</sup> mice, I bred a combination of Advillin-loxP-tdTomato-Stop-loxP-DTA, PV-Cre and *Pirt*-GCaMP3 mice to produce offspring that were either PV<sup>DTA</sup>;GCaMP3, PV;GCaMP3, or DTA;GCaMP3, the former were used as test animals and the latter two genotypes were used as WT littermate controls. As in the Piezo2 imaging experiments, all imaging was performed on the left DRG at lumbar level 4 (L4), the neurons of which innervate the hind paw. The stimuli applied to the ipsilateral hind paw (see methods for stimulus protocol) were predominantly mechanical, encompassing as broad a range of discrete mechanical sensations as possible. Noxious heat and noxious cold stimuli were used as modality controls. I injected the inflammatory agent PGE<sub>2</sub> (20 µl of 500 µM concentration) into the hind paw of the animal after performing an initial round of the stimulus protocol. I then repeated the protocol 5 minutes after administration of PGE<sub>2</sub> to see if/how neuron responses differed.

I again used a WT control for these experiments to confirm consistency between these GCaMP imaging experiments and those already published. Under basal conditions the majority of responding neurons in the WT mice respond to the most noxious stimuli, i.e. pinch and 55 °C (Figure 5.5.B), with approximately 20% of all responding neurons categorised as polymodal (Figure 5.5.C). The greatest proportion of polymodal neurons were those that responded to both mechanical and heat stimuli (Figure 5.5.B), this is consistent with a publication also comparing the response profile of neurons to thermal and mechanical stimuli (Wang et al., 2018). By classifying the cross-sectional area of neurons as small <650 µm<sup>2</sup>, medium >650 µm<sup>2</sup> <900 µm<sup>2</sup>, and large >900 µm<sup>2</sup> (Wang et al., 2018) I found that predominantly small diameter neurons respond to noxious stimuli, consistent with classical nociceptors (data not shown).

Injecting PGE<sub>2</sub> into the hind paw of WT mice was an insightful means of establishing GCaMP imaging as an effective surrogate for behaviour assays, as we can directly observe the changing profile of neuron responses in this well characterised model of acute inflammatory pain. In this study, PGE<sub>2</sub> visibly increased the number of WT neuron responses (Figure 5.5.A). Surprisingly, the proportion of pinch-only responding neurons was substantially reduced (Figure 5.5.B). This can be explained by the increase in the proportion of pinch-responding neurons now also responding to other modalities – i.e. a phenotypic switch to polymodality. In this instance, of the 82 neurons responding to pinch under basal conditions, 22 of these also responded to 55°C (no pinch responders responded to noxious cooling). After the application of PGE<sub>2</sub> 97 neurons

responded to pinch, 38 of which also responded to 55°C, and 4 of which responded to 0°C. This resulted in an increase in the proportion polymodal neurons from ~27% to ~43% after PGE<sub>2</sub> injection. Exploring these responses in greater depth, also reveals a change in the repertoire of the neurons responding, not just a recruitment of pinch-responding neurons after PGE<sub>2</sub> injection. For example, despite the number of responses to pinch rising from 82 to 97 after the addition of PGE<sub>2</sub>, the pinch response was lost from 35 cells. However, a response from a further 50 cells was elicited, 17 of which I classified as “silent” nociceptors, as they were those that had not responded to any stimuli under basal conditions. This change in the repertoire of cells responding to noxious mechanical stimuli after the addition of inflammatory agents is also described by Smith-Edwards et al., (2016). They describe this phenomenon as responsible for the shaping of the inflammatory pain response by the PNS. I also observe an overall increase in the proportion of neurons responding to 55°C after the addition of PGE<sub>2</sub>, previously described by Emery et al., (2016). Further investigation again revealed a population of neurons responding to 55°C were lost, with a concomitant recruitment of *de novo* responding neurons. A proportion of these were also classified as silent nociceptors. I observed an overall increase in neuronal polymodality following PGE<sub>2</sub> administration, increasing from ~20% to ~31% (Figure 5.5.C). This phenotypic shift towards polymodality is expected, although I observed a greater increase than previously described (Emery et al., 2016). This is likely due to the broader spectrum of mechanical stimuli used within this study that provides a more granular characterisation of evoked neuronal responses. Thus, my results are in-keeping with published data, creating a reliable means of comparison against the responses of DRG neurons in the PV<sup>DTA</sup> mice.



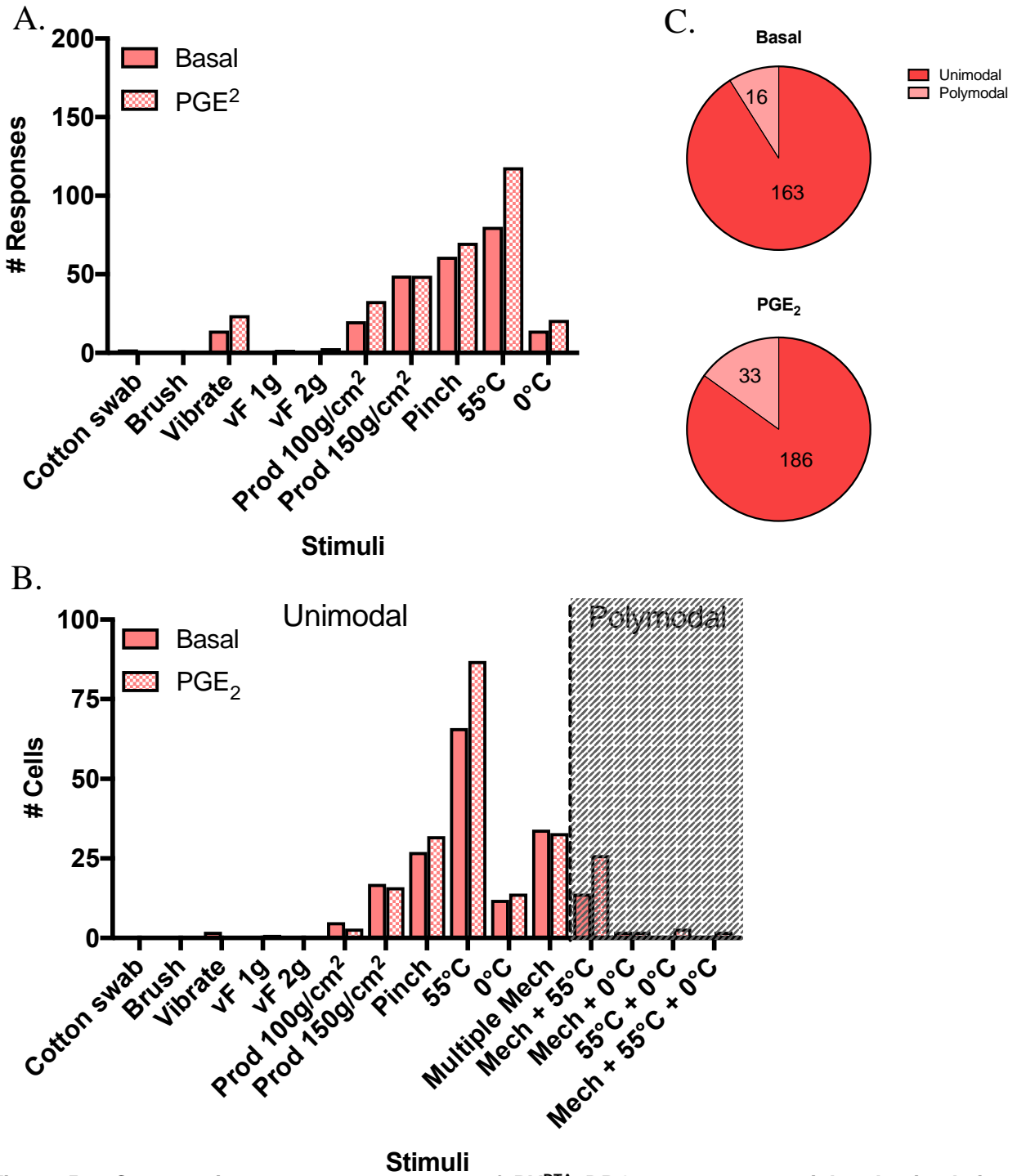
**Figure 5.5. *In vivo* GCaMP imaging Stimuli used to compare responses of WT DRG neurons to peripheral stimulation before and after induction of acute inflammatory pain**

**A.** The number of total neuron responses in the DRG of WT animals to stimuli applied to the hind paw, either pre intraplantar injection of PGE<sub>2</sub> or 5 minutes after. **B.** The number of total cells responding to either one type of stimuli, modality ('Multiple Mech' refers to neurons responding to multiple types of mechanical stimulation including pinch, and are deemed as unimodal within this study), or as polymodal i.e those responding to more than one modality in the case of 'Mech + 55°C', 'Mech + 0°C', '55°C + 0°C', and 'Mech + 55°C + 0°C'. **C.** The number of polymodal versus unimodal responding neurons of WT animals pre and post-PGE<sub>2</sub> injection. (n=4 mice)

#### 5.4.5 The neuron response profiles of PV<sup>DTA</sup> mice are comparable to WT mice

Using the same stimulation protocol described above, I recorded the responses of DRG neurons in PV<sup>DTA</sup>;GCaMP3 (now referred to as PV<sup>DTA</sup>) mice pre and post PGE<sub>2</sub>-induced inflammation. Something to mention from the outset is that despite using the same number of animals for each *in vivo* experiment, I recorded far fewer responses in PV<sup>DTA</sup> animals overall. This can be explained by the anatomy of the animals themselves, a more prominent curve of the spine on the z axis meant that a smaller portion of DRG could be viewed in any one plane, however, the proportions of responses to each stimulus were comparable to the WT dataset. For example, under basal conditions I see a similar proportion of responses to pinch in comparison to the WT (~25% of total responses in PV<sup>DTA</sup> and ~21% in WT) , and to 55 °C (~33% of total responses in PV<sup>DTA</sup> and ~38% in WT) (Figure 5.6.A and 5.5.A). After PGE<sub>2</sub> injection I also observe an increase in the total number of responses and total responding neurons in PV<sup>DTA</sup> animals, which is proportional to those I observe in the WT. An in-depth analysis of the data again revealed not only a *de novo* recruitment of neurons in response to inflammation, but a change in the repertoire of neurons responding after the injection of PGE<sub>2</sub>. For example, of the total population of neurons responding to pinch under basal conditions (61), 35 responding neurons were lost after the addition of PGE<sub>2</sub> but a further 44 responding neurons were gained. A similar occurrence (but with fewer neurons lost) is seen within the population of neurons responding to 55 °C. One discrepancy between the two datasets, however, is the extent of polymodality observed in the DRG of PV<sup>DTA</sup> animals versus the WT. Under basal and acute inflammatory conditions I see ~ 9 % and ~15 % of total responding neurons responding to more than one modality, respectively. (Figure 5.6.C). These percentages are substantially lower than those reported in WT animals within this experiment. This difference could be due to the substantial increase in neurons responding to either pinch or 55 °C only in the DRG of PV<sup>DTA</sup> animals after PGE<sub>2</sub> injection, which isn't observed in the WT (Figure 5.6.B and 5.5.B).





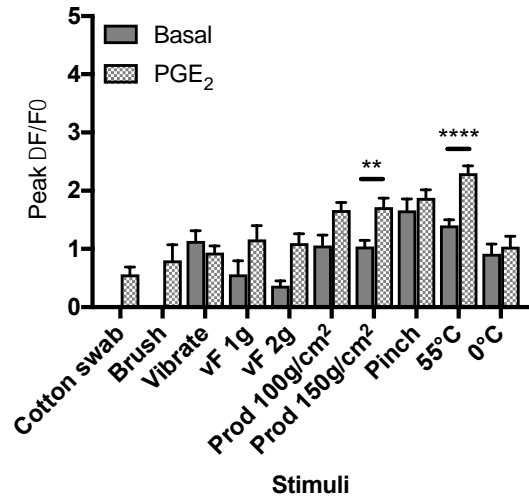
**Figure 5.6. Comparative responses of PV<sup>DTA</sup> DRG neurons to peripheral stimulation before and after induction of acute inflammatory pain**

**A.** The number of total neuron responses in the DRG of PV<sup>DTA</sup> animals to stimuli applied to the hind paw, either pre intraplantar injection of PGE<sub>2</sub> or 5 minutes after. **B.** The number of total cells responding to either one type of stimuli, modality, or as polymodal. **C.** The number of polymodal versus unimodal responding neurons of PV<sup>DTA</sup> animals pre and post PGE<sub>2</sub> (n=4 mice). For clarity, 'PV<sup>DTA</sup>' refers to mice with the genotype 'PV<sup>DTA</sup>;GCaMP3' in this figure.

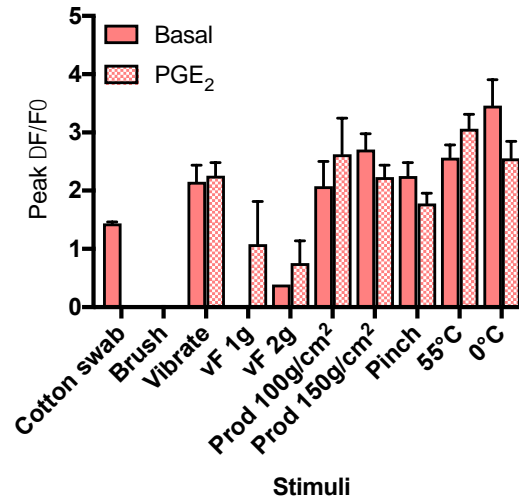
#### 5.4.6 The activity of responding neurons is increased in PV<sup>DTA</sup> mice in comparison to the WT, under basal conditions

As a further means of investigating if there any differences between the responses of DRG neurons in the WT and PV<sup>DTA</sup> mice pre- and post-PGE<sub>2</sub> injection, I compared the peak fluorescence of all neuron responses as a measure of their extent of activation. The corresponding area under the curve (AUC) was also plotted to investigate variability in the duration of neuron activation. The AUC yielded very similar patterns of neuron activity to that portrayed by peak fluorescence. I observe that peak fluorescence (i.e., activity) of neurons responding to 150g/cm<sup>2</sup> prod ( $1.045 \pm 0.105 \Delta F/F_0$  pre-PGE<sub>2</sub>;  $1.718 \pm 0.154 \Delta F/F_0$  post-PGE<sub>2</sub>;  $p=0.0006$ ) and 55°C ( $1.405 \pm 0.097 \Delta F/F_0$  pre-PGE<sub>2</sub>;  $2.304 \pm 0.123 \Delta F/F_0$  post-PGE<sub>2</sub>;  $p= <0.0001$ ) significantly increases in the WT mice after injection of PGE<sub>2</sub> (Figure 5.7.A.i.). This increased excitability of neurons to noxious stimuli mirrors the hypersensitivity observed in behaving WT animals after PGE<sub>2</sub> injection and in a similar DRG *in vivo* GCaMP study (Emery et al., 2016). Interestingly the peak fluorescence of PV<sup>DTA</sup> neurons compared to WT neurons under basal conditions is significantly increased in response to 150g/cm<sup>2</sup> prod ( $2.705 \pm 0.273 \Delta F/F_0$  PV<sup>DTA</sup>;  $p= <0.0001$ ), 55°C ( $2.568 \pm 0.219 \Delta F/F_0$  PV<sup>DTA</sup>;  $p= <0.0001$ ), and 0 °C ( $0.917 \pm 0.167 \Delta F/F_0$  WT;  $3.461 \pm 0.445 \Delta F/F_0$  PV<sup>DTA</sup>;  $p= <0.0001$ ) (Figure 5.7.C.i.). The peak fluorescence of responding PV<sup>DTA</sup> neurons does not increase with the addition of PGE<sub>2</sub> (Figure 5.7.B.i.). This is perhaps indicative of a disinhibition of the DRG somatosensory neurons in PV<sup>DTA</sup> mice, or at least those associated with noxious sensation, under basal conditions. Whether this correlates with a hypersensitivity to acute noxious stimuli, or a hyposensitivity to acute inflammatory pain in the behaving PV<sup>DTA</sup> mouse subsequently became a source of further investigation. Figure 5.7.D shows example traces of individual neurons of WT and PV<sup>DTA</sup> animals responding to either 150g/cm<sup>2</sup> prod or 55 °C, pre and post PGE<sub>2</sub> injection.

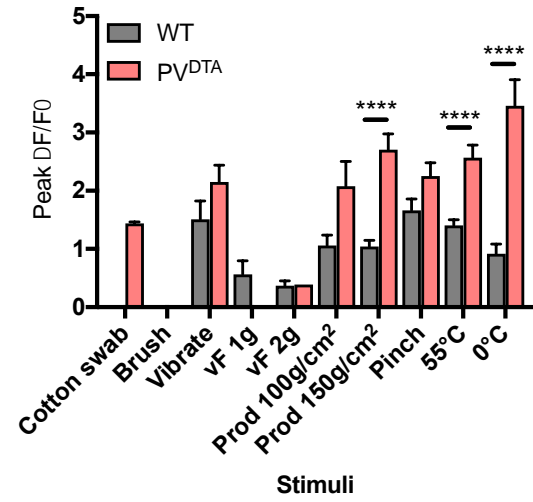
A.i.



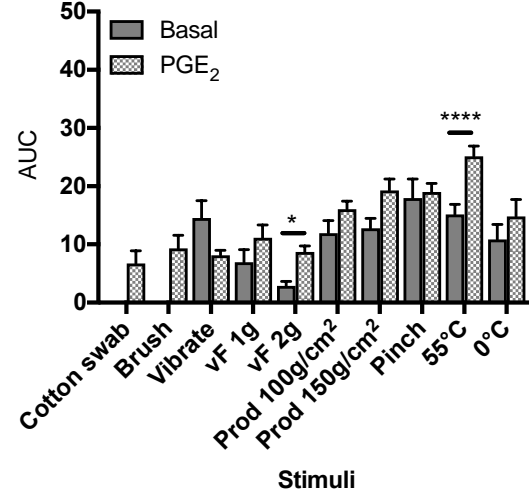
B.i



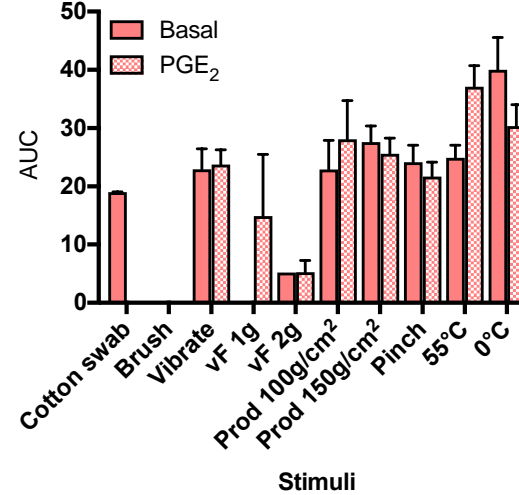
C.i.



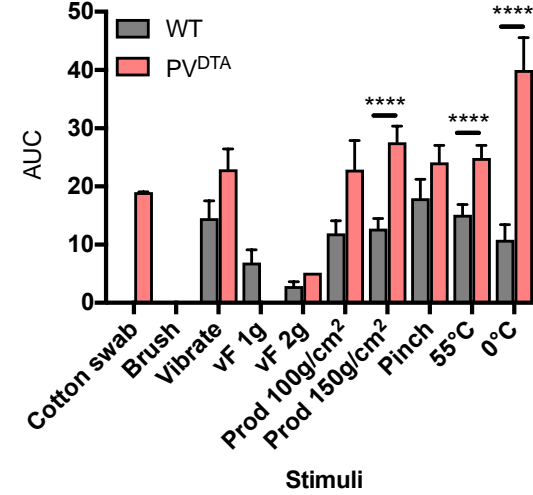
A.ii.

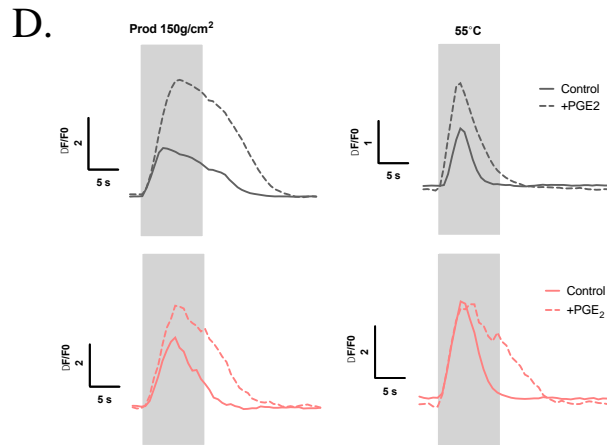


B.ii



C.ii.





**Figure 5.7. Peak fluorescence as a measure of activity of responding DRG neurons in  $PV^{DTA}$  mice verses WT controls to peripheral stimulation before and after induction of acute inflammatory pain**

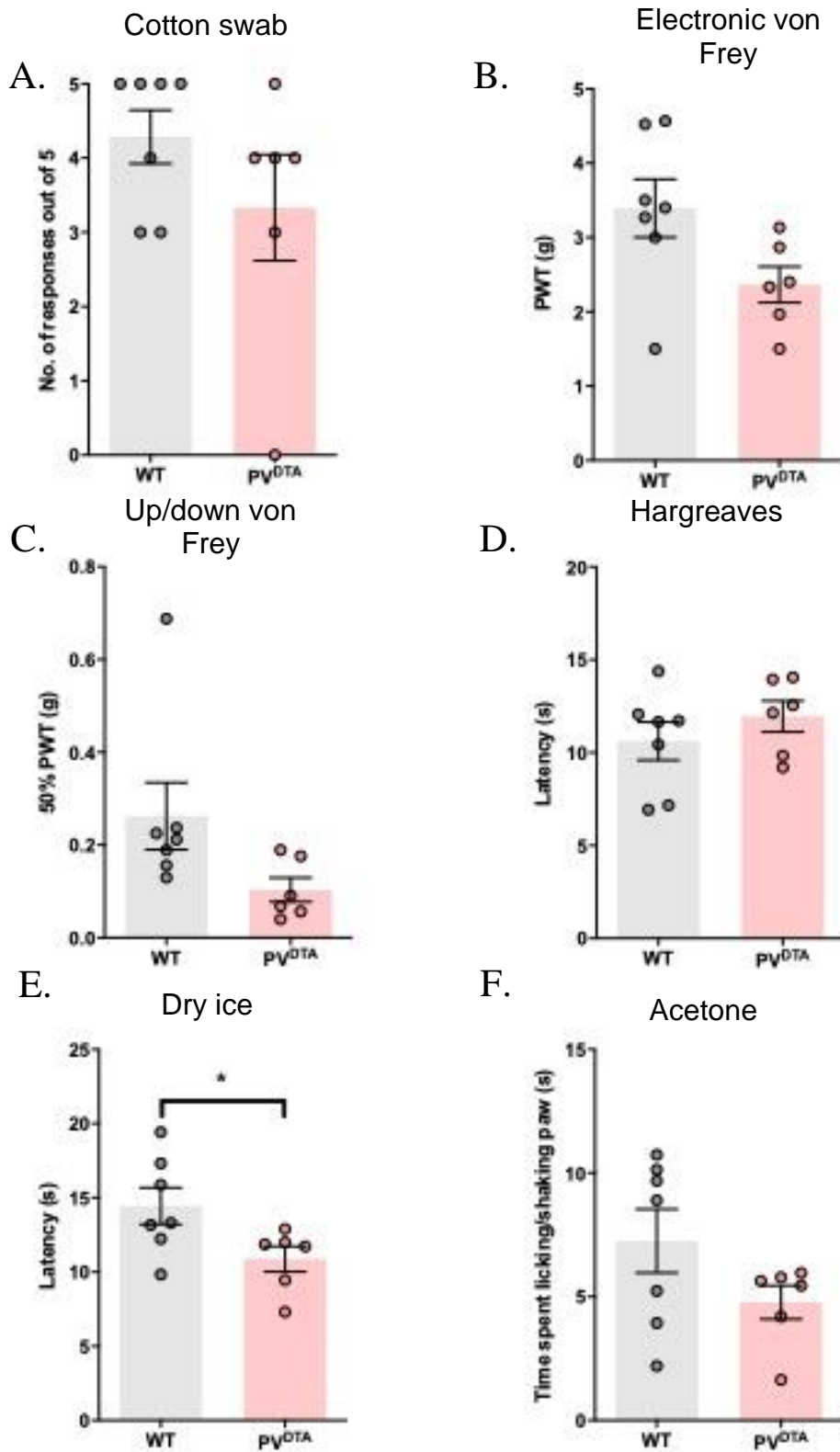
**A.** Peak fluorescence **(i)** and corresponding area under the curve (AUC) **(ii)** of neurons in WT animals. For most stimuli an increase in activity is observed after  $PGE_2$  injection, and significantly so in those neurons responding to  $150g/cm^2$  prod and  $55^\circ C$  water. **B.** Peak fluorescence **(i)** and corresponding AUC **(ii)** in  $PV^{DTA}$  animals. A significant increase in peak fluorescence to any stimuli, including those that are noxious, is not observed after  $PGE_2$  injection. **C.** A comparison of the basal responses of WT and  $PV^{DTA}$  neurons demonstrates that fluorescence, hence activity, of  $PV^{DTA}$  neurons responding to  $150g/cm^2$  prod, and  $55^\circ C$  and  $0^\circ C$  water is significantly greater than WT responding neurons, with both peak fluorescence **(i)**, and corresponding AUC **(ii)**. **D.** Representative traces of a responding WT (grey) and  $PV^{DTA}$  (pink) neuron's peak fluorescence to  $150g/cm^2$  prod and  $55^\circ C$  pre and post  $PGE_2$  exposure. Data are shown as Mean  $\pm$  SEM. Statistical analysis was performed using the multiple unpaired Student's t test. (WT  $n=4$ ;  $PV^{DTA}$   $n=4$ )

#### 5.4.7 PV<sup>DTA</sup> mice are hypersensitive to noxious cold

The increased peak fluorescence of responding DRG neurons to hind paw stimulation in PV<sup>DTA</sup> versus WT mice during *in vivo* GCaMP imaging indicated that PV<sup>DTA</sup> animals may have a behavioural hypersensitivity to somatosensory stimuli. As discussed in the previous Piezo2 chapter, it is exceptionally important to take the proprioceptive function of the animals to be tested into consideration as this may confound their ability to respond to pain threshold testing irrespective of their perception of the stimulus. As such, I approached these pain behaviour assays with great caution. In line with my imaging data, I found a reduction in the time/force taken for PV<sup>DTA</sup> animals to respond to certain stimuli, reassuring me that it was a hypersensitivity that we were observing. Perhaps if motor coordination was not impaired, I may have observed an even further reduction in response time. Unfortunately, the severe proprioceptive deficit in PV<sup>DTA</sup> animals made it impossible to accurately perform certain pain behaviour experiments as they rely upon the coordinated movement of the whole animal rather than the withdrawal of one hind paw. I will discuss later how these issues may be overcome using alternate pain behaviour assays that unfortunately could not be utilised within this study.

I performed the cotton swab assay (Figure 5.8.A) as a means of determining the sensitivity of PV<sup>DTA</sup> animals to innocuous dynamic mechanical stimulation of the hind paw. I found no significant difference in comparison to WT mice, although there is a perceivable diminution in their number of responses perhaps due to their motor deficit. To determine the response of animals to punctate mechanical stimuli I used the electronic von Frey assay (dynamic plantar aesthesiometer), and the manual up/down von Frey assay. I observe a trend in hypersensitivity in PV<sup>DTA</sup> animals in response to the electronic von Frey assay ( $2.367 \pm 0.2416$  g) in comparison to WT animals ( $3.394 \pm 0.3911$  g) that does not quite reach significance ( $p=0.0554$ ) (Figure 5.8.B). The same trend was observed in the manual up/down von Frey assay (Figure 5.8.C). This is in line with my imaging data, which suggests that DRG neurons responding to mechanical stimuli, do so with increased excitability in PV<sup>DTA</sup> mice. Unfortunately, I could not glean reliable data from the Randall-Selitto assay as a measure of sensitivity to noxious mechanical stimuli, due to the inability of PV<sup>DTA</sup> animals to produce a coordinated and discernible nocifensive response either when the apparatus was applied to the tail, or to the hind paw. An alternate means of assessing sensitivity to noxious mechanical stimuli in the future could be to use the pinprick assay (Murthy et al., 2018). This is the punctate stimulation of one hind paw with a needle whilst the animal is positioned (after acclimatisation) in a von Frey stand. To limit human error, attaching this needle to a von Frey filament would ensure that the needle is applied with similar (if not the same) force (Dhandapani et al., 2018).

To assess the response of PV<sup>DTA</sup> animals to a noxious heat stimulus I performed the Hargreaves assay, again finding no significant difference in heat pain thresholds between these and WT animals (Figure 5.8.D). This could be perceived as contradictory to my imaging findings, which suggest that PV<sup>DTA</sup> animals are hypersensitive to noxious heat. It is important to note that the Hargreaves assay (with a temperature cut-off of 50°C) is not directly comparable with the 55°C water applied to the hind paw during imaging experiments. A more appropriate comparison would be the use of the hot plate assay, which at its most noxious also assesses the response of animals to 55°C heat. Unfortunately, I also did not achieve reliable results with this assay, as the PV<sup>DTA</sup> animals are incapable of rearing or jumping. If possible, it would have been beneficial to adapt the Hargreaves apparatus to allow for direct stimulation of one hind paw with 55°C heat excluding a ramp. Other studies have published data using the thermal probe assay (Murthy et al., 2018) although this has its own caveats including the 1g of pressure applied to the hind paw with the correct positioning of the probe. To assess sensitivity to noxious cold, I performed the dry ice assay (Figure 5.8.E). This particular behavioural test requires animals to be placed on the same glass surface as in the Hargreaves assay, while dry ice is applied to the area of glass under the hind paw. I observe a significant reduction in the time taken for PV<sup>DTA</sup> animals to withdraw their hind paw ( $10.87 \pm 0.8525$  s) versus WT animals ( $14.45 \pm 1.235$  s) ( $p = 0.0421$ ), supporting the increased activity I observed in the DRG neurons during *in vivo* GCaMP imaging experiments in response to 0°C water. No significant difference was observed using the acetone assay to assess behaviour to innocuous cooling, however (Figure 5.8.F).



**Figure 5.8. Acute behavioural characterisation of PV<sup>DTA</sup> mice**

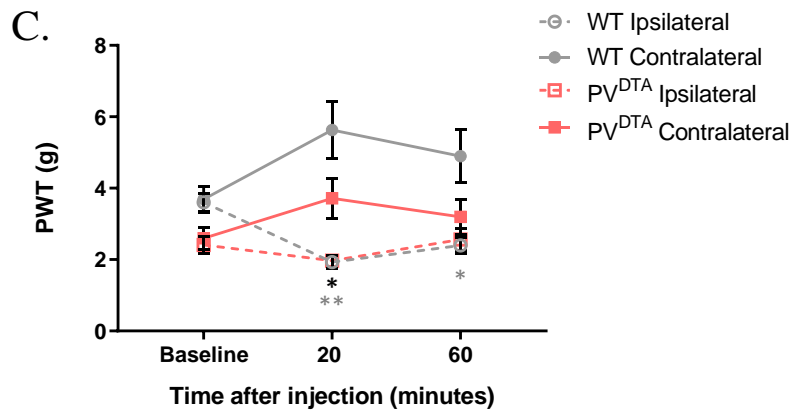
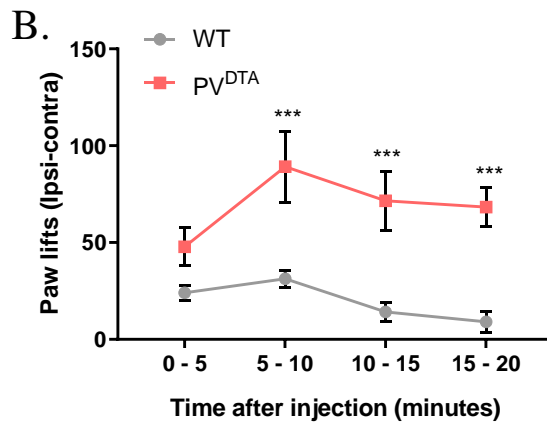
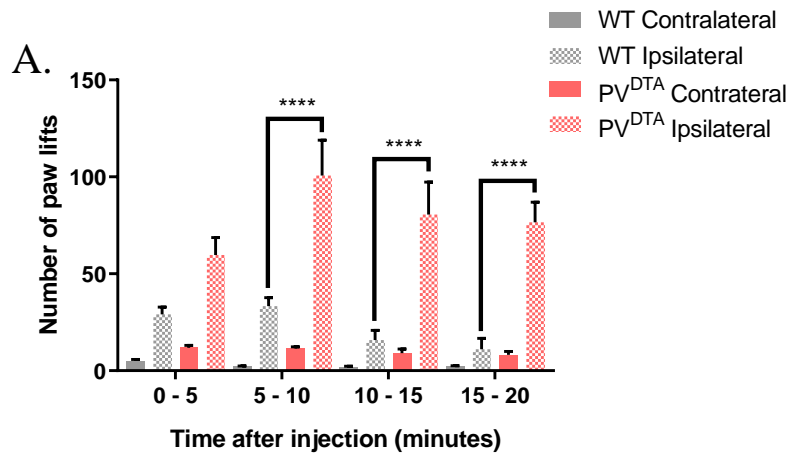
**A.** Cotton swab test assessing innocuous dynamic mechanical sensitivity. Statistical analysis performed using the Mann-Whitney test. **B.** Electronic von Frey. **C.** Manual up/down von Frey. **D.** Hargreaves assay. **E.** Dry ice assay. **F.** Acetone assay. Data are shown as Mean  $\pm$  SEM. Statistical analysis was performed using the unpaired Student's t test unless stated otherwise. (WT n=7; PV<sup>DTA</sup> n=6).

#### **5.4.8 Stimulus-independent pain is dramatically increased in PV<sup>DTA</sup> animals in comparison to WT animals following induction of acute inflammation**

As the PGE<sub>2</sub> model of acute inflammation is an assay I used during the *in vivo* GCaMP imaging experiments, I chose to repeat this assay in the behaving animals. Something that is exceptionally difficult to glean using *in vivo* GCaMP imaging is spontaneous activity of peripheral neurons. I found a dramatic increase in stimulus-independent hypersensitivity in awake, behaving PV<sup>DTA</sup> animals in comparison to WT animals as evidenced by observing flicking, shaking, biting, licking behaviours of the ipsilateral hind paw for a duration of 20 minutes immediately after PGE<sub>2</sub> injection (Figure 5.9.A and B). This comparative hypersensitivity peaked at 5–10 minutes post PGE<sub>2</sub> injection where PV<sup>DTA</sup> animals lifted their paws on average  $100.7 \pm 18.2$  times over 5 minutes and WT animals only  $33.3 \pm 4.4$  times ( $p = <0.0001$ ) (Figure 5.9.A). These findings suggest that peripheral PV<sup>+</sup> neurons are responsible for providing a tonic level of input into the spinal cord under inflammatory conditions, which helps to modulate the nocifensive response of the animal to inflammatory insults.

After 20 minutes of stimulus-independent observation I looked at mechanically-evoked behaviours at 20 minutes and 60 minutes post-PGE<sub>2</sub> injection using the electronic von Frey assay (Figure 5.9.C). The ipsilateral hind paw of WT animals was significantly hypersensitive to the von Frey stimulus in comparison to the contralateral hind paw at 20 minutes post injection, and to the ipsilateral baseline recording at both 20 and 60 minutes post injection (Figure 5.9.C). Reassuringly, the hypersensitivity of PV<sup>DTA</sup> animals to the electronic von Frey assay in comparison to WT animals is again observed at baseline, and there appears to be a slight increase in this hypersensitivity at 20 minutes post- PGE<sub>2</sub> injection (but is not significant). Potential differences in mechanical pain thresholds could have been more accurately determined using manual von Frey filaments and the up/down paradigm that could provide better resolution of fine thresholds. Another indication of a possible hypersensitivity is that I observe a corresponding hyposensitivity in the contralateral hind paw, similar to that seen in the WT animals.





**Figure 5.9. Stimulus-independent and stimulus-dependent behaviours observed in WT versus PVDTA animals in response to intraplantar PGE<sub>2</sub> injection**

**A.** The number of paw lifts observed as a measure of nocifensive behaviour due to 20  $\mu$ l 500 mM intraplantar injection of PGE<sub>2</sub>. PV<sup>DTA</sup> mice demonstrate a significantly greater number of ipsilateral hind paw lifts in comparison to the ipsilateral hind paw of WT animals. **B.** The same observation presented as the mean number of contralateral paw lifts subtracted from the mean number of ipsilateral paw lifts. **C.** Electronic von Frey applied to both ipsilateral and contralateral hind paws. A significant hypersensitivity in the ipsilateral hind paw of WT mice is observed at 20 minutes post PGE<sub>2</sub> injection in comparison to contralateral hind paw. This hypersensitivity begins to wear off an hour after injection. A perceivable hypersensitivity in PV<sup>DTA</sup> animals in comparison to WT animals to electronic von Frey is observed in both ipsi- and contralateral hind paws at baseline. A further hypersensitivity (although not significant) is observed in the ipsilateral hind paw of PV<sup>DTA</sup> animals 20 minutes after PGE<sub>2</sub> injection. Data are shown as Mean  $\pm$  SEM. Statistical analysis was performed using RM two-way ANOVA with Tukey's multiple comparisons test to compare ipsilateral and contralateral hind paw lifts in WT and PV<sup>DTA</sup> animals, and PWT in both genotypes in response to electronic von Frey. RM one-way ANOVA with Dunnett's multiple comparisons test was used to compare subsequent von Frey recordings to the baseline. Black stars represent significance in comparison to WT. Grey stars represent WT significance in comparison to baseline recording. (WT n=7; PV<sup>DTA</sup> n=6).

#### 5.4.9 Evidence for peripheral sensory neuron hypersensitivity is observed in the spinal cord of PV<sup>DTA</sup> animals as determined by *in vivo* electrophysiology

*Performed in collaboration with Dr. Shafaq Sikandar, WHRI, QMUL*

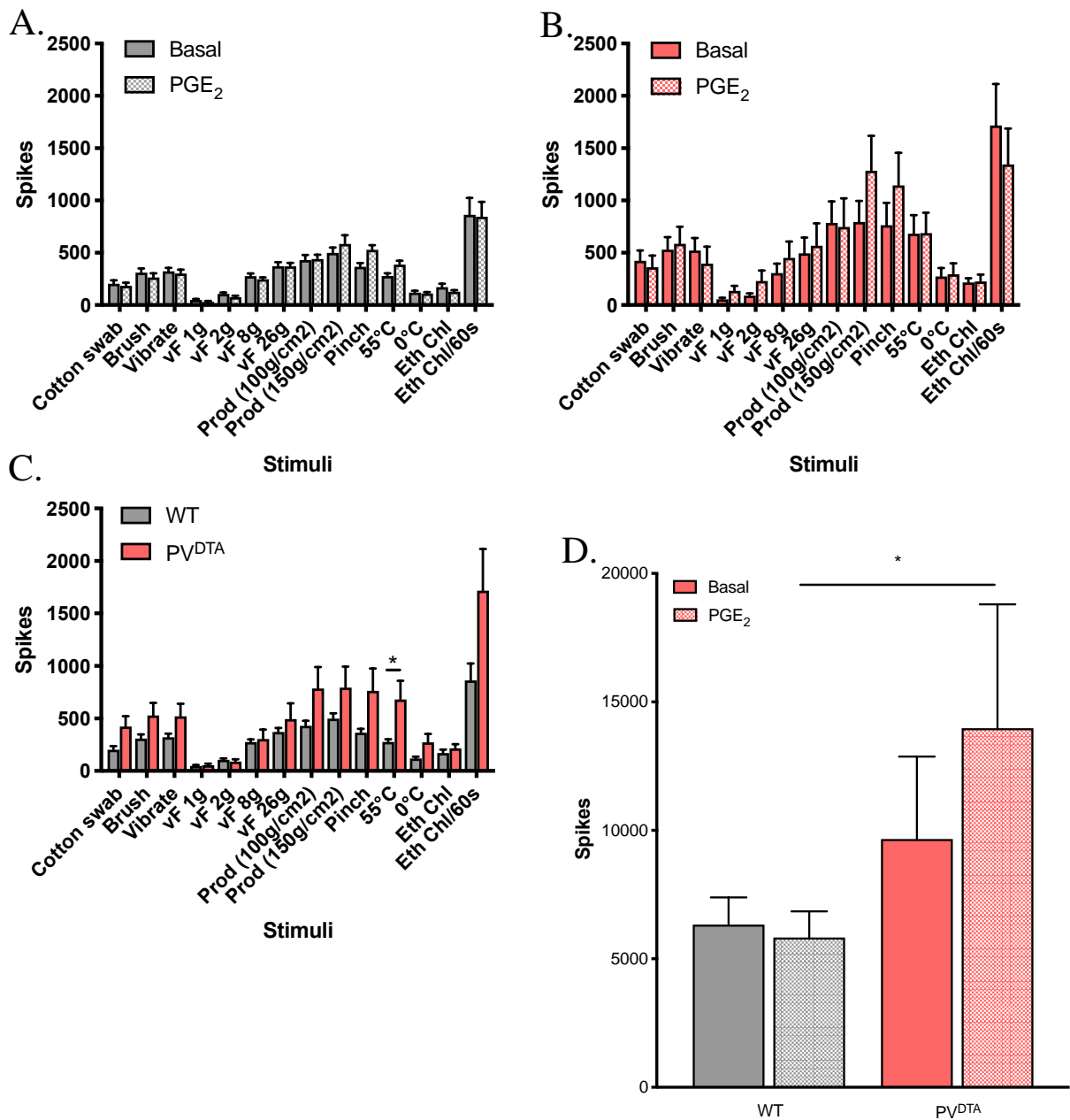
As a further means of corroborating the hypersensitivity I observe in PV<sup>DTA</sup> animals, I chose to explore their sensitivity at the level of the spinal cord to the same stimuli used in the *in vivo* GCaMP imaging experiments. To do so, we recorded extracellular spikes (action potentials) from wide dynamic range (WDR) neurons located in the deep dorsal horn (laminae III-V), a region of the spinal cord that receives inputs from both mechanosensitive innocuous and noxious afferents, and which we identified by their responses to dynamic and punctate mechanical stimuli, and a noxious heat stimulus. WDR neurons include both interneurons involved in polysynaptic reflexes, and projection neurons that transmit sensory information from the spinal cord to the brain through the spinothalamic and spinoreticular tracts. This experimental paradigm is regularly used to determine the sensitivity of neurons to peripheral innocuous and noxious insults, both under basal conditions and in the presence of inflammatory and neuropathic insults. However, interpretation of these experimental techniques should be approached with some caution as although it is believed that WDR neurons show a consistent increase in spontaneous activity in response to inflammatory and neuropathic insults, inconsistencies have been observed in stimulus-dependent responses under the same conditions (Zain & Bonin, 2019). This particular technique did however allow us to explore spontaneous activity to a greater extent.

Where we observe a significant increase in activity in response to noxious mechanical and heat stimuli in the DRG neurons of WT animals after exposure to PGE<sub>2</sub>, our stimulus-dependent *in vivo* electrophysiology recordings demonstrate a modest but insignificant increase in the firing rate of WDR neurons in response to pinch and 55°C stimuli after PGE<sub>2</sub> injection (Figure 5.10.A). The WDR neurons of PV<sup>DTA</sup> animals also appear hypersensitive to noxious mechanical stimuli after PGE<sub>2</sub> injection although again not to a significant extent (Figure 5.10.B). When we compare the evoked activity of both WT and PV<sup>DTA</sup> WDR neurons under basal conditions (Figure 5.10.C), we observe significantly increased activity (spikes/10 s) in response to 55°C in PV<sup>DTA</sup> animals ( $277.2 \pm 25.5$  WT;  $683.2 \pm 176.2$  PV<sup>DTA</sup>;  $p= 0.0109$ ). This is in line with the significant increase in activity observed in the DRG in response to 55°C. However, we do not observe here the same significant increase in response to noxious mechanical and cold stimuli. We only observe a trend with pinch ( $364.8 \pm 36.1$  WT;  $763.1 \pm 213.2$  PV<sup>DTA</sup>;  $p= 0.0786$ ) and 0°C ( $120.7 \pm 15.6$  WT;  $274.5 \pm 77.9$  PV<sup>DTA</sup>;  $p= 0.0714$ ). Further experiments are required to validate these findings, although increased activity is likely considering the cold hypersensitivity I observe in the behaving animals, and the trend in increased mechanical sensitivity. Both *in vivo* imaging and *in vivo* electrophysiology datasets

suggest that a behavioural heat hypersensitivity would be evident with the appropriate behavioural assay.

To assess stimulus-independent (spontaneous) activity of WDR neurons in response to PGE<sub>2</sub> injection we performed a 5 minute baseline recording prior to the natural stimulus protocol. This was then compared to a 5 minute recording from the same neurons beginning immediately after PGE<sub>2</sub> injection into the ipsilateral hind paw. We found that spontaneous activity in the WDR neurons of PV<sup>DTA</sup> animals was significantly greater than in WT WDR neurons after intraplantar PGE<sub>2</sub> injection, as measured by total spikes over the duration of the 5 minute recordings (5829 ± 1021 WT; 13979 ± 4817 PV<sup>DTA</sup>; p= 0.0129) (Figure 5.10.D). This is in line with the enhanced hypersensitivity observed in the behaving PV<sup>DTA</sup> animals. However, somewhat peculiarly we do not observe an increase in spontaneous activity after administration of PGE<sub>2</sub> in the WDR neurons of WT animals.

Whilst performing these experiments, an interesting observation was that the hind paw sensory neurons in PV<sup>DTA</sup> animals appeared to innervate a greater length of the dorsal horn than their WT counterparts. This is a likely indication of developmental compensation and also highlights the difficulty we had in isolating and recording from WDR neurons in these animals. Immunohistochemistry experiments using retrograde tracers injected into the hind paw would be an excellent means of assessing the somatotopic organisation of these peripheral sensory neurons, by examining lumbar DRG for tracer expression in neurons of PV<sup>DTA</sup> animals in comparison to WT animals, the innervation pattern of which we would normally expect to be L3-L5 DRG.



**Figure 5.10. *In vivo* electrophysiology in WDR neurons of the dorsal horn of the spinal cord in WT versus PV<sup>DTA</sup> animals**

**A.** Activity of WDR neurons in the dorsal horn of WT animals measured as the number of spikes produced over the 10 second stimulation period, pre and post intraplantar PGE<sub>2</sub> injection. Spontaneous activity to the ethyl chloride stimulus was measured for a subsequent 60 seconds after the initial 10 second recording **B.** Activity of WDR neurons in the dorsal horn of PV<sup>DTA</sup> animals. **C.** A comparison of the number of spikes produced by WDR neurons in the dorsal horn under basal conditions in both the WT and PV<sup>DTA</sup> mice. **D.** Stimulus independent activity in WDR neurons as a consequence of 20  $\mu$ l 500 mM intraplantar injection of PGE<sub>2</sub>. Basal activity of WDR neurons was recorded for 5 minutes prior to the first stimulation protocol, and stimulus-independent activity of the same neurons was recorded for 5 minutes after intraplantar injection of PGE<sub>2</sub>. Data are shown as Mean  $\pm$  SEM. Statistical analysis was performed using the multiple unpaired Student's t test for evoked activity, and ordinary one-way ANOVA for stimulus-independent activity. (WT basal and PGE<sub>2</sub> n= 45; PV<sup>DTA</sup> basal n= 17; PV<sup>DTA</sup> PGE<sub>2</sub> n= 13 ).

#### **5.4.10 Peripheral cutaneous PV+ neurons respond to a range of stimuli including noxious mechanical and thermal stimuli pre and post PGE<sub>2</sub> injection**

As a means of directly determining which stimuli peripheral PV+ neurons respond to, I crossed PV<sup>Tom</sup> animals with those globally expressing GCaMP6s to generate PV<sup>Tom</sup>;GCaMP6s progeny. This allowed for the identification of PV+ DRG neurons with red fluorescence on a background of green GCaMP6s-expressing DRG neurons during *in vivo* imaging experiments. Global GCaMP6s expressing mice were chosen for this particular experiment due to minimal expression of *Pirt*-driven GCaMP3 in PV+ sensory neurons (see appendices for details). I used the same natural stimulus protocol as utilised in the PV<sup>DTA</sup>;GCaMP3 *in vivo* imaging studies, and all other methods associated with it. If PV+ cutaneous neurons are responsible for closing the ‘pain gate’ in the spinal cord, one may assume they are activated in response to noxious stimuli.

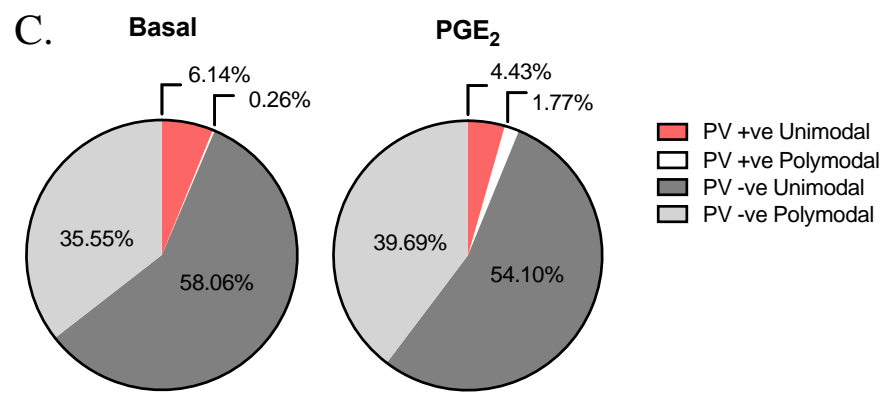
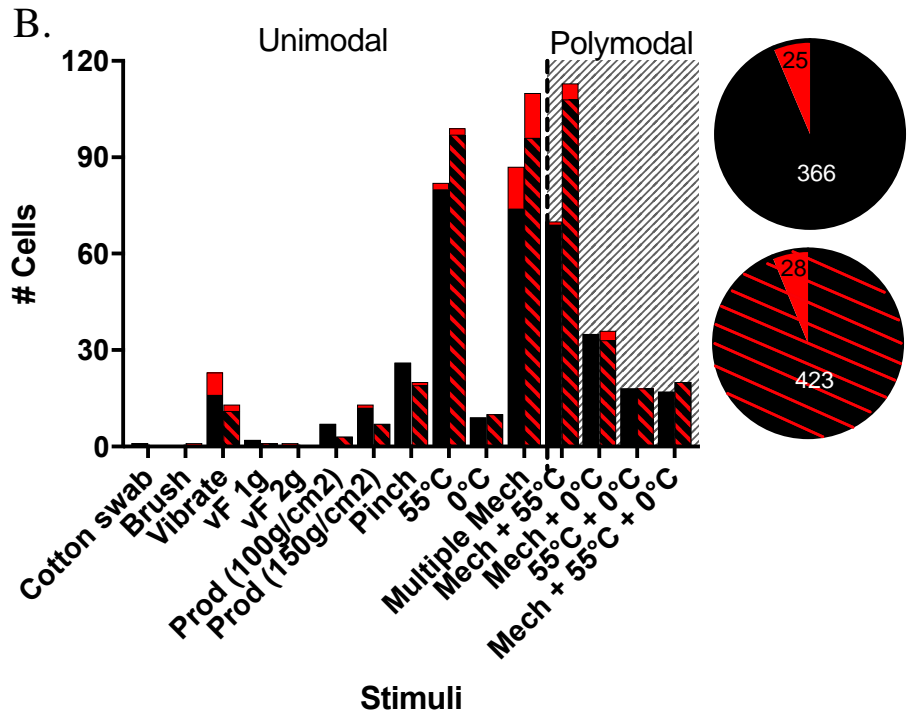
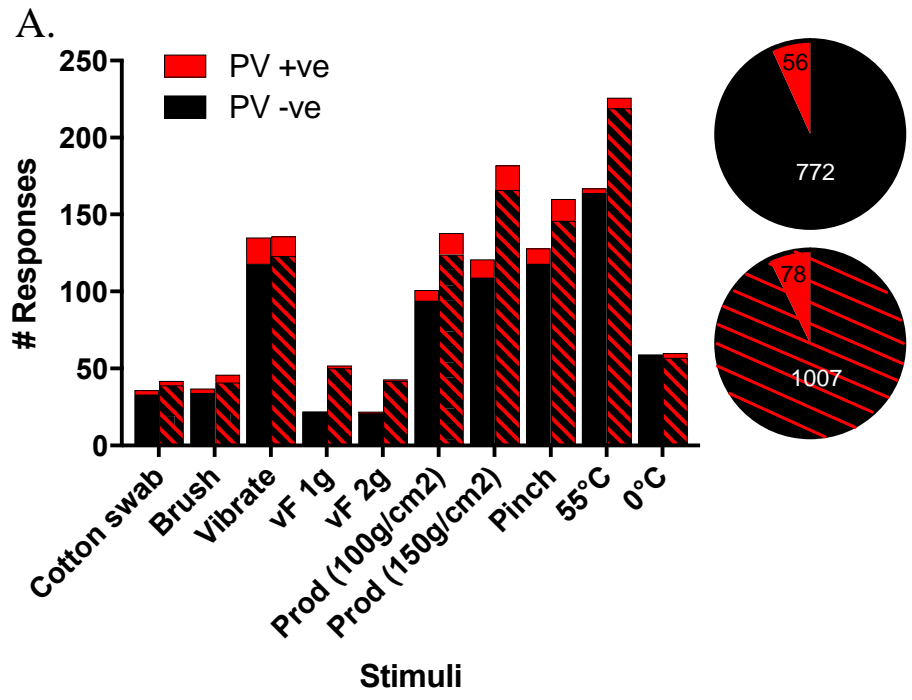
Before discussing the data with emphasis placed upon the PV+ population of sensory neurons, only, it is important to first note the different profile of total DRG neuron responses gleaned as a consequence of global GCaMP6s expression instead of *Pirt*-driven GCaMP3 expression. As mentioned, there is a proportion of sensory neurons that don’t express the molecular marker *Pirt*, which are predominantly LTMRs including those expressing PV. As such there is reduced bias towards responses induced by noxious stimuli, and we see a more even distribution of responses across all stimuli. I also observe a greater proportion of polymodal neurons both under basal and acute inflammatory conditions. One would argue that this is a much more accurate representation of the neuron response profile within the DRG.

As expected, I observe only a small portion of total responding cells as PV+. We know from previous studies that PV+ neurons make up ~25% of total L4 DRG neurons, and only a small portion of these are vibration-sensitive cutaneous afferents. In my recordings, I found that ~30% of PV neurons responded to vibration stimuli under basal conditions, which is in line with data indicating PV expression in Pacinian corpuscles (de Nooij et al., 2013), the sensory neuron end organs responsible for sensing vibration (Abraira & Ginty, 2013) (Figure 5.11.A). Under basal conditions I also observe responses to noxious mechanical cues including pinch, and interestingly to 55°C (which make up ~5% of total PV neuron responses), but none to 0°C. It is possible that the latter observation can be explained by the comparatively small number of total neurons that respond to noxious cooling rather than noxious heating, and that perhaps PV+ neurons outside of our field of view do indeed respond to this stimulus. When I assign each of these responses to individual neurons (Figure 5.11.B) I observe a significant proportion of PV+ neurons responding to vibration only under basal conditions, and that the

majority of those that respond to noxious mechanical stimuli are in fact responding to a number of different types of mechanical stimuli (classified as 'multiple mech' neurons). I only report one polymodal PV+ neuron here out of 25 PV+ neurons recorded in total, which responds both to a mechanical stimulus, and 55°C.

After the addition of PGE<sub>2</sub>, total responses in the PV+ population increased from 56 to 78, and total responding cells increased from 25 to 28. This is in proportion to the increases observed in the non-PV expressing population (Figure 5.11.A and B). This data indicates that peripheral PV neurons also have a propensity for PGE<sub>2</sub>-mediated sensitisation. I observe a very slight diminution of responses to vibration (from 17 to 13), and a modest increase in the number of responses to noxious mechanical (from 10 to 14) and noxious thermal stimuli (from 3 to 10). Interestingly I also observe *de novo* responses to 0°C (Figure 5.11.A). When looking at the combined responses within the individual PV neurons themselves, I observe an increase in the number of polymodal PV+ neurons, from 1 to 8, which again increases proportionally alongside PV-negative sensory neurons (Figure 5.11.B and C). Those PV+ neurons responding to 0°C are all polymodal and respond to mechanical stimuli too.

Here I confirm that cutaneous PV+ neurons are indeed sensitive to vibration stimulus, but that they are also capable of responding to noxious mechanical and thermal stimuli, a phenomenon that has not been reported until now. As will be debated within the discussion, it is possible (and must be the case) that peripheral PV neurons do express thermosensors. This fits nicely with the idea of them acting as inhibitory with respect to noxious thermosensing, evidence for which is the thermal hypersensitivity I observe in PV<sup>DTA</sup> animals.





**Figure 5.11. *In vivo* GCaMP6s imaging comparing responses of PV+ and PV-negative neurons to peripheral stimulation before and after induction of acute inflammatory pain in PV<sup>Tom</sup>;GCaMP6s mice**

Red represents tdTomato-expressing PV+ neurons, black represents non-tdTomato-expressing PV-negative neurons. Red stripes indicate post-PGE<sub>2</sub> injection.

**A.** The number of total neuron responses in the DRG of animals to stimuli applied to the hind paw, either pre intraplantar injection of PGE<sub>2</sub> or 5 minutes after. Pie charts represent the total number of responses of both PV+ and PV-negative neurons pre and post PGE<sub>2</sub>. **B.** The number of total cells responding to either one type of stimuli, modality ('Multiple Mech' refers to neurons responding to multiple types of mechanical stimulation including pinch, and are deemed as unimodal within this study), or as polymodal i.e those responding to more than one modality in the case of 'Mech + 55°C', 'Mech + 0°C', '55°C + 0°C', and 'Mech + 55°C + 0°C'. Pie charts represent the total number of responding cells pre and post PGE<sub>2</sub>. **C.** The proportion (expressed as percentage of total) of polymodal versus unimodal responding neurons of animals pre and post PGE<sub>2</sub>. (n=6).

## 5.5 Discussion

I used a comprehensive means of assessing the sensitivity of PV<sup>DTA</sup> animals to a broad range of innocuous and noxious stimuli by combining *in vivo* DRG imaging, dorsal horn electrophysiology, and behavioural assays. This combinatorial approach has given me confidence in reporting a mechanical and thermal hypersensitivity in animals as a consequence of peripheral PV neuron ablation, despite the proprioceptive deficits also incurred as a result. This is the first study to suggest that the cutaneous population of PV+ sensory neurons are essential to the negative regulation of both acute and acute inflammatory nociception, likely via mechanisms described in the gate control theory of pain. These data presented here pave the way for future experiments to further understand how this population of sensory neurons contributes to normal pain perception, and if it can be manipulated to provide analgesia in chronic pain conditions.

### 5.5.1 Is this means of targeted peripheral PV+ neuron ablation an appropriate choice for the experiments I set out to perform?

As a preliminary means of investigating the contribution of cutaneous PV+ neurons to acute pain sensing, this study certainly identifies intriguing areas for future exploration. It is however, difficult to take all of these findings at face value for the lack of temporal and spatial control over the DTA-mediated ablation strategy. For example, a major caveat to any constitutive DTA-mediated neuron ablation study is that it does not take the developmental and perhaps transient expression of the marker gene within the developing mouse into account. Reassuringly, our immunohistochemistry studies described here suggest significant overlap between PV antibody and constitutive tomato expression within the PV+ population of DRG neurons, however, transient protein expression has had serious implications for other DTA-mediated ablated sensory neurons studies in the past. This includes those originally describing the role of TRPV1-expressing nociceptors (Mishra et al., 2011). This research found that TRPV1 is an embryonic marker for many nociceptors including cold-sensitive TRPM8 neurons, and as a consequence, mice that had undergone DTA-mediated TRPV1 neuron ablation had a marked insensitivity to hot and cold whilst retaining normal touch and noxious touch sensation. Subsequent studies using temporally-controlled DTR/DTX-mediated TRPV1 ablation generated mice that retained normal responses to cold but had a diminished aversion to noxious heat (Pogorzala et al., 2013). Similarly DTR/DTX-mediated TRPM8 ablation led to retainment of noxious heat sensing but an inhibition of noxious cold sensing (Mishra et al., 2011). These particular studies emphasise the importance of temporal control, as subset-specific markers in the adult may also be embryonic markers for other modality-specific somatosensory neurons.

Where I demonstrate that transient PV-expression in the developing mouse is unlikely to be a problem, it is important to also address the possibility of central (or indeed peripheral) compensatory plasticity as a consequence of the ablation of whole neuron subsets. An example of such developmental plasticity is highlighted in an inducible peripheral PV neuron ablation study, which focused on the role of PV+ proprioceptors (Takeoka & Arber, 2019). This research used the same *PV-Cre* as I do here, intercrossed with *Advillin<sup>iDTR</sup>* and *Rosa26-LSL-tdTomato* mouse lines, the key difference being that they had temporal control over PV neuron ablation via systemic injection of DTX. The group reported that juvenile mice (P1 and P14) injected with DTX were capable of developing the central circuitry to compensate for this early disruption of proprioceptive feedback, as assessed by their improvement in performing a locomotor treadmill task. Adult mice (P60), in which the locomotor circuits were fully formed, failed to improve in their performance of this task. It is possible (despite observing significant proprioceptive and sensory deficits) that similar compensatory plasticity takes place in *PV<sup>DTA</sup>* animals, as indicated by the disruption of the somatotopic peripheral neuron organisation we noted during *in vivo* electrophysiology experiments.

To address the spatial specificity of the PV neuron ablation strategy described here, it is worth first addressing the use of the promoter for the *Advillin* gene to drive DTA expression in the peripheral population of PV+ neurons. Recent evidence suggests *Advillin* may not be as sensory neuron specific as first reported and considering the widespread expression of PV throughout the peripheral and central nervous systems, it is essential that we rule out any argument for off-target PV neuron ablation. Promoter-based recombination using *Advillin-Cre* in mice was identified as sensory neuron-specific some time ago (Zurborg et al., 2011). This study subsequently led to dozens of others using *Advillin* as a promoter to explore the role of various proteins specifically within peripheral sensory neurons, including pain studies (Minett et al., 2012). However, the authors of a recent publication reported *Advillin* expression in all adult neural crest-derived neurons, which includes those of the autonomic nervous system, subsequently advising caution when using *Advillin* to target peripheral sensory neurons only (Hunter et al., 2018). How can we be sure that the phenotype I observe is as a consequence of peripheral PV+ neuron-specific ablation? Unfortunately, I cannot rely upon the phenotype of these animals alone for reassurance that all PV neurons in the spinal cord remain intact. This is because I observe a similar mechanical hypersensitivity in these animals as is reported with dorsal horn PV interneuron ablation (Petitjean et al., 2015). Reassuringly, the latest *Advillin* study, like the first, does not find *Advillin* expression

in the spinal cord of adult mice (other than the presence of afferent terminals in laminae lii), nor is there any evidence to suggest that PV expression is found within the autonomic nervous system. Furthermore, in the Takeoka & Arber (2019) PV<sup>iDTR</sup> study, in which they used a very similar Advillin-based genetic paradigm to specifically ablate peripheral PV neurons, PV interneurons in the spinal cord all remained intact. In summary Advillin appears to be a suitable means of restricting DTA-expression to the peripheral population of PV neurons.

As I have emphasised throughout this chapter, the focus of this study was to investigate cutaneous PV-expressing sensory neurons, as opposed to the muscle-innervating proprioceptive afferents. Where these imaging, electrophysiological, and behavioural strategies have targeted the cutaneous population by only assessing responses in the animal to hind paw stimulation, some of these studies have been marred by the proprioceptive deficits of PV<sup>DTA</sup> mice. Thus it would also be prudent to address the spatial control we have over this PV+ neuron ablation strategy. With the growing number of single cell RNA-seq studies published, it is increasingly likely that a marker specific to the cutaneous population of PV-expressing neurons will be identified. In the most recent large-scale DRG neuron RNA-seq study, genetic markers such as *Nog*, *Cgnl1*, and *Sertm1*, appear to specifically identify a population of PV neurons outside of the proprioceptor subset (Amit Zeisel et al., 2018). Hence genetic manipulation of mice using these markers may help us to tease the cutaneous and proprioceptive population of PV sensory neurons apart in future experiments. A recent preprint has addressed this problem by intercrossing PV-Cre and Rx3-FlpO mice with an Ai65:double stop:tdTomato reporter, to generate progeny expressing tdTomato only in the proprioceptive muscle afferents (Oliver et al., 2020). In doing so they were able to perform single cell RNA sequencing which revealed a further five distinct neuronal clusters which correspond to either Ia or II fibres terminating as muscle spindles, or Ib fibres terminating as Golgi tendon organs. If we could adopt a similar strategy instead using a marker specific to PV afferents innervating Meissner and Pacinian corpuscles, this would allow for a much more refined approach to studying their contribution to pain, thus circumventing the proprioceptive deficits I observe here.

### **5.5.2 The contribution of peripheral PV+ neurons to mechanical nociception and the gate control theory of pain**

The combined behaviour, electrophysiological, and imaging data I describe identifies a role for cutaneous PV+ neurons in modulating mechanical sensitivity. I observe a possible hypersensitivity in the behaving PV<sup>DTA</sup> animal to von Frey stimulation of the hind paw, which is corroborated by an increase in activity in the DRG neurons in response to mechanical insults, as

well as the WDR neurons of the deep dorsal horn. However, a complete marrying of these individual findings has been complicated by the difficulty in replicating the stimuli used in the imaging and electrophysiology experiments, in the behaving PV<sup>DTA</sup> animal. This is due to their severe motor deficits. As I will discuss later, there are possible ways to better explore this in future work.

I propose here that peripheral PV+ neurons contribute to the integrative sensory pathways described by the gate control theory of pain. Until recently, the identity of the A $\beta$  fibres responsible for closing the so-called pain gate had remained elusive but an intricate optogenetic study in mice has reported a subset responsible for repressing acute mechanical pain in the behaving animal under normal conditions (Arcourt et al., 2017). By optogenetically labelling (with ChR2) a combination of mechanonociceptors - Npy2r and LTMRs (MafA) - they found that the severe nocifensive reflex observed with optogenetic stimulation of the Npy2r+ peripheral neurons was dramatically attenuated with the co-activation of the MafA+ subpopulation of sensory neurons. The reflex that they observe with stimulation of Npy2r neurons alone is much more severe than when applying a natural noxious mechanical stimulus, and the group surmise that the latter will inevitably activate LTMRs irrespective of the intensity of the mechanical stimulation, thus acting to suppress at least some of the signal transmitted by mechanonociceptors. The group also found that the analgesic effect observed upon activation of the MafA+ neurons was stronger at low frequencies, consistent with gate control theory that proposes that the inhibitory effect of LTMR input on pain transmission is blocked as nociceptor activity increases. They also observed that LTRM activation was required for fine-tuning the reflex coordination observed in the behaving animal in response to a noxious insult. Thus, I suggest that the cutaneous PV-population of sensory neurons play a role in modulating the pain gate in the dorsal horn, consistent with the increase in activity we observe in the integrative WDR neurons of the spinal cord, and the hypersensitivity to mechanical stimuli reported in the PV<sup>DTA</sup> animals. Furthermore, the enhanced activity observed in the DRG of PV<sup>DTA</sup> animals would suggest that there is a loss of presynaptic inhibitory control of peripheral sensory neurons, which is mediated by LTMRs in normal animals, via an inhibitory interneuron intermediate in the dorsal horn (Mendell, 2014).

Further argument for the contribution of PV+ neurons to gating mechanical pain can be drawn from recent observations in Piezo2 conditional KO animals. As discussed in depth in the previous chapter, Piezo2 is the main mechanotransducer in peripheral PV+ sensory neurons (Woo et al., 2015), with its deletion in this population causing severe proprioceptive deficits in the behaving

animals. What the group failed to report upon in this instance was any phenotype occurring in innocuous or noxious mechanical behaviour assays. Subsequent widespread constitutive conditional KO of Piezo2 within the sensory neuron population using an Advillin-Cre, reveals not only that these animals had defective touch sensation and proprioception, but also that they were sensitised to noxious mechanical stimuli (Zhang et al., 2019). This group hypothesised that this was due to Piezo2-mediated gentle touch sensation having an inhibitory role in mechanical pain. It would be interesting to take another look at the Piezo2<sup>Pvalb</sup> mice to determine if we observe a similar mechanical hypersensitivity in these animals when compared to PV<sup>DTA</sup> mice.

To the best of my knowledge, this study is the first to demonstrate that cutaneous peripheral PV+ neurons have a role in closing the mechanonociceptive gate in the dorsal horn of the spinal cord. They do not overlap with those expressing the LTMR marker MafA (Bourane et al., 2009), and are likely to do so via the activation of the low-threshold mechanotransducer, Piezo2.

### **5.5.3 Is there a role for peripheral PV+ neurons in gating noxious thermal stimuli?**

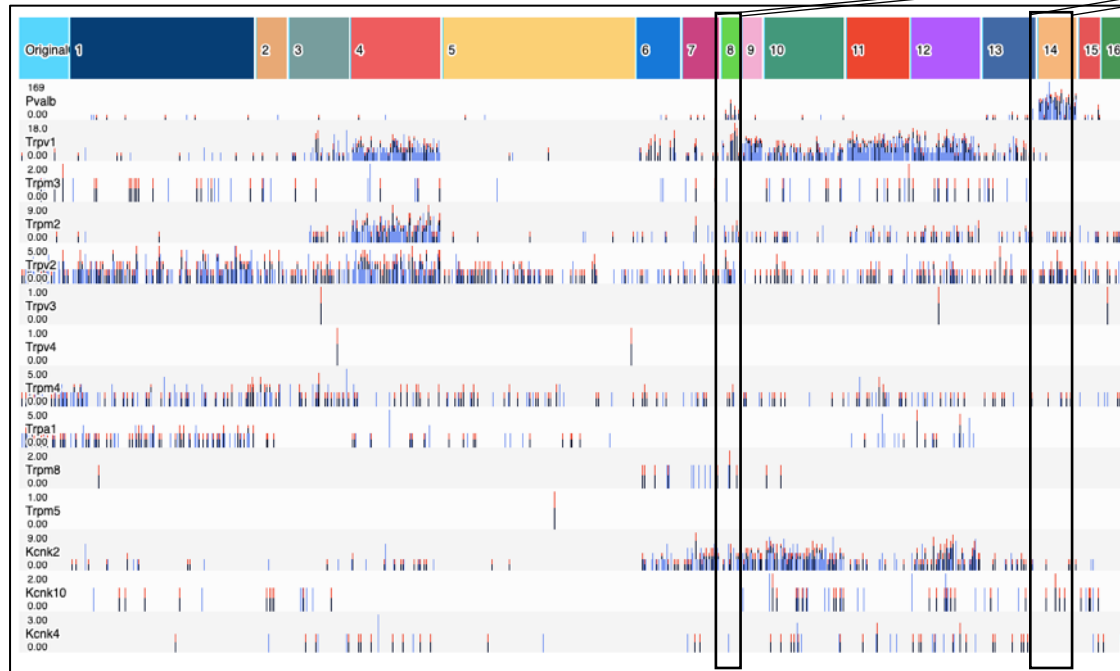
Somewhat surprisingly, these data suggest that the cutaneous PV+ population of neurons may also be responsible for the inhibitory modulation of noxious cold and heat perception, as evidenced by the increase in activity of peripheral neurons and spinal WDR neurons in response to 55°C and 0°C in the PV<sup>DTA</sup> mice. Where marrying these findings with our behaviour has proven difficult for some sensory modalities, I observe a clear and significant hypersensitivity to the dry ice noxious cold assay in the behaving PV<sup>DTA</sup> animals. Unfortunately, the same cannot be said for noxious heat, as I was unable to use a 55°C heat behavioural assay equivalent. Given that my mechanical and noxious cooling behavioural findings are in line with the imaging and electrophysiology data, it is highly likely that I would also observe a behavioural hypersensitivity to noxious heat with the appropriate pain behaviour test. My DRG *in vivo* imaging data in the PV<sup>Tom</sup> animals ties in with the idea of PV+ neurons providing inhibitory modulation of noxious heat, given that PV neurons respond to 55°C under basal conditions. With reference to noxious cooling, one could so far as to suggest that PV neurons are capable of a response (as evidenced in the presence of PGE<sub>2</sub>) but as the overall number of neurons responding to cooling is so low in general, perhaps these remained outside of my field of view under basal conditions. Transcriptional studies would appear to corroborate these findings, as there is a clear overlap between the recently identified PSPEP8 PV population of sensory neurons (likely to be the cutaneous PV positive population of sensory neurons), the putative noxious heat sensor TRPV1, and the noxious cooling sensor TRPM8 (Zeisel et al., 2018). These expression patterns are not

seen in the traditional proprioceptive PV+ population, PSNF2 (previously NF4/5 (Usoskin et al., 2015)) (Figure 5.12). Reassuringly, immunohistochemical studies have also indicated a modest overlap between PV, TRPV1, and TRMP8 protein, in the DRG of rats and mice respectively (Takashima et al., 2010; Zachařová & Paleček, 2009).

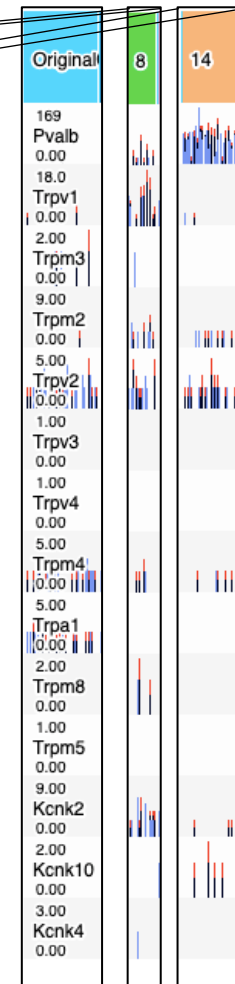
How might the response of cutaneous PV sensory neurons contribute to noxious thermosensing modulation? Unlike mechanical pain, the gating of noxious thermal insults in the spinal cord has proved much more elusive. Where constitutive ablation of dorsal horn SOM<sup>+</sup> excitatory interneurons does not result in any thermal deficits (Duan et al., 2014), acute pharmacogenetic inhibition of these neurons causes both noxious mechanical and thermal sensory deficits, suggesting compensatory mechanisms in mediating thermal nociception after SOM<sup>+</sup> neuronal ablation (Christensen et al., 2016). Ablation of the calbindin2/calretinin (CR<sup>+</sup>) lineage excitatory interneurons also impairs mechanical nociception and in this case heat nociception measured by affective licking behaviour at high heat (55°C) but not at intermediate heat (50°C) (Duan et al., 2014). Subsequent use of *in vivo* spinal cord imaging has demonstrated that both SOM<sup>+</sup> and CR<sup>+</sup> neurons (of which compose 11 out of 15 dorsal horn excitatory subtypes in a recent RNA sequencing study (Håring et al., 2018)) respond to both heat and cold stimuli (Ran & Chen, 2019).

Is it possible that the peripheral PV+ population synapse with the inhibitory interneurons responsible for providing input to the excitatory SOM<sup>+</sup> and CR<sup>+</sup> populations and in this manner regulate noxious thermosensation? The fact that we observe a hypersensitivity in WDR neurons to a 55°C stimulus, but do not observe a hypersensitivity in the behaving animal to lower heat temperatures may suggest that peripheral PV+ neurons do indeed provide input to inhibitory interneurons that make contact with the 55°C-sensitive CR<sup>+</sup> population.

A.



B.



**Figure 5.12. Transcriptional profiles of putative thermosensors within two distinct PV populations of sensory neurons reveal overlapping expression of noxious thermosensors and PV**

Data extracted from the Linnarsson ‘Peripheral sensory neurons’ dataset, and visualised using the Loom Viewer web tool. Genes are listed on the left-hand side of both A and B, with *Pvalb* placed at the top for reference, and thermosensing genes listed underneath. X axis labels “Original-16” refer to DRG clusters PSNP2, PSNP3, PSNP4, PSNP5, PSNP6, PSNP1, PSPEP7, PSPEP6, PSPEP8, PSPEP5, PSPEP4, PSPEP3, PSPEP2, PSPEP1, PSNF2, PSNF3, PSNF1, respectively

**A.** Transcriptional profile of Parvalbumin and selected thermosensors across all peripheral sensory neuron clusters as defined by Usoskin et al. (2015) and Zeisel et al. (2018). **B.** An isolated view of the two PV-rich clusters PSPEP8 and PSNF2 (the latter previously labelled as groups N4/5 in the Usoskin et al. (2015) dataset). The noxious heat sensor *Trpv1* and the noxious cold sensor *Trpm8* appear enriched within the PSPEP8 cluster, which is likely to correspond to the cutaneous population of PV+ sensory neurons.



#### 5.5.4 The contribution of peripheral PV+ neurons to gating acute inflammatory pain

Another surprising finding within this study was that stimulus-independent pain in PV<sup>DTA</sup> mice was greatly increased in the behaving animals after PGE<sub>2</sub> injection into the hind paw, much more so than in WT littermates. Concomitant activity in the WDR neurons of PV<sup>DTA</sup> animals was also significantly increased, the same was not observed in the WT dorsal horn.

It is well-established that PGE<sub>2</sub> contributes to various pain states as NSAIDs which inhibit the COX enzymes responsible for prostaglandin production, induce analgesia. In the periphery PGE<sub>2</sub> exerts its nociceptive effects via four G-protein-coupled receptors EP1-4 which are unevenly distributed throughout peripheral sensory neurons. A number of studies have looked at the impact of various EP receptor knockdowns, knockouts, and antagonists on pain, including comprehensive studies of combinatorial receptor knockouts in mice (Popp et al., 2009). However, it is widely accepted that specific receptor antagonists are a more accurate means of assessing EP receptor function due to the proposed compensatory/developmental redundancy within EP receptor KO animals. Consequently there has been particular emphasis on the importance of the EP4 receptor with respect to hyperalgesia in PGE<sub>2</sub>-mediated sensitisation of DRG neurons (Lin et al., 2006). Cumulative antagonist studies indicate that PGE<sub>2</sub>-mediated hyperalgesia exerts its effects via the activation of the EP1 (which also has a significant role in contributing to hyperalgesia within the dorsal horn (Minami et al., 2001)), and EP4 receptors in peripheral nociceptors. PGE<sub>2</sub> binding to each receptor causes an upregulation of cytosolic PKC and PKA, respectively, which leads to the sensitisation of nociceptive ion channels including TRPV1, and Na<sub>v</sub>1.9, both linked to thermal hyperalgesia, and Na<sub>v</sub>1.8 and T-type calcium channels such as the Ca<sub>v</sub>3.2 isoform, believed to contribute to PGE<sub>2</sub>-mediated mechanical hyperalgesia (Kawabata, 2011).

Due to the observation of enhanced stimulus-independent (and to a certain extent stimulus-evoked) hypersensitivity in PV<sup>DTA</sup> animals as a consequence of PGE<sub>2</sub> injection into the hind paw, one may propose that PV+ neurons also have a role in gating acute inflammation and as such must also be sensitised by PGE<sub>2</sub> injection via PGE<sub>2</sub>-EP receptor binding. However, both the Usoskin et al. (2015) and Zeisel et al. (2018) single cell transcriptomic datasets suggest that although proprioceptive peripheral PV+ neurons express the PGE<sub>2</sub> receptor EP4, the PSPEP8 subset of peripheral PV neurons do not, instead only weakly expressing transcript for the EP2 receptor. These observations have yet to be complimented with immunohistochemical studies. Irrespective of this I do still observe a *de novo* recruitment of PV+ neurons in the *in vivo* PV<sup>Tom</sup>

GCaMP6s studies presented here, in response to noxious thermal and mechanical insults. If this is not as a consequence of direct PGE<sub>2</sub> activation, it is possible that it could be due to inflammatory-mediated neuronal coupling as described by Kim et al. (2016). This study demonstrated that coupled activation could occur between small diameter nociceptors and large diameter LTMRs via gap-junctions in glial cells after inflammation or nerve injury. The authors surmised that this phenomenon contributed to mechanical hyperalgesia by allowing nociceptors to recruit additional nociceptors in response to noxious stimuli, and allodynia by allowing LTMRs to recruit nociceptors in response to innocuous stimuli. As such, the PV+ neuron responses I observe to noxious stimuli after addition of PGE<sub>2</sub> may be due to a coupling between PV+ neurons and nociceptors, which reciprocally allows nociceptors to activate LTMRs in response to noxious stimuli. It is possible that nociceptors below my field of view are responsible for the *de novo* activation of PV neurons I observe. If coupling does indeed occur in these animals after PGE<sub>2</sub> application, this is strong evidence for a direct role of PV+ neurons in shaping the perception of acute inflammatory pain.

It is also important to note here that there are inconsistencies to address with respect to the data gleaned from my PGE<sub>2</sub>-mediated inflammatory pain experiments. This includes a lack of evidence in support of stimulus-independent activity in DRG neurons during *in vivo* imaging experiments, for both PV<sup>DTA</sup> and PV<sup>Tom</sup> studies. Irrespective of the experiment it remains technically challenging to observe spontaneous activity using this experimental paradigm. This is possibly explained by the use of general anaesthetic during the experiments. A recent study has successfully imaged the DRG in awake mice using a chronic implantation window method, whilst the animal is restrained. Using GCaMP6s this group demonstrated that spontaneous activity in awake mice occurred in at least 14.1% of DRG sensory neurons, dropping to 4.3% in anaesthetised mice (Chen et al., 2019). However, this experimental technique comes with caveats of its own, including stress of the animal, and the animal's ability to move within its restraint, likely contributing to erroneous sensory neuron activation.

### **5.5.5 Could these observations aid our understanding of current non-pharmaceutical approaches to pain management?**

My findings indicate that cutaneous peripheral PV+ neurons are likely to play an inhibitory role in the regulation of normal pain processing via gate control. These could have powerful implications in advancing our understanding of current non-pharmaceutical approaches to managing pain, which rely on the recruitment of subpopulations of as yet unknown A $\beta$  LTMRs. These approaches include the TENS device, where electrodes are placed near to the site of injury and/or pain and

emit electrical pulses which activate local peripheral afferents. Significant efficacy has been reported in acute postoperative and non-postoperative pain, as well as in chronic pain conditions such as diabetic peripheral neuropathy, and fibromyalgia. However, this efficacy relies heavily upon both the intensity and frequency of the electrical stimulation emitted by the TENS device (Vance et al., 2014). It is believed varying these parameters recruits different endogenous mechanisms of analgesia but it remains to be delineated if certain parameters work best for different underlying causes of pain. Conventional gate-control TENS uses low intensity (5-10 mA) but high frequency (100-120 Hz) stimulation, which recruits A $\beta$  fibres and induces analgesia immediately, lasting for a few minutes to hours, and is restricted to the ipsilateral region of placement. Evidence has been put forward to suggest that the recruitment of deep joint afferents over cutaneous afferents is required for inducing this mode of TENS analgesia (Radhakrishnan & Sluka, 2005), many other studies offer speculative views arguing either way. Somewhat less-relevant to my findings, acupuncture-like TENS relies upon low frequency (4-20Hz) and high intensity (15-60 mA) stimulation, and recruits A $\delta$  and C-fibre nociceptors, resulting in a delayed onset of analgesia (15-20 minutes) which lasts for several hours. In this instance, it is believed that analgesia is induced through the recruitment of the DNIC (Diffuse Noxious Inhibitory Control) pathway, pain relief is subsequently more diffuse, and also abolished with naloxone treatment (Coutaux, 2017; Peng et al., 2019).

Another less conventional means of recruiting the somatosensory system in the management of pain is the use of vibration therapy, either targeting the whole body (WBV), or a focal region (FV). PV is expressed in both end organs responsible for sensing vibrations in the skin, Meissner and Pacinian corpuscles (Vega et al., 1996), sensitive to low frequency (~5-100Hz) and high frequency stimuli (200-300Hz) respectively (Fleming & Luo, 2013). Thus, this mode of treatment is arguably more specific to my findings. In the case of WBV, vibration is administered to the patient by means of an oscillating platform of a pre-set frequency (10–60 Hz) and amplitude, which they are required to stand on. This particular form of non-pharmaceutical intervention has successfully been used to improve muscle strength, balance, and bone density, but its use in managing chronic pain is slowly gaining traction (Alev et al., 2017; Hong et al., 2015). For example, prolonged analgesia is induced in diabetic peripheral neuropathy patients treated with WBV, where pharmaceutical interventions had previously failed (Hong et al., 2015; Kessler & Hong, 2013). Analgesia has also been reported with FV, which relies upon a small mechanical device placed directly over the painful region. Studies have suggested analgesic efficacy in patients suffering from chronic pain conditions including knee osteoarthritis (Rabini et al., 2015), and in patients with painful upper

limb contractures (Costantino et al., 2017). Similar to TENS therapy, the extent of analgesia induced by both vibration methods relies upon the frequency of vibration delivered, but also the duration and frequency of treatments. Importantly, improvements in gait (Hong et al., 2015), and in limb coordination for those with upper limb contractures (Costantino et al., 2017) are observed, speculated to be as a consequence of the recruitment of muscle spindle fibres Ia and II, ultimately strengthening central motor circuitry. Whether these fibres also contribute to gate control-mediated analgesia is possible as they share the same anatomical path as A $\beta$  fibres into the dorsal horn (Baxter, 2019).

The findings I report within this study likely aid our understanding of these non-pharmaceutical approaches to treating pain, the intricate mechanisms of which are predominantly speculative. Importantly, the efficacy of these treatments also strengthens my argument that cutaneous PV afferents are responsible for the inhibitory regulation of pain. However, they also further highlight the importance of delineating the contribution of cutaneous versus proprioceptive PV afferents to gate control.

## 5.6 Future directions

This study is the first to focus on the contribution of cutaneous PV+ neurons to acute and acute inflammatory pain. Using animals with constitutive peripheral PV positive neuron ablation, I demonstrate that a loss of peripheral PV+ neurons causes a mechanical, thermal, and inflammatory hypersensitivity in the behaving mouse, which correlates with an increase in activity of sensory neurons and excitatory dorsal horn neurons. Labelling of PV neurons and subsequent *in vivo* imaging of the DRG reveals that PV+ neurons are capable of responding to noxious mechanical and noxious thermal cues, indicative of a role for cutaneous PV sensory neurons in closing the 'pain gate', thus inhibitory regulation of the normal pain response. However, cutaneous PV neuron characterisation could be improved by the refinement of a number of techniques used here such as the behavioural assays used, the means of peripheral PV neuron ablation, and caveats associated with DRG GCaMP imaging studies. Furthermore, I propose here that cutaneous PV+ neurons are necessary for regulating the pain response, future directions should include a means of assessing their sufficiency in doing so.

With regards to the acute pain behaviour assays, one area of improvement would be to use those that more closely reflect the stimuli used during the imaging and electrophysiology experiments, particularly with respect to noxious heat. I have already mentioned some appropriate alternate tests, including the thermal probe assay as a measure of sensitivity to noxious heating, and the noxious mechanical pinprick assay, both of which allow for individual hind paw stimulation. This is of particular importance when taking the proprioceptive deficits of the PV<sup>DTA</sup> animal into account. Unfortunately, without the appropriate equipment (in the case of the thermal probe) and licencing this has not been possible as part of this study, but my data indicates a need to do so. To address my behavioural assays with respect to PGE<sub>2</sub>-induced acute inflammatory pain, it would be appropriate to repeat this study using manual von Frey filaments as they are more sensitive than the electronic von Frey equipment, possibly enabling us to tease out any enhanced mechanical hypersensitivity after PGE<sub>2</sub> injection in PV<sup>DTA</sup> animals. These alternate behavioural tests are predominantly required as a consequence of the proprioceptive deficits of PV<sup>DTA</sup> mice. The need for these assays could perhaps be circumvented if we were to adopt alternate strategies of genetically targeted neuron ablation, as mentioned within the discussion. This would include identifying a genetic marker for the cutaneous population of PV+ afferents, as Oliver et al. (2020) did with PV+ proprioceptors. With growing access to large DRG single cell RNA-seq datasets, the opportunity to do so is ever increasing. To further improve upon the reliability of my results, it

would also be prudent to adopt a temporal means of neuron ablation, such as the inducible DTR/DTX strategy used by Takeoka & Arber (2019) in their study of PV+ proprioceptors.

The data I present here, and the improvements I mention above all contribute to the argument that PV neurons are necessary for the negative regulation of pain under normal conditions. Therefore, future experiments should also focus on their sufficiency to do so by adopting a strategy of cutaneous PV neuron activation. One such strategy would be the use of optogenetics, which is an incredibly powerful tool for manipulating specific somatosensory neuron subpopulations. Expressing ChR2 in peripheral PV+ neurons would allow us to activate the cutaneous population of peripheral PV neurons via transdermal illumination of the hind paw and observe for any aversive behaviours under normal conditions. Illumination of the hind paw only would also eliminate the need to specifically genetically target the cutaneous PV+ population. Adopting a similar experimental strategy to Arcourt et al. (2017), we could optogenetically label nociceptive neurons and observe if co-activation of both PV+ neurons and nociceptors ameliorates any increased sensitivity observed with nociceptor activation alone. This would be an exceptionally informative means of confirming if PV+ neurons are responsible for shaping the acute pain response.

Optogenetic activation of peripheral PV neurons would also allow for the exploration of the role of cutaneous PV afferents in chronic models of pain. This is an area of investigation that I had initially intended to explore but was hindered by the PV<sup>DTA</sup> animal's severe deficits in motor coordination (as the induction of neuropathic pain would be unethical, and it would be challenging to discern any additional hypersensitivity that may arise as a consequence of neuropathy), and the difficulty in visualising DRG neuron responses (spontaneous and evoked) during *in vivo* GCaMP imaging after the implementation of a model of neuropathic pain. Optogenetics would provide a means of establishing whether peripheral PV neurons contribute to pain, or if they can be activated to ameliorate it. A way of exploring this would be to implement a model of chronic pain (or even acute inflammatory pain) and generate a place preference assay, whereby in one area, freely moving chronic pain animals receive pulses of yellow light to the ipsilateral hind paw (negative control), and in the other, pulses of blue light. An aversion or inclination to the area where blue light is administered would be an indication of the contribution of cutaneous PV afferents to pain or alleviation of pain, respectively. With respect to the contribution of peripheral PV neurons to chronic pain, an alternate strategy to investigate this would be to activate the cutaneous PV population using natural stimuli, i.e. a vibration stimulus. The application of a vibration stimulus to

awake behaving mice has previously been performed in a place preference paradigm (Ranade et al., 2014). Using a similar approach to the optogenetic studies, we could provide chronic pain animals with one area/surface that vibrates at a given frequency, and another that does not. If WT chronic pain animals are drawn to the vibrating surface (similar to vibration therapy we mentioned earlier) it would imply that vibration-sensitive cutaneous PV neurons are capable of ameliorating chronic pain in this instance. Further investigation would be required to confirm this, such as combining the chronic pain and vibration place preference assay with a cutaneous-specific PV neuron ablation strategy.

This study provides a solid foundation and argument for further investigations exploring the role of cutaneous peripheral PV+ neurons in pain. I have outlined just some of the possible ways of improving upon and extending my current findings, which would provide us not only with a significant leap forward in our understanding of the complex mechanisms underpinning the perception of pain, but the identification of a novel endogenous system that could be manipulated for the treatment of chronic pain.

## 6 Discussion

The work presented in this thesis addresses a number of unanswered questions in the pain field. In Chapters 3 and 4 this includes an investigation into the contribution of Aqp1 and Piezo2 to noxious mechanotransduction/sensation, respectively. Where Piezo2 has been ascribed to innocuous mechanosensation and proprioception, efforts to identify a noxious mechanotransducer(s) are ongoing. Isolation of these has been hampered by the limited and diffuse expression of mechanotransducers in the PNS. In this thesis I have delved into the literature to identify and characterise Aqp1 and any potential role it may have in mechanical pain sensing, finding that it is not a *bona fide* mechanotransducer. Similar attempts to screen known channels for mechanotransducer properties have also had limited success (Katanosaka et al., 2018; Vilceanu & Stucky, 2010). These findings in conjunction with my own emphasise the need to develop novel strategies to identify new candidates. Where chemical and thermal activation of cultured cells in combination with calcium imaging for high-throughput screens of the relevant chemically and/or thermally activated transducers is relatively straightforward, it has been difficult to apply the mechanical equivalent to the same high-throughput approach. Low-throughput screens have been used in the past (as was the case in identifying the Piezos) which utilise a functional genomic siRNA screen using cell membrane indentation and electrophysiological recording (Beaulieu-Laroche et al., 2020; Coste et al., 2010; Hong et al., 2016), the major caveat being the time taken to do this. Recent efforts have developed high-throughput systems which have allowed for the mechanical stimulation of many cells at once, using sheer stress in this instance (Xu et al., 2018). This method led to the successful identification of the novel mechanotransducer, GPR68, responsible for sensing shear stress in the endothelial cells of small-diameter arteries. While this is a promising step forward, different types of mechanical force (e.g. cell stretch and osmotic challenge) activate specific mechanotransducers, therefore this particular high through-put approach needs adapting to better suit a noxious mechanotransducer screen (Delmas et al., 2011). The success of this method also depends on the cell line tested. To address this issue, our lab has since implemented a cell/candidate identification method that compares the proteomes of undifferentiated versus differentiated neuronal cell lines after mechanical sensitivity characterisation. If a cell line is identified that produces SA currents (affiliated with noxious mechanosensation) only after differentiation, a proteome comparison between the undifferentiated and differentiated cell will be made in the hope of identifying candidates expressed in the differentiated group. Identification of a *bona fide* noxious mechanotransducer will not only improve our understanding of the physiological mechanisms that underpin pain but provide us with a possible therapeutic target for much-needed novel analgesics.



Where this thesis demonstrates that Piezo2 expression in nociceptors does not contribute to acute mechanical pain, recent evidence suggests that Piezo2 could in fact contribute to the negative regulation of noxious mechanosensation. This was demonstrated by Zhang et al. (2019) who used a peripherally-restricted pan-neuronal Cre (*Advil-Cre*) to delete Piezo2 expression in all sensory neurons. While this led to the expected reduction in sensitivity to innocuous mechanical stimuli in mice, it also enhanced sensitivity to noxious mechanical insults, contrary to previous reports. This is in line with the negative regulation of mechanical nociception I report in Chapter 5 by the peripheral population of PV+ neurons, which are known to express Piezo2. Therefore, a further source of investigation is to determine if it is expression of Piezo2 that drives the negative regulation of noxious mechanosensation by PV+ neurons.

There are very few examples of known peripheral sensory neuron subpopulations that contribute to the negative regulation of pain via the gate control theory. Here however, in Chapter 5 I identify the PV+ population of sensory neurons as necessary for negatively regulating acute mechanical, thermal, and inflammatory pain. Although an investigation into their sufficiency to do so is required, this observation is an important step towards our understanding of this complex pain circuitry. In addition to building upon this seminal theory, the findings presented within this thesis may provide further evidence for very recent observations of neuronal communication at the level of the DRG. With the use of *in vivo* GCaMP imaging, I demonstrate that increased activity is evident in the DRG of PV<sup>DTA</sup> animals in response to noxious stimuli. Where there is the likelihood that this arises due to a dysregulation of PSI in the dorsal horn (a form of gate control at the level of the spinal cord), it is possible that PV+ sensory neurons provide inhibitory input to nociceptors at the level of the soma. This phenomenon is evidenced by Du et al. (2017), who show functional GABAergic transmission within the DRG that is responsible for modulating the pain response in rodents. They describe this as a novel form of gate control in the PNS.

Additional evidence for the regulation of pain signalling at the level of the DRG is in the findings presented by Kim et al. (2016) who describe gap junction-mediated coupling at the soma of DRG neurons after the induction of inflammatory and neuropathic pain. In these chronic pain models, coupling allows for nociceptors to recruit additional nociceptors in response to noxious stimuli, and allodynia by allowing LTMRs to recruit nociceptors in response to innocuous stimuli. This phenomenon could rationalise the *de novo* recruitment of PV+ DRG neurons I observe in PV<sup>tdTom</sup> animals after the induction of acute inflammation, which may have an inhibitory role in this

instance, explaining the significant increase in acute inflammatory pain behaviour observed in PV<sup>DTA</sup> animals. Research into the contribution of peripheral PV+ neurons to chronic pain is still required, however. Pain signalling and plasticity at the level of the DRG is a novel observation that challenges traditional views of nociception and is an exceptionally exciting avenue for further exploration.

Studies into the areas listed above will build upon my finding that cutaneous PV+ neurons negatively regulate pain. They will aid our understanding of, and ability to better manipulate the mechanisms underpinning non-pharmacological approaches to managing pain, such as vibration and TENS therapy. These treatments aim to recruit endogenous mechanisms of analgesia and are rapidly increasing in popularity as they avoid the unwanted and sometimes fatal side-effects of current therapeutic approaches to managing acute and chronic pain.

## 7 Summary

This thesis utilises transgenic mice to either globally or conditionally delete genes, or to ablate entire populations of sensory neurons, to explore their contribution to pain sensation. In doing so I describe the role of the water and ion channel Aqp1, as well as the role (or lack of) of the known mechanotransducer Piezo2, in noxious mechanosensation. Ablation of peripheral PV+ neurons demonstrates that the cutaneous population of these are required for regulating normal pain sensation.

The mechanotransducer responsible for noxious mechanosensation remains for the most part, elusive. Using electrophysiological and behavioural techniques to characterise Aqp1 KO mice, I establish that Aqp1 contributes to noxious MA currents in DRG neurons and is required for mechanical pain perception *in vivo*. However, my data suggests that it is unlikely to form the pore of an MA channel itself. Piezo2 is the mechanotransducer responsible for light touch sensation and proprioception, but its contribution to acute mechanical pain is debated. I exclude a role for Piezo2 in acute mechanical pain sensing by characterising animals which have undergone mechanonociceptor-specific Piezo2 deletion. As a consequence of the outcome of these two studies, the noxious mechanotransducer remains unidentified. Excitingly, these findings have since led to the generation of a list of novel noxious mechanotransducer candidates in our lab. Should identification of a noxious mechanotransducer prove successful, our understanding of the mechanisms underpinning mechanical pain will be vastly improved and may provide a novel therapeutic target for pain management in the future.

Characterisation of cutaneous PV+ afferents has been limited. Using a combination of behaviour, imaging, and electrophysiology assays in mice with PV+ sensory neuron ablation, I show that this population of neurons is responsible for negatively regulating normal and inflammatory pain sensations. This is likely via their ability to close the 'pain gate' in the dorsal horn. Where I demonstrate that these neurons are necessary for normal pain sensation, further experiments to confirm their sufficiency will be required. These findings may provide further insight into the physiological mechanisms underpinning non-pharmacological approaches to treating pain (i.e. TENS). As current pharmacological approaches to treating chronic pain are poorly efficacious, an understanding of how we may harness endogenous pain pathways to treat pain using non-pharmacological approaches would prove incredibly beneficial.

## 8 References

- Abdo, H., Calvo-Enrique, L., Lopez, J. M., Song, J., Zhang, M., Usoskin, D., ... Ernfors, P. (2019). Specialized cutaneous Schwann cells initiate pain sensation. *Science*, 365(6454), 695–699. <https://doi.org/10.1126/science.aax6452>
- Abrahamsen, B., Zhao, J., Asante, C. O., Cendan, C. M., Marsh, S., Martinez-Barbera, J. P., ... Wood, J. N. (2008). The cell and molecular basis of mechanical, cold, and inflammatory pain. *Science (New York, N. Y.)*, 321(5889), 702–705. <https://doi.org/10.1126/science.1156916>
- Abraira, V., & Ginty, D. (2013). The Sensory Neurons of Touch. *Neuron*, 79(4), 618–639. <https://doi.org/10.1016/j.neuron.2013.07.051>
- Akay, T., Tourtellotte, W. G., Arber, S., & Jessell, T. M. (2014). Degradation of mouse locomotor pattern in the absence of proprioceptive sensory feedback. *Proceedings of the National Academy of Sciences*, 111(47), 16877–16882. <https://doi.org/10.1073/pnas.1419045111>
- Akerboom, J., Rivera, J. D. V., Rodríguez Guilbe, M. M., Malavé, E. C. A., Hernandez, H. H., Tian, L., ... Schreier, E. R. (2009). Crystal structures of the GCaMP calcium sensor reveal the mechanism of fluorescence signal change and aid rational design. *Journal of Biological Chemistry*, 284(10), 6455–6464. <https://doi.org/10.1074/jbc.M807657200>
- Akopian, A. N., Sivilotti, L., & Wood, J. N. (1996). A tetrodotoxin-resistant voltage-gated sodium channel expressed by sensory neurons. *Nature*, 379(6562), 257–262. <https://doi.org/10.1038/379257a0>
- Akopian, A. N., Souslova, V., England, S., Okuse, K., Ogata, N., Ure, J., ... Wood, J. N. (1999). The tetrodotoxin-resistant sodium channel SNS has a specialized function in pain pathways. *Nature Neuroscience*, 2(6), 541–548. <https://doi.org/10.1038/9195>
- Alev, A., Mihriban, A., Bilge, E., Ayça, E., Merve, K., Şeyma, C., ... Mahmut, G. S. (2017). Effects of whole body vibration therapy in pain, function and depression of the patients with fibromyalgia. *Complementary Therapies in Clinical Practice*, 28, 200–203. <https://doi.org/10.1016/j.ctcp.2017.06.008>
- Alloui, A., Zimmermann, K., Mamet, J., Duprat, F., Noël, J., Chemin, J., ... Lazdunski, M. (2006). TREK-1, a K<sup>+</sup> channel involved in polymodal pain perception. *EMBO Journal*, 25(11), 2368–2376. <https://doi.org/10.1038/sj.emboj.7601116>
- Amaya, F., Wang, H., Costigan, M., Allchorne, A. J., Hatcher, J. P., Egerton, J., ... Woolf, C. J. (2006). The voltage-gated sodium channel Nav1.9 is an effector of peripheral inflammatory pain hypersensitivity. *Journal of Neuroscience*, 26(50), 12852–12860. <https://doi.org/10.1523/JNEUROSCI.4015-06.2006>
- Anderson, E. O., Schneider, E. R., Matson, J. D., Gracheva, E. O., & Bagriantsev, S. N. (2018). TMEM150C/Tentonin3 Is a Regulator of Mechano-gated Ion Channels. *Cell Reports*, 23(3), 701–708. <https://doi.org/10.1016/j.celrep.2018.03.094>
- Andersson, D. a, Gentry, C., Moss, S., & Bevan, S. (2009). Cloquinol and pyrithione activate TRPA1 by increasing intracellular Zn<sup>2+</sup>. *Proceedings of the National Academy of Sciences of the United States of America*, 106(20), 8374–8379. <https://doi.org/10.1073/pnas.0812675106>
- Arcourt, A., Gorham, L., Dhandapani, R., Prato, V., Taberner, F. J., Wende, H., ... Lechner, S. G. (2017). Touch Receptor-Derived Sensory Information Alleviates Acute Pain Signaling and Fine-Tunes Nociceptive Reflex Coordination. *Neuron*, 93(1), 179–193. <https://doi.org/10.1016/j.neuron.2016.11.027>
- Árnadóttir, J., & Chalfie, M. (2010). Eukaryotic Mechanosensitive Channels. *Annual Review of Biophysics*, 39(1), 111–137. <https://doi.org/10.1146/annurev.biophys.37.032807.125836>
- Autzen, H. E., Julius, D., & Cheng, Y. (2019). Membrane mimetic systems in CryoEM: keeping membrane proteins in their native environment. *Current Opinion in Structural Biology*, 58, 259–268. <https://doi.org/10.1016/j.sbi.2019.05.022>
- Bai, C., Fukuda, N., Song, Y., Ma, T., Matthay, M. A., & Verkman, A. S. (1999). Lung fluid transport

- in aquaporin-1 and aquaporin-4 knockout mice. *Journal of Clinical Investigation*, 103(4), 555–561. <https://doi.org/10.1172/JCI4138>
- Bang, H., Kim, Y., & Kim, D. (2000). TREK-2, a new member of the mechanosensitive tandem-pore K<sup>+</sup> channel family. *Journal of Biological Chemistry*, 275(23), 17412–17419. <https://doi.org/10.1074/jbc.M000445200>
- Bao, F., Chen, M., Zhang, Y., & Zhao, Z. (2010). Hypoalgesia in mice lacking aquaporin-4 water channels. *Brain Research Bulletin*, 83(6), 298–303. <https://doi.org/10.1016/j.brainresbull.2010.08.015>
- Basbaum, A. I., Bautista, D. M., Scherrer, G., & Julius, D. (2009). Cellular and Molecular Mechanisms of Pain. *Cell*, 139(2), 267–284. <https://doi.org/10.1016/j.cell.2009.09.028>
- Baxter, A. (2019). Vibration for Chronic Pain. *Practical Pain Management*, 19(2), 60–63; 67.
- Beaulieu-Laroche, L., Christin, M., Donoghue, A. M., Agosti, F., Yousefpour, N., Petitjean, H., ... Sharif-Naeini, R. (2018). TACAN is an essential component of the mechanosensitive ion channel responsible for pain sensing. *bioRxiv*. <https://doi.org/10.1101/338673>
- Beaulieu-Laroche, Lou, Christin, M., Donoghue, A., Agosti, F., Yousefpour, N., Petitjean, H., ... Sharif-Naeini, R. (2020). TACAN Is an Ion Channel Involved in Sensing Mechanical Pain. *Cell*, 180(5), 956-967.e17. <https://doi.org/10.1016/j.cell.2020.01.033>
- Benarroch, E. E. (2007). Sodium channels and pain. *Neurology*, 68(3), 233–236. <https://doi.org/10.1212/01.wnl.0000252951.48745.a1>
- Bennett, D. L., Clark, X. A. J., Huang, J., Waxman, S. G., & Dib-Hajj, S. D. (2019). The role of voltage-gated sodium channels in pain signaling. *Physiological Reviews*, 99(2), 1079–1151. <https://doi.org/10.1152/physrev.00052.2017>
- Berrier, C., Pozza, A., De Lacroix De Lavalette, A., Chardonnet, S., Mesneau, A., Jaxel, C., ... Ghazi, A. (2013). The purified mechanosensitive channel TREK-1 is directly sensitive to membrane tension. *Journal of Biological Chemistry*, 288(38), 27307–27314. <https://doi.org/10.1074/jbc.M113.478321>
- Black, J. A., Cummins, T. R., Plumpton, C., Chen, Y. H., Hormuzdiar, W., Clare, J. J., & Waxman, S. G. (1999). Upregulation of a silent sodium channel after peripheral, but not central, nerve injury in DRG neurons. *Journal of Neurophysiology*, 82(5), 2776–2785. <https://doi.org/10.1152/jn.1999.82.5.2776>
- Black, J. A., Nikolajsen, L., Kroner, K., Jensen, T. S., & Waxman, S. G. (2008). Multiple sodium channel isoforms and mitogen-activated protein kinases are present in painful human neuromas. *Annals of Neurology*, 64(6), 644–653. <https://doi.org/10.1002/ana.21527>
- Boassa, D., Stamer, W. D., & Yool, A. J. (2006). Ion channel function of aquaporin-1 natively expressed in choroid plexus. *J Neurosci*, 26(30), 7811–7819. <https://doi.org/10.1523/jneurosci.0525-06.2006>
- Borsani, E., Bernardi, S., Albertini, R., Rezzani, R., & Rodella, L. F. (2009). Alterations of AQP2 expression in trigeminal ganglia in a murine inflammation model. *Neuroscience Letters*, 449(3), 183–188. <https://doi.org/10.1016/j.neulet.2008.11.014>
- Bourane, S., Garces, A., Venteo, S., Pattyn, A., Hubert, T., Fichard, A., ... Carroll, P. (2009). Low-Threshold Mechanoreceptor Subtypes Selectively Express MafA and Are Specified by Ret Signaling. *Neuron*, 64(6), 857–870. <https://doi.org/10.1016/j.neuron.2009.12.004>
- Boyle, K. A., Gradwell, M. A., Yasaka, T., Dickie, A. C., Polgár, E., Ganley, R. P., ... Hughes, D. I. (2019). Defining a Spinal Microcircuit that Gates Myelinated Afferent Input: Implications for Tactile Allodynia. *Cell Reports*, 28(2), 526-540.e6. <https://doi.org/10.1016/j.celrep.2019.06.040>
- Braz, J., Solorzano, C., Wang, X., & Basbaum, A. I. (2014). Transmitting Pain and Itch Messages: A Contemporary View of the Spinal Cord Circuits that Generate Gate Control. *Neuron*, 82(3), 522–536. <https://doi.org/10.1016/j.neuron.2014.01.018>
- Brenner, D. S., Golden, J. P., & Gereau, R. W. (2012). A Novel Behavioral Assay for Measuring Cold Sensation in Mice. *PLoS ONE*, 7(6), e39765.

- <https://doi.org/10.1371/journal.pone.0039765>
- Brohawn, S. G., Su, Z., & MacKinnon, R. (2014). Mechanosensitivity is mediated directly by the lipid membrane in TRAAK and TREK1 K<sup>+</sup> channels. *Proceedings of the National Academy of Sciences of the United States of America*, 111(9), 3614–3619. <https://doi.org/10.1073/pnas.1320768111>
- Buffoli, B., Borsani, E., Rezzani, R., & Rodella, L. F. (2009). Chronic constriction injury induces aquaporin-2 expression in the dorsal root ganglia of rats. *Journal of Anatomy*, 215(5), 498–505. <https://doi.org/10.1111/j.1469-7580.2009.01143.x>
- Carlton, S. M., Lekan, H. A., Kim, S. H., & Chung, J. M. (1994). Behavioral manifestations of an experimental model for peripheral neuropathy produced by spinal nerve ligation in the primate. *Pain*, 56(2), 155–166. [https://doi.org/10.1016/0304-3959\(94\)90090-6](https://doi.org/10.1016/0304-3959(94)90090-6)
- Cavanaugh, D. J., Lee, H., Lo, L., Shields, S. D., Zylka, M. J., Basbaum, A. I., & Anderson, D. J. (2009). Distinct subsets of unmyelinated primary sensory fibers mediate behavioral responses to noxious thermal and mechanical stimuli. *Proceedings of the National Academy of Sciences*, 106(22), 9075–9080. <https://doi.org/10.1073/pnas.0901507106>
- Celio, M. R., & Heizmann, C. W. (1981). Calcium-binding protein parvalbumin as a neuronal marker. *Nature*, 293(5830), 300–302. <https://doi.org/10.1038/293300a0>
- Chaplan, S. R., Bach, F. W., Pogrel, J. W., Chung, J. M., & Yaksh, T. L. (1994). Quantitative assessment of tactile allodynia in the rat paw. *Journal of Neuroscience Methods*, 53(1), 55–63. [https://doi.org/10.1016/0165-0270\(94\)90144-9](https://doi.org/10.1016/0165-0270(94)90144-9)
- Chelur, D. S., Ernstrom, G. G., Goodman, M. B., Yao, C. A., Chen, L., O' Hagan, R., & Chalfie, M. (2002). The mechanosensory protein MEC-6 is a subunit of the *C. elegans* touch-cell degeneration channel. *Nature*, 420(6916), 669–673. <https://doi.org/10.1038/nature01205>
- Chen, C., Zhang, J., Sun, L., Zhang, Y., Gan, W. B., Tang, P., & Yang, G. (2019). Long-term imaging of dorsal root ganglia in awake behaving mice. *Nature Communications*, 10(1), 1–11. <https://doi.org/10.1038/s41467-019-11158-0>
- Chesler, A. T., Szczot, M., Bharucha-Goebel, D., Čeko, M., Donkervoort, S., Laubacher, C., ... Bönnemann, C. G. (2016). The Role of PIEZO2 in Human Mechanosensation. *New England Journal of Medicine*, 375(14), 1355–1364. <https://doi.org/10.1056/NEJMoa1602812>
- Chisholm, K. I., Khovanov, N., Lopes, D. M., La Russa, F., & McMahon, S. B. (2018). Large Scale In Vivo Recording of Sensory Neuron Activity with GCaMP6. *ENEURO*, 5(1), ENEURO.0417-17.2018. <https://doi.org/10.1523/ENEURO.0417-17.2018>
- Christensen, A. J., Iyer, S. M., François, A., Vyas, S., Ramakrishnan, C., Vesuna, S., ... Delp, S. L. (2016). In Vivo Interrogation of Spinal Mechanosensory Circuits. *Cell Reports*, 17(6), 1699–1710. <https://doi.org/10.1016/j.celrep.2016.10.010>
- Christensen, A. P., & Corey, D. P. (2007). TRP channels in mechanosensation: Direct or indirect activation? *Nature Reviews Neuroscience*, 8(7), 510–521. <https://doi.org/10.1038/nrn2149>
- Colburn, R. W., Lubin, M. Lou, Stone, D. J., Wang, Y., Lawrence, D., D'Andrea, M. R. R., ... Qin, N. (2007). Attenuated Cold Sensitivity in TRPM8 Null Mice. *Neuron*, 54(3), 379–386. <https://doi.org/10.1016/j.neuron.2007.04.017>
- Costantino, C., Galuppo, L., & Romiti, D. (2017). Short-term effect of local muscle vibration treatment versus sham therapy on upper limb in chronic post-stroke patients: A randomized controlled trial. *European Journal of Physical and Rehabilitation Medicine*, 53(1), 32–40. <https://doi.org/10.23736/S1973-9087.16.04211-8>
- Coste, B., Houge, G., Murray, M. F., Stitzel, N., Bandell, M., Giovanni, M. A., ... Patapoutian, A. (2013). Gain-of-function mutations in the mechanically activated ion channel PIEZO2 cause a subtype of Distal Arthrogryposis. *Proceedings of the National Academy of Sciences of the United States of America*, 110(12), 4667–4672. <https://doi.org/10.1073/pnas.1221400110>
- Coste, B., Mathur, J., Schmidt, M., Earley, T. J., Ranade, S., Petrus, M. J., ... Patapoutian, A. (2010). Piezo1 and Piezo2 are essential components of distinct mechanically-activated cation channels. *Science*, 330(6000), 55–60. Bertrand.

- <https://doi.org/10.1126/science.1193270>.Piezo1
- Coutaux, A. (2017). Non-pharmacological treatments for pain relief: TENS and acupuncture. *Joint Bone Spine*, 84(6), 657–661. <https://doi.org/10.1016/j.jbspin.2017.02.005>
- Cox, C. D., Bae, C., Ziegler, L., Hartley, S., Nikolova-Krstevski, V., Rohde, P. R., ... Martinac, B. (2016). Removal of the mechanoprotective influence of the cytoskeleton reveals PIEZO1 is gated by bilayer tension. *Nature Communications*, 7(1), 10366. <https://doi.org/10.1038/ncomms10366>
- Cox, J. J., Reimann, F., Nicholas, A. K., Thornton, G., Roberts, E., Springell, K., ... Woods, C. G. (2006). An SCN9A channelopathy causes congenital inability to experience pain. *Nature*, 444(7121), 894–898. <https://doi.org/10.1038/nature05413>
- Craner, M. J., Klein, J. P., Renganathan, M., Black, J. A., & Waxman, S. G. (2002). Changes of sodium channel expression in experimental painful diabetic neuropathy. *Annals of Neurology*, 52(6), 786–792. <https://doi.org/10.1002/ana.10364>
- Cui, L., Miao, X., Liang, L., Abdus-Saboor, I., Olson, W., Fleming, M. S., ... Luo, W. (2016). Identification of Early RET+ Deep Dorsal Spinal Cord Interneurons in Gating Pain. *Neuron*, 91(5), 1137–1153. <https://doi.org/10.1016/j.neuron.2016.07.038>
- Cummins, T. R., Dib-Hajj, S. D., Black, J. A., Akopian, A. N., Wood, J. N., & Waxman, S. G. (1999). A novel persistent tetrodotoxin-resistant sodium current in SNS-null and wild-type small primary sensory neurons. *The Journal of Neuroscience: The Official Journal of the Society for Neuroscience*, 19(24), 1–6. <https://doi.org/10.1523/JNEUROSCI.19-24-j0001.1999>
- D’Mello, R., & Dickenson, A. H. (2008). Spinal cord mechanisms of pain. *British Journal of Anaesthesia*, 101(1), 8–16. <https://doi.org/10.1093/bja/aen088>
- De Ieso, M. L., Pei, J. V., Nourmohammadi, S., Smith, E., Chow, P. H., Kourghi, M., ... Yool, A. J. (2019). Combined pharmacological administration of AQP1 ion channel blocker AqB011 and water channel blocker Bacopaside II amplifies inhibition of colon cancer cell migration. *Scientific Reports*, 9(1), 1–17. <https://doi.org/10.1038/s41598-019-49045-9>
- de Nooij, J. C., Doobar, S., & Jessell, T. M. (2013). Etv1 Inactivation Reveals Proprioceptor Subclasses that Reflect the Level of NT3 Expression in Muscle Targets. *Neuron*, 77(6), 1055–1068. <https://doi.org/10.1016/j.neuron.2013.01.015>
- Dekkers, J., Bayley, P., Dick, J. R. T., Schwaller, B., Berchtold, M. W., & Greensmith, L. (2004). Over-expression of parvalbumin in transgenic mice rescues motoneurons from injury-induced cell death. *Neuroscience*, 123(2), 459–466. <https://doi.org/10.1016/j.neuroscience.2003.07.013>
- Delle Vedove, A., Storbeck, M., Heller, R., Hölker, I., Hebbar, M., Shukla, A., ... Wirth, B. (2016). Biallelic Loss of Proprioception-Related PIEZO2 Causes Muscular Atrophy with Perinatal Respiratory Distress, Arthrogryposis, and Scoliosis. *American Journal of Human Genetics*, 99(5), 1206–1216. <https://doi.org/10.1016/j.ajhg.2016.09.019>
- Delmas, P., Hao, J., & Rodat-Despoix, L. (2011). Molecular mechanisms of mechanotransduction in mammalian sensory neurons. *Nature Reviews Neuroscience*, 12(3), 139–153. <https://doi.org/10.1038/nrn2993>
- Delmas, P., Korogod, S. M., & Coste, B. (2020). Noxious Mechanosensation. In John N. Wood (Ed.), *The Oxford Handbook of the Neurobiology of Pain* (Vol. 1, pp. 199–232). Oxford University Press. <https://doi.org/10.1093/oxfordhb/9780190860509.013.14>
- Deuis, J. R., Dvorakova, L. S., & Vetter, I. (2017). Methods Used to Evaluate Pain Behaviors in Rodents. *Frontiers in Molecular Neuroscience*, 10(September), 1–17. <https://doi.org/10.3389/fnmol.2017.00284>
- Deuis, J. R., & Vetter, I. (2016). The thermal probe test: A novel behavioral assay to quantify thermal paw withdrawal thresholds in mice. *Temperature*, 3(2), 199–207. <https://doi.org/10.1080/23328940.2016.1157668>
- Devices, M. (2020). Axon Guide - Electrophysiology and Biophysics Laboratory Techniques |

- Molecular Devices, (June), 1–273.
- Devor, M. (2009). Ectopic discharge in A $\beta$  afferents as a source of neuropathic pain. *Experimental Brain Research*, 196(1), 115–128. <https://doi.org/10.1007/s00221-009-1724-6>
- Dhandapani, R., Arokiaraj, C. M., Taberner, F. J., Pacifico, P., Raja, S., Nocchi, L., ... Heppenstall, P. A. (2018). Control of mechanical pain hypersensitivity in mice through ligand-targeted photoablation of TrkB-positive sensory neurons. *Nature Communications*, 9(1), 1640. <https://doi.org/10.1038/s41467-018-04049-3>
- Dib-Hajj, S. D., Rush, A. M., Cummins, T. R., Hisama, F. M., Novella, S., Tyrrell, L., ... Waxman, S. G. (2005). Gain-of-function mutation in Nav1.7 in familial erythromelalgia induces bursting of sensory neurons. *Brain*, 128(8), 1847–1854. <https://doi.org/10.1093/brain/awh514>
- Domenichiello, A. F., Wilhite, B. C., Keyes, G. S., & Ramsden, C. E. (2017). A dose response study of the effect of prostaglandin E2 on thermal nociceptive sensitivity. *Prostaglandins, Leukotrienes and Essential Fatty Acids*, 126(3), 20–24. <https://doi.org/10.1016/j.plefa.2017.08.015>
- Drenth, J. P. H., & Waxman, S. G. (2007). Mutations in sodium-channel gene SCN9A cause a spectrum of human genetic pain disorders. *Journal of Clinical Investigation*, 117(12), 3603–3609. <https://doi.org/10.1172/JCI33297>
- Drew, L. J., Rohrer, D. K., Price, M. P., Blaver, K. E., Cockayne, D. a, Cesare, P., & Wood, J. N. (2004). Acid-sensing ion channels ASIC2 and ASIC3 do not contribute to mechanically activated currents in mammalian sensory neurones. *The Journal of Physiology*, 556(3), 691–710. <https://doi.org/10.1113/jphysiol.2003.058693>
- Drew, L. J., Rugiero, F., Cesare, P., Gale, J. E., Abrahamsen, B., Bowden, S., ... Wood, J. N. (2007). High-threshold mechanosensitive ion channels blocked by a novel conopeptide mediate pressure-evoked pain. *PLoS ONE*, 2(6), e515. <https://doi.org/10.1371/journal.pone.0000515>
- Drew, L. J., & Wood, J. N. (2007). FM1-43 is a Permeant Blocker of Mechanosensitive Ion Channels in Sensory Neurons and Inhibits Behavioural Responses to Mechanical Stimuli. *Molecular Pain*, 3(1), 1744–8069. <https://doi.org/10.1186/1744-8069-3-1>
- Drew, L. J., Wood, J. N., & Cesare, P. (2002). Distinct mechanosensitive properties of capsaicin-sensitive and -insensitive sensory neurons. *The Journal of Neuroscience*, 22(12), 1–5. <https://doi.org/Rc228>
- Du, X., Hao, H., Yang, Y., Huang, S., Wang, C., Gigout, S., ... Gamper, N. (2017). Local GABAergic signaling within sensory ganglia controls peripheral nociceptive transmission. *Journal of Clinical Investigation*, 127(5), 1741–1756. <https://doi.org/10.1172/JCI86812>
- Duan, B., Cheng, L., Bourane, S., Britz, O., Padilla, C., Garcia-Campmany, L., ... Ma, Q. (2014). Identification of spinal circuits transmitting and gating mechanical pain. *Cell*, 159(6), 1417–1432. <https://doi.org/10.1016/j.cell.2014.11.003>
- Duan, B., Cheng, L., & Ma, Q. (2018). Spinal Circuits Transmitting Mechanical Pain and Itch. *Neuroscience Bulletin*, 34(1), 186–193. <https://doi.org/10.1007/s12264-017-0136-z>
- Duan, G., Han, C., Wang, Q., Guo, S., Zhang, Y., Ying, Y., ... Zhang, X. (2016). A SCN10A SNP biases human pain sensitivity. *Molecular Pain*, 12, 1–16. <https://doi.org/10.1177/1744806916666083>
- Dubin, A. E., Murthy, S., Lewis, A. H., Brosse, L., Cahalan, S. M., Grandl, J., ... Patapoutian, A. (2017). Endogenous Piezo1 Can Confound Mechanically Activated Channel Identification and Characterization. *Neuron*, 94(2), 266-270.e3. <https://doi.org/10.1016/j.neuron.2017.03.039>
- Eijkelkamp, N., Linley, J. E., Torres, J. M., Bee, L., Dickenson, A. H., Gringhuis, M., ... Wood, J. N. (2013). A role for Piezo2 in EPAC1-dependent mechanical allodynia. *Nature Communications*, 4(1), 1682. <https://doi.org/10.1038/ncomms2673>
- Emery, E. C., Young, G. T., Berrocoso, E. M., Chen, L., & McNaughton, P. A. (2011). HCN2 Ion Channels Play a Central Role in Inflammatory and Neuropathic Pain. *Science*, 333(6048),



- 1462–1466. <https://doi.org/10.1126/science.1206243>
- Emery, E. C., Luiz, A. P., Sikandar, S., Magnúsdóttir, R., Dong, X., & Wood, J. N. (2016). In vivo characterization of distinct modality-specific subsets of somatosensory neurons using GCaMP. *Science Advances*, 2(11), e1600990. <https://doi.org/10.1126/sciadv.1600990>
- Emery, Edward C., & Wood, J. N. (2019). Somatosensation a la mode: plasticity and polymodality in sensory neurons. *Current Opinion in Physiology*, 11, 29–34. <https://doi.org/10.1016/j.cophys.2019.04.014>
- Faber, C. G., Lauria, G., Merkies, I. S. J., Cheng, X., Han, C., Ahn, H. S., ... Waxman, S. G. (2012). Gain-of-function Nav1.8 mutations in painful neuropathy. *Proceedings of the National Academy of Sciences of the United States of America*, 109(47), 19444–19449. <https://doi.org/10.1073/pnas.1216080109>
- Fayaz, A., Croft, P., Langford, R. M., Donaldson, L. J., & Jones, G. T. (2016). Prevalence of chronic pain in the UK: A systematic review and meta-analysis of population studies. *BMJ Open*, 6(6). <https://doi.org/10.1136/bmjopen-2015-010364>
- Ferrari, L. F., Bogen, O., Green, P., & Levine, J. D. (2015a). Contribution of Piezo2 to endothelium-dependent pain. *Molecular Pain*, 11(1), 65. <https://doi.org/10.1186/s12990-015-0068-4>
- Ferrari, L. F., Bogen, O., Green, P., & Levine, J. D. (2015b). Contribution of Piezo2 to endothelium-dependent pain. *Molecular Pain*, 11. <https://doi.org/10.1186/s12990-015-0068-4>
- Filice, F., Blum, W., Lauber, E., & Schwaller, B. (2019). Inducible and reversible silencing of the Pvalb gene in mice: An in vitro and in vivo study. *European Journal of Neuroscience*, 50(4), 2694–2706. <https://doi.org/10.1111/ejn.14404>
- Filice, F., Lauber, E., Vörckel, K. J., Wöhr, M., & Schwaller, B. (2018). 17- $\beta$  estradiol increases parvalbumin levels in Pvalb heterozygous mice and attenuates behavioral phenotypes with relevance to autism core symptoms. *Molecular Autism*, 9(1), 1–13. <https://doi.org/10.1186/s13229-018-0199-3>
- Filice, F., Vörckel, K. J., Sungur, A. Ö., Wöhr, M., & Schwaller, B. (2016). Reduction in parvalbumin expression not loss of the parvalbumin-expressing GABA interneuron subpopulation in genetic parvalbumin and shank mouse models of autism. *Molecular Brain*, 9(1), 1–17. <https://doi.org/10.1186/s13041-016-0192-8>
- Fink, M., Duprat, F., Lesage, F., Reyes, R., Romey, G., Heurteaux, C., & Lazdunski, M. (1996). Cloning, functional expression and brain localization of a novel unconventional outward rectifier K<sup>+</sup> channel. *The EMBO Journal*, 15(24), 6854–6862. <https://doi.org/10.1002/j.1460-2075.1996.tb01077.x>
- Fink, M., Lesage, F., Duprat, F., Heurteaux, C., Reyes, R., Fosset, M., & Lazdunski, M. (1998). A neuronal two P domain K<sup>+</sup> channel stimulated by arachidonic acid and polyunsaturated fatty acids. *EMBO Journal*, 17(12), 3297–3308. <https://doi.org/10.1093/emboj/17.12.3297>
- Firestein, S. (2001). How the olfactory system makes sense of scents. *Nature*, 413(6852), 211–218. <https://doi.org/10.1038/35093026>
- Fleming, M. S., & Luo, W. (2013). The anatomy, function, and development of mammalian A $\beta$  low-threshold mechanoreceptors. *Frontiers in Biology*, 8(4), 408–420. <https://doi.org/10.1007/s11515-013-1271-1>
- Fukuoka, T., Miyoshi, K., & Noguchi, K. (2015). De novo expression of Nav1.7 in injured putative proprioceptive afferents: Multiple tetrodotoxin-sensitive sodium channels are retained in the rat dorsal root after spinal nerve ligation. *Neuroscience*, 284, 693–706. <https://doi.org/10.1016/j.neuroscience.2014.10.027>
- Gandal, M. J., Nesbitt, A. M., McCurdy, R. M., & Alter, M. D. (2012). Measuring the maturity of the fast-spiking interneuron transcriptional program in autism, schizophrenia, and bipolar disorder. *PLoS ONE*, 7(8), 1–8. <https://doi.org/10.1371/journal.pone.0041215>
- Gao, H., He, C., Fang, X., Hou, X., Feng, X., Yang, H., ... Ma, T. (2006). Localization of aquaporin-

- 1 water channel in glial cells of the human peripheral nervous system. *Glia*, 53(7), 783–787. <https://doi.org/10.1002/glia.20336>
- Garrison, S. R., Dietrich, a., & Stucky, C. L. (2012). TRPC1 contributes to light-touch sensation and mechanical responses in low-threshold cutaneous sensory neurons. *Journal of Neurophysiology*, 107(3), 913–922. <https://doi.org/10.1152/jn.00658.2011>
- Ghitani, N., Barik, A., Szczot, M., Thompson, J. H., Li, C., Le Pichon, C. E., ... Chesler, A. T. (2017). Specialized Mechanosensory Nociceptors Mediating Rapid Responses to Hair Pull. *Neuron*, 95(4), 944-954.e4. <https://doi.org/10.1016/j.neuron.2017.07.024>
- Gibson, S. J., Polak, J. M., Bloom, S. R., Sabate, I. M., Mulderry, P. M., Ghatel, M. A., ... Evans, R. M. (1984). Calcitonin gene-related peptide immunoreactivity in the spinal cord of man and of eight other species. *Journal of Neuroscience*, 4(12), 3101–3111. <https://doi.org/10.1523/jneurosci.04-12-03101.1984>
- Giglio, C. A., Defino, H. L. A., da-Silva, C. A., de-Souza, A. S., & Del Bel, E. A. (2006). Behavioral and physiological methods for early quantitative assessment of spinal cord injury and prognosis in rats. *Brazilian Journal of Medical and Biological Research*, 39(12), 1613–1623. <https://doi.org/10.1590/S0100-879X2006001200013>
- Gingras, J., Smith, S., Matson, D. J., Johnson, D., Nye, K., Couture, L., ... McDonough, S. I. (2014). Global nav1.7 knockout mice recapitulate the phenotype of human congenital indifference to pain. *PLoS One*, 9(9), e105895. <https://doi.org/10.1371/journal.pone.0105895>
- Gold, M. S., & Gebhart, G. F. (2010). Nociceptor sensitization in pain pathogenesis. *Nature Medicine*, 16(11), 1248–1257. <https://doi.org/10.1038/nm.2235>
- Goldberg, Y. P., MacFarlane, J., MacDonald, M. L., Thompson, J., Dube, M.-P., Mattice, M., ... Hayden, M. R. (2007). Loss-of-function mutations in the Nav1.7 gene underlie congenital indifference to pain in multiple human populations. *Clinical Genetics*, 71(4), 311–319. <https://doi.org/10.1111/j.1399-0004.2007.00790.x>
- Goodman, M. B., Ernstom, G. G., Chelur, D. S., O'Hagan, R., Yao, C. A., & Chalfie, M. (2002). MEC-2 regulates C. elegans DEG/ENaC channels needed for mechanosensation. *Nature*, 415(6875), 1039–1042. <https://doi.org/10.1038/nature00853>
- Grienberger, C., & Konnerth, A. (2012). Imaging Calcium in Neurons. *Neuron*, 73(5), 862–885. <https://doi.org/10.1016/j.neuron.2012.02.011>
- Guo, D., & Hu, J. (2014). Spinal presynaptic inhibition in pain control. *Neuroscience*, 283, 95–106. <https://doi.org/10.1016/j.neuroscience.2014.09.032>
- Haliloglu, G., Becker, K., Temucin, C., Talim, B., Küçüksahin, N., Pergande, M., ... Cirak, S. (2017). Recessive PIEZO2 stop mutation causes distal arthrogyrosis with distal muscle weakness, scoliosis and proprioception defects. *Journal of Human Genetics*, 62(4), 497–501. <https://doi.org/10.1038/jhg.2016.153>
- Halsey, A., Conner, A., Bill, R., Logan, A., & Ahmed, Z. (2018). Aquaporins and Their Regulation after Spinal Cord Injury. *Cells*, 7(10), 174. <https://doi.org/10.3390/cells7100174>
- Hamann, S., Zeuthen, T., Cour, M. La, Nagelhus, E. A., Ottersen, O. P., Agre, P., & Nielsen, S. (1998). Aquaporins in complex tissues: distribution of aquaporins 1–5 in human and rat eye. *American Journal of Physiology-Cell Physiology*, 274(5), 1332–1345. <https://doi.org/10.1152/ajpcell.1998.274.5.C1332>
- Han, S., Soleiman, M. T., Soden, M. E., Zweifel, L. S., & Palmiter, R. D. (2015). Elucidating an Affective Pain Circuit that Creates a Threat Memory. *Cell*, 162(2), 363–374. <https://doi.org/10.1016/j.cell.2015.05.057>
- Hao, J., & Delmas, P. (2010). Multiple Desensitization Mechanisms of Mechanotransducer Channels Shape Firing of Mechanosensory Neurons. *Journal of Neuroscience*, 30(40), 13384–13395. <https://doi.org/10.1523/JNEUROSCI.2926-10.2010>
- Hargreaves, K., Dubner, R., Brown, F., Flores, C., & Joris, J. (1988). A new and sensitive method for measuring thermal nociception in cutaneous hyperalgesia. *Pain*, 32(1), 77–88. [https://doi.org/10.1016/0304-3959\(88\)90026-7](https://doi.org/10.1016/0304-3959(88)90026-7)

- Häring, M., Zeisel, A., Hochgerner, H., Rinwa, P., Jakobsson, J. E. T., Lönnerberg, P., ... Ernfors, P. (2018). Neuronal atlas of the dorsal horn defines its architecture and links sensory input to transcriptional cell types. *Nature Neuroscience*, 21(6), 869–880. <https://doi.org/10.1038/s41593-018-0141-1>
- Haroutounian, S., Nikolajsen, L., Bendtsen, T. F., Finnerup, N. B., Kristensen, A. D., Hasselstrøm, J. B., & Jensen, T. S. (2014). Primary afferent input critical for maintaining spontaneous pain in peripheral neuropathy. *Pain*, 155(7), 1272–1279. <https://doi.org/10.1016/j.pain.2014.03.022>
- Hendry, S., & Hsiao, S. (2012). The Somatosensory System. *Fundamental Neuroscience: Fourth Edition*, 531–551. <https://doi.org/10.1016/B978-0-12-385870-2.00024-X>
- Ho Kim, S., & Mo Chung, J. (1992). An experimental model for peripheral neuropathy produced by segmental spinal nerve ligation in the rat. *Pain*, 50(3), 355–363. [https://doi.org/10.1016/0304-3959\(92\)90041-9](https://doi.org/10.1016/0304-3959(92)90041-9)
- Honda, C. N. (1995). Differential distribution of calbindin-D28k and parvalbumin in somatic and visceral sensory neurons. *Neuroscience*, 68(3), 883–892. [https://doi.org/10.1016/0306-4522\(95\)00180-Q](https://doi.org/10.1016/0306-4522(95)00180-Q)
- Hong, G., Lee, B., Wee, J., Kim, G. H., Kim, I., Oh, U., ... Jung, J. (2016). Mechanosensitive Currents in Dorsal-Root Ganglion Neurons with Proprioceptive Function Article Tentonin 3 / TMEM150c Confers Distinct Mechanosensitive Currents in Dorsal-Root Ganglion Neurons with Proprioceptive Function. *Neuron*, 91(1), 1–12. <https://doi.org/10.1016/j.neuron.2016.05.029>
- Hong, J., Barnes, M. J., & Kessler, N. J. (2015). Case study: Use of vibration therapy in the treatment of diabetic peripheral small fiber neuropathy. *International Journal of Diabetes Mellitus*, 3(1), 72–75. <https://doi.org/10.1016/j.ijdm.2011.01.010>
- Hongo, N., Takamura, Y., Nishimaru, H., Matsumoto, J., Tobe, K., Saito, T., ... Nishijo, H. (2020). Astaxanthin Ameliorated Parvalbumin-Positive Neuron Deficits and Alzheimer's Disease-Related Pathological Progression in the Hippocampus of AppNL-G-F/NL-G-F Mice. *Frontiers in Pharmacology*, 11(March), 1–15. <https://doi.org/10.3389/fphar.2020.00307>
- Huang, J., Polgár, E., Solinski, H. J., Mishra, S. K., Tseng, P. Y., Iwagaki, N., ... Hoon, M. A. (2018). Circuit dissection of the role of somatostatin in itch and pain. *Nature Neuroscience*, 21(5), 707–716. <https://doi.org/10.1038/s41593-018-0119-z>
- Hunter, D. V., Smaila, B. D., Lopes, D. M., Takatoh, J., Denk, F., & Ramer, M. S. (2018). Advillin Is Expressed in All Adult Neural Crest-Derived Neurons. *Eneuro*, 5(5), 1–16. <https://doi.org/10.1523/ENEURO.0077-18.2018>
- Ivanova, A., Signore, M., Caro, N., Greene, N. D. E., Copp, A. J., & Martinez-Barbera, J. P. (2005). In vivo genetic ablation by Cre-mediated expression of diphtheria toxin fragment A. *Genesis*, 43(3), 129–135. <https://doi.org/10.1002/gene.20162>
- Jaggi, A. S., Jain, V., & Singh, N. (2011). Animal models of neuropathic pain. *Fundamental & Clinical Pharmacology*, 25(1), 1–28. <https://doi.org/10.1111/j.1472-8206.2009.00801.x>
- Jarvis, M. F., Honore, P., Shieh, C. C., Chapman, M., Joshi, S., Zhang, X. F., ... Krafft, D. S. (2007). A-803467, a potent and selective Nav1.8 sodium channel blocker, attenuates neuropathic and inflammatory pain in the rat. *Proceedings of the National Academy of Sciences of the United States of America*, 104(20), 8520–8525. <https://doi.org/10.1073/pnas.0611364104>
- Ji, R.-R., Berta, T., & Nedergaard, M. (2013). Glia and pain: Is chronic pain a gliopathy? *Pain*, 154(SUPPL. 1), S10–S28. <https://doi.org/10.1016/j.pain.2013.06.022>
- Ji, R. R., Kohno, T., Moore, K. A., & Woolf, C. J. (2003). Central sensitization and LTP: Do pain and memory share similar mechanisms? *Trends in Neurosciences*, 26(12), 696–705. <https://doi.org/10.1016/j.tins.2003.09.017>
- Jia, Z., Ikeda, R., Ling, J., Viatchenko-Karpinski, V., & Gu, J. G. (2016). Regulation of Piezo2 Mechanotransduction by Static Plasma Membrane Tension in Primary Afferent Neurons.

- Julius, D., & Basbaum, A. I. (2001). Molecular mechanisms of nociception. *Nature*, 413(6852), 203–210. <https://doi.org/10.1038/35093019>
- Kang, L., Gao, J., Schafer, W. R., Xie, Z., & Xu, X. Z. S. (2010). C. elegans TRP Family Protein TRP-4 Is a Pore-Forming Subunit of a Native Mechanotransduction Channel. *Neuron*, 67(3), 381–391. <https://doi.org/10.1016/j.neuron.2010.06.032>
- Kassuya, C. A. L., Ferreira, J., Claudino, R. F., & Calixto, J. B. (2007). Intraplantar PGE 2 causes nociceptive behaviour and mechanical allodynia: The role of prostanoid e receptors and protein kinases. *British Journal of Pharmacology*, 150(6), 727–737. <https://doi.org/10.1038/sj.bjp.0707149>
- Katanosaka, K., Takatsu, S., Mizumura, K., Naruse, K., & Katanosaka, Y. (2018). TRPV2 is required for mechanical nociception and the stretch-evoked response of primary sensory neurons. *Scientific Reports*, 8(1), 1–10. <https://doi.org/10.1038/s41598-018-35049-4>
- Kato, J., Takai, Y., Hayashi, M. K., Kato, Y., Tanaka, M., Sohma, Y., ... Yasui, M. (2014). Expression and localization of aquaporin-4 in sensory ganglia. *Biochemical and Biophysical Research Communications*, 451(4), 562–567. <https://doi.org/10.1016/j.bbrc.2014.08.026>
- Katz, J., & Seltzer, Z. (2009). Transition from acute to chronic postsurgical pain: risk factors and protective factors. *Expert Review of Neurotherapeutics*, 9(5), 723–744. <https://doi.org/10.1586/ern.09.20>
- Kawabata, A. (2011). Prostaglandin E2 and pain - An update. *Biological and Pharmaceutical Bulletin*, 34(8), 1170–1173. <https://doi.org/10.1248/bpb.34.1170>
- Kessler, N. J., & Hong, J. (2013). Whole body vibration therapy for painful diabetic peripheral neuropathy: A pilot study. *Journal of Bodywork and Movement Therapies*, 17(4), 518–522. <https://doi.org/10.1016/j.jbmt.2013.03.001>
- Kim, Y. S., Anderson, M., Park, K., Zheng, Q., Agarwal, A., Gong, C., ... Dong, X. (2016). Coupled Activation of Primary Sensory Neurons Contributes to Chronic Pain. *Neuron*, 91(5), 1085–1096. <https://doi.org/10.1016/j.neuron.2016.07.044>
- Kindt, K. S., Viswanath, V., Macpherson, L., Quast, K., Hu, H. Z., Patapoutian, A., & Schafer, W. R. (2007). Caenorhabditis elegans TRPA-1 functions in mechanosensation. *Nature Neuroscience*, 10(5), 568–577. <https://doi.org/10.1038/nn1886>
- King, L. S., Kozono, D., & Agre, P. (2004). From structure to disease: The evolving tale of aquaporin biology. *Nature Reviews Molecular Cell Biology*, 5(9), 687–698. <https://doi.org/10.1038/nrm1469>
- King, L. S., Choi M, Fernandez PC, Cartron JP, A. P. (2001). Defective urinary concentrating ability due to a complete deficiency of aquaporin-1. *N Engl J Med*, 345(3), 175–179.
- Knowlton, W. M., Palkar, R., Lippoldt, E. K., McCoy, D. D., Baluch, F., Chen, J., & McKemy, D. D. (2013). A Sensory-Labeled Line for Cold: TRPM8-Expressing Sensory Neurons Define the Cellular Basis for Cold, Cold Pain, and Cooling-Mediated Analgesia. *Journal of Neuroscience*, 33(7), 2837–2848. <https://doi.org/10.1523/JNEUROSCI.1943-12.2013>
- Kremeyer, B., Lopera, F., Cox, J. J., Momin, A., Rugiero, F., Marsh, S., ... Ruiz-Linares, A. (2010). A Gain-of-Function Mutation in TRPA1 Causes Familial Episodic Pain Syndrome. *Neuron*, 66(5), 671–680. <https://doi.org/10.1016/j.neuron.2010.04.030>
- Kretschmer, T., Happel, L. T., England, J. D., Nguyen, D. H., Tiel, R. L., Beuerman, R. W., & Kline, D. G. (2002). Accumulation of PN1 and PN3 sodium channels in painful human neuroma-evidence from immunocytochemistry. *Acta Neurochirurgica*, 144(8), 803–810. <https://doi.org/10.1007/s00701-002-0970-1>
- Kuhn, D. C., & Willis, A. L. (1973). Prostaglandin E2, inflammation and pain threshold in rat paws. *Brit.J.Pharmacol.*, 49(1), 183–184.
- Kung, C. (2005). A possible unifying principle for mechanosensation. *Nature*, 436(7051), 647–654. <https://doi.org/10.1038/nature03896>

- Kwan, K. Y., Allchorne, A. J., Vollrath, M. A., Christensen, A. P., Zhang, D. S., Woolf, C. J., & Corey, D. P. (2006). TRPA1 Contributes to Cold, Mechanical, and Chemical Nociception but Is Not Essential for Hair-Cell Transduction. *Neuron*, *50*(2), 277–289. <https://doi.org/10.1016/j.neuron.2006.03.042>
- Lallemend, F., & Ernfors, P. (2012). Molecular interactions underlying the specification of sensory neurons. *Trends in Neurosciences*, *35*(6), 373–381. <https://doi.org/10.1016/j.tins.2012.03.006>
- Larson, A. A; Brown, David R; El-Atrasha, Samy ; Walser, M. M. (1986). Pain Threshold Changes in Adjuvant- Induced Inflammation : A Possible Model of Chronic Pain in the Mouse I i. *Pharmacology Biochemistry and Behavior*, *24*, 49–53. [https://doi.org/10.1016/0091-3057\(86\)90043-2](https://doi.org/10.1016/0091-3057(86)90043-2)
- Lawson, S. N., Fang, X., & Djouhri, L. (2019). Nociceptor subtypes and their incidence in rat lumbar dorsal root ganglia (DRGs): focussing on C-polymodal nociceptors, A $\beta$ -nociceptors, moderate pressure receptors and their receptive field depths. *Current Opinion in Physiology*, *11*, 125–146. <https://doi.org/10.1016/j.cophys.2019.10.005>
- Leipold, E., Liebmann, L., Korenke, G. C., Heinrich, T., Gießelmann, S., Baets, J., ... Kurth, I. (2013). A de novo gain-of-function mutation in SCN11A causes loss of pain perception. *Nature Genetics*, *45*(11), 1399–1407. <https://doi.org/10.1038/ng.2767>
- Leith, J. L., Koutsikou, S., Lumb, B. M., & Apps, R. (2010). Spinal processing of noxious and innocuous cold information: Differential modulation by the periaqueductal gray. *Journal of Neuroscience*, *30*(14), 4933–4942. <https://doi.org/10.1523/JNEUROSCI.0122-10.2010>
- Lennertz, R. C., Kossyeva, E. A., Smith, A. K., & Stucky, C. L. (2012). TRPA1 mediates mechanical sensitization in nociceptors during inflammation. *PLoS ONE*, *7*(8), 1–11. <https://doi.org/10.1371/journal.pone.0043597>
- Lesage, F., Guillemare, E., Fink, M., Duprat, F., Lazdunski, M., Romey, G., & Barhanin, J. (1996). TWIK-1, a ubiquitous human weakly inward rectifying K<sup>+</sup> channel with a novel structure. *The EMBO Journal*, *15*(5), 1004–1011. <https://doi.org/10.1002/j.1460-2075.1996.tb00437.x>
- Lesage, F., Terrenoire, C., Romey, G., & Lazdunski, M. (2000). Human TREK2, a 2P Domain Mechano-sensitive K<sup>+</sup> Channel with Multiple Regulations by Polyunsaturated Fatty Acids, Lysophospholipids, and Gs, Gi, and Gq Protein-coupled Receptors. *Journal of Biological Chemistry*, *275*(37), 28398–28405. <https://doi.org/10.1074/jbc.M002822200>
- Levin, M. F., & Hui-Chan, C. W. Y. (1993). Conventional and acupuncture-like transcutaneous electrical nerve stimulation excite similar afferent fibers. *Archives of Physical Medicine and Rehabilitation*, *74*(1), 54–60. <https://doi.org/10.5555/uri:pii:000399939390383L>
- Li, J., Patil, R. V., & Verkman, A. S. (2002). Mildly abnormal retinal function in transgenic mice without Müller cell aquaporin-4 water channels. *Investigative Ophthalmology and Visual Science*, *43*(2), 573–579.
- Li, J., & Verkman, A. S. (2001). Impaired Hearing in Mice Lacking Aquaporin-4 Water Channels. *Journal of Biological Chemistry*, *276*(33), 31233–31237. <https://doi.org/10.1074/jbc.M104368200>
- Lin, C.-R., Amaya, F., Barrett, L., Wang, H., Takada, J., Samad, T. A., & Woolf, C. J. (2006). Prostaglandin E2 Receptor EP4 Contributes to Inflammatory Pain Hypersensitivity. *Journal of Pharmacology and Experimental Therapeutics*, *319*(3), 1096–1103. <https://doi.org/10.1124/jpet.106.105569>
- Litman, T., Søggaard, R., & Zeuthen, T. (2017). Ammonia and Urea Permeability of Mammalian Aquaporins. In *Aquaporins* (Vol. 969, pp. 327–358). Berlin, Heidelberg: Springer Berlin Heidelberg. [https://doi.org/10.1007/978-3-540-79885-9\\_17](https://doi.org/10.1007/978-3-540-79885-9_17)
- Liu, M., & Wood, J. N. (2011). The Roles of Sodium Channels in Nociception : *Pain Medicine*, *12*, 93–99. <https://doi.org/10.1111/j.1526-4637.2011.01158.x>
- Livak, K. J., & Schmittgen, T. D. (2001). Analysis of relative gene expression data using real-time quantitative PCR and the 2- $\Delta\Delta$ CT method. *Methods*, *25*(4), 402–408.

- <https://doi.org/10.1006/meth.2001.1262>
- Lolignier, S., Bonnet, C., Gaudioso, C., Noël, J., Ruel, J., Amsalem, M., ... Busserolles, J. (2015). The Nav1.9 Channel Is a Key Determinant of Cold Pain Sensation and Cold Allodynia. *Cell Reports*, 11(7), 1067–1078. <https://doi.org/10.1016/j.celrep.2015.04.027>
- Lu, D. C., Zhang, H., Zador, Z., & Verkman, A. S. (2008). Impaired olfaction in mice lacking aquaporin-4 water channels. *The FASEB Journal*, 22(9), 3216–3223. <https://doi.org/10.1096/fj.07-104836>
- Lu, Y., Ma, X., Sabharwal, R., Snitsarev, V., Morgan, D., Rahmouni, K., ... Abboud, F. M. (2009). The Ion Channel ASIC2 Is Required for Baroreceptor and Autonomic Control of the Circulation. *Neuron*, 64(6), 885–897. <https://doi.org/10.1016/j.neuron.2009.11.007>
- Luiz, A. P., MacDonald, D. I., Santana-Varela, S., Millet, Q., Sikandar, S., Wood, J. N., & Emery, E. C. (2019). Cold sensing by Na V 1.8-positive and Na V 1.8-negative sensory neurons. *Proceedings of the National Academy of Sciences of the United States of America*, 116(9), 3811–3816. <https://doi.org/10.1073/pnas.1814545116>
- Ma, T. H., Gao, H. W., Fang, X. D., & Yang, H. (2011). Expression and function of aquaporins in peripheral nervous system. *Acta Pharmacologica Sinica*, 32(6), 711–715. <https://doi.org/10.1038/aps.2011.63>
- Ma, T., Yang, B., Carlson, E. J., Epstein, C. J., Verkman, A. S., & Gillespie, A. (1998). Severely Impaired Urinary Concentrating Ability in Transgenic Mice Lacking Aquaporin-1 Water Channels. *The Journal of Biological Chemistry*, 273(8), 4296–4299. <https://doi.org/10.1074/jbc.273.8.4296>
- Ma, W., Chabot, J. G., Vercauteren, F., & Quirion, R. (2010). Injured nerve-derived COX2/PGE2 contributes to the maintenance of neuropathic pain in aged rats. *Neurobiology of Aging*, 31(7), 1227–1237. <https://doi.org/10.1016/j.neurobiolaging.2008.08.002>
- Macias, M. Y., Syring, M. B., Pizzi, M. A., Crowe, M. J., Alexanian, A. R., & Kurpad, S. N. (2006). Pain with no gain: Allodynia following neural stem cell transplantation in spinal cord injury. *Experimental Neurology*, 201(2), 335–348. <https://doi.org/10.1016/j.expneurol.2006.04.035>
- Mahmud, A. A., Nahid, N. A., Nassif, C., Sayeed, M. S. B., Ahmed, M. U., Parveen, M., ... Michaud, J. L. (2017). Loss of the proprioception and touch sensation channel PIEZO2 in siblings with a progressive form of contractures. *Clinical Genetics*, 91(3), 470–475. <https://doi.org/10.1111/cge.12850>
- Martinac, B., Rohde, P. R., Battle, A. R., Petrov, E., Pal, P., Foo, A. F. W., ... Kloda, A. (2010). Studying Mechanosensitive Ion Channels Using Liposomes. In *Liposomes: Methods and Protocols* (Vol. 606, pp. 31–53). [https://doi.org/10.1007/978-1-60761-447-0\\_4](https://doi.org/10.1007/978-1-60761-447-0_4)
- Mauthner, S. E., Hwang, R. Y., Lewis, A. H., Xiao, Q., Tsubouchi, A., Wang, Y., ... Tracey, W. D. (2014). Balboa binds to pickpocket in vivo and is required for mechanical nociception in drosophila larvae. *Current Biology*, 24(24), 2920–2925. <https://doi.org/10.1016/j.cub.2014.10.038>
- Mayer, D. J., & Price, D. D. (1976). Central nervous system mechanisms of analgesia. *Pain*, 2(4), 379–404. [https://doi.org/10.1016/0304-3959\(76\)90080-4](https://doi.org/10.1016/0304-3959(76)90080-4)
- McCarter, G. C., Reichling, D. B., & Levine, J. D. (1999). Mechanical transduction by rat dorsal root ganglion neurons in vitro. *Neuroscience Letters*, 273(3), 179–182.
- McCoy, E. S., Taylor-Blake, B., Street, S. E., Pribisko, A. L., Zheng, J., & Zylka, M. J. (2013). Peptidergic CGRP $\alpha$  Primary Sensory Neurons Encode Heat and Itch and Tonically Suppress Sensitivity to Cold. *Neuron*, 78(1), 138–151. <https://doi.org/10.1016/j.neuron.2013.01.030>
- Mccoy, E., & Sontheimer, H. (2010). MAPK induces AQP1 expression in astrocytes following injury. *Glia*, 58(2), 209–217. <https://doi.org/10.1002/glia.20916>
- McMillin, M. J., Beck, A. E., Chong, J. X., Shively, K. M., Buckingham, K. J., Gildersleeve, H. I. S., ... Bamshad, M. J. (2014). Mutations in PIEZO2 cause Gordon syndrome, Marden-Walker Syndrome, and distal arthrogyriposis type 5. *American Journal of Human Genetics*, 94(5), 734–744. <https://doi.org/10.1016/j.ajhg.2014.03.015>

- Medici, T., & Shortland, P. J. (2015). Effects of peripheral nerve injury on parvalbumin expression in adult rat dorsal root ganglion neurons. *BMC Neuroscience*, *16*(1), 93. <https://doi.org/10.1186/s12868-015-0232-9>
- Melzack, R., & Wall, P. D. (1965). Pain Mechanisms: A New Theory. *Science*, *150*.
- Mendell, L. M. (2014). Constructing and deconstructing the gate theory of pain. *Pain*, *155*(2), 210–216. <https://doi.org/10.1016/j.pain.2013.12.010>
- Meng, J. H., Ma, X. C., Li, Z. M., & Wu, D. C. (2007). Aquaporin-1 and aquaporin-3 expressions in the temporomandibular joint condylar cartilage after an experimentally induced osteoarthritis. *Chinese Medical Journal*, *120*(24), 2191–2194. <https://doi.org/10.1097/00029330-200712020-00006>
- Mikhailov, N., Leskinen, J., Fagerlund, I., Poguzhelskaya, E., Giniatullina, R., Gafurov, O., ... Giniatullin, R. (2019). Mechanosensitive meningeal nociception via Piezo channels: Implications for pulsatile pain in migraine? *Neuropharmacology*, *149*(October 2018), 113–123. <https://doi.org/10.1016/j.neuropharm.2019.02.015>
- Minami, T., Nakano, H., Kobayashi, T., Sugimoto, Y., Ushikubi, F., Ichikawa, A., ... Ito, S. (2001). Characterization of EP receptor subtypes responsible for prostaglandin E2-induced pain responses by use of EP1 and EP3 receptor knockout mice. *British Journal of Pharmacology*, *133*(3), 438–444. <https://doi.org/10.1038/sj.bjp.0704092>
- Minett, M. S., Eijkelkamp, N., & Wood, J. N. (2014). Significant Determinants of Mouse Pain Behaviour. *PLoS ONE*, *9*(8), e104458. <https://doi.org/10.1371/journal.pone.0104458>
- Minett, M. S., Falk, S., Santana-Varela, S., Bogdanov, Y. D., Nassar, M. A., Heegaard, A. M., & Wood, J. N. (2014). Pain without nociceptors? Nav1.7-independent pain mechanisms. *Cell Reports*, *6*(2), 301–312. <https://doi.org/10.1016/j.celrep.2013.12.033>
- Minett, M. S., Nassar, M. a, Clark, A. K., Passmore, G., Dickenson, A. H., Wang, F., ... Wood, J. N. (2012). Distinct Nav1.7-dependent pain sensations require different sets of sensory and sympathetic neurons. *Nature Communications*, *3*(1), 791. <https://doi.org/10.1038/ncomms1795>
- Minett, M. S., Pereira, V., Sikandar, S., Matsuyama, A., Lollignier, S., Kanellopoulos, A. H., ... Wood, J. N. (2015). Endogenous opioids contribute to insensitivity to pain in humans and mice lacking sodium channel Nav1.7. *Nature Communications*, *6*(1), 8967. <https://doi.org/10.1038/ncomms9967>
- Mishra, S. K., & Hoon, M. A. (2010). Ablation of TrpV1 neurons reveals their selective role in thermal pain sensation. *Molecular and Cellular Neuroscience*, *43*(1), 157–163. <https://doi.org/10.1016/j.mcn.2009.10.006>
- Mishra, S. K., Tisel, S. M., Orestes, P., Bhangoo, S. K., & Hoon, M. A. (2011). TRPV1-lineage neurons are required for thermal sensation. *EMBO Journal*, *30*(3), 582–593. <https://doi.org/10.1038/emboj.2010.325>
- Mobasheri, A., Wray, S., & Marples, D. (2005). Distribution of AQP2 and AQP3 water channels in human tissue microarrays. *Journal of Molecular Histology*, *36*(1–2), 1–14. <https://doi.org/10.1007/s10735-004-2633-4>
- Mogil, J. S., Breese, N. M., Witty, M. F., Ritchie, J., Rainville, M. L., Ase, A., ... Séguéla, P. (2005). Transgenic expression of a dominant-negative ASIC3 subunit leads to increased sensitivity to mechanical and inflammatory stimuli. *Journal of Neuroscience*, *25*(43), 9893–9901. <https://doi.org/10.1523/JNEUROSCI.2019-05.2005>
- Moroni, M., Servin-Vences, M. R., Fleischer, R., Sánchez-Carranza, O., & Lewin, G. R. (2018). Voltage gating of mechanosensitive PIEZO channels. *Nature Communications*, *9*(1), 1096. <https://doi.org/10.1038/s41467-018-03502-7>
- Mulligan, S. J., & MacVicar, B. A. (2006). VRACs CARVe a Path for Novel Mechanisms of Communication in the CNS. *Science's STKE*, *2006*(357), pe42–pe42. <https://doi.org/10.1126/stke.3572006pe42>
- Murthy, S. E., Loud, M. C., Daou, I., Marshall, K. L., Schwaller, F., Kühnemund, J., ... Patapoutian,

- A. (2018). The mechanosensitive ion channel Piezo2 mediates sensitivity to mechanical pain in mice. *Science Translational Medicine*, 10(462), eaat9897. <https://doi.org/10.1126/scitranslmed.aat9897>
- Nagi, S. S., Marshall, A. G., Makdani, A., Jarocka, E., Liljencrantz, J., Ridderström, M., ... Olausson, H. (2019). An ultrafast system for signaling mechanical pain in human skin. *Science Advances*, 5(7), 1–11. <https://doi.org/10.1126/sciadv.aaw1297>
- Nandasena, B. G. T. L., Suzuki, A., Aita, M., Kawano, Y., Nozawa-Inoue, K., & Maeda, T. (2007). Immunolocalization of aquaporin-1 in the mechanoreceptive Ruffini endings in the periodontal ligament. *Brain Research*, 1157, 32–40. <https://doi.org/10.1016/j.brainres.2007.04.033>
- Nassar, M. A., Baker, M. D., Levato, A., Ingram, R., Mallucci, G., McMahon, S. B., & Wood, J. N. (2006). Nerve injury induces robust allodynia and ectopic discharges in Nav 1.3 null mutant mice. *Molecular Pain*, 2, 1–10. <https://doi.org/10.1186/1744-8069-2-33>
- Nassar, M. A., Stirling, L. C., Forlani, G., Baker, M. D., Matthews, E. A., Dickenson, A. H., & Wood, J. N. (2004). Nociceptor-specific gene deletion reveals a major role for Nav1.7 (PN1) in acute and inflammatory pain. *Proceedings of the National Academy of Sciences*, 101(34), 12706–12711. <https://doi.org/10.1073/pnas.0404915101>
- Nesic, O., Guest, J. D., Zivadinovic, D., Narayana, P. A., Herrera, J. J., Grill, R. J., ... Lee, J. (2010). Aquaporins in spinal cord injury: The janus face of aquaporin 4. *Neuroscience*, 168(4), 1019–1035. <https://doi.org/10.1016/j.neuroscience.2010.01.037>
- Nesic, O., Lee, J., Unabia, G. C., Johnson, K., Ye, Z., Vergara, L., ... Perez-Polo, J. R. (2008). Aquaporin 1 - A novel player in spinal cord injury. *Journal of Neurochemistry*, 105(3), 628–640. <https://doi.org/10.1111/j.1471-4159.2007.05177.x>
- Nesic, O., Lee, J., Johnson, K. M., Ye, Z., Xu, G. Y., Unabia, G. C., ... Perez-Polo, J. R. (2005). Transcriptional profiling of spinal cord injury-induced central neuropathic pain. *Journal of Neurochemistry*, 95(4), 998–1014. <https://doi.org/10.1111/j.1471-4159.2005.03462.x>
- Noël, J., Zimmermann, K., Busserolles, J., Deval, E., Alloui, A., Diochot, S., ... Lazdunski, M. (2009). The mechano-activated K<sup>±</sup> channels TRAAK and TREK-1 control both warm and cold perception. *EMBO Journal*, 28(9), 1308–1318. <https://doi.org/10.1038/emboj.2009.57>
- Nonomura, K., Woo, S. H., Chang, R. B., Gillich, A., Qiu, Z., Francisco, A. G., ... Patapoutian, A. (2017). Piezo2 senses airway stretch and mediates lung inflation-induced apnoea. *Nature*, 541(7636), 176–181. <https://doi.org/10.1038/nature20793>
- O'Hagan, R., Chalfie, M., & Goodman, M. B. (2005). The MEC-4 DEG/ENaC channel of *Caenorhabditis elegans* touch receptor neurons transduces mechanical signals. *Nature Neuroscience*, 8(1), 43–50. <https://doi.org/10.1038/nn1362>
- Oklinski, M. K., Choi, H. J., & Kwon, T. H. (2015). Peripheral nerve injury induces aquaporin-4 expression and astrocytic enlargement in spinal cord. *Neuroscience*, 311, 138–152. <https://doi.org/10.1016/j.neuroscience.2015.10.025>
- Okubo, M., Fujita, A., Saito, Y., Komaki, H., Ishiyama, A., Takeshita, E., ... Sasaki, M. (2015). A family of distal arthrogyrosis type 5 due to a novel PIEZO2 mutation. *American Journal of Medical Genetics, Part A*, 167(5), 1100–1106. <https://doi.org/10.1002/ajmg.a.36881>
- Okuda, H., Noguchi, A., Kobayashi, H., Kondo, D., Harada, K. H., Youssefian, S., ... Koizumi, A. (2016). Infantile pain episodes associated with novel Nav1.9 mutations in familial episodic pain syndrome in Japanese families. *PLoS ONE*, 11(5), 1–23. <https://doi.org/10.1371/journal.pone.0154827>
- Oliver, K. M., Florez-Paz, D. M., Badea, T. C., Mentis, G. Z., Menon, V., & Nooij, J. C. de. (2020). Molecular development of muscle spindle and Golgi tendon organ sensory afferents revealed by single proprioceptor transcriptome analysis. *BioRxiv*, 2020.04.03.023986. <https://doi.org/10.1101/2020.04.03.023986>
- Oshio, K., Watanabe, H., Song, Y., Verkman, A. S., & Manley, G. T. (2005). Reduced cerebrospinal fluid production and intracranial pressure in mice lacking choroid plexus water



- channel Aquaporin-1. *The FASEB Journal*, 19(1), 76–78. <https://doi.org/10.1096/fj.04-1711fje>
- Oshio, K., Watanabe, H., Yan, D., Verkman, A. S., & Manley, G. T. (2006). Impaired pain sensation in mice lacking Aquaporin-1 water channels. *Biochemical and Biophysical Research Communications*, 341(4), 1022–1028. <https://doi.org/10.1016/j.bbrc.2006.01.062>
- Papadopoulos, M. C., & Verkman, A. S. (2013). Aquaporin water channels in the nervous system. *Nature Reviews. Neuroscience*, 14(4), 265–277. <https://doi.org/10.1038/nrn3468>
- Patel, A. J., Honoré, E., Maingret, F., Lesage, F., Fink, M., Duprat, F., & Lazdunski, M. (1998). A mammalian two pore domain mechano-gated S-like K<sup>+</sup> channel. *EMBO Journal*, 17(15), 4283–4290. <https://doi.org/10.1093/emboj/17.15.4283>
- Peirs, C., Dallel, R., & Todd, A. J. (2020). Recent advances in our understanding of the organization of dorsal horn neuron populations and their contribution to cutaneous mechanical allodynia. *Journal of Neural Transmission*, 127(4), 505–525. <https://doi.org/10.1007/s00702-020-02159-1>
- Peirs, C., Williams, S. P. G., Zhao, X., Walsh, C. E., Gedeon, J. Y., Cagle, N. E., ... Seal, R. P. (2015). Dorsal Horn Circuits for Persistent Mechanical Pain. *Neuron*, 87(4), 797–812. <https://doi.org/10.1016/j.neuron.2015.07.029>
- Peng, W. W., Tang, Z. Y., Zhang, F. R., Li, H., Kong, Y. Z., Iannetti, G. D., & Hu, L. (2019). Neurobiological mechanisms of TENS-induced analgesia. *NeuroImage*, 195(March), 396–408. <https://doi.org/10.1016/j.neuroimage.2019.03.077>
- Pereira, V., Busserolles, J., Christin, M., Devilliers, M., Poupon, L., Legha, W., ... Noël, J. (2014). Role of the TREK2 potassium channel in cold and warm thermosensation and in pain perception. *Pain*, 155(12), 2534–2544. <https://doi.org/10.1016/j.pain.2014.09.013>
- Petitjean, H., Pawlowski, S. A., Fraine, S. L., Sharif, B., Hamad, D., Fatima, T., ... Sharif-Naeini, R. (2015). Dorsal Horn Parvalbumin Neurons Are Gate-Keepers of Touch-Evoked Pain after Nerve Injury. *Cell Reports*, 13(6), 1246–1257. <https://doi.org/10.1016/j.celrep.2015.09.080>
- Pogorzala, L. A., Mishra, S. K., & Hoon, M. A. (2013). The cellular code for mammalian thermosensation. *Journal of Neuroscience*, 33(13), 5533–5541. <https://doi.org/10.1523/JNEUROSCI.5788-12.2013>
- Poole, K., Herget, R., Lapatsina, L., Ngo, H.-D., & Lewin, G. R. (2014). Tuning Piezo ion channels to detect molecular-scale movements relevant for fine touch. *Nature Communications*, 5(1), 3520. <https://doi.org/10.1038/ncomms4520>
- Popp, L., Häussler, A., Olliges, A., Nüsing, R., Narumiya, S., Geisslinger, G., & Tegeder, I. (2009). Comparison of nociceptive behavior in prostaglandin E, F, D, prostacyclin and thromboxane receptor knockout mice. *European Journal of Pain*, 13(7), 691–703. <https://doi.org/10.1016/j.ejpain.2008.09.001>
- Prato, V., Taberner, F. J., Hockley, J. R. F., Callejo, G., Arcourt, A., Tazir, B., ... Lechner, S. G. (2017). Functional and Molecular Characterization of Mechanoinsensitive “Silent” Nociceptors. *Cell Reports*, 21(11), 3102–3115. <https://doi.org/10.1016/j.celrep.2017.11.066>
- Preston, G. M., & Agre, P. (1991). Isolation of the cDNA for erythrocyte integral membrane protein of 28 kilodaltons: Member of an ancient channel family. *Proceedings of the National Academy of Sciences of the United States of America*, 88(24), 11110–11114. <https://doi.org/10.1073/pnas.88.24.11110>
- Preston, G., Smith, B., Zeidel, M., Moulds, J., & Agre, P. (1994). Mutations in aquaporin-1 in phenotypically normal humans without functional CHIP water channels. *Science*, 265(5178), 1585–1587. <https://doi.org/10.1126/science.7521540>
- Price, D. D., & Dubner, R. (1977). Mechanisms of first and second pain in the peripheral and central nervous systems. *Journal of Investigative Dermatology*, 69(1), 167–171. <https://doi.org/10.1111/1523-1747.ep12497942>
- Price, M. P., McIlwrath, S. L., Xie, J., Cheng, C., Qiao, J., Tarr, D. E., ... Welsh, M. J. (2001). The DRASIC cation channel contributes to the detection of cutaneous touch and acid stimuli in

- mice. *Neuron*, 32(6), 1071–1083. [https://doi.org/10.1016/S0896-6273\(01\)00547-5](https://doi.org/10.1016/S0896-6273(01)00547-5)
- Qi, Y., Andolfi, L., Frattini, F., Mayer, F., Lazzarino, M., & Hu, J. (2015). Membrane stiffening by STOML3 facilitates mechanosensation in sensory neurons. *Nature Communications*, 6, 1–13. <https://doi.org/10.1038/ncomms9512>
- Qiu, F., Jiang, Y., Zhang, H., Liu, Y., & Mi, W. (2012). Increased expression of tetrodotoxin-resistant sodium channels Nav1.8 and Nav1.9 within dorsal root ganglia in a rat model of bone cancer pain. *Neuroscience Letters*, 512(2), 61–66. <https://doi.org/10.1016/j.neulet.2012.01.069>
- Quick, K., Zhao, J., Eijkelkamp, N., Linley, J. E., Rugiero, F., Cox, J. J., ... Wood, J. N. (2012). TRPC3 and TRPC6 are essential for normal mechanotransduction in subsets of sensory neurons and cochlear hair cells. *Open Biology*, 2(5), 120068. <https://doi.org/10.1098/rsob.120068>
- Rabini, A., De Sire, A., Marzetti, E., Gimigliano, R., Ferriero, G., Piazzini, D. B., ... Gimigliano, F. (2015). Effects of focal muscle vibration on physical functioning in patients with knee osteoarthritis: a randomized controlled trial. *European Journal of Physical and Rehabilitation Medicine*, 51(5), 513–520.
- Radhakrishnan, R., & Sluka, K. A. (2005). Deep tissue afferents, but not cutaneous afferents, mediate transcutaneous electrical nerve stimulation-induced antihyperalgesia. *Journal of Pain*, 6(10), 673–680. <https://doi.org/10.1016/j.jpain.2005.06.001>
- Raffaelli, W., & Arnaudo, E. (2017). Pain as a disease: An overview. *Journal of Pain Research*, 10, 2003–2008. <https://doi.org/10.2147/JPR.S138864>
- Ran, C., & Chen, X. (2019). Probing the coding logic of thermosensation using spinal cord calcium imaging. *Experimental Neurology*, 318(March), 42–49. <https://doi.org/10.1016/j.expneurol.2019.04.009>
- Ranade, S. S., Syeda, R., & Patapoutian, A. (2015). Mechanically Activated Ion Channels. *Neuron*, 87(6), 1162–1179. <https://doi.org/10.1016/j.neuron.2015.08.032>
- Ranade, S. S., Woo, S.-H., Dubin, A. E., Moshourab, R. A., Wetzel, C., Petrus, M., ... Patapoutian, A. (2014). Piezo2 is the major transducer of mechanical forces for touch sensation in mice. *Nature*, 516(7529), 121–125. <https://doi.org/10.1038/nature13980>
- Randall, I. O., & Selitto, J. J. (1957). A method for measurement of analgesic activity on inflamed tissue. *Archives Internationales de Pharmacodynamie et de Therapie*, 111(4), 409–419.
- Raouf, R., Lolignier, S., Sexton, J. E., Millet, Q., Santana-Varela, S., Biller, A., ... Wood, J. N. (2018). Inhibition of somatosensory mechanotransduction by annexin A6. *Science Signaling*, 11(535), eaao2060. <https://doi.org/10.1126/scisignal.aao2060>
- Raouf, R., Quick, K., & Wood, J. N. (2010). Review series Pain as a channelopathy. *The Journal of Clinical Investigation*, 120(11), 3745–3752. <https://doi.org/10.1172/JCI43158.to>
- Ren, H., Yang, B., Molina, P. A., Sands, J. M., & Klein, J. D. K. (2015). NSAIDs alter phosphorylated forms of AQP2 in the inner medullary tip. *PLoS ONE*, 10(10), 1–14. <https://doi.org/10.1371/journal.pone.0141714>
- Rexed, B. (1954). A cytoarchitectonic atlas of the spinal cord in the cat. *The Journal of Comparative Neurology*, 100(2), 297–379. <https://doi.org/10.1002/cne.901000205>
- Richardson, S. M., Knowles, R., Marples, D., Hoyland, J. A., & Mobasher, A. (2008). Aquaporin expression in the human intervertebral disc. *Journal of Molecular Histology*, 39(3), 303–309. <https://doi.org/10.1007/s10735-008-9166-1>
- Rojek, A., Führtbauer, E. M., Kwon, T. H., Frøkiær, J., & Nielsen, S. (2006). Severe urinary concentrating defect in renal collecting duct-selective AQP2 conditional-knockout mice. *Proceedings of the National Academy of Sciences of the United States of America*, 103(15), 6037–6042. <https://doi.org/10.1073/pnas.0511324103>
- Rugiero, F., Drew, L. J., & Wood, J. N. (2010). Kinetic properties of mechanically activated currents in spinal sensory neurons. *The Journal of Physiology*, 588(Pt 2), 301–314. <https://doi.org/10.1113/jphysiol.2009.182360>

- Rugiero, F., & Wood, J. N. (2009). The mechanosensitive cell line ND-C does not express functional thermoTRP channels. *Neuropharmacology*, *56*(8), 1138–1146. <https://doi.org/10.1016/j.neuropharm.2009.03.012>
- Rush, A. M., Dib-Hajj, S. D., Liu, S., Cummins, T. R., Black, J. A., & Waxman, S. G. (2006). A single sodium channel mutation produces hyper- or hypoexcitability in different types of neurons. *Proceedings of the National Academy of Sciences*, *103*(21), 8245–8250. <https://doi.org/10.1073/pnas.0602813103>
- Saadé, N. E., Massaad, C. A., Ochoa-Chaar, C. I., Jabbur, S. J., Safieh-Garabedian, B., & Atweh, S. F. (2002). Upregulation of proinflammatory cytokines and nerve growth factor by intraplantar injection of capsaicin in rats. *Journal of Physiology*, *545*(1), 241–253. <https://doi.org/10.1113/jphysiol.2002.028233>
- Samad, O. A., Tan, A. M., Cheng, X., Foster, E., Dib-Hajj, S. D., & Waxman, S. G. (2013). Virus-mediated shRNA knockdown of Na v 1.3 in rat dorsal root ganglion attenuates nerve injury-induced neuropathic pain. *Molecular Therapy*, *21*(1), 49–56. <https://doi.org/10.1038/mt.2012.169>
- Sandkühler, J. (2009). Models and Mechanisms of Hyperalgesia and Allodynia. *Physiological Reviews*, *89*(2), 707–758. <https://doi.org/10.1152/physrev.00025.2008>
- Sangameswaran, L., Delgado, S. G., Fish, L. M., Koch, B. D., Jakeman, L. B., Stewart, G. R., ... Herman, R. C. (1996). Structure and Function of a Novel Voltage-gated, Tetrodotoxin-resistant Sodium Channel Specific to Sensory Neurons. *Journal of Biological Chemistry*, *271*(11), 5953–5956. <https://doi.org/10.1074/jbc.271.11.5953>
- Sauer, B., & Henderson, N. (1988). Site-specific DNA recombination in mammalian cells by the Cre recombinase of bacteriophage P1. *Proceedings of the National Academy of Sciences of the United States of America*, *85*(14), 5166–5170. <https://doi.org/10.1073/pnas.85.14.5166>
- Schwaller, B., Dick, J., Dhoot, G., Carroll, S., Vrbova, G., Nicotera, P., ... Celio, M. R. (1999). Prolonged contraction-relaxation cycle of fast-twitch muscles in parvalbumin knockout mice. *American Journal of Physiology - Cell Physiology*, *276*(2 45-2), 395–403. <https://doi.org/10.1152/ajpcell.1999.276.2.c395>
- Sexton, J. E., Desmonds, T., Quick, K., Taylor, R., Abramowitz, J., Forge, A., ... Wood, J. N. (2016). The contribution of TRPC1, TRPC3, TRPC5 and TRPC6 to touch and hearing. *Neuroscience Letters*, *610*, 36–42. <https://doi.org/10.1016/j.neulet.2015.10.052>
- Shields, S. D., Ahn, H. S., Yang, Y., Han, C., Seal, R. P., Wood, J. N., ... Dib-Hajj, S. D. (2012). Na v1.8 expression is not restricted to nociceptors in mouse peripheral nervous system. *Pain*, *153*(10), 2017–2030. <https://doi.org/10.1016/j.pain.2012.04.022>
- Shields, S. D., Mazario, J., Skinner, K., & Basbaum, A. I. (2007). Anatomical and functional analysis of aquaporin 1, a water channel in primary afferent neurons. *Pain*, *131*(1–2), 8–20. <https://doi.org/10.1016/j.pain.2006.11.018>
- Shortland, P. J., & Mahns, D. A. (2016). Differing roles for parvalbumin neurons after nerve injury. *Neural Regeneration Research*, *11*(8), 1241–1242. <https://doi.org/10.4103/1673-5374.189179>
- Sivilotti, L., & Woolf, C. J. (1994). The contribution of GABA(A) and glycine receptors to central sensitization: Disinhibition and touch-evoked allodynia in the spinal cord. *Journal of Neurophysiology*, *72*(1), 169–179. <https://doi.org/10.1152/jn.1994.72.1.169>
- Smith-Edwards, K. M., DeBerry, J. J., Saloman, J. L., Davis, B. M., & Woodbury, C. J. (2016). Profound alteration in cutaneous primary afferent activity produced by inflammatory mediators. *ELife*, *5*(NOVEMBER2016), 1–18. <https://doi.org/10.7554/eLife.20527>
- Soattin, L., Fiore, M., Gavazzo, P., Viti, F., Facci, P., Raiteri, R., ... Vassalli, M. (2016). The biophysics of piezo1 and piezo2 mechanosensitive channels. *Biophysical Chemistry*, *208*, 26–33. <https://doi.org/10.1016/j.bpc.2015.06.013>
- Solenov, E. I., Vetrivel, L., Oshio, K., Manley, G. T., & Verkman, A. S. (2002). Optical measurement of swelling and water transport in spinal cord slices from aquaporin null mice.

- Journal of Neuroscience Methods*, 113(1), 85–90. [https://doi.org/10.1016/S0165-0270\(01\)00481-2](https://doi.org/10.1016/S0165-0270(01)00481-2)
- Sosa, M. A. G., De Gasperi, R., & Elder, G. A. (2010). Animal transgenesis: An overview. *Brain Structure and Function*, 214(2–3), 91–109. <https://doi.org/10.1007/s00429-009-0230-8>
- Sukhotinsky, I., Ben-Dor, E., Raber, P., & Devor, M. (2004). Key role of the dorsal root ganglion in neuropathic tactile hypersensitivity. *European Journal of Pain*, 8(2), 135–143. [https://doi.org/10.1016/S1090-3801\(03\)00086-7](https://doi.org/10.1016/S1090-3801(03)00086-7)
- Syeda, R., Florendo, M. N., Cox, C. D., Kefauver, J. M., Santos, J. S., Martinac, B., & Patapoutian, A. (2016). Piezo1 Channels Are Inherently Mechanosensitive. *Cell Reports*, 17(7), 1739–1746. <https://doi.org/10.1016/j.celrep.2016.10.033>
- Szczot, M., Liljencrantz, J., Ghitani, N., Barik, A., Lam, R., Thompson, J. H., ... Chesler, A. T. (2018). PIEZO2 mediates injury-induced tactile pain in mice and humans. *Science Translational Medicine*, 10(462), eaat9892. <https://doi.org/10.1126/SCITRANSLMED.AAT9892>
- Szczot, M., Pogorzala, L. A., Solinski, H. J., Young, L., Yee, P., Le Pichon, C. E., ... Hoon, M. A. (2017). Cell-Type-Specific Splicing of Piezo2 Regulates Mechanotransduction. *Cell Reports*, 21(10), 2760–2771. <https://doi.org/10.1016/j.celrep.2017.11.035>
- Tait, M. J., Saadoun, S., Bell, B. A., & Papadopoulos, M. C. (2008). Water movements in the brain: role of aquaporins. *Trends in Neurosciences*, 31(1), 37–43. <https://doi.org/10.1016/j.tins.2007.11.003>
- Takashima, Y., Ma, L., & McKemy, D. D. (2010). The development of peripheral cold neural circuits based on TRPM8 expression. *Neuroscience*, 169(2), 828–842. <https://doi.org/10.1016/j.neuroscience.2010.05.039>
- Takeoka, A., & Arber, S. (2019). Functional Local Proprioceptive Feedback Circuits Initiate and Maintain Locomotor Recovery after Spinal Cord Injury. *Cell Reports*, 27(1), 71–85.e3. <https://doi.org/10.1016/j.celrep.2019.03.010>
- Tan, A. M., Samad, O. A., Dib-Hajj, S. D., & Waxman, S. G. (2015). Virus-mediated knockdown of Nav1.3 in dorsal root ganglia of STZ-induced diabetic rats alleviates tactile allodynia. *Molecular Medicine*, 21, 544–552. <https://doi.org/10.2119/molmed.2015.00063>
- Theile, J. W., & Cummins, T. R. (2011). Recent Developments Regarding Voltage-Gated Sodium Channel Blockers for the Treatment of Inherited and Acquired Neuropathic Pain Syndromes. *Frontiers in Pharmacology*, 2(October), 1–14. <https://doi.org/10.3389/fphar.2011.00054>
- Tian, L., Andrew Hires, S., & Looger, L. L. (2012). Imaging neuronal activity with genetically encoded calcium indicators. *Cold Spring Harbor Protocols*, 7(6), 647–656. <https://doi.org/10.1101/pdb.top069609>
- Todd, A. J. (2010). Neuronal circuitry for pain processing in the dorsal horn. *Nature Reviews Neuroscience*, 11(12), 823–836. <https://doi.org/10.1038/nrn2947>
- Todd, A. J., & Wang, F. (2020). Central Nervous System Pain Pathways. In John N. Wood (Ed.), *The Oxford Handbook of the Neurobiology of Pain* (pp. 414–444). Oxford University Press. <https://doi.org/10.1093/oxfordhb/9780190860509.013.5>
- Tracey, W. D., Wilson, R. I., Laurent, G., & Benzer, S. (2003). painless, a Drosophila gene essential for nociception. *Cell*, 113(2), 261–273. [https://doi.org/10.1016/S0092-8674\(03\)00272-1](https://doi.org/10.1016/S0092-8674(03)00272-1)
- Tsantoulas, C., Laínez, S., Wong, S., Mehta, I., Vilar, B., & McNaughton, P. A. (2017). Hyperpolarization-activated cyclic nucleotide-gated 2 (HCN2) ion channels drive pain in mouse models of diabetic neuropathy. *Science Translational Medicine*, 9(409), eaam6072. <https://doi.org/10.1126/scitranslmed.aam6072>
- Tsunoda, S. P., Wiesner, B., Lorenz, D., Rosenthal, W., & Pohl, P. (2004). Aquaporin-1, Nothing but a Water Channel. *Journal of Biological Chemistry*, 279(12), 11364–11367. <https://doi.org/10.1074/jbc.M310881200>
- Umenishi, F., & Schrier, R. W. (2003). Hypertonicity-induced Aquaporin-1 (AQP1) Expression Is

- Mediated by the Activation of MAPK Pathways and Hypertonicity-responsive Element in the AQP1 Gene. *Journal of Biological Chemistry*, 278(18), 15765–15770. <https://doi.org/10.1074/jbc.M209980200>
- Usoskin, D., Furlan, A., Islam, S., Abdo, H., Lönnerberg, P., Lou, D., ... Ernfors, P. (2015). Unbiased classification of sensory neuron types by large-scale single-cell RNA sequencing. *Nature Neuroscience*, 18(1), 145–153. <https://doi.org/10.1038/nn.3881>
- Van Den Bosch, L., Schwaller, B., Vleminckx, V., Meijers, B., Stork, S., Ruehlicke, T., ... Berchtold, M. W. (2002). Protective effect of parvalbumin on excitotoxic motor neuron death. *Experimental Neurology*, 174(2), 150–161. <https://doi.org/10.1006/exnr.2001.7858>
- Vance, C. G. T., Dailey, D. L., Rakel, B. A., & Sluka, K. A. (2014). Using TENS for pain control: the state of the evidence. *Pain Management*, 4(3), 197–209. <https://doi.org/10.2217/pmt.14.13>
- Vega, J. A., Haro, J. J., & Del Valle, M. E. (1996). Immunohistochemistry of human cutaneous Meissner and Pacinian corpuscles. *Microscopy Research and Technique*, 34(4), 351–361. [https://doi.org/10.1002/\(SICI\)1097-0029\(19960701\)34:4<351::AID-JEMT6>3.0.CO;2-R](https://doi.org/10.1002/(SICI)1097-0029(19960701)34:4<351::AID-JEMT6>3.0.CO;2-R)
- Verkman, A. S., Yang, B., Song, Y., Manley, G. T., & Ma, T. (2000). Role of water channels in fluid transport studied by phenotype analysis of aquaporin knockout mice. *Experimental Physiology*, 85(s1), 233s-241s. <https://doi.org/10.1111/j.1469-445X.2000.tb00028.x>
- Verkman, A. S. (2012). Aquaporins in Clinical Medicine. *Annual Review of Medicine*, 63(1), 303–316. <https://doi.org/10.1146/annurev-med-043010-193843>
- Verkman, A. S., Smith, A. J., Phuan, P. wah, Tradtrantip, L., & Anderson, M. O. (2017). The aquaporin-4 water channel as a potential drug target in neurological disorders. *Expert Opinion on Therapeutic Targets*, 21(12), 1161–1170. <https://doi.org/10.1080/14728222.2017.1398236>
- Vierck, C. J., Whitsel, B. L., Favorov, O. V., Brown, A. W., & Tommerdahl, M. (2013). Role of primary somatosensory cortex in the coding of pain. *Pain*, 154(3), 334–344. <https://doi.org/10.1016/j.pain.2012.10.021>
- Vilceanu, D., & Stucky, C. L. (2010). TRPA1 Mediates Mechanical Currents in the Plasma Membrane of Mouse Sensory Neurons. *PLoS ONE*, 5(8), e12177. <https://doi.org/10.1371/journal.pone.0012177>
- Wang, A. Y., Lohmann, K. M., Yang, C. K., Zimmerman, E. I., Pantazopoulos, H., Herring, N., ... Konradi, C. (2011). Bipolar disorder type 1 and schizophrenia are accompanied by decreased density of parvalbumin- and somatostatin-positive interneurons in the parahippocampal region. *Acta Neuropathologica*, 122(5), 615–626. <https://doi.org/10.1007/s00401-011-0881-4>
- Wang, F., Bélanger, E., Côté, S. L., Desrosiers, P., Prescott, S. A., Côté, D. C., & De Koninck, Y. (2018). Sensory Afferents Use Different Coding Strategies for Heat and Cold. *Cell Reports*, 23(7), 2001–2013. <https://doi.org/10.1016/j.celrep.2018.04.065>
- Wang, J., La, J.-H., & Hamill, O. P. (2019). PIEZO1 Is Selectively Expressed in Small Diameter Mouse DRG Neurons Distinct From Neurons Strongly Expressing TRPV1. *Frontiers in Molecular Neuroscience*, 12(July), 1–15. <https://doi.org/10.3389/fnmol.2019.00178>
- Wang, L., Zhou, H., Zhang, M., Liu, W., Deng, T., Zhao, Q., ... Xiao, B. (2019). Structure and mechanogating of the mammalian tactile channel PIEZO2. *Nature*, 573(7773), 225–229. <https://doi.org/10.1038/s41586-019-1505-8>
- Weiss, J., Pysrski, M., Jacobi, E., Bufe, B., Willnecker, V., Schick, B., ... Zufall, F. (2011). Loss-of-function mutations in sodium channel Nav1.7 cause anosmia. *Nature*, 472(7342), 186–190. <https://doi.org/10.1038/nature09975>
- Wetzel, C., Pifferi, S., Picci, C., Gök, C., Hoffmann, D., Bali, K. K., ... Lewin, G. R. (2017). Small-molecule inhibition of STOML3 oligomerization reverses pathological mechanical hypersensitivity. *Nature Neuroscience*, 20(2), 209–218. <https://doi.org/10.1038/nn.4454>
- Wise, J. (2017). Gabapentinoids should not be used for chronic low back pain, meta-analysis

- concludes. *BMJ (Online)*, 358, 1–2. <https://doi.org/10.1136/bmj.j3870>
- Wöhr, M., Orduz, D., Gregory, P., Moreno, H., Khan, U., Vörckel, K. J., ... Schwaller, B. (2015). Lack of parvalbumin in mice leads to behavioral deficits relevant to all human autism core symptoms and related neural morphofunctional abnormalities. *Translational Psychiatry*, 5(January 2014), e525. <https://doi.org/10.1038/tp.2015.19>
- Woo, S.-H., Lukacs, V., de Nooij, J. C., Zaytseva, D., Criddle, C. R., Francisco, A., ... Patapoutian, A. (2015). Piezo2 is the principal mechanotransduction channel for proprioception. *Nature Neuroscience*, 18(12), 1756–1762. <https://doi.org/10.1038/nn.4162>
- Woo, S., Ranade, S., Weyer, A. D., Dubin, A. E., Baba, Y., Qiu, Z., ... Patapoutian, A. (2014). Piezo2 is required for Merkel-cell mechanotransduction. *Nature*, 509(7502), 622–626. <https://doi.org/10.1038/nature13251>
- Wood, J. N., Bevan, S. J., Coote, P. R., Dunn, P. M., Harmar, A., Hogan, P., ... Wheatley, S. (1990). Novel Cell Lines Display Properties of Nociceptive Sensory Neurons. *Proceedings of the Royal Society B: Biological Sciences*, 241(1302), 187–194. <https://doi.org/10.1098/rspb.1990.0084>
- Woolf, C. J., & Salter, M. W. (2000). Neuronal plasticity: Increasing the gain in pain. *Science*, 288(5472), 1765–1768. <https://doi.org/10.1126/science.288.5472.1765>
- Woolfe, G., & Macdonald, A. D. (1944). The Evaluation Of The Analgesic Action Of Pethidine Hydrochloride (Demerol). *Journal of Pharmacology and Experimental Therapeutics*, 80(3), 300 LP – 307.
- Wu, J., Lewis, A. H., & Grandl, J. (2017). Touch, Tension, and Transduction – The Function and Regulation of Piezo Ion Channels. *Trends in Biochemical Sciences*, 42(1), 57–71. <https://doi.org/10.1016/j.tibs.2016.09.004>
- Xie, W., Strong, J. A., & Zhang, J. M. (2017). Active nerve regeneration with failed target reinnervation drives persistent neuropathic pain. *ENeuro*, 4(1), 1–16. <https://doi.org/10.1523/ENEURO.0008-17.2017>
- Xu, J., Mathur, J., Vessières, E., Hammack, S., Nonomura, K., Favre, J., ... Patapoutian, A. (2018). GPR68 Senses Flow and Is Essential for Vascular Physiology. *Cell*, 173(3), 762–775.e16. <https://doi.org/10.1016/j.cell.2018.03.076>
- Xu, Q., & Yaksh, T. L. (2011). A brief comparison of the pathophysiology of inflammatory versus neuropathic pain. *Current Opinion in Anaesthesiology*, 24(4), 400–407. <https://doi.org/10.1097/ACO.0b013e32834871df>
- Xu, Z. Z., Kim, Y. H., Bang, S., Zhang, Y., Berta, T., Wang, F., ... Ji, R. R. (2015). Inhibition of mechanical allodynia in neuropathic pain by TLR5-mediated A-fiber blockade. *Nature Medicine*, 21(11), 1326–1331. <https://doi.org/10.1038/nm.3978>
- Yaksh, T. L., Al-Rodhan, N. R. F., & Jensen, T. S. (1988). Sites of action of opiates in production of analgesia. *Progress in Brain Research*, 77(C), 371–394. [https://doi.org/10.1016/S0079-6123\(08\)62803-4](https://doi.org/10.1016/S0079-6123(08)62803-4)
- Yamaguchi, T., Takano, K., Inaba, Y., Morikawa, M., Motobayashi, M., Kawamura, R., ... Kosho, T. (2019). PIEZO2 deficiency is a recognizable arthrogryposis syndrome: A new case and literature review. *American Journal of Medical Genetics, Part A*, 179(6), 948–957. <https://doi.org/10.1002/ajmg.a.61142>
- Yan, Z., Zhang, W., He, Y., Gorczyca, D., Xiang, Y., Cheng, L. E., ... Jan, Y. N. (2013). Drosophila NOMPC is a mechanotransduction channel subunit for gentle-touch sensation. *Nature*, 493(7431), 221–225. <https://doi.org/10.1038/nature11685>
- Yang, Y., Wang, Y., Li, S., Xu, Z., Li, H., Ma, L., ... Shen, Y. (2004). Mutations in SCN9A, encoding a sodium channel alpha subunit, in patients with primary erythralgia. *Journal of Medical Genetics*, 41(3), 171–174. <https://doi.org/10.1136/jmg.2003.012153>
- Yasul, M., Hazama, A., Kwon, T. H., Nielsen, S., Guggino, W. B., & Agre, P. (1999). Rapid gating and arton permeability of an intracellular aquaporin. *Nature*, 402(6758), 184–187. <https://doi.org/10.1038/46045>

- Yekkirala, A. S., Roberson, D. P., Bean, B. P., & Woolf, C. J. (2017). Breaking barriers to novel analgesic drug development. *Nature Reviews Drug Discovery*, *16*(8), 545–564. <https://doi.org/10.1038/nrd.2017.87>
- Yu, J., Yool, A. J., Schulten, K., & Tajkhorshid, E. (2006). Mechanism of Gating and Ion Conductivity of a Possible Tetrameric Pore in Aquaporin-1. *Structure*, *14*(9), 1411–1423. <https://doi.org/10.1016/j.str.2006.07.006>
- Zacharová, G., & Paleček, J. (2009). Parvalbumin and TRPV1 receptor expression in dorsal root ganglion neurons after acute peripheral inflammation. *Physiological Research*, *58*(2), 305–309. <https://doi.org/1738> [pii]
- Zain, M., & Bonin, R. P. (2019). Alterations in evoked and spontaneous activity of dorsal horn wide dynamic range neurons in pathological pain: A systematic review and analysis. *Pain*, *160*(10), 2199–2209. <https://doi.org/10.1097/j.pain.0000000000001632>
- Zappia, K. J., O'Hara, C. L., Moehring, F., Kwan, K. Y., & Stucky, C. L. (2017). Sensory Neuron-Specific Deletion of TRPA1 Results in Mechanical Cutaneous Sensory Deficits. *ENEURO*, *4*(1), ENEURO.0069-16.2017. <https://doi.org/10.1523/ENEURO.0069-16.2017>
- Zeisel, A., Hochgerner, H., Lönnerberg, P., Johnsson, A., Memic, F., van der Zwan, J., ... Linnarsson, S. (2018). Molecular Architecture of the Mouse Nervous System. *Cell*, *174*(4), 999–1014.e22. <https://doi.org/10.1016/j.cell.2018.06.021>
- Zeng, W. Z., Marshall, K. L., Min, S., Daou, I., Chapleau, M. W., Abboud, F. M., ... Patapoutian, A. (2018). PIEZO2 mediates neuronal sensing of blood pressure and the baroreceptor reflex. *Science*, *362*(6413), 464–467. <https://doi.org/10.1126/science.aau6324>
- Zhang, H., & Verkman, A. S. (2010). Aquaporin-1 tunes pain perception by interaction with Nav1.8 Na<sup>+</sup> channels in dorsal root ganglion neurons. *Journal of Biological Chemistry*, *285*(8), 5896–5906. <https://doi.org/10.1074/jbc.M109.090233>
- Zhang, H., & Verkman, A. S. (2015). Aquaporin-1 water permeability as a novel determinant of axonal regeneration in dorsal root ganglion neurons. *Experimental Neurology*, *265*, 152–159. <https://doi.org/10.1016/j.expneurol.2015.01.002>
- Zhang, M., Wang, Y., Geng, J., Zhou, S., & Xiao, B. (2019). Mechanically Activated Piezo Channels Mediate Touch and Suppress Acute Mechanical Pain Response in Mice Article Mechanically Activated Piezo Channels Mediate Touch and Suppress Acute Mechanical Pain Response in Mice. *Cell Reports*, *26*(6), 1419–1431.e4. <https://doi.org/10.1016/j.celrep.2019.01.056>
- Zhang, W., Cheng, L. E., Kittelmann, M., Li, J., Petkovic, M., Cheng, T., ... Jan, Y. N. (2015). Ankyrin Repeats Convey Force to Gate the NOMPC Mechanotransduction Channel. *Cell*, *162*(6), 1391–1403. <https://doi.org/10.1016/j.cell.2015.08.024>
- Zhao, Q., Zhou, H., Chi, S., Wang, Y., Wang, J., Geng, J., ... Xiao, B. (2018). Structure and mechanogating mechanism of the Piezo1 channel. *Nature*, *554*(7693), 487–492. <https://doi.org/10.1038/nature25743>
- Zimmerman, A., Bai, L., & Ginty, D. D. (2014). The gentle touch receptors of mammalian skin. *Science*, *346*(6212), 950–954. <https://doi.org/10.1126/science.1254229>
- Zimmerman, A. L., Kovatsis, E. M., Pozsgai, R. Y., Tasnim, A., Zhang, Q., & Ginty, D. D. (2019). Distinct Modes of Presynaptic Inhibition of Cutaneous Afferents and Their Functions in Behavior. *Neuron*, *102*(2), 420–434.e8. <https://doi.org/10.1016/j.neuron.2019.02.002>
- Zimmermann, K., Leffler, A., Babes, A., Cendan, C. M., Carr, R. W., Kobayashi, J. I., ... Reeh, P. W. (2007). Sensory neuron sodium channel Nav1.8 is essential for pain at low temperatures. *Neuroforum*, *13*(3), 100–101. <https://doi.org/10.1038/nature05880>
- Zurborg, S., Piszczek, A., Martínez, C., Hublitz, P., Al Banchaabouchi, M., Moreira, P., ... Heppenstall, P. A. (2011). Generation and characterization of an Advillin-Cre driver mouse line. *Molecular Pain*, *7*, 1–10. <https://doi.org/10.1186/1744-8069-7-66>

## 9 Appendices

### 9.1 *Appendix A: Additional methods and results for chapter 5*

#### 9.1.1 *In vitro* GCaMP imaging

Mice were culled in accordance with the Animals (Scientific Procedures) Act 1986. DRG were freshly harvested from PV<sup>tdTom</sup>;GCaMP3 mice and digested for 45 min at 37°C in Ca<sup>2+</sup>- and Mg<sup>2+</sup>-free Hanks' balanced salt solution (HBSS) containing 5 mM 4-(2-hydroxyethyl)-1-piperazineethanesulfonic acid (HEPES), 10 mM glucose, 5 mg/ml collagenase and 10 mg/ml dispase. DRG were then mechanically triturated in Dulbecco's modified Eagle's medium (DMEM) containing 10% foetal bovine serum (FBS) using fire-polished glass pipettes. Cells were plated onto 13 mm glass coverslips precoated with poly-L-lysine (1 mg/ml) and laminin (1 mg/ml) and maintained in DMEM containing 10% FBS and 125 ng/ml nerve growth factor (NGF) and 40 ng/ml neurotrophin 3 (NT3). Neurons were kept at 37°C in 5% CO<sub>2</sub> and used for *in vitro* imaging studies 12-24 hours after culturing.

Coverslips were placed into a perfusion chamber mounted on an upright Leica confocal microscope (SP8). Using a gravity fed perfusion system they were perfused with standard extracellular solution containing (in mM): 140 NaCl, 4 KCl, 1.8 CaCl<sub>2</sub>, 1 MgCl<sub>2</sub>, 10 HEPES and 5 glucose (adjusted to pH 7.4 using NaOH). After a baseline recording of 30 seconds, standard extracellular solution was switched for a high concentration KCl solution containing (in mM): 74 NaCl, 70 KCl, 1.8 CaCl<sub>2</sub>, 1 MgCl<sub>2</sub>, 10 HEPES and 5 glucose (adjusted to pH 7.4 using NaOH) for 1.5 minutes (or until maximal fluorescence was observed) and then washed with extracellular solution. Cells were incubated with 10 μM Fluo4-AM for 45 minutes at room temperature, washed with standard extracellular solution, and the protocol repeated. Data were analysed as described for *in vivo* DRG imaging experiments.

#### 9.1.2 Cold plate

A hot/cold plate (Ugo Basile) was used for this experiment. Mice were habituated to the apparatus for 2 minutes the day before testing. On the day, a mirror was placed behind the plate in order to observe the animal from all angles, and the plate was cooled and held at 10 °C. The mouse was placed on the plate and the duration of forepaw lifts over a 5 minute period recorded as a measure of cold sensitivity. This was repeated at 5 °C.



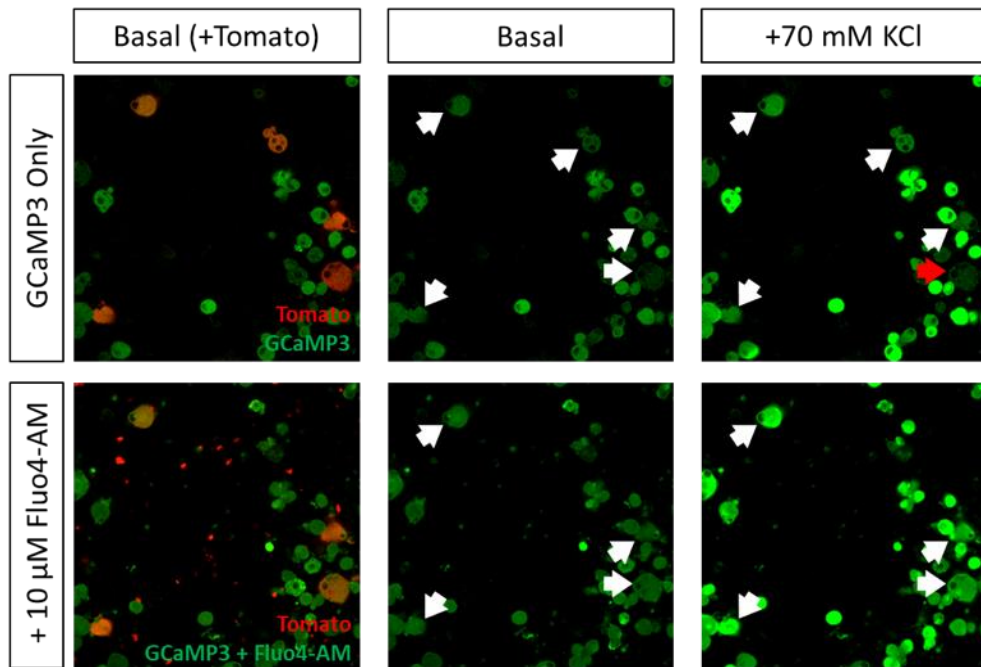
### 9.1.3 GCaMP3 is poorly expressed in the PV+ neurons of PV<sup>tdTom</sup>;Pirt-GCaMP3 mice

For a more definitive indication as to what role cutaneous PV+ neurons may have in peripheral somatosensation by directly observing their responses to hind paw stimulation, we created a mouse expressing tomato in PV+ neurons on a background of GCaMP3 expressed in all peripheral sensory neurons. We did so by crossing PV-Cre, Pirt-GCaMP3 and Rosa26-LSL-tdTomato reporter mice to produce PV<sup>tdTom</sup>;Pirt-GCaMP3 mice. Using the same stimulation protocol described in previous chapters it quickly became apparent that we could not visualise any responses in PV+ neurons, even to proprioceptive stimuli (a foot flex in this case).

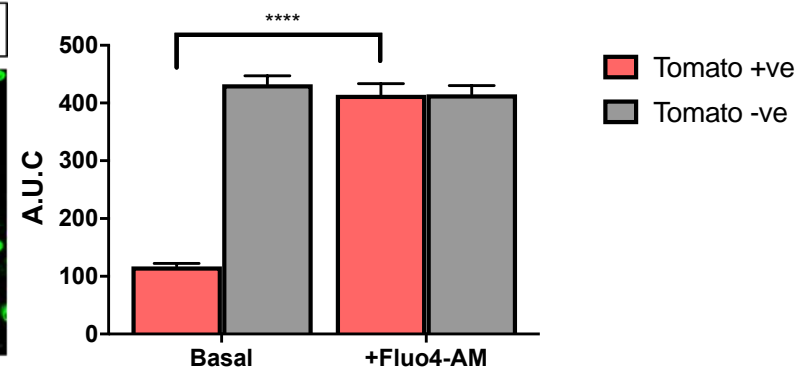
We questioned whether this was due to an inherent quality of PV+ neurons. As PV binds Ca<sup>2+</sup>, one may assume that Ca<sup>2+</sup> buffering by PV leaves a reduced concentration of cytosolic Ca<sup>2+</sup> available for GCaMP3 to bind to, therefore producing a weaker fluorescent signal when the neuron is activated. To determine if this was the case we dissociated and cultured PV<sup>tdTom</sup>;Pirt-GCaMP3 neurons and imaged them *in vitro*. We first maximally stimulated them with a high potassium solution (70 mM KCl), performed a washout, then incubated them with the membrane-permeable calcium indicator Fluo-4 AM, and repeated exposure to 70 mM KCl. PV+ neuron fluorescence in response to 70 mM KCl after incubation with Fluo-4 AM but not before, would suggest that there was sufficient cytosolic Ca<sup>2+</sup> within the neuron for effective binding of a Ca<sup>2+</sup> indicator. In this case poor fluorescence prior to incubation with Fluo4-AM would likely be due to limited expression of GCaMP3, and not due to PV's Ca<sup>2+</sup> binding properties. This is exactly what we found (Figure 9.1.A). GCaMP3-only expressing PV+ neurons had a peak fluorescence of  $1.46 \pm 0.158$  ( $\Delta F/F_0$ ), but incubation with Fluo4-AM significantly increased peak fluorescence to  $4.196 \pm 0.662$  ( $\Delta F/F_0$ ) when exposed to 70 mM KCl (Figure 9.1.B) ( $p= 0.0010$ , paired Student's t test). Fluo4-AM-incubated PV+ neuron fluorescence was comparable to the PV-negative neurons pre ( $5.7 \pm 0.4152$  ( $\Delta F/F_0$ )) and post ( $4.39 \pm 0.5249$  ( $\Delta F/F_0$ )) Fluo4-AM incubation (Figure 9.1.B). Calculating the area under the curve reveals a similar finding (Figure 9.1.C)

The recent single cell RNA sequencing dataset published alongside the study by Usoskin et al., (2015) corroborates this finding by demonstrating that there is minimal overlap between PV and Pirt RNA expression in the DRG neurons of mice. As GCaMP3 expression is driven by the Pirt promoter in this instance, you could assume poor expression of GCaMP3 protein in PV+ neurons.

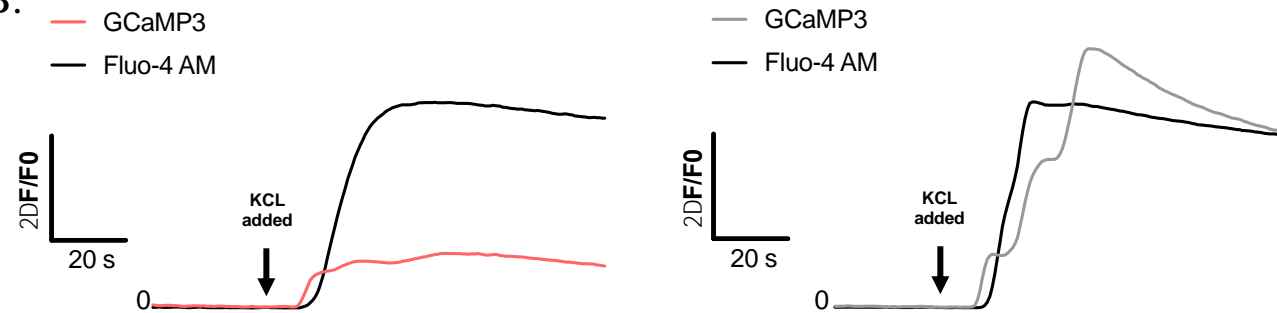
A.



C.



B.

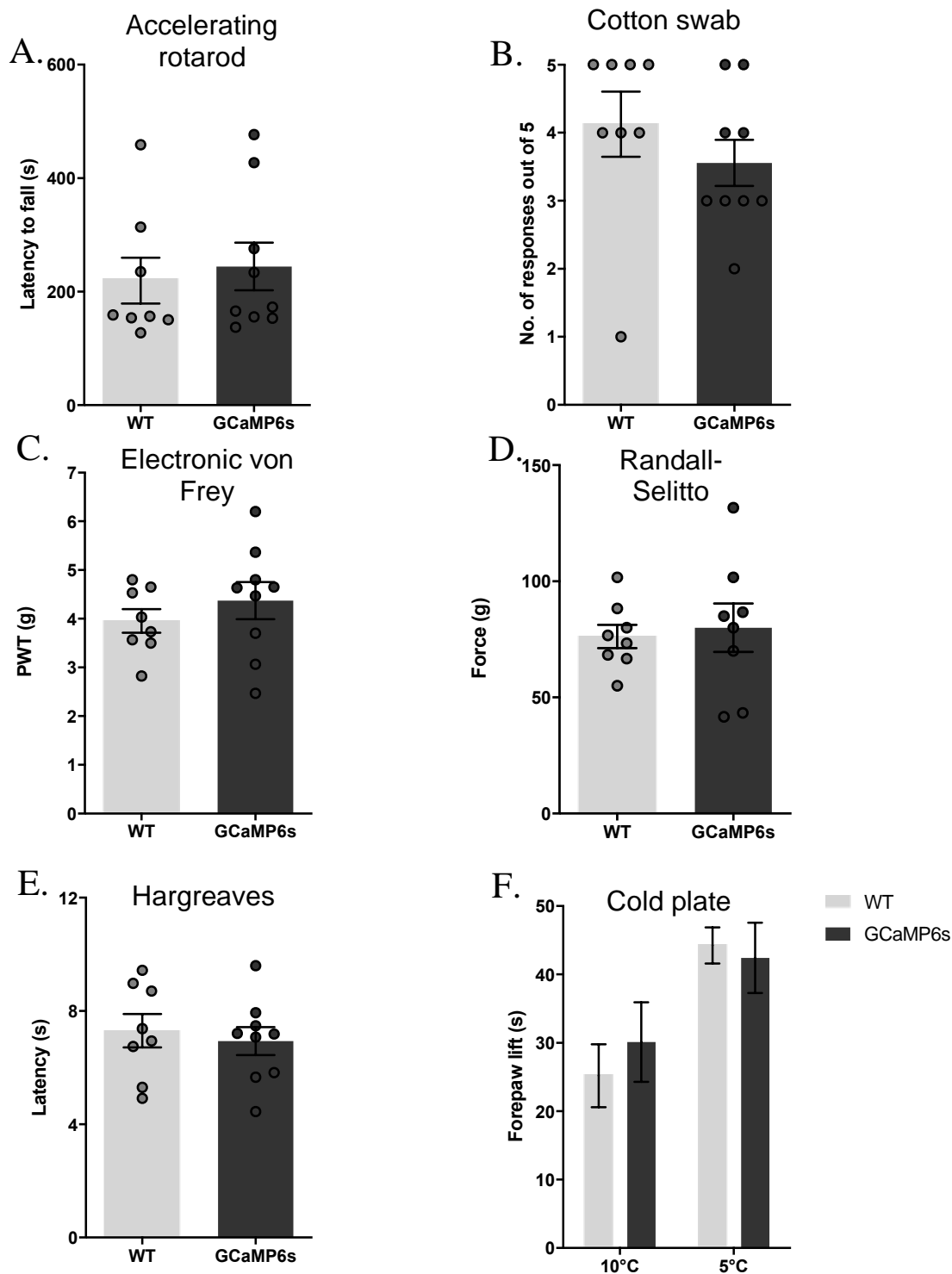


**Figure 9.1. GCaMP3-expressing PV+ neurons do not fluoresce as readily as the non-PV population in the presence of high concentration potassium solution, but do after incubation with the calcium indicator Fluo4-AM**

**A.** Example images of neurons responding to addition of 70 mM KCl before and after incubation with the calcium indicator Fluo-4 AM. Images on the far-left show tomato expression in PV+ population. PV+ neurons are denoted with an arrow. A red arrow indicates a cell that does not respond after addition of 70 mM KCl. **B.** Mean peak fluorescence traces of tomato+ neurons on the left, and tomato- neurons on the right, pre and post incubation with Fluo4-AM **C.** Depicts the A.U.C of the traces in B (n=20 per group). Data shown as Mean  $\pm$  SEM. Regular two-way ANOVA with Tukey's multiple comparison test performed for A.U.C.

#### **9.1.4 Global GCaMP6s mice are behaviourally normal**

To ensure global expression of GCaMP6s does not cause any behavioural deficits, we performed a range of behaviour assays on global GCaMP6s mice including the rotarod test to ensure normal motor coordination, as well pain behaviour experiments encompassing all modalities. We found no significant differences between adult mice globally expressing GCaMP6s, and WT C57BL/6J mice. Of note, GCaMP6s mice develop normally and exhibit no other form of physical or behavioural abnormality (Figure 9.2.A-F).



**Figure 9.2. There is no significant behavioural difference between WT and global GCaMP6 mice**  
**A.** Accelerating rotarod test. Time at which animal fell from rod displayed. **B.** Cotton swab applied to the hind paw. The number of withdrawal responses out of 5 tests was recorded. Data displayed as Mean  $\pm$  SEM with Mann-Whitney test. **C.** Electronic von Frey. An increasing force (ramp speed 0.5 g/s) applied to the hind paw, the force at which the animal withdrew recorded. **D.** Randall-Selitto performed on the hind paw as a measure of noxious mechanosensitivity. **E.** Hargreaves as a measure of sensitivity to noxious heat stimuli. **F.** Cold plate assay quantified as the amount of time animals spent with their forepaws lifted over a period of 5 minutes. Data are shown as Mean  $\pm$  SEM. Statistical analysis was performed using the unpaired Student's t test unless stated otherwise. (WT (C57BL/6J) n=8; global GCaMP6s, n=9).